The Age-Old Question of ANCA-Associated Vasculitis

Isabella Batten

B.A. Natural Sciences, Mod. Molecular Medicine

14314548

A thesis submitted to The University of Dublin, Trinity College for the degree of Doctor of Philosophy

Under the supervision of:

Dr. Nollaig Bourke, Prof. Mark Little & Dr. Mark Robinson

31st March 2023

Declaration

I declare that this thesis has not been submitted as an exercise for a degree at this or any other university and it is entirely my own work.

I agree to deposit this thesis in the University's open access institutional repository or allow the library to do so on my behalf, subject to Irish Copyright Legislation and Trinity College Library conditions of use and acknowledgement.

I consent to the examiner retaining a copy of the thesis beyond the examining period, should they so wish (EU GDPR May 2018).

I declare that this thesis contains work carried out by others that are duly noted. Datasets for *ELOVL2* methylation validation analysis from chapter 3 were provided by The Irish Longitudinal Cohort on Ageing (TILDA) and Prof. Dominic Ciavatta's group from the University of North Carolina at Chapel Hill. Pyrosequencing of the AAV samples were carried out in collaboration with Dr. Caroline Conway (Ulster University). Matt McElheron (Trinity College Dublin) was responsible for the computational modelling and statistical analysis of raw pyrosequencing data, the results of which are outlined in Chapter 3. Dr. Emma Leacy (Royal college of Surgeons) provided metabolic analyses of monocytes stimulated with ANCA added into the discussion section of chapter 3. The validation of the flow panel used to measure NETosis outlined in chapter 4 was undergone in collaboration with Amrita Dwivedi (Trinity College Dublin). The cellular assays outlined in chapter 4 were undergone in collaboration with undergraduate students, Mylène Lopez (EPISEN ISBS Paris) and Aisling O'Rourke (Trinity College Dublin) as part of their undergraduate thesis projects. Dr. Arthur White (Trinity College Dublin) assisted with the power analysis of interferon data outlined in Chapter 5.

Signed: _Isabella Batten_

Date: 30.03.23

Acknowledgments

There are so many people who deserve acknowledging for the work done over the past 4 years so strap in.

Firstly, to my absolutely amazing supervisors, Nollaig Bourke, Mark Little and Mark Robinson, I don't know how I got so lucky as to have you 3 incredibly talented academics as mentors over the past four years and I cannot thank you all enough for your endless advice, and tireless commitment to our biweekly meetings. I genuinely could not have done it without you all, and although 3 opinionated cooks may seem like a lot, you'll end up with a meal you can be proud of!

Nollaig, I can't believe my time in your lab is almost up! You have been the most important guiding figure in my career to date and I don't think I would have made it this far without having such a patient, kind and relentlessly enthusiastic supervisor. It has been an absolute pleasure working with you over the past 5+ years and you have been an overwhelmingly positive influence on my career and future as we know it. Thank you so much for your constant support. Exciting and scary times ahead and I hope our paths will cross again.

Mark L., your dedication to your work, lab and everyone in it is just incredible. I honestly do not understand where you find the time for it all! I have loved being part of the RIG group over the past couple of years and you have definitely brought me out of my comfort zone academically, particularly in the clinic! I have nothing but good words to say about you Mark, and it has been a real privilege to have had the opportunity to work with you.

Mark R., considering you are no longer in the same building as the rest of us I honestly cannot believe how involved you have been in this project! The advice you have provided on every aspect of this work over the years has been invaluable and I hope you know how much it is appreciated. I wish you the best in the future and cannot thank you enough.

To my N.B lab members, Liam, Adam, Matt and Conor, having the 4 of you in the lab (never at the same time thank God!) has been such an experience. I genuinely feel like I have witnessed what it must be like to have 4 brothers and I cannot help but laugh at some

of the memories made in that time. There is never a dull moment with you guys, and I wouldn't have it any other way. You are all absolutely incredible friends and scientists who I know are going to excel in the future and I have loved working with all of you.

To my original RIG lab members and office buddies, Amrita, Aisling, Emma, Grainne and Derv you are all just so fantastic. The number of questions I must have asked you over the years would probably fill a thesis in itself! Aisling, Grainne and Emma, I was so proud to have watched you all graduate last year and Derv and Amrita I am so delighted you were stuck with me thereafter! Thank you guys so much for creating such a wonderful atmosphere to work in.

Gareth Brady, Derek Doherty, Clíona Ní Cheallaigh and Aisling O' Halloran, although not my main supervisors, you have provided me with an abundance of both academic and general life advice throughout my time here and I have thoroughly enjoyed chatting with you guys whether in the lab, the office or the pub. Your relationship with your students is fantastic and I am grateful to have experienced that.

Conor Finlay, you for sure deserve an honourable mention after all that time spent on the cellstream software with me! Clara and Margaret, Friday wine days were my absolute favourite days. Ola one word, waltzters, a memory I will never forget no matter how much I try. Ashanty, our Tom, Tom Dineen, Nawal, Niall, Stephen, Marcus, Snow, Makala, Fiana, Cathal, Arlena, Tara, Daniel, Nicole, Ailbhe, Aifric, Anjali, Sarah, Emily, Donal, Sharee, Kevin, Bahareh, Ryan, Carla, Emma C. and all my friends and colleagues at TTMI, particularly those at 1 o'clock lunch, you are all amazing and I couldn't have asked for better people to spend my days with. Thank you all! There is no better team to be a part of.

I can't go without thanking Kevin Thompson from IT services and past and present members of security particularly Aogan, Ciaran, Marie and Paul. Thank you so much for being such reassuring and kind faces in the building and letting me in to park in times of desperation! I've had the pleasure of working with some fantastic students over the years, in particular Aisling O' Rourke and Mylène Lopez who have contributed to this thesis. Thank you for being a wonderful addition to this journey and I am positive you have bright futures ahead of you. To Mary Breen and the Silver Surfers, it was an absolute

pleasure to meet you all. You are truly a fantastic community, and this work would not have been possible without your help! And of course, to Pamela O' Neill and all of the staff working at the nephrology clinic in TUH thank you so much for being so kind and welcoming, and for helping through my recruitment process.

To my friends outside of TTMI, in particular my school friends and college crew, thank you all so much for your constant support, distractions when needed and praise when undeserved! It is an amazing thing to be surrounded by support systems like you guys who I can celebrate the big and small achievements in life with.

I must of course acknowledge my family, Jessie, Nicola, Michael, Mom, Dad and of course Charlie. No matter what the situation their support and encouragement is a constant in my life and I am forever grateful. Particularly to my parents who feed my ego with academic praise, thank you for everything you have given me in life. I am 100% here today because of your influence and the confidence and ambition that you have both instilled in me.

Last but not least, to my incredible fiancé Daniel and his family. Carol and Dave, thank you for always having an open door and cake at the ready! I couldn't have asked for better. Daniel, you have been there for all the best times and all the worst times over the course of not one, but two degrees! I am so excited with what this year has left to come for us. Thank you for constantly supporting not just my academic ideas but also all of my life choices without a minute's hesitation. For the dinners you've cooked me, the late-night collections, the distractions from stress, the back rubs to aid my horrific posture during the writing of this thesis and all the other small things you have done during the course of this degree I am so thankful. It would have been twice the battle without you, and I cannot wait to celebrate this milestone with you by my side.

Table of Contents

List of Figures

List of Tables

List of Abbreviations

AAV	ANCA Associated Vasculitis
AAV A	ANCA Associated Vasculitis Active
AAV R	ANCA Associated Vasculitis Remission
ABCs	Age associated B Cell
ACTB	Beta Actin
AG	Aicardi Goutier Syndrome
AID	Activation-induced cytidine deaminase
ANCA	Anti-Neutrophil Cytoplasmic autoantibody
ANXA3	Annexin A3
APC	Antigen Presenting Cell
Approx.	Approximately
Aza	Azathioprine
BCR	B Cell Receptor
BP	Base Pairs
BVAS	Birmingham Vasculitis Activity score
CCL19	Chemokine (C-C motif) Ligand 19
CD	Cluster of differentiation
cDNA	compliment DNA
CKD	Chronic Kidney Disease
Chr	Chromosome
CRP	C-Reactive Protein
CS	Corticosteroids
CSR	Class Switch Recombination
CP	Chronic Pyelonephritis
CpG	Cytosine-phosphate-guanine
CVD	Cardiovascular Disease
CXCL10	C-X-C motif Chemokine 10
CXCR3	C-X-C motif Chemokine Receptor 3
Cyclo	Cyclophosphamide
DAMPs	Danger-Associated Molecular Patterns
DAPI	4,6-Diamidino2-Phenylindole
DC	Disease Controls

pDC	Plasmacytoid Dendritic Cell
DHEA	dehydroepiandrosterone
DHR123	Dihydrorhodamine-123
DKD	Diabetic Kidney Disease
DM	Dermatomyositis
DMSO	Dimethyl sulfoxide
DNA	Deoxyribonucleic Acid
DNAm	DNA methylation
dNTP	Deoxynucleotide Triphosphate
EAA	Epigenetic Age Acceleration
EDTA	Ethylenediaminetetraacetic acid
EEAA	Extrinsic Epigenetic Age Acceleration
ECTS	European Credit Transfer and Accumulation System
eGFR	Estimated Glomerular Filtration Rate
EGPA	Eosinophilic Granulomatosis Polyangiitis
ELISA	Enzyme-Linked Immunosorbent Assay
ELOLV2	Elongation of very long chain fatty acids like 2
ESPRI	The EULAR Sjogren's Syndrome Patient Reported Index
Eppys	Eppendorf tubes
FACs	fluorescence-activated cell sorting
FCS	Foetal Calf Serum
FCγ	Fragment crystallizable gamma
fMLP	N-formyl-Methionyl-Leucyl-Phenylalanine
GBM	Glomerular Basement Membrane
GPA	Granulomatosis with Polyangiitis
HC	Healthy Controls
HCL	Hydrochloric acid
HCQ	Hydroxychloroquine
HLA	Human Leukocyte Antigen
Hr	Hour
IEAA	Intrinsic Epigenetic Age Acceleration
Ig	Immunoglobulin
IL-5	Interleukin-5
IL-6	Interleukin-6

IL-8	Interleukin-8
IL-1β	Interleukin-1 Beta
ISG15	Interferon Stimulated Gene 15
IFIT1	Interferon Induced Protein with Tetratricopeptide Repeats 1
IFI27	Interferon Alpha Inducible Protein 1
IFI44L	Interferon Induced Protein 44 Like
IFN	Interferon
IQR	Interquartile Range
JAK	Janus Kinase
LPS	Lipopolysaccharide
mAb	Monoclonal Antibody
MCP-1	Monocyte Chemoattractant Protein 1
MCT	Microcentrifuge Tube
MHC	Major Histocompatibility Complex
Min	Minute
MMF	Mycophenolate Mofetil
MMP8	Matrix Metalloproteinase 8
MPA	Microscopic polyangiitis
MPO	Myeloperoxidase
MS	Multiple Sclerosis
Mtx	Methotrexate
NaCl	Sodium Chloride
NaOH	Sodium Hydroxide
NaHCO$_3$	Sodium Bicarbonate
NEI VF OP	National Eye Institute Vision Functioning Ocular Pain
NH$_4$CL	Ammonium Chloride
NET	Neutrophil Extracellular Trap
Neut	Neutrophil
NF-H2O	Nuclease-Free Water
NFκB	Nuclear Factor kappa light chain enhancer of activated B cells
NLR	NOD-like Receptors
NOD	Nucleotide Oligomerization Domain
normDNA	Normalised DNA
NK	Natural Killer

OAZ1	Ornithine Decarboxylase Antizyme 1
OSDI	Ocular surface disease index
PAMPs	Pathogen-Associated Molecular Patterns
PAN	Polyarteritis Nodosa
PBMC	Peripheral blood mononuclear cells
PBS	Phosphate Buffered Saline
PCR	Polymerase Chain Reaction
PFA	Paraformaldehyde
PMA	Phorbol 12-myristate 13-acetate
PPIA	Peptidyl propyl Isomerase A
PRR	Pattern Recognition Receptor
PR3	Proteinase 3
pSS	Primary Sjogren's Syndrome
PT	Processing Tube
PUFA	Polyunsaturated Fatty Acids
RA	Rheumatoid Arthritis
RBC	Red Blood Cell
RIG	Retinoic Acid Inducible Gene
Ritux	Rituximab
RKD	Rare Kidney Disease
rhGH	recombinant human Growth Hormone
RLR	RIG-Like Receptor
ROS	Reactive Oxygen Species
RNA	Ribonucleic Acid
mRNA	messenger RNA
RNFD	DNase I
RPMI	Roswell Parks Memorial Institute Medium
RPL27	Ribosomal Protein L27
RPM	Revolutions Per Minute
RPS13	Ribosomal Protein S13
RSAD2	Radical SAM Domain-Containing 2
RT	Room temperature
RTase	Reverse transcriptase
RV	Rheumatoid Vasculitis

SASP	Senescence Associated Secretory Phenotype
Sec	Seconds
SIGLEC1	Sialic Acid Binding Ig Like Lectin 1
SIGLEC8	Sialic Acid Binding Ig Like Lectin 8
SHM	Somatic Hypermutation
SLE	Systemic Lupus Erythematosus
SLEDAI	SLE Disease Activity Index
SOCS1	Suppressor of Cytokine Signalling 1
STAT1	Signal Transducer and Activator of Transcription 1
Strep-HrP	Streptavidin horseradish peroxidase
TBP	TATA-Box Binding protein
TCR	T Cell Receptor
TBE	Tris Borate EDTA
TE	Tris-EDTA
TILDA	The Irish Longitudinal Study of Ageing
TLR	Toll-Like Receptor
TMB	Tetramethylbenzidine
TNF	Tumour Necrosis Factor
TRIM	Thymus Regeneration Immunorestoration
Tx	Treated
TxN	Treatment Naïve
UN	Unstimulated
USP18	Ubiquitin Specific Peptidase 18
VLC-PUFA	Very long chain PUFA
WB	Whole blood
Yrs	Years

Publications From this Work

Funding

Oral Presentations

- "The Age-Old Question of ANCA Associated Vasculitis"
  Trinity Translational Medicine Institute Seminar Series, December 2022

- "The Age-Old Question of ANCA Associated Vasculitis"
  Discipline of Medical Gerontology Postgraduate Research Day, MISA, St. James's Hospital, April 2023

- "The Age-Old Question of ANCA Associated Vasculitis"
  Trinity Translational Medicine Institute Conference, March 2022

- "Investigating a Role for Type I Interferon Cytokines in the Pathogenesis of ANCA Associated Vasculitis"
  The Meath Foundation Research Symposium, November 2021

- "Investigating a Role for Type I Interferon Cytokines in the Pathogenesis of ANCA Associated Vasculitis"
  Trinity college Dublin Immunology Research Forum, March 2021

- "Exploring the role of type I interferons in inflammageing".
  Precision Medicine Cancer Symposium, Trinity Translational Medicine Institute, March 2019

Poster Presentations

- "Exploration into Epigenetic Ageing in ANCA-Associated Vasculitis"
  yEFIS Symposium, November 2022

- "The Age-Old Question of ANCA Associated Vasculitis"
  ISI Annual Conference, September 2022

- "The Age-Old Question of ANCA Associated Vasculitis"
  20th International Vasculitis and ANCA Workshop, April 2022

- "Exploring the Role of Type I Interferon Responses in ANCA Associated
  Vasculitis"
  British Society of Immunology Annual Conference, November 2021

- "Exploring Type I Interferon Activity in ANCA-Associated Vasculitis"
  6th European Congress of Immunology Virtual Conference, September 2021
  Included Oral Video

- "Exploring the Role of Type I Interferons in ANCA-Associated Vasculitis"
  American Society of Nephrology (ASN) Kidney Week Virtual Conference,
  October 2020
  Included Oral Video

- "Exploring the Role of Type I Interferons in ANCA Associated Vasculitis"
  ISI Annual Conference, September 2019

Abstract

Anti-Neutrophil Cytoplasmic Autoantibody (ANCA)-Associated Vasculitis (AAV) is a group of systemic autoimmune disorders characterised by severe inflammation of the small blood vessels. Unusually for an autoimmune disease, AAV primarily affects older individuals, however the reasons behind this later-in-life development remains unknown. Although chronological age is widely accepted as an important factor in AAV development, biological ageing, a concept defined by ageing-specific cellular and molecular biomarkers as opposed to chronological time, has received little attention in this disease. With various measurement techniques now available, biological age has been shown to correlate closely with both lifespan and health span, making it an interesting approach for the risk assessment of age-associated diseases. Despite biological age measures being a superior method of capturing how the ageing body can lead to disease, biological age has not been assessed in AAV.

Accelerated ageing, which can be determined using these measures of biological age, is often associated with a chronic, low-grade inflammation, a process known as "inflammageing". A key early step in AAV development is the reaction of autoantibodies, known as ANCAs, with innate immune cells leading to their activation and subsequent inflammatory response. The effect that age has on these cells in the context of AAV remains unclear.

Additionally, recent evidence indirectly links AAV pathology and type I interferon (IFN) proteins, a family of innate immune cytokines. The inflammation seen in certain autoimmune conditions, termed type I interferonopathies, is largely due to an overproduction of these type I IFNs and their responses. Our lab has also noted a dysregulation of type I IFN regulated genes with age, possibly indicating a role for these cytokines in the process of inflammageing. However, to our knowledge this protein family are yet to be comprehensively assessed in AAV.

Therefore, during this PhD project we aimed to investigate the relationship between ageing and AAV activity. Our work has demonstrated that AAV patients experience age acceleration compared to healthy controls, using a DNA-methylation (DNAm) based measure of biological age. We have shown that chronological ageing can affect certain

immune functions specific to particular immune cell types in response to ANCA stimulation. Finally, we demonstrated that type I IFN signalling is not systemically dysregulated in AAV and therefore AAV should not be considered a type I interferonopathy. Overall, our work indicates important roles for the biological mechanisms associated with ageing in the pathogenesis of AAV.

Lay Abstract

Anti-neutrophil cytoplasmic autoantibody (ANCA)-associated vasculitis, or AAV, is an autoimmune disease that causes severe damage to the small blood vessels and nearby organs. Although rare, AAV is a serious disorder that if left untreated can result in organ failure and subsequent death. AAV predominantly affects older individuals, however the reasons behind this later-in-life development remains unknown. Although chronological age, a measure of time, is widely accepted as an important factor in AAV development, biological ageing, a measure of biological changes, has remained unstudied in this disease. Various scientific techniques are now available that measure biological ageing and these measurements have proven to be excellent predictors of lifespan and individual risk of disease development.

Accelerated ageing, which can be determined using measurements of biological age, is often associated with poor health outcomes possibly due to the influence that age can have on various aspects of the immune system. The effects that age has on the function of key immune cells known to be involved in AAV development remains unclear.

Type I interferons are a family of proteins with several immune functions. When these proteins become over-produced, they are known to cause certain autoimmune conditions named type I interferonopathies. These proteins are also known to become dysregulated with age, however, whether these proteins are overexpressed in AAV is unknown.

Therefore, we aimed to study the relationship between ageing and AAV activity. We have shown that biological ageing is accelerated in AAV patients. We have also noted that some immune responses are altered with age in response to stimulation with important triggers of AAV activity. Finally, we have demonstrated that type I IFN immune responses are not dysregulated in AAV patients and so AAV should not be classified as a type I interferonopathy. Together, this body of research reveals a role for the biological effects of ageing in AAV

1 Introduction

1.1 Ageing

Ageing can be defined as a progressive accumulation of physical, psychological and social changes over time eventually leading to impaired physical and cognitive function and an increased risk of death [1]. It is the biggest risk factor for the most prominent diseases in the world today including neurodegenerative disorders [2], cardiovascular disease [3, 4] and cancer [5] and so, with an ever-ageing population, gerontological research has received much interest in the scientific and medical community. A major focus of such research has been to identify cellular and molecular changes that occur with age in an attempt to better understand age as a risk factor for disease and to develop means of prolonging the average health span [6, 7]. With this in mind, a number of hallmarks have been described that characterise the cellular processes associated with ageing. These include genomic instability, epigenetic alterations, loss of proteostasis, deregulated nutrient-sensing, mitochondrial dysfunction, cellular senescence, stem cell exhaustion, altered intercellular communication, chronic inflammation, dysbiosis and disabled macroautophagy [1, 8]. This cellular and molecular approach to ageing is often referred to as "biological ageing" (Figure1.1.1). These hallmarks are associated with changes to all bodily systems and, importantly, biological ageing has been shown to correlate strongly with both lifespan and health span, representing a superior approach of disease risk assessment when compared to chronological time [7, 9-11]. Numerous methods have been described that measure the biological age of a sample, each of which have their own advantages and disadvantages, the most accurate predictors of biological age to date are thought to be epigenetic clocks [10, 12, 13].

Figure 1.1.1:
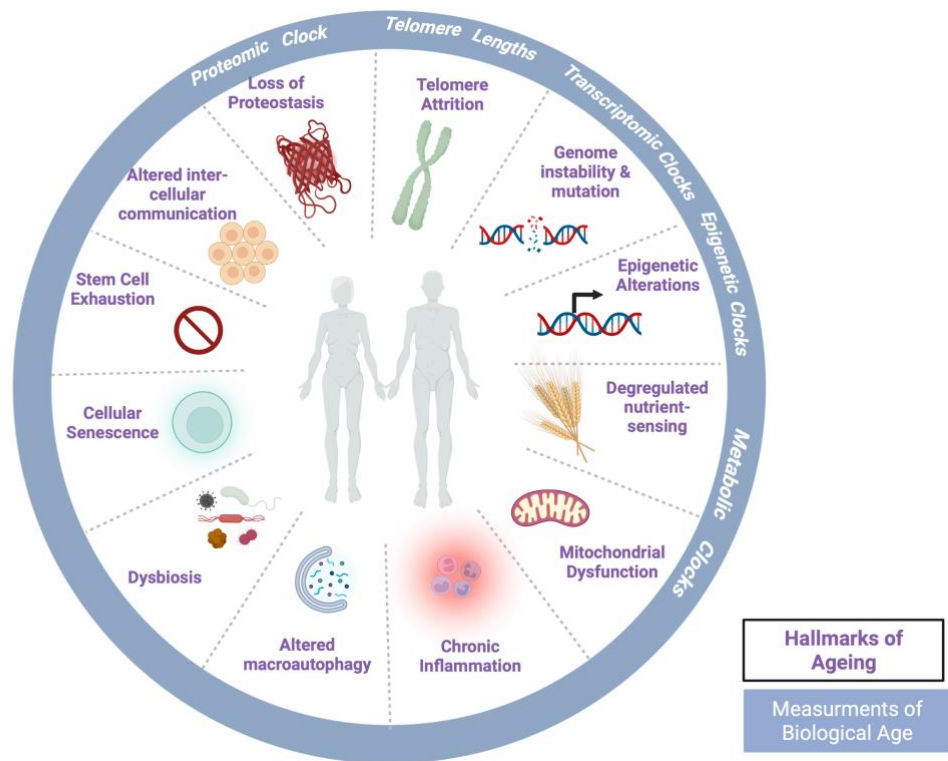
Figure 1.1.1The Hallmarks of Ageing

Biological hallmarks of ageing as outlined by Lopez-Otin et al. and the current techniques and tools utilised to measure biological ageing that are based off of these hallmarks **[1, 8, 14]**.

1.2 Epigenetics and Epigenetic Clocks as tools for quantifying biological ageing

1.2.1 Epigenetics

As mentioned above, genetic and epigenetic regulation are key components of ageing, particularly biological ageing. Deoxyribonucleic acid (DNA) refers to the genetic code found within every cell of an organism. Despite all cells containing the same sequence of DNA, each cell is capable of differentially expressing genes within this sequence, allowing for various functions and phenotypes to arise and this differential gene expression is regulated by epigenetic modifications [15, 16]. Epigenetics describes a change in the transcriptional output of the genetic code without changing the DNA sequence itself and importantly, these changes are thought to be both hereditable and reversible. Various mechanisms of epigenetic modifications have been described to date. These include DNA methylation, histone modification and epigenetic alterations regulated by various non-coding ribonucleic acids (RNAs) [17, 18]. These modifications begin at development where each cell eventually acquires a generally stable epigenetic pattern that regulates their transcription allowing for cellular differentiation and the formation of specific cell types and functions [19]. Environmental factors such as nutrition [20], smoking [21], and alcohol consumption [22] have been shown to greatly impact epigenetic signatures and, unsurprisingly, these epigenetic modifications are known to accumulate with age [1]. Interestingly, certain epigenetic modifications that occur in response to environmental influences, particularly early on in life, have been associated with a myriad of diseases ranging from cardiovascular disease and metabolic disorders [23-25] to autoimmune diseases and cancer [26, 27]. With these changes being, in theory, reversible, epigenetic drugs and therapies have become a promising field of research [28].

1.2.2 DNA Methylation

DNA methylation is an epigenetic mechanism involving the transfer of a methyl group, via methyl transferases, onto the C5 position of a cytosine nucleotide in the DNA sequence. The majority of DNA methylation modifications occur on cytosines present on regions of the DNA known as cytosine-phosphate-guanine (CpG) islands. These CpG islands refer to regions of the genome greater than 200 base pairs (bp) in length that are primarily composed of CpG dinucleotides (a cytosine nucleotide bound to a guanine

nucleotide by a phosphate bond). Many of these islands are found within the promotor regions of DNA. Methylation of these sites often act to suppress gene expression by either recruiting transcriptional repressors or inhibiting the binding of transcription factors to DNA (Figure 1.2.1) [29, 30].

Figure 1.2.1
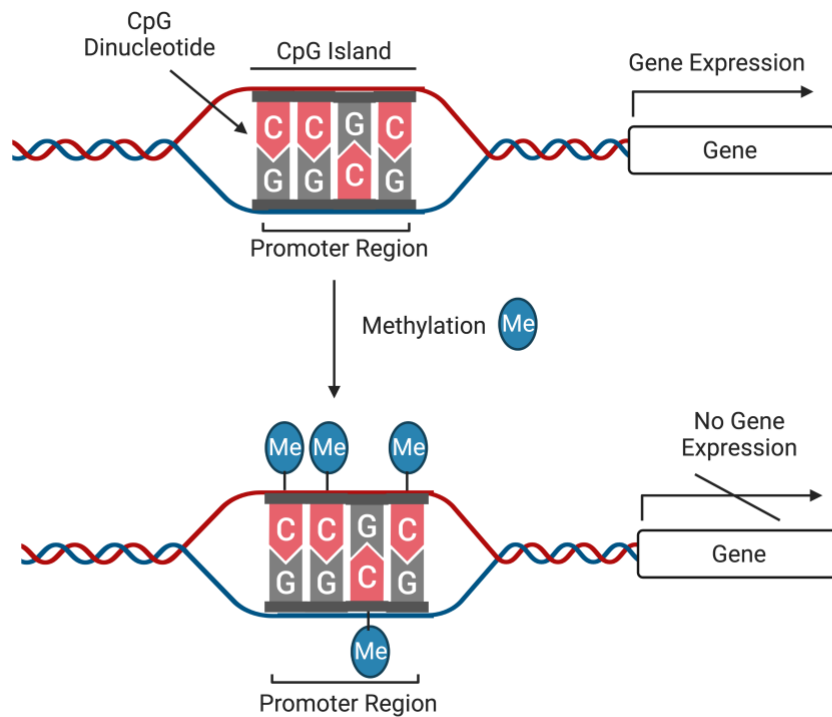
Figure 1.2.1 Methylation of CpG Sites Represses Gene Transcription

The addition of a methyl group to the cytosine of a CpG dinucleotide located on a CpG island situated on the promoter region of a gene results in transcriptional repression and so the gene is no longer expressed [14, 29, 30].

1.2.3 Epigenetic Clocks

With the recognition of epigenetic alterations as a hallmark of ageing came the development of epigenetic clocks; tools that are currently regarded as the most accurate estimators of biological age [1, 8, 10, 13]. It has been shown that a number of CpG sites become either hypomethylated or hypermethylated with age [31]. By measuring specific CpG methylation sites and using computational algorithms to analyse this data, epigenetic clocks can be modelled for human samples that estimate the approximate age of the sample donor. A number of clocks have been described to date, each with their unique advantages and disadvantages. These include, but are not limited to, Horvath's clock [31],

Hannum's Clock [32], Levine's PhenoAge clock [9], Lu's GrimAge clock [10] and *ELOVL2* methylation clocks [12, 33].

The first of these clocks to have been described, so called first generation epigenetic clocks, were Hannum's blood clock and Horvath's multi-tissue clock in 2013 [31, 32]. While Hannum's clock was mathematically derived from a total of 79 specific CpG sites in human blood, Horvath's clock measures a set of 353 CpG sites in human tissue chosen using a penalized regression model using a transformed version of chronological age as an outcome measure. Unlike Horvath's clock, as Hannum's clock was developed on human blood samples it is highly influenced by changes in blood cell composition. Importantly, these clocks were able to identify outliers of biological age i.e., individuals whose epigenetic age diverged from their chronological age. With this, epigenetic age acceleration (EAA) could be measured as the difference between the epigenetic age of an individual and their corresponding chronological age and importantly this difference was shown to be an accurate marker of mortality risk.

With the aim of increasing the ability of epigenetic clocks to detect morbidity and mortality, second generation clocks were constructed including Levine's PhenoAge clock and the GrimAge clock [9, 10]. Both use novel two-step approaches to epigenetic clock modelling involving the incorporation of DNA methylation-based markers associated with factors of morbidity and mortality. Both of these second generation clocks have been shown to correlate much more strongly with mortality, multi-morbidity and health span in comparison to the first-generation clocks making them extremely useful in the risk assessment of many diseases [9, 10].

Although the above clocks are well utilized in the world of biological ageing research, they do require extensive sequencing of the entire genome making it quite a costly venture with complex analysis. With this in mind, the creation of a single gene epigenetic clock has been a highly investigated avenue which could allow for a much more widespread implementation of epigenetic ageing analysis with potential diagnostic value.

ELOVL2 is a protein-coding gene that codes for an enzyme involved in the long-chain fatty acid elongation cycle, therefore acting as a master regulator of polyunsaturated fatty acids [34]. Interestingly, the methylation status of *ELOVL2* has been shown to be one of

the most powerful methylation predictors of not just chronological age, but also biological age [12, 35, 36]. Several studies have noted an overall hypermethylated state of *ELOVL2* with age, corresponding to decreased gene expression and this decreased expression has recently been reported to contribute to the ageing phenotype, including mitochondrial dysfunction, cellular senescence, and stem cell exhaustion [12, 34-36]. With this in mind, epigenetic clock models have been created based off the methylation status of a small numbers of CpG sites surrounding the promoter region of *ELOVL2* alone. This allows for biological age estimations of human samples through the analysis of a single gene marker, making for a much more feasible and accessible means of calculating biological ageing [12, 33].

Due to these clocks being excellent predictors of morbidity and mortality they are extremely useful tools in the risk assessment of older individuals. These clocks are now being exploited to predict multi-morbidity, premature mortality, risk of disease progression/relapse and the effects of age-reversal drugs [37-39]. However, several questions regarding the feasibility of these clocks as biomarkers of ageing and disease remain, specifically regarding the effect of pharmacological treatment on epigenetic clock measures. Sehl *et al.* investigated the effects of radiotherapy and chemotherapy on the epigenetic ageing profiles of breast cancer patients. Interestingly they found that epigenetic age acceleration significantly increases post-treatment, and this may be a result of increased cellular senescence, however, the long-term effect that this has on patients remains to be determined [40]. On the other hand, Fahy *et al.* looked at the effect that drug administration has on DNAm epigenetic ageing in healthy individuals, publishing one of the few papers to suggest the possibility of age reversal by pharmacological intervention [37]. This paper outlined the results of the TRIIM (Thymus Regeneration, Immunorestoration and Insulin Mitigation) trial, a study aimed to investigate the possibility of using recombinant human growth hormone (rhGH) in combination with dehydroepiandrosterone (DHEA) and metformin to reverse signs of immunosenescence in healthy older males. They concluded that the administration of these drugs resulted in increased predicted human lifespan based on DNAm epigenetic age estimators. However, it is worth noting that results varied depending on the DNAm clock model used and only the GrimAge predictor showed a persistent effect post-treatment [37]. Both of these studies show contrasting results in response to various drug treatments, but both have highlighted a potential role for immune modulation in the mediation of the changes.

1.3 The Immune System

It comes as no surprise that both health span and biological ageing are highly associated with immune system changes. Our immune system can be broadly categorised into innate and adaptive immunity with specialised immune cell types associated with each [41-43]. The innate immune system, which includes neutrophils, eosinophils, monocytes/macrophages, natural killer (NK) cells and dendritic cells, is the initial detector and responder of threats and rapidly initiates and propagates inflammatory responses [41, 42]. The adaptive immune system on the other hand, which includes T and B lymphocytes, is largely thought of as a far more specialised and targeted defence mechanism and is responsible for the generation of long-term protective immunity against pathogens. It requires innate immune signals, antigen presentation and time to initiate this response (Table 1.3.1) [41, 43].

Table 1.3.1:

Cell Type	Function	Percentage of Leukocytes in Adult Peripheral Blood	Phenotypic Identifiers
Innate Immune Cells			
Monocyte	• ROS production • Cytokine production • Antigen Presentation • Differentiation into macrophages and dendritic cells	2-10%	CD14+, CD16, CD11b+
Macrophage	• Phagocytosis • Antigen Presentation • Cytokine Production	Variable	CD14+, CD11b+, HLA-DR+
Neutrophil	• NETosis • Phagocytosis • Degranulation - enzyme, proteases and cytokine release • Chemotaxis • ROS Production	40-70%	CD15+, CD66B+
Eosinophil	• EETosis • Degranulation • ROS Production • Chemotaxis	0.5-5%	CD11B+, CD62L+, SIGLEC8+
Dendritic Cell	• Phagocytosis • Antigen Presentation • Cytokine Production	1-2%	CD11c+, HLA-DR+ (Markers dependent on dendritic cell subtype)
NK Cell	• Cell killing (pathogens, infected and cancerous cells etc.) via cytokine, granzyme and perforin production	10-30%	CD56+ CD3-
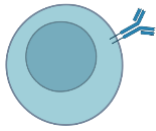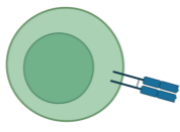
Adaptive Immune Cells			
B Cell	• Antibody production • Immune memory • Cytokine/chemokine production	5-10%	CD19+
T cell	• Cytotoxicity • Regulation and homeostasis of immune response • Cytokine/chemokine production • Immune memory	20-60%	CD3+ CD4+ CD8+ (Markers are dependent on T cell subtype)

Table 1.3.1: Cells of the Immune System

The name, function, frequency in the peripheral blood and common phenotypic markers of primary immune cells of both the innate and adaptive immune systems [14, 41-45].

1.3.1 Immune cells

Neutrophils

Neutrophils are the most abundant immune cell type in peripheral blood, accounting for up to 70% of total leukocytes [45]. They are thought to be short lived multi-lobed cells, with a half-life of only a few hours, however, reports of longer-lived neutrophils have recently been published [46]. Neutrophils represent a heterogenous population of cells with phenotypic and functional diversity in both homeostatic and disease settings [47]. Their primary function is in the protection against and killing of invading microbes and they deploy multiple mechanisms to carry this out. Cytoplasmic granules are key to this function, and, in the case of a neutrophil, three subtypes of granules exist each of which are comprised of various enzymes and proteins: azurophilic (primary) granules, specific (secondary) granules and gelatinase (tertiary) granules. One way in which a neutrophil can protect against invading pathogens is through phagocytosis, a process through which a microbe is sensed, tracked and engulfed by the cell. Once engulfed, the pathogen is transported to the azurophilic granules where it is destroyed by antimicrobial enzymes, proteins and the alkaline environment. Neutrophils can also degranulate, during which the neutrophilic granules are sequentially released, often into a phagosome to prevent host cell damage, facilitating the killing of any microbes as well as stimulating further immune

and inflammatory responses [48]. Additionally, neutrophils can undergo NETosis, a specialised form of programmed cell death in which nuclear chromatin condenses and fuses with the granules to form a net-like structure known as a neutrophil extracellular trap (NET). These NETs are expelled from the neutrophil into the extracellular space where it is capable of physically trapping pathogens for future phagocytosis as well as directly killing and degrading pathogenic components via granular enzymes and proteins [48-50]. Finally, neutrophils also release chemokines, cytokines and reactive oxygen species (ROS) further propagating inflammation at the sites of infection and recruiting and activating other immune cell types [48].

Monocytes

Monocytes are mononuclear myeloid cells that make up approximately 10% of leukocytes in peripheral blood [45]. These cells are derived from bone marrow precursors which enter the circulation where they can migrate to specific tissues and organs and differentiate further into macrophages or dendritic cells. Monocytes function primarily in host defence, being major stimulators of innate inflammation through the production and release of both pro- and anti-inflammatory cytokine, chemokines and reactive oxygen species. Monocytes are also capable of clearing infections through phagocytosis and have roles in homeostasis and wound healing as well as in the activation of the adaptive immune response through antigen presentation [51, 52]. Three subtypes of monocytes are recognised based on the expression of the FcγIII receptor CD16: classical monocytes (CD14++CD16-), intermediate monocytes (CD14++CD16+) and non-classical (CD14+CD16++). These subsets have been shown to be both phenotypically, transcriptionally and functionally distinct [52].

Eosinophils

Eosinophils, along with neutrophils, are a subpopulation of multi-lobed granulocytes that accounts for less than 5% of leukocytes in the peripheral blood [45]. They are derived in the bone marrow where they rely on IL-5 to regulate their maturation and differentiation. Similar to neutrophils, they are thought to have a very short half-life of just a few hours in peripheral blood, however, can survive as tissue resident cells for several weeks [53]. Very like neutrophils, eosinophils contain granules that are vital for their function. Eosinophilic cytoplasm's are thought to possess approximately 200 granules each containing numerous proteins including but not limited to major basic protein, eosinophilic derived endotoxin, eosinophilic cationic protein and eosinophil peroxidase

which mediate pathogen killing through degranulation and eosinophilic extracellular trap (EET) formation. Although less abundant than neutrophils, eosinophils are larger cells that are capable of releasing and producing multiple cytokines and chemokines, making them a crucial initiator and propagator of the innate immune response [53, 54]. Their primary function is in the protection against multi-cellular parasites such as helminths however they are also involved in the proliferation, activation, and differentiation of T cells [53].

T Cells:

T cells are specialised lymphocytes of the adaptive immune system that originate in the bone marrow and mature in the thymus where they are trained to express unique T cell receptors that recognise specific antigens. Multiple subsets of T cells have been described to date including the classical subsets CD4+ helper and CD8+ cytotoxic as well as other subsets that include natural killer, innate-like and γδ T cells. CD4+ T cells can also be further categorised into subsets that include Th1, Th2, Th17 and Treg cells, each of which are associated with specific immune responses. The main functions of T cells are in the direct killing of pathogen infected host cells, the production of cytokines to further induce inflammation and also to regulate the immune response ensuring both the production of inflammation but also the resolution of this when needed in order to prevent tissue damage [43, 45].

B Cells:

B cells are specialised cells of the adaptive immune system that are produced in the bone marrow and migrate to secondary lymphoid organs (e.g. the lymph nodes and spleen) where they undergo functional maturation [43, 45]. Their primary function is to produce specialised antibodies that are capable of recognising and targeting hundreds of thousands of specific antigens. This incredible repertoire is possible through the functional rearrangement of the B cell receptor, (VDJH and VJL rearrangement), antigen-induced clonal expansion, class switch recombination (CSR) at the IgH locus, somatic hypermutation (SHM) of V_H genes, and selection for increased affinity of a BCR for its unique antigenic epitope through affinity maturation [55]. B cells are also capable of differentiating into memory B cells following an encounter with a pathogen. Memory B cells can persist in the circulation for years following an initial encounter with a pathogen. Upon reinfection with the same pathogenic antigen, memory B cells are capable of rapid

proliferation and the production of specific antibodies targeting this pathogen, resulting in swift pathogenic elimination, often before any inflammation arises [56].

1.3.2 Inflammation

The generation of inflammation is a critical aspect of the immune response to biological threats and the detection of such stimuli leads to the rapid production and release of various inflammatory mediators such as cytokines and chemokines by surrounding cells [57]. Inflammatory cytokines are initially produced following activation of the innate immune system, which can respond to pathogen derived signals (pathogen associated molecule patterns; PAMPs) such as lipopolysaccharide (LPS), peptidoglycans [58] and N-formyl-methionyl-leucyl-phenylalanine (fMLP) [59], as well as to signals of danger (danger associated molecule patterns; DAMPs), which include cholesterol crystals, uric acid crystals and other cellular components, such as DNA, leaked into the extracellular environment during tissue damage and necrosis [57, 60]. These PAMPs and DAMPs are sensed by conserved innate immune receptors, known as pattern recognition receptor (PRRs), that are expressed on both immune and non-immune cells. A number of pattern recognition receptors have been described to date including but not limited to Toll-like receptors (TLRs), NOD-like receptors (NLRs) and RIG-1-like receptors (RLRs). Binding of ligands to these receptors results in the activation of specific cell signalling cascades which leads to the activation of two main signalling pathways: (i.) the transcription factor NFκB pathway and (ii.) the interferon regulatory factor (IRF) transcription pathways (Table 1.3.1) [60-62]. While activation of the NFκB pathway generally regulates the gene expression of inflammatory cytokines such as IL-6, IL-1β and TNF-α, the IRF transcription pathways, particularly IRF3 and IRF7, leads to the induction of type I and III IFNs (Figure 1.3.1) [63, 64]. These IFNs subsequently activate a broad anti-viral response in the body and their ability to activate and regulate other immune cells is a crucial step in activating adaptive immune responses required for induction of long-term protective immunity against a pathogen, including in the context of vaccination. Under homeostatic conditions these inflammatory processes are tightly regulated often through complex negative regulatory pathways allowing for the appropriate resolution of any inflammation once the threat has been removed [63, 65].

Figure 1.3.1:
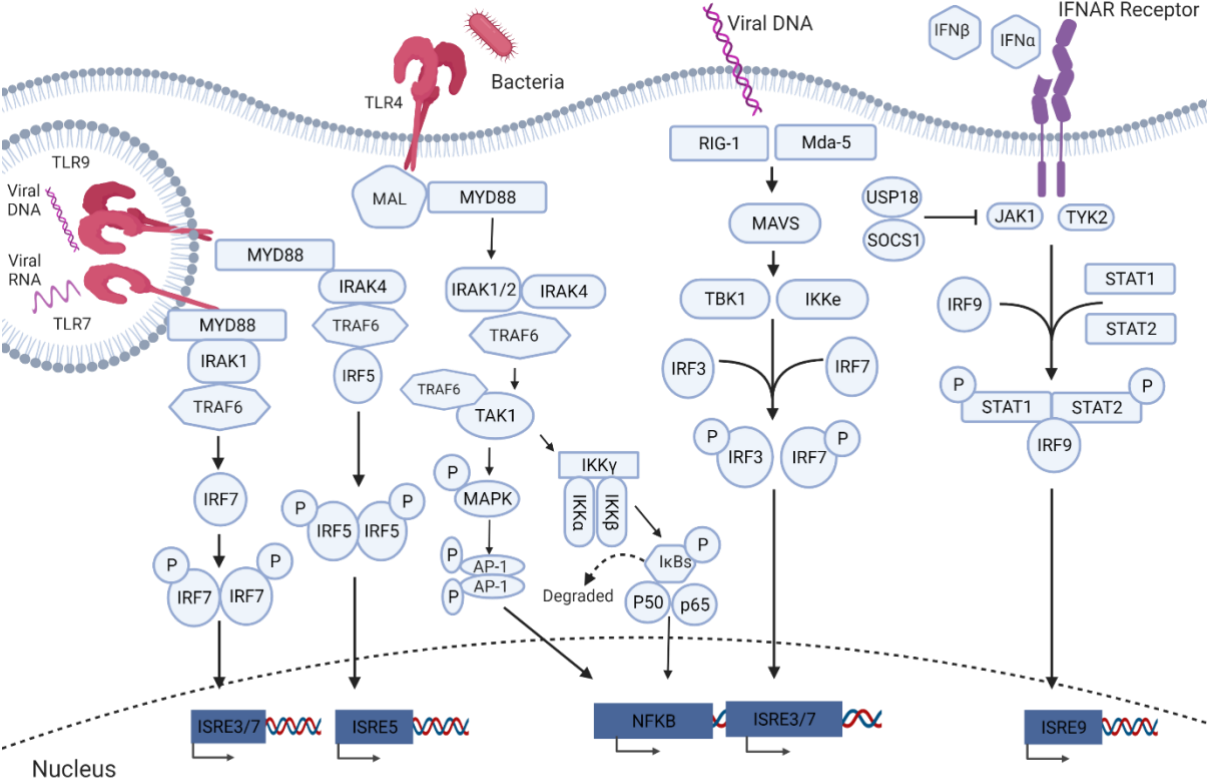
Figure 1.3.1 NFκB and IRF Transcription Signalling Pathways [14].

1.4   Immune Changes with Age

Ageing can cause alterations to the function of all immune cell types, often putting older individuals at greater risk of infection and disease (Table 1.4.1)[66]. Two major ageing immune phenotypes that have emerged as being strongly linked to health and disease as we age are inflammageing and cellular senescence.

1.4.1   Inflammageing

A failure to adequately control and resolve inflammatory responses can lead to tissue destruction and poor health outcomes [41]. As the human body ages, there is a propensity for low-level inflammatory responses to be chronically activated, a phenomenon known as "inflammageing" [67]. Multiple factors have been implicated in the development of inflammageing including long-term exposure to various antigens, adaptations to stress signals, changes in metabolic function, microbiome alterations and accumulation of cellular debris [68-73] and although much remains unknown regarding the molecular mechanisms that regulate inflammageing, it is clear that inflammageing plays a major role in the development and pathophysiology of age-related diseases. Hallmarks of inflammageing include elevated systemic levels of pro-inflammatory cytokines and acute-phase proteins, such as IL-6, TNF-α and CRP [6, 74]. Indeed many human studies on ageing have focused on these proteins as markers of inflammageing as their expression is elevated and often predictive of disease incidence in many ageing associated conditions such as frailty [67, 75], cardiovascular disease (CVD) [67, 76, 77], neurocognitive impairment [78, 79], cancer [80] and diabetes [81, 82]. How exactly the activation of a baseline pro-inflammatory state, like inflammageing, results in morbidity remains a topic of much research and seems to have various roles depending on the specifics of the disease. While multiple studies have suggested a heightened and overactive immune response to certain stimuli in older individuals [83], several studies have also shown that this chronic inflammation leads to a condition of refractory immune signalling meaning that when these vital innate immune pathways are slightly activated, they cannot be activated further to their full extent when needed [84]. A study by Shen-Orr *et al.* for example, found that in people with higher baseline inflammatory cytokines, many important immune cell types were unable to activate JAK-STAT signalling, an intracellular signalling pathway, to the same extent as people with lower baseline

inflammatory status. This chronic inflammation, quantified using a cytokine response scoring method, was shown to be clinically associated with markers of diastolic dysfunction and atherosclerosis, implicating increased basal inflammation as a causative factor of cardiovascular disease [85]. Interestingly, many hallmarks of ageing have been shown to contribute to this phenomenon of inflammageing, in particular, increased cellular senescence.

1.4.2 Senescence and inflammation

Senescence describes a cellular state in which the cell has lost long-term proliferative capacity yet does not undergo apoptosis and is still metabolically active [86]. It occurs in response to a number of triggers including cellular stress or DNA damage and has been reported to have important roles in processes such as embryogenesis, wound healing and ageing and their clearance has been shown to promote pathology such as fibrosis and pulmonary hypertension (Figure 1.4.1) [86-89]. Although cellular senescence is a part of normal homeostasis, protecting against afflictions such as cancer and fibrosis, the accumulation of these cells over time is thought to contribute to the process of inflammageing and the development of age-related morbidity and mortality through the loss of cell function [86, 87]. Several studies have demonstrated the negative impact of senescent cell accumulation with age. For example, Xu et al. showed that the transplantation of senescent cells into healthy mice results in decreased lifespan compared to controls leaving them more susceptible to frailty and tissue dysfunction [90]. Elevated numbers of senescent cells along with increased rates of cellular senescence are noted in humans that have been diagnosed with conditions associated with an accelerated ageing phenotype such as down syndrome [91] and progeria [92]. Human genome-wide association studies have also shown that variations in the INK4/ARF gene locus, which encodes for several key effector molecules of cellular senescence, correlate with increased susceptibility to diseases such as cancer and cardiovascular disease, suggesting a major role for these cells in age-associated disease [93, 94].

A number of these senescent cells can take on an altered secretory phenotype, termed senescence-associated secretory phenotype (SASP) resulting in the production and release of various inflammatory cytokines, chemokines, growth factors and extracellular matrix proteases, thus strongly linking the accumulation of these cells with the inflammageing phenotype [90, 95]. The effect of removing/minimising the secretory

capacity of these cells is currently an area of huge research with several senolytic and senomorphic therapies being investigated in both mice and humans [90, 96-98].

Figure 1.4.1:
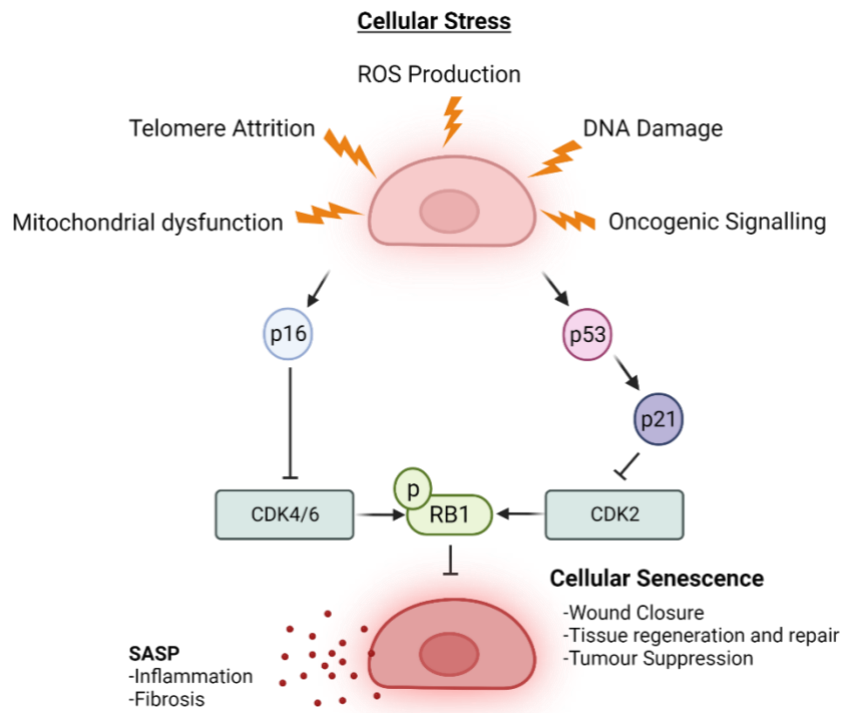
Figure 1.4.1: p16 and p53 mediated cellular senescent pathways [14].

1.4.3   Immunosenescence

Immunosenescence refers to the functional decline of the immune system with age leading to the reduced ability to respond to new antigens and an increased susceptibility to infection and disease. Both Inflammageing and cellular senescence contributes to this phenomenon [99]. Although both innate and adaptive immune responses are affected (Table 1.4.1), due to their role in antigen specific responses, changes in T cell and B cell immunity with age are often regarded as the key drivers of this process.

A major feature of immunosenescence is the reduction of naïve T cells accompanied by the accumulation of memory or memory-like T cells [99, 100], a phenomenon that is partially explained by thymic involution which begins at puberty but increases exponentially later-in-life with only trace amounts of functional thymic tissue reported to remain in individuals over 70 [101]. This also results in the reduced ability to respond to new pathogens and a shrinkage of the T cell receptor repertoire over time. Furthermore,

chronic and repeated exposure to pathogens such as human cytomegalovirus and influenza virus results in the clonal expansion and proliferation of late-differentiated effector T cells that often exhibit features of replicative senescence again culminating in an overall change in the T cell profile of aged individuals and contributing to inflammageing [100]. T cells play a central role in modulating protective versus tolerogenic outcomes in response to antigens. The accumulation of cellular damage with age is also accompanied by the increased circulation of self-antigens such as circulating DNA which can contribute towards the breakdown of T cell tolerance with age. Breakdown in T cell tolerance has been reported to contribute towards immune activation, chronic inflammation and the development of autoimmunity [102].

B cell numbers can also decrease with increasing age as well as experience shifts in subset abundances; decreased mature, naive B cell frequencies with increased memory B cell frequencies [103]. As a result, a loss of B cell receptor diversity has been consistently reported in older individuals having implications on B cell activation and antibody production [104, 105]. While somatic hypermutation appears to remain unchanged in B cells with age, decreased B cell isotype switching occurs. This results in decreased antibody specificity and effector functions leading to a weakened ability to recognise and respond to new antigens and a decreased ability to distinguish self-antigens [106]. Similarly, to T cells, an increased propensity towards cellular senescence is seen with age in B cells contributing to the decline in B cell function and overall immunodeficiency.

All of these immune changes leave older individuals more susceptible to both infection and disease. Age-associated changes to both the innate and adaptive immune system are also associated with the development of autoimmunity and autoimmune disease.

Table 1.4.1:

Innate Immune Cells	Dysregulation with Age
Monocyte	• Become major producers of the pro-inflammatory cytokines such as TNFα contributing to a state of inflammageing [107].
Macrophage	• Shifts in macrophage polarization [108, 109] • Reduced/altered function; chemotaxis, phagocytosis, ROS production, signal transduction, apoptosis, antigen recognition and presentation, cytokine production etc [110] • Impaired autophagy and mitophagy [111]
Neutrophil	• Increased numbers [112] • Reduced function; chemotaxis, phagocytosis, ROS production, signal transduction and apoptosis [113, 114] • Increased production of neutrophil extracellular traps [112]
Eosinophils	• Decreased response to activation signals resulting in decreased degranulation and decreased ROS production [115]
Dendritic Cell	• Reduced/altered function; co-stimulatory molecule expression, cytokine production, antigen presentation, TLR-mediated signalling, chemotaxis and endocytosis [116, 117]
NK Cell	• Changes in subset abundances; increased CD56^{dim} CD16+ cells and decreased CD56^{bright} CD16- subsets which results in elevated cytokine production and cytotoxic granule release as well as decreased dendritic cell maturation, monocyte activation and T cell differentiation [118-120] • The accumulation of senescent NK cells indicated by CD57 expression [120] • Decreased NK cell activity on a per cell basis, reduced expression of NK cell receptors leading to decreased cell recognition and killing, and decreased production of cytokines and chemokines [117, 121]
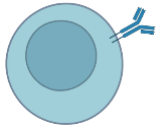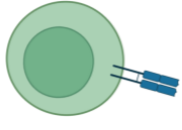
Adaptive Immune Cells	
B Cell	• Decreased Naïve B cells, IgM and IgD serum levels [99, 103] • Increased memory B cells, ABCs, IgG and IgA serum levels [99, 103] • Restricted BCR repertoire, reduced class-switch recombination and AID expression [104] • Reduced antibody production [122, 123]
T cell	• Decreased naïve T cells and TCR diversity [101, 124, 125] • Altered T cell subset proportions often leading to reduced antigen recognition and response [100, 126] • Altered activation, differentiation and cytokine production [101, 127]

Table 1.4.1: Changes in Immune Cell Profiles with Age [14].

1.5 Ageing and Autoimmune Disease

Autoimmunity refers to the presence of antibodies, B cells and T cells that target self- or auto-antigens. Although autoimmunity is common, with many healthy individuals having some levels of autoantibodies present within their systems, these autoantibodies and autoreactive T cells can become pathogenic and result in damage to healthy tissues and organs, a feature that characterises an autoimmune disease [128, 129]. Just over 80 distinct autoimmune diseases have been described to date with an estimated prevalence of about 3-5% worldwide. Interestingly, a clear sex bias has been noted in many autoimmune conditions, with females having an overall three-fold higher risk of autoimmune development compared to males [130, 131]. Although most forms of autoimmune disease develop in early to mid-adulthood, between the ages of 16 and 45, various autoimmune diseases have shown a later age of onset including diseases such giant cell arteritis, autoimmune pancreatitis, autoimmune thyroiditis, and ANCA-associated vasculitis [130, 132, 133]. The reasons behind a later-in-life development for autoimmune disease is an area of great interest and the effect that later life age-of-onset has on disease outcome remains under-explored.

Many of the molecular changes associated with age are thought to contribute to the development of age-associated autoimmunity and autoimmune disease. Several hallmarks of ageing have been shown to occur in patients with autoimmune disorders compared to healthy controls including genomic instability, epigenetic alterations, mitochondrial dysfunction, loss of proteostasis and cellular senescence [134-136]. Patients with age-related systemic lupus erythematosus for example, a systemic autoimmune disease with varied clinical manifestations and pathogenesis, have shown significant epigenetic alterations and genomic instability while rheumatoid arthritis patients, an autoimmune disease characterised by inflammation of the joint tissue, is accompanied by a loss of proteostasis and increased cellular senescence compared to healthy controls [26, 136-139].

Age related changes in both the innate and adaptive immune system are known to contribute towards the development of autoimmune diseases later-in-life. Inflammageing for example, is thought to prime cells for activation in the absence of a known threat. Monocyte, macrophage, NK cell and neutrophil impairments with age have been shown

to contribute towards an inflammatory environment characteristic of autoimmune diseases (Table 1.4.1). Dysregulated autophagy, mitophagy and phagocytosis as well as impaired APC signalling by monocytes, macrophages and dendritic cells with age are also thought to increase autoreactivity and autoantibody production in older individuals [110, 140]. The prevalence of autoantibodies and autoreactive T cells increases with age, a feature thought to be largely driven by cellular senescence and immunosenescence [141, 142]. Older individuals show increased levels of self-antigens such as circulating DNA due to increased cellular senescence and cell death. These increased autoantigen levels promote the production of autoantibodies and autoreactive T cells [143-145].

Although the links between ageing and autoimmunity are beginning to emerge, very little research is done regarding the role of age in the development of many of these diseases, including ANCA-associated vasculitis.

1.6 ANCA Associated Vasculitis

Anti-neutrophil cytoplasmic autoantibody (ANCA)-associated vasculitis (AAV) is a group of relapsing-remitting systemic autoimmune disorders characterised by severe inflammation of the small blood vessels and surrounding organs [146]. AAV is a rare disease, with a reported annual incidence of 4.6-18.4 cases per 100,000 individuals, dependent on location [133, 147, 148]. Although rare, it is extremely life-threatening, with a 1-year mortality rate of >80% if left untreated, dropping to about 20% following treatment; rates that make clear the need for further research into this disease [149].

Three forms of AAV are recognised, each of which are associated with different clinical presentations: microscopic polyangiitis (MPA), granulomatosis with polyangiitis (GPA) and eosinophilic granulomatosis with polyangiitis (EGPA). Although all three classify as AAV based on small vessel inflammation and the common presence of ANCAs, each subtype is histologically and immunologically distinguishable [146, 150]. GPA and EGPA show granuloma formation compared to MPA and while EGPA is largely an eosinophil driven disease, often accompanied by asthma and allergy responses, GPA and MPA are predominantly thought to be neutrophil driven. Genetic and epigenetic variation between each subtype has also been reported and various responses to multiple treatments have been observed [135, 151]. While GPA is most commonly associated with autoantibodies that target PR3 proteins (anti-PR3 ANCA), MPA and EGPA often show positivity for autoantibodies against MPO (anti-MPO ANCA)(Table 1.6.1)[146, 150].

Table 1.6.1:

	GPA	**MPA**	**EGPA**
Pathology	Necrotising granulomatous inflammation effecting small to medium blood vessel (e.g., capillaries, venules, arterioles and arteries)	Necrotising vasculitis predominantly effecting small to blood vessel (e.g., capillaries, venules, and arterioles)	Necrotising granulomatous inflammation effecting small to medium blood vessel (e.g., capillaries, venules, arterioles and arteries)
Granuloma Formation	Yes	No	Yes
Immune Cells involved	Neutrophil Driven	Neutrophil Driven	Eosinophil Driven
Asthma and eosinophilia	No	No	Yes
ANCA specificity	Commonly associated with anti-PR3 ANCA (80-90% of cases)	Commonly associated with anti-MPO ANCA (70-80% of cases)	40% of cases have anti-MPO ANCA
ANCA Staining pattern	c-ANCA	p-ANCA	p-ANCA
Systems commonly affected	Respiratory tract, renal system, skin and rarely the PNS	Respiratory tract, Renal system, skin and rarely the PNS	Respiratory tract, circulatory system including heart, renal system, skin and PNS
Geographic Distribution	Most common in Northern Europe and America	Most common in Southern Europe and East Asia	Most common in Europe and America but extremely rare

Table 1.6.1 AAV Classification: Clinical and immunological characteristics of GPA, MPA and EGPA.

Although there are currently no curative measures for the treatment of AAV, remission is often induced and maintained through the use of various immunosuppressive agents. Cyclophosphamide (cyclo) and rituximab (ritux) are two of the most commonly prescribed remission induction therapies for these patients [152]. Cyclophosphamide is a DNA alkylating agent that has been in clinical use for over 40 years, revolutionising the treatment and survival outcomes of AAV patients. It targets and inhibits the cell cycle,

preventing cellular proliferation, including that of immune cells, resulting in the non-specific systemic reduction of inflammatory responses [153, 154]. Rituximab on the other hand, gained approval for the treatment of AAV over a decade ago and has been noted to induce remission in AAV patients both on its own and in combination with other treatments [154, 155]. Rituximab is a monoclonal antibody that specifically targets CD20+ B cells, resulting in B cell depletion and a subsequent decrease in ANCA titres and immune responses in AAV patients. Despite drastically improving patient outcomes, both cyclophosphamide and rituximab can have various adverse effects on these patients and indeed the leading cause of death in treated AAV patients are treatment related complications [149, 156].

1.6.1 Immune Cells Involved in AAV

Neutrophils

Neutrophils are consistently reported as key cells involved in AAV development and progression [47, 50, 157, 158]. As the primary sources of MPO and PR3, the most common targets of ANCAs, neutrophils are thought to initiate immune intolerance via autoantigen release to which autoantibodies (ANCA) are produced. Following their production, ANCAs can then work to activate neutrophils resulting in the initiation of a pro-inflammatory response and vascular damage, commencing a positive feedback loop of autoantigen release, ANCA production and neutrophil activation. Activated neutrophils are capable of adhering to vascular endothelial cells and migrating into the vascular wall where they can accumulate and undergo NETosis and degranulation releasing inflammatory cytokines, enzymes, ROS and chemokines. These activated immune cells are also capable of inducing cell apoptosis and tissue lesions resulting in vascular endothelial destruction and substantial tissue damage [50, 157-160]. The importance of these cells in the pathogenesis of AAV has been demonstrated in numerous studies throughout the years. Neutrophils are known to infiltrate the kidneys during active AAV and neutrophil numbers in AAV patients have been shown to associate with AAV pathology and increase with disease severity [158, 161, 162]. As well as this, neutrophils isolated from AAV patients have shown upregulated expression of both MPO and PR3 compared to healthy controls, a feature that correlates with clinical outcomes in these patients [134, 163]. Neutrophils isolated from AAV patients also show increased

activation (degranulation, NETosis, cytokine release etc.) at baseline compared to healthy controls further demonstrating their pro-inflammatory role in AAV [50, 158].

Monocytes

Although extremely important in the maintenance of innate immune responses, chronic and spontaneous activation of monocytes results in damage to healthy tissue and indeed this has been shown to occur in AAV [164, 165]. Although neutrophils are often regarded as the primary innate immune drivers of AAV, monocytes have also been shown to contribute to AAV pathology through the propagation of inflammation. Both *in vivo* and *in vitro* studies show that ANCAs upregulate activation markers such as CD14 and TLR expression on monocytes [165]. Intermediate monocyte populations are increased in AAV patients compared to healthy controls and both MPO and PR3 have been shown to be preferentially expressed on these subsets. Ex vivo stimulation of monocytes with anti-MPO result in pro-inflammatory cytokine production such as IL-1β, IL-6 and IL-8, contributing to the pro-inflammatory environment of AAV [166]. Increased MCP-1 levels, a chemokine involved in monocyte recruitment and activation, has been reported to be elevated in AAV patient kidney biopsies and as such, monocytes and macrophages have been shown to be major infiltrates into the glomeruli of these patients [162, 167, 168]. As well as this, monocytes are thought to have a major impact on adaptive immune cells, in particular T cells during AAV. MHCII molecules are crucial antigen presenting molecules coded by the HLA genes and their expression is increased in monocytes isolated from AAV patients compared to healthy controls, having important effects on autoreactive T cell activation, recruitment and polarisation during active AAV [164, 165].

Eosinophils

Like many other immune cells, eosinophilia and dysregulated eosinophil activation can be harmful to healthy tissue and is highly associated with asthma and allergy as well as other autoimmune conditions including AAV, specifically EGPA [169]. EGPA patients present with eosinophilia and numbers of eosinophils have been shown to correlate with disease activity [162]. Clinical trials for drugs targeting eosinophils in EGPA are currently underway and are showing some success in the treatment of EGPA. Indeed, mepolizumab, a monoclonal antibody that targets IL-5, has become the first approved

drug for the treatment of EGPA that targets eosinophil maturation, activation, and survival [170].

T cells

T cell dysregulation has been noted in almost all known autoimmune diseases including AAV. T lymphocytes have been shown to infiltrate kidney tissues and other affected areas in AAV animal models and patients [162]. Polarisation towards a Th1 and Th17 response is associated with AAV pathology, propagating a pro-inflammatory environment. In addition to this numbers of Tregs are shown to decrease during active AAV and their function declines. The cytokines released by these T cells interact with other immune cells including neutrophils, monocytes and B cells, causing their recruitment and activation, further enhancing endothelial and vascular damage [171, 172].

B cells

With autoantibodies being characteristic features of autoimmune disease, it is no surprise that B cell activity is associated with AAV. B cells produce the autoantibodies ANCA which are found in most cases of AAV and are linked to pathogenicity within these disorders. B cell depletion using the monoclonal antibody rituximab has become a very successful treatment option for AAV patients and has been shown to decrease circulating ANCA titres in these individuals [154, 155]. Despite this, treatment with rituximab increases the risk of severe and chronic infection and may not be a suitable treatment option for all patients.

1.6.2   ANCA

AAV is usually characterised by the presence of autoantibodies, ANCAs, most commonly directed against the proteins myeloperoxidase (MPO) or proteinase 3 (PR3). There are two main immunofluorescent staining patterns of ANCA; one showing cytoplasmic localisation of the staining (c-ANCA) which commonly associates with anti-PR3 and the second being a perinuclear pattern of staining (p-ANCA) which is usually specific to anti-MPO ANCA. While c-ANCA is typically found in GPA patients, p-ANCA is associated more with MPA and EGPA vasculitis. Although very useful diagnostic biomarkers of AAV, the pathogenic role of ANCAs in AAV is still highly debated [173, 174]. Several studies have shown an association between ANCA titres and disease activity supporting

the idea that ANCAs propagate inflammation in AAV [155, 175, 176]. As well as this, rituximab, a monoclonal antibody that results in B cell depletion and decreased ANCA titres, has proven to be an effective treatment for AAV [155]. Furthermore, multiple animal models have been described that require the introduction of ANCAs to induce pathology, again hinting at their involvement in AAV development and progression [177]. In contrast to this however, Finkielman *et al*. reported only very weak associations between ANCA levels and disease activity in a cohort of GPA patients and noted that ANCA titres did not associate with time to remission or relapse [178]. As well as this, not all AAV patients show ANCA positivity. It has been reported that c-ANCA are present in 80-95% of new-onset GPA patients and p-ANCA in 70-80% of newly diagnosed MPA patients and only 30-40% of EGPA patients. However, it is worth noting that, particularly with EGPA, patients that are ANCA positive have a higher risk of granuloma formation and renal involvement compared to those without, hinting at a pathological role for these autoantibodies [179]. Additionally, ANCAs have been reported to occur in several diseases other than AAV as well as in about 5% of the healthy population, leaving their precise pathophysiological mechanism in AAV still to be determined [180, 181].

One commonly accepted hypothesis for the role of ANCA in AAV is that an underlying disorder such as an infection results in the release of pro-inflammatory mediators, which bring MPO and PR3 to the surface of circulating neutrophils and monocytes. ANCAs bind with these now exposed FCγ receptor targets, resulting in immune cell activation, inducing a rapid onset pro-inflammatory response which damages endothelial cells and causes tissue injury [182](Figure 1.6.1).
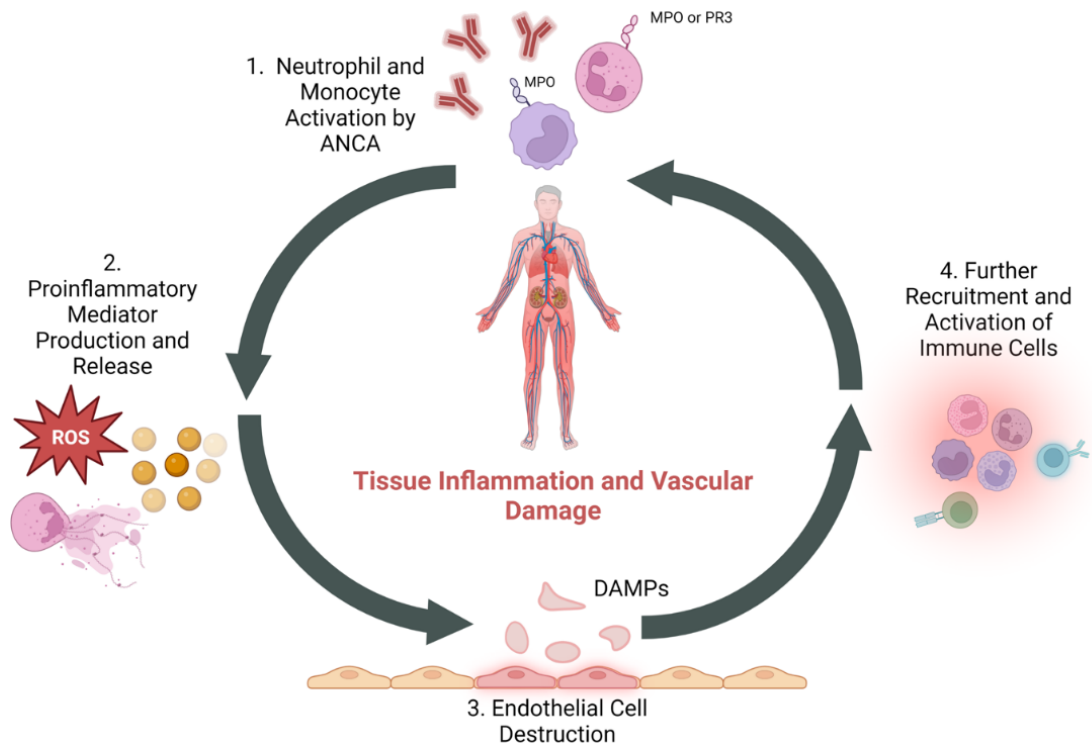
Figure 1.6.1 Depiction of the immunopathology of AAV:

1. Following an unknown priming event, the neutrophilic proteins MPO and PR3 migrate to the surface of neutrophils and monocytes allowing autoantibodies (ANCA) to bind, causing cellular activation. 2. This activation results in the release of pro-inflammatory cytokines and chemokines, reactive oxygen species release and NETosis production. 3. This pro-inflammatory onslaught causes severe damage to the endothelial cells of surrounding blood vessels releasing DAMPs into the circulation. 4. Both the pro-inflammatory response and chemokines produced as well as the DAMPs released by dying cells works to attract other immune cells to the site of inflammation, primarily monocytes, which are capable of migrating through the endothelium, maturing into macrophages and becoming major producers of pro-inflammatory cytokines such as TNFα and IL-1β [14].

Although the precise role of ANCA in AAV is still unknown, a clear distinction can be seen between anti-MPO ANCA patients and anti-PR3 ANCA patients. Current research often categorises AAV solely by GPA, MPA and EGPA status, however, arguments have been made to categorise these patients further based on ANCA subtype, particularly during clinical trials and treatment reception [152, 183]. Although clinically similar in terms of histopathology and clinical outcomes, anti-MPO mediated AAV and anti-PR3

mediated AAV show differences in pathophysiology, genetic and epigenetic signatures, demographics, aetiology, clinical presentations etc. [134, 135, 151, 184, 185] [186]

1.6.3   Anti-MPO AAV versus Anti-PR3 AAV

MPO is a heme protein typically found within the azurophilic granules of a neutrophil and plays an important role in the maintenance of an alkaline environment within these granules as well as in the protection against microbes during degranulation and NETosis [187]. Although generally found within the cell, priming of a neutrophil with stimuli such as TNFα can bring MPO to the surface where it may act as an adhesion molecule and promote cellular activation through the binding of anti-MPO ANCA [188]. PR3 on the other hand is a serine protease that plays an important role in protein degradation both intracellularly and extracellularly. Similar to MPO, PR3 can be found within the azurophilic granules of neutrophils, however in contrast to MPO, PR3 has also been shown to be constitutively expressed on the cell surface, an observation that may contribute to the production of anti-PR3 ANCA and allows the interaction between PR3 and anti-PR3 antibodies resulting in cellular activation [189]. Despite being less commonly investigated, MPO and PR3 are also expressed on the surface of monocytes and binding of ANCAs to these targets results in oxygen radical production and the release of pro-inflammatory cytokines such as IL-8 [166]. Although overall, a higher incidence rate of AAV is noted in males compared to females, the male-to-female ratio is higher in anti-PR3 AAV compared to anti-MPO AAV [186]. Anti-PR3 AAV patients also show a higher frequency of granulomatous lesions, respiratory involvement, and a higher risk of relapse compared to anti-MPO patients [174, 185]. Despite this, anti-MPO patients often show greater renal involvement and worse renal outcomes compared to anti-PR3 patients, a greater risk of cardiovascular events and an overall worse prognosis [184, 185]. Finally, several genetic and epigenetic factors have been associated with the presence of each autoantibody. Notably, while polymorphisms within the HLA gene region represents the biggest genetic risk factor of AAV, polymorphisms at distinct regions are associated with ANCA specificity. While polymorphisms in the HLA-DPB1 locus shows a strong association with anti-PR3 AAV, HLA-DQA and DQB1 polymorphisms show a stronger association with anti-MPO AAV [135, 151]. In terms of epigenetics, most epigenetic studies to date have focused on the genes encoding the MPO and PR3 proteins, *MPO* and *PRTN3* respectively. A recent study by Jones et. al showed that DNA methylation around

these 2 genes was lower in active AAV patients compared to patients in remission and healthy controls and that this correlated with levels of circulating ANCA. As well as this, remission patients with higher methylation levels surrounding the *PRTN3* gene showed prolonged relapse-free periods while those with lower methylation levels surrounding this gene showed a greater risk of relapse. The same observation was not noted with regards to the methylation of *MPO*. Interestingly these findings were independent of ANCA serotype in patients (Table 1.6.2) [134].

Table 1.6.2:

	Anti-MPO ANCA	**Anti-PR3 ANCA**
AAV Subtype Association	MPA and EGPA	GPA
Male: Female Ratio	0.3-1	1-1.9
Age at diagnosis	Often within the 6th-7th decade of life	Often within the 5th-6th decade of life
Immunofluorescent Staining Pattern	P-ANCA	C-ANCA
Pathology	Worse renal outcomes and higher morbidity	Higher risk of respiratory tract involvement
Genetics	HLA-DQA and HLA DQB1 polymorphism	HLA-DPB1, SERPINA1 and PRTN3 polymorphisms

Table 1.6.2 ANCA Classification. Differences between anti-MPO and anti-PR3 ANCA AAV.

Unusually for an autoimmune disease, AAV tends to develop later-in-life, with an average age of onset reported to be between the fifth and seventh decades of life, however the reasons behind this later-in-life development remain unknown [133, 147, 190]. Ageing is also known to effect the prognosis and outcome for AAV patients, with older patients experiencing increased mortality, end-stage renal failure and treatment-related complications compared to younger AAV patients, highlighting the influence that age has on both disease initiation and trajectory [191]. Of note, although not always the case, several studies have noticed a later age of onset for anti-MPO AAV patients compared to anti-PR3 patients, an observation that our lab have also recognised [184, 186, 192, 193]. Although chronological ageing is widely accepted to be a risk factor for AAV development, biological ageing is yet to be explored in the context of this disease.

Regardless of subtype, early diagnosis and treatment of these disorders is crucial in preventing serious organ damage and death. However, due to a lack of knowledge regarding the underlying biology of this disease, no curative measures are currently available for AAV. Treatment options generally rely on broad immunosuppression using drugs such as corticosteroids which dampen the uncontrolled inflammation. Although these treatments reduce the cell and tissue destruction created by immune dysregulation, the nonspecific nature of these treatments often results in adverse effects and poor outcomes for patients [194]. More specific and targeted treatment options are currently being explored in AAV in order to improve patient outcomes and, with this goal in mind, a better understanding of the specific mechanisms driving this disease is needed [154, 195]. Considering the importance of neutrophils and monocytes in AAV activity, current research often focuses on innate immune responses [50, 157, 196]. Despite this, one aspect of the innate immune response that has received little attention in the context of AAV is type I IFN immunity.

1.7 Interferons and Type I Interferons

Interferons are a family of innate cytokines that were first identified in the 1950's and have long been associated with the anti-viral immune response. Three classifications of interferons have been described to date: type I IFNs which are comprised of numerous subsets (IFN-α, IFN-β, IFN-δ IFN-ε, IFN-ω, IFN-κ and IFN-τ), type II IFNs which only includes IFN-γ and type III interferons of which there are four subtypes (IFN-λ1, IFN-λ2, IFN-λ3 and IFN-λ4)[197].. Together this family of cytokines regulate hundreds of genes and have numerous effector functions. While type I and type III IFNs can be expressed by almost all cell types, type II production is thought to be T cell, macrophage and NK cell specific. Although all members of this family are crucial for efficient immune function, type I IFNs arguably have the most extensive range of immunomodulatory effects [64, 197, 198].

1.7.1 Type I IFNs

Type I IFNs are essential mediators of the innate immune response noted for their anti-viral, anti-proliferative and immuno-regulatory properties [198]. With these cytokines having such essential and diverse roles in immunity, they are equipped with an extensive and complex production and regulatory system. As aforementioned, type I IFNs are formed through various signalling mechanisms involving the recognition of danger signals by specific receptors [199]. For many cells, the most common means of type I IFN production is via the interaction of RLRs, such as RIG-1, with viral or foreign components such as double stranded RNA [65]. However, the primary producers of type I IFNs during viral infections are plasmacytoid dendritic cells (pDCs) and these cells are known to utilise the Toll-like receptors, specifically TLR7 and TLR9, to carry out this process. Once produced, IFNs can act either as autocrine or endocrine molecules resulting in the upregulation of several gene products including the further production of type I IFNs themselves and various interferon regulated genes (IRGs) with numerous functions. Type I IFNs also act to stimulate negative regulators of type I IFN production such as SOCS1 and USP18 creating negative feedback loops which allow for the controlled production of these cytokines (Figure 1.3.1)[199].

1.7.2 Type I IFNs as a Bridge Between Innate and Adaptive Immune Responses

Type I interferons can act as both autocrine and paracrine cytokines and can have numerous and varying effects on different cell types, including effects on the migration, differentiation, and survival of multiple immune cells. Studies have demonstrated roles for these cytokines in NK cell cytotoxic activity, ROS production in monocytes/macrophages and neutrophils as well as antigen presentation by dendritic cells [200-202]. Indeed, the effect of type I IFNs on antigen presenting cells (APCs) such as dendritic cells are critical for the efficient activation of the adaptive immune response. T and B lymphocyte maturation and expansion are dependent on the efficient presentation of pathogen epitopes via MHC molecules on APCs. Not only do type I IFNs promote the maturation and survival of various APCs, but they also upregulate the expression of MHC and co-stimulatory molecules on these cell types [202, 203]. Additionally, type I IFNs are capable of inducing T cell activation and proliferation through the upregulation of various chemokines and cytokines including CXCL10 and CXCR3 [204]. Type I IFNs are also required for the maturation of B lymphocytes, upregulation of B cell survival factors and isotype switching following activation of these cells [205, 206].

The dysregulation of immune responses, including the chronic release of pro-inflammatory mediators, can drive the development and progression of autoimmune and autoinflammatory disease. Due to type I interferons having such a major impact on both the innate and adaptive immune response, it is unsurprising that dysregulation of this family of cytokines has been reported to result in poor health outcomes including neurodegenerative disease, autoinflammatory disease and autoimmune disease [207-209]. Interestingly, dysregulated type I IFN signalling has also been noted with age [209, 210].

1.7.3 Type I Interferonopathies

The idea that an inadequate and uncontrolled type I interferon response could potentially be harmful was initially posed in the 1970s following Ion Gresser's report outlining the lethal effect of type I Interferons on new-born mice [211]. Several years later, the first indication of type I IFNs having a pathogenic role in humans was reported by Lebon *et al*. regarding Aicardi-Goutier syndrome. However, it wasn't until 2011 following a study on systemic lupus erythematosus (SLE) that the term type I interferonopathy was first coined, referring to a classification of autoimmune diseases characterised by the systemic dysregulation of type I IFN responses [212, 213]. Advances in scientific techniques and

screening assays such as next-generation sequencing have resulted in an increase in the number of known type I interferonopathies with up to 40 discrete genotypes described to date, and the recognition of a remarkably broad associated phenotypic spectrum [214].

As previously discussed, one of the most well-defined interferonopathies described to date is Aicardi-Goutier syndrome, a disorder defined by Mendelian inborn errors that are linked to type I IFN production, resulting in systemically increased basal levels of type I IFN responses and this overproduction is largely accepted to be a key driver of the immunopathology observed in these patients [215]. Although there is some overlap in terms of genetic and immunological features between type I interferonopathies, allowing for type I interferonopathy signatures to be described and tested for, there are also large phenotypic variations between these diseases, with the only defined feature of commonality being type I IFN dysregulation [208, 216]. Skin involvement is frequent among this classification of autoimmune disease and innate immune cells, particularly neutrophils and monocytes, are often regarded as key drivers of pathogenesis. Other examples of type I interferonopathies include a monogenic form of SLE, dermatomyositis and Sjogren's syndrome [207, 208, 217, 218].

With the emergence of novel treatments designed to specifically target aspects of the type I IFN signalling pathway, it has become more important than ever to correctly recognise, classify and diagnose type I interferonopathies so that the best treatment plans can be provided to these patients [219].

Although AAV shares both clinical and immunological similarities with known type I interferonopathies such as SLE and past studies have suggested a role for type I IFNs in AAV severity [50, 220], to our knowledge, type I IFNs have never been conclusively investigated as causative factors of AAV initiation or progression. Given the possible role of type I IFNs in ageing and inflammageing this analysis could also serve to explain the later-in-life development of AAV.

1.8 Study Design and Rationale

1.8.1 Hypothesis

We hypothesize that individuals with AAV experience accelerated biological ageing, increasing their risk of disease development and progression when compared to healthy individuals of similar chronological age. Considering the differences in chronological age at diagnosis between anti-MPO and anti-PR3 mediated AAV patients, we suggest that biological ageing may also differ depending on ANCA specificity. Furthermore, we propose that biological changes that occur with ageing contribute to the abnormal innate immune responses observed in AAV, specifically innate immune cell dysfunction. Finally, given the known changes in type I IFN signalling with age and the similarities between AAV and known type I interferonopathies, we hypothesize that systemic type I IFN regulated responses are dysregulated in AAV patient's indicative of a type I interferonopathy.

1.8.2 Specific Aims

1. To determine the biological age of a mixed cohort of AAV patients via epigenetic clock analysis and determine whether epigenetic age differs depending on ANCA subtype, whether treatment effects these measures and whether these individuals experience accelerated ageing in comparison to a healthy control cohort.

2. To investigate the effect of age on innate immune cell function in response to stimulation with ANCAs

3. To determine whether type I IFN responses are dysregulated in AAV, characteristic of type I interferonopathies and to examine whether this profile correlates to disease activity.

Figure 1.8.1:
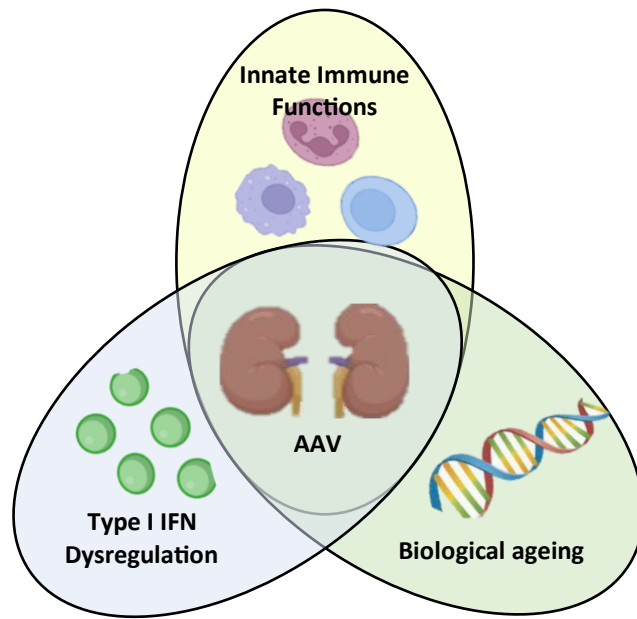
Figure 1.8.1: The Interplay Between Biological Ageing, Immune Dysfunction and AAV Development.

Biological ageing is associated with abnormal innate immune cell function and IFN dysregulation. The effect that this has on AAV development and progression remains unclear [14].

2 Materials and Methods

2.1 Reagents

Product	Company
4% paraformaldehyde (PFA)	Santa Cruz, Texas, USA
BD FACS lysing solution	BD Biosciences, Oxford, UK
Bovine serum Albumin (BSA)	Thermo Fisher Scientific, Loughborough, UK
Dextran	Sigma-Aldrich, Missouri, USA
DMSO	Thermo Fisher Scientific, Loughborough, UK
EDTA	Sigma Aldrich, Wicklow, Ireland
Ethanol	Sigma Aldrich, Wicklow, Ireland
Molecular Grade Ethanol	Thermo Fisher Scientific, Loughborough, UK
Molecular Grade Isopropanol	Thermo Fisher Scientific, Loughborough, UK
FCS	Sigma Aldrich, Wicklow, Ireland
Hoechst dye	Thermo Fisher Scientific, Loughborough, UK
Lithium heparin vacuettes	Greiner Bio-One, Kremsmunster, Austria
NaOH	Sigma Aldrich, Wicklow, Ireland
NH_4Cl	Sigma Aldrich, Wicklow, Ireland
OneComp beads	eBioscience, California, USA
Percoll	GE healthcare, Uppsala, Sweden
Phosphate buffered Saline (PBS)	Thermo Fisher Scientific, Loughborough,UK
Power SYBR Green PCR Master	Bio-Sciences Ltd, Thermo Fisher Scientific, Loughborough, UK
fMLP	Sigma Aldrich, Wicklow, Ireland
TNFα	Biolegend, Amsterdam, Netherlands
PMA	Sigma Aldrich, Wicklow, Ireland
LPS	Sigma Aldrich, Wicklow, Ireland
Cytochalasin B	Sigma Aldrich, Wicklow, Ireland
Goat Serum	Sigma Aldrich, Wicklow, Ireland

TMB	Thermo Fisher Scientific, Loughborough, UK
Permafluor Mountant	Thermo Fisher Scientific, Loughborough, UK
Roswell Parks Memorial Institute Medium (RPMI)	Thermo Fisher Scientific, Loughborough, UK
Trypan Blue	Sigma Aldrich, Wicklow, Ireland
Tween 20	Fisher Scientific
Virkon	Thermo Fisher Scientific, Loughborough, UK

2.2   Kits

Product	Company
High-Capacity cDNA Reverse Transcription Kit	BD Biosciences, Oxford, UK
DNase I, Amplification Grade	Bio-Sciences Ltd, Thermo Fisher Scientific, Loughborough, UK
PAXgene Blood RNA Kit (50)	Qiagen LTD, Manchester UK
PureLink RNA extraction kit	Bio-Sciences Ltd, Thermo Fisher Scientific, Loughborough, UK
EZ DNA Methylation Kit	Zymo Research, Cambridge, UK
PyroMark PCR kit	Qiagen Ltd, Manchester, UK
PyroMark 48 sequencing kit	Agilent, Santa Clara, USA
Hu IL-6 OptEIA ELISA Set	BD Biosciences, Oxford, UK
Hu IP-10 (CXCL10) OptEIA ELISA Set	BD Biosciences, Oxford, UK
Hu TNFα OptEIA ELISA Set	BD Biosciences, Oxford, UK
Hu MCP-1 OptEIA ELISA Set	BD Biosciences, Oxford, UK
Hu MPO DuoSet ELISA Kit	R&D Systems, UK
Hu CCL19 DuoSet ELISA Kit	R&D Systems, UK

2.3 Equipment

Equipment	Company
96 well plate	Sarstedt, Co. Wexford, Ireland
Centrifuge	Eppendorf Hamburg, Germany
Eppendorf tubes	Sarstedt, Co. Wexford, Ireland
FACS Canto II flow cytometer	BD, San Jose, USA
Amnis Cellstream Flow Cytometer	Luminex, Amnis Corporation, Seattle, WA
FACs tubes	Thermo Fisher Scientific, Loughborough, UK
Light Microscope	Olympus Corporation, Japan
Multichannel pipette	Thermo Fisher Scientific, Loughborough, UK
Pipettes (p2, p20, p200, p1000)	Thermo Fisher Scientific, Loughborough, UK
NanoDrop™ 2000/2000c Spectrophotometer.	Labtech International, UK
Ph Meter	Hanna Instruments, UK
Pipette Gun	VWR International Ltd., Ballycoolin, Dublin, Ireland.
Pipette tips p2/p200/p1000	Sarstedt, Co. Wexford, Ireland
Filter pipette tips p2/p200/p1000	Thermo Fisher Scientific, Loughborough, UK
Pipettes 5/10/25ml	Corning, New York, USA
Plate Reader	Molecular Devices, California, USA
Syringes 10/50ml	Terumo N.V, Belgium
Tissue culture plates 6/24	Sarstedt, Co. Wexford, Ireland
MiniAmp Plus Thermal Cycler	Applied Biosystems by Thermofisher, UK
2100 Bioanalyzer Instrument	Agilent, Santa Clara, USA
Fluorescent microscope	Olympus Corporation, Japan
QuantStudio 5 Real-Time PCR Machine	Applied Biosystems by Thermofisher, UK

2.4 Fluorescent and monoclonal antibodies

Product	Fluorochrome	Clone	Company
Anti-histone Ab	N/A	H11-4	Merk Millipore Ltd. Ireland
Goat anti-mouse IgG secondary Ab	Alexa Fluor 568	N/A	Thermo Fisher Scientific, Loughborough, UK
CD15	PerCP-Cy5.5	W6D3	Biolegend, Amsterdam, Netherlands
CD14	PE-Cy7	61D3	Biolegend. Amsterdam, Netherlands
CD16	APC-Cy7	3G8	BD Biosciences, Oxford, UK
CD45	PE	HI30	BD Biosciences, Oxford, UK
DAPI	Pacific Blue	N/A	Sigma-Aldrich , Missouri, USA
Sytox Red	APC	N/A	Invitrogen by Thermo Fisher Scientific, Loughborough, UK
DHR-123	FITC	N/A	Invitrogen by Thermo Fisher Scientific, Loughborough, UK
Anti-MPO	PE	2C7	Bio-Rad, Co. Kildare, Ireland
Anti-PR3	FITC	W6M2	Abcam, UK
CD45	Pacific Blue	HI30	Invitrogen by Thermo Fisher Scientific
Anti-PR3 mAb	N/A	N/A	Abcam, Cambridge, UK
Anti-MPO mAb	N/A	N/A	Origene, Germany
Isotype IgG Control	N/A	IE2.2	Merk Millipore Ltd. Ireland

2.5   Buffers

Buffer	Components
2% Dextran	2% dextran in PBS
2% PFA	4% PFA in FACs buffer (1:1 ratio)
Cell Culture Medium	RPMI-1640 + 0.5% BSA
FACS buffer	2% foetal calf serum in PBS
RBC lysis buffer	155mM NH_4Cl, 0.1mM EDTA, 12mM $NaHCO_3$ pH 7.4
Blocking Buffer (Microscopy)	5% Goats serum in PBS

2.6   Software

Software	Company
FACSDiva software	BD Oxford, UK
GraphPad Prism v9.1.1 software	GraphPad Software, San Diego, CA, USA
Amnis Cellstream Software	Luminex, Amnis Corporation, Seattle, WA
Kaluza software Version 2.1	Beckman Coulter, USA
QuantStudio™ Real-Time PCR Software 1.3	Applied Biosystems by Thermo Fisher Scientific, Loughborough, UK
R (version 4.2.1)	Free Software Foundation GNU Project, Austria
Python (version 3.9.7)	Python Software Foundation, Delaware, USA
Image J Fiji	National Institute of Health
GeneSys software	GeneSys software Company, California, USA
Agilent bioanalyzer software	Agilent, Santa Clara, USA
Agilent PyroMark 48 software	Agilent, Santa Clara, USA
Biorender 2023	Biorender, Canada

2.7 RKD Participant Recruitment

All AAV, disease control (DC) and healthy control (HC) participant samples used in this study were recruited using the Rare Kidney Disease (RKD) Registry and Biobank of Ireland (www.tcd.ie/medicine/thkc/research/rare.php) which has full ethical approval for the sampling and processing of human biological samples from the ethical committees of each participating hospital (St. Vincent's Hospital Research ethics committee, Tallaght Hospital Research ethics committee, St. James' Hospital Research ethics committee, and Beaumont Hospital Research ethics committee). All participants provided informed consent and biological samples were collected and stored in accordance with the RKD sample and data collection and management protocol from participating centres across the country. A detailed record of clinical and demographical data is also available for each participant which excludes any personal information that would allow for participant identification.

2.8 Molecular Biology

2.8.1 Bisulphite Conversion of DNA

Bisulphite conversion of 500ng of DNA was carried out using the Zymo Research EZ DNA Methylation Kit. 5μl of the normDNA was added to 5μl of M-Dilution buffer and adjusted to a total volume of 50μl using nuclease free water (NF-H$_2$O). This was gently mixed by pipetting and incubated at 42°C for 30mins. Following incubation 100μl of CT conversion reagent was added to each sample and mixed. The samples were added to a thermocycler set at (95°C for 30sec, 50°C for 60mins) x16 cycles followed by a 4°C hold for minimally 10mins. Following this 400μl of binding buffer was added to a Zymo-Spin IC column placed inside a collection tube. Each sample was added into these spin columns and the sample mixed by inverting the columns several times. The samples were then centrifuged at full speed (>10,000g) for 30sec. The flow through was discarded. 100μl of M-Wash Buffer was added to each column and the mixture centrifuged at full speed for a further 30sec. 200μl of M-Desulphonation buffer was added to each column and left to stand at room temperature (RT) (20-30°C) for 15-20mins. Once this incubation was complete the samples were centrifuged for 30sec at full speed. 200μl of M-Wash buffer was then added to the column and centrifuged at full speed for 30sec. Following this a further 200μl of M-Wash buffer was added to the columns and centrifuged at full speed

for 30sec. The column was then placed inside a microcentrifuge tube. 10μl of M-Elution buffer was added directly into the column matrix and centrifuged at full speed for 30sec. This step is repeated for a final elution volume of 20μl. The bisulphite converted DNA sample can be immediately used for downstream processes or stored long term at -80°C.

2.8.2   PCR Amplification for Pyrosequencing

PCR Amplification was carried out following the Qiagen PyroMark PCR kit and protocol. Firstly, all reagents were removed from the freezer and allowed to thaw at room temperature. The reaction mix was then set up according to Table 2.8.1.

Table 2.8.1:

Component	Volume per Reaction (μl)	Final Concentration
PyroMark PCR Master Mix, 2X	12.5	Contains HotStar Taq DNA Polymerase, 1X PyroMark PCR Buffer and dNTPs
Coral Load Concentrate, 10X	2.5	1X
Primer A (Forward) AGGGGAGTAGGGTAAGTGAGG	Variable	0.2μM
Primer B (Reverse) AACAAAACCATTTCCCCCTAATAT	Variable	0.2μM
RNase-Free H20	Variable	-
Template DNA CCRTAAACRTTAAACCRCCRCRCRAAACCRAC	Variable	<500ng/reaction or 10-20ng bisulphite converted DNA
Total Volume	25	

Table 2.8.1 PyroMark PCR Reaction kit volumes per test

A mastermix of the above reagents excluding the DNA was made and the mastermix was gently mixed through pipetting up and down before adding 20μl of it to individual PCR tubes. 5ul of the template DNA was subsequently added to the PCR tube. NF-H$_2$O was added to a PCR tube to act as a negative control. The thermocycler was programmed according to Table 2.8.2. The PCR tubes were placed inside the thermocycler set with a heated lid and the programme was started. Once complete, the PCR products were stored at 4-8°C short term or at-20°C for long term storage. All primers were designed using the PyroMark Assay Design software version 2.0.

Table 2.8.2:

PCR Step	Time	Temperature (°C)	Cycles	Comments
Initial PCR Activation Step	15min	95	1	HotStar Taq DNA Polymerase is activated by this step
3 Step Cycling			45	
Denaturing	30sec	94		
Annealing	30sec	56		
Extension	30sec	72		
Final Extension	10mins	72	1	

Table 2.8.2: PyroMark PCR Reaction settings

2.8.3 PCR Agarose Gel Electrophoresis

To make up the 1.5% agarose gel 1.5g of agarose was added to 98.5ml of TBE buffer. This mixture was heated until the agarose was fully dissolved and then allowed to cool before adding 3ul of gel red nucleic acid stain. The mixture was subsequently added to a template, the comb inserted, and the gel allowed to set at room temperature. Once set, 3µl of the ladder and samples were loaded into the appropriate wells and the power pack was switched on. The gels were allowed to run for 30-40 minutes before being imaged using GeneSys software.

2.8.4 Pyrosequencing Using the PyroMark 48

Pyrosequencing was undergone using the Agilent PyroMark 48 sequencer. The pyromark run was set up on the machine as an automatic run following the instructions outlined in the manual. All reagents were removed from the fridge/freezer and allowed to come to room temperature. The primers were then diluted to 4µM in annealing buffer and all reagents pipetted into the appropriate cartridges following the instructions outlined on the machine (volumes are specific to each run). Once complete the cartridge lids were closed and locked. Injector priming and testing was then selected. During this time the PyroMark Q48 magnetic beads and sample were loaded into the PyroMark Q48 disk. This was done by vortexing the magnetic beads and immediately pipetting 3µl of this suspension into 3-5 wells. It is important to note that the magnetic beads will fall out of suspension quickly

due to their high density and so can only be pipetted for a brief period (3-5 wells) before requiring resuspension via vortexing. 10μl of biotinylated PCR product was then added to the wells. If 10μl was unavailable, then the remaining volume was made up with NF-H$_2$O. Once fully loaded the disk was inserted into the machine and locked into position using the lock nut. The programme was started by pressing the "start" button on the screen. Once complete the plate was discarded and the machine was cleaned by pipetting NF-H$_2$O into each cartridge in the volumes indicated on the machine. When the machine had completed the clean step the absorber strip was discarded, and the cartridge lids left slightly ajar to allow any residual liquid to evaporate. The machine was then turned off.

2.8.5   Cell lysate RNA Extractions

RNA extractions from isolated PBMCs were carried out using the PureLink RNA mini kit, following the protocols provided. 400μl of the 70% ethanol solution was added to each of the previously isolated PBMC samples and vortexed until well mixed. 700μl of this solution was added to separate, labelled spin cartridges inside a collection tube provided within the kit. The tubes were centrifuged at 12,000g for 20 seconds. The flow through was discarded and this step was repeated using the remaining sample. 700μl of wash buffer I was then added to each cartridge, and these were again centrifuged at 12,000 g for 20 seconds. Once spun the flow through was discarded and the collection tubes replaced. 500ml of wash buffer II was subsequently added to each tube and centrifuged at 12,000g for 20 seconds. The flow through was discarded and this wash step was repeated however this time spun for 1 minute. Each of the samples were then centrifuged for a further 2 minutes at 12,000g. The collection tubes for each sample were replaced with labelled eppys and 30μl of NF-H$_2$0 was carefully pipetted into the centre of each of the spin cartridge filters, making sure not to touch the filter with the pipette tip. The samples were incubated for 1 minute at room temperature and subsequently centrifuged for 1 minute at 8000-10,000g. Spin cartridges were discarded, and the eluted RNA was quantified using a NanoDrop spectrophotometer and the samples stored at -80°C for later use in cDNA synthesis and qPCR.

2.8.6   Whole Blood Paxgene RNA Extractions

Whole blood RNA Extractions were performed following the Paxgene RNA extraction kit protocol. Briefly, blood previously collected and stored at -80 degrees Celsius in

Qiagen Paxgene blood tubes were thawed to room temperature. They were then incubated at room temperature for a further 2 hours. Following incubation, the blood tubes were centrifuged at 4000g for 10mins. The supernatants were discarded, the pellet resuspended in 4ml of NF-H$_2$O and the blood tube lid replaced. These were then centrifuged for a further 10mins at 4000g. Following centrifugation, the entire supernatant was carefully discarded, and the pellet was resuspended in 350μl of buffer 1. This sample was added to a 1.5ml microcentrifuge tube (MCT) along with 300μl of buffer 2 and 40μl phosphokinase 1. This mixture was vortexed briefly and then incubated for 10mins at 55 degrees Celsius using a shaker incubator set to 500rpm. The entire lysate was pipetted into a paxgene shredder column and centrifuged for 2mins at 20,000g. The resultant supernatant was transferred to a fresh MCT along with 350ul of molecular grade ethanol and briefly vortexed. 700μl of this mixture was pipetted into a paxgene RNA column placed inside a 2ml processing tube (PT) and spun at 20,000g for 1 minute. The flow through was discarded, the column placed inside a fresh PT and the remaining sample was added to the column and spun at 20,000g for 1 min. Again, the flow through was discarded and PT replaced. 350μl of buffer 3 was added to the spin column and this was centrifuged for 2mins at 20,000g. In the meantime, 10μl of DNase 1 (RNFD) was added to 70μl of RDD buffer for each sample processed and mixed by gently flicking. Following the spin, the supernatant was discarded and PT replaced. 80μl of the DNase mixture was added to the spin column and left to incubate at room temperature for 15mins. Following incubation, a further 350μl of buffer 3 was added to the column and this was centrifuged for 1min at 20,000g. The supernatant was discarded, PT replaced, 500μl of buffer 4 added to the spin column and the tube was centrifuged at 20,000g for 1min. Again, the supernatant was discarded, PT replaced, 500μl of buffer 4 added to the spin column and the tube was centrifuged at 20,000g for 3mins. Following this, the supernatant was discarded, PT replaced, and the column was spun dry for 2mins at 20,000g. The spin column was then placed inside a labelled MCT, 40μl of buffer 5 was added to the filter and this was centrifuged for 1min at 18,000g. This step was repeated twice. The eluate was then incubated at 65 degrees Celsius for 5mins. Following this it was immediately placed on ice, nanodropped and then stored in the –80°C freezer.

2.8.7   Bioanalysis

Bioanalysis of each RNA sample was performed using an Agilent 2100 Bioanalyzer following the procedures described in the Agilent RNA 6000 Nano kit guide. In brief, the

electrodes were cleaned by resting them in the cleaning chip filled with 350μl of RNAzap followed by NF-H$_2$O for 30sec each. The gel was prepared by pipetting 550μl of the RNA gel stock into a spin filter and centrifuging for 10mins at 1500g. This was then aliquoted into 65μl aliquots to be stored at 4 degrees Celsius for 1 month. The gel dye mix was prepared by adding 1μl of the RNA dye, which had been allowed to equilibrate to room temperature, to a 65μl aliquot of the prepared RNA gel. This mix was vortexed well and centrifuged for 10mins at 13,000g. The gel dye mix, samples and ladder were then loaded onto the chip, being careful to add the correct reagent to the appropriate wells, centrifuged for 1min and read on the bioanalyzer (Figure 2.8.1).

Figure 2.8.1:
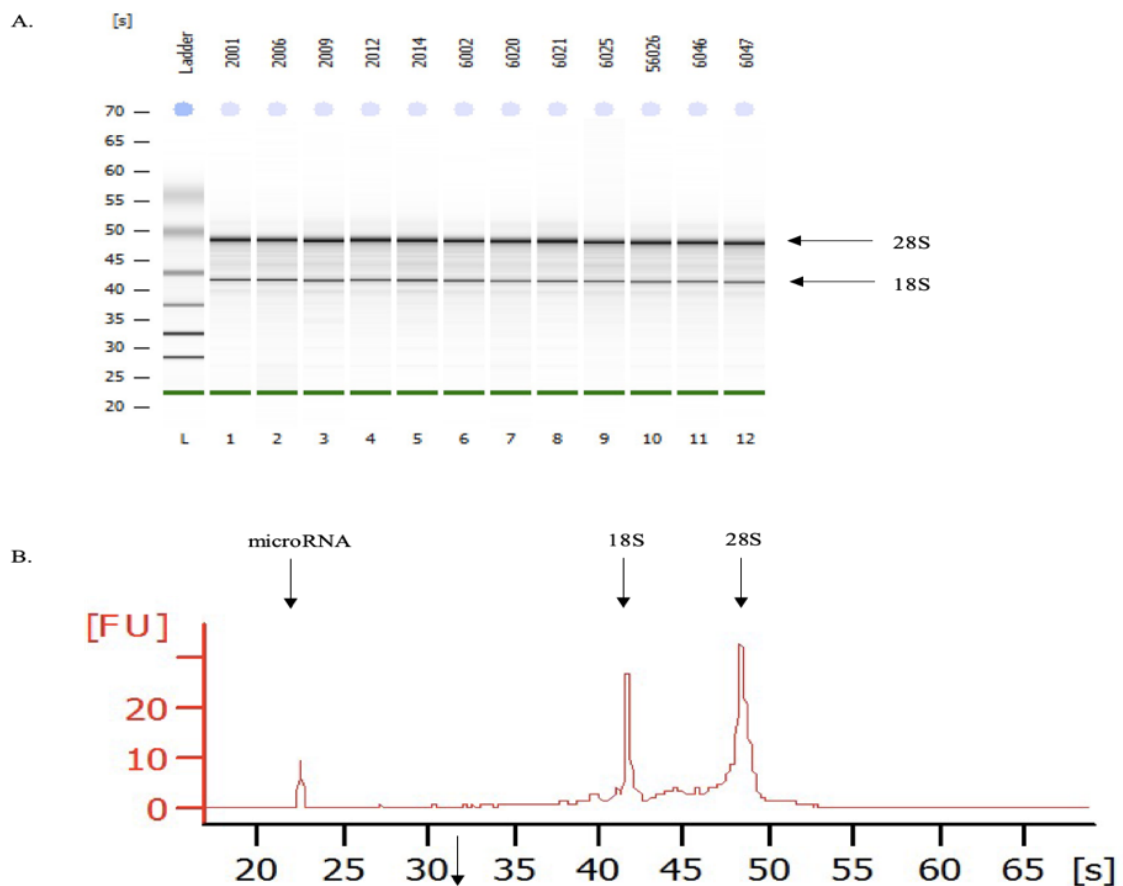
Figure 2.8.1: Representations of RNA Integrity values detected using the Agilent Bioanalyzer.
(A.) Profiles of RNA samples isolated from whole blood of 12 healthy controls. (B.) An electropherogram representing one of the healthy control samples analysed. RNA quality in these samples is assessed by analysing degradation visible as either additional (A) bands or (B) peaks other than those of 28S and 18S.

2.8.8 cDNA Synthesis

250ng of high-quality RNA was reverse transcribed into cDNA using the ThermoFisher High-Capacity cDNA Reverse Transcription Kit. The reagents provided were used according to the volumes outlined in Table 2.8.3.

Table 2.8.3:

	+RTase	**-RTase (control)**
10X Assay Buffer	2.5µl	2.5µl
25X dNTP	0.8µl	0.8µl
10X RT Random Primers	2µl	2µl
Reverse transcriptase (RTase)	0.5µl	0µl
NF-H$_2$O	9.2µl	9.7µl

Table 2.8.3: High-capacity reverse transcription kit component volumes per test

15µl of the appropriate master mix was added to the labelled PCR tubes followed by 10µl of the RNA sample. Reverse transcription of the samples was subsequently carried out using a thermocycler set to the following conditions (Table 2.8.4):

Table 2.8.4:

	Step 1	Step 2	Step 3	Step 4
Temperature (°C)	25	37	85	4
Time (mins)	10	120	5	∞

Table 2.8.4: cDNA synthesis thermocycler settings

The cDNA produced was stored at -20°C.

2.8.9 Primer Design

All primers were designed using the NCBI Primer BLAST database (https://www.ncbi.nlm.nih.gov/tools/primer-blast). Primers were designed to amplify a product of maximum 200 bps and to be intron spanning where possible (Table 2.8.5). Primers were synthesised by IDT technologies.

Table 2.8.5:

Gene	Forward	Reverse	Product Length
18S	GTAACCCGTTGAACCCCATT	CCATCCAATCGGTAGTAGCG	151
b-actin	ACAGAGCCTCGCCTTTGCC	GATATCATCATCCATGGTGAGCTGG	70
PPIA	TGAGGTAAGGGGCCTGGATAC	GTCTGCAAACAGAAGGCAAAAT	173
TBP	TGACCCAGGGTGCCATGA	GGGTCAGTCCAGTGCCATAA	72
RPS13	CTTTCGTTGCCTGATCGCC	ACTTCAACCAAGTGGGGACG	107
RPL27	GGGTGGTTGCTGCCGAA	GGTGCCATCATCAATGTTCTTCAC	116
OAZ1	CAGCAGCAGTGAGAGGGTC	TCTGACTATTCCCTCGCCCA	120
STAT1	TGCGCGCAGAAAAGTTCCATT	AGACATCCTGCCACCTTGTG	171
ISG15	GCGAACTCATCTTTGCCAGT	AGCATCTTCACCGTCAGGTC	91
SIGLEC1	CTCTGCCTCTACCTCCACCT	AAACACGCCTCCTTCTCCAG	152
IFIT1	AGCTTACACCATTGGCTGCT	CCATTTGTACTCATGGTTGCTGT	
RSAD2	CCCCAACCAGCGTCAACTAT	TCTTCTCCATACCAGCTTCCT	147
IFI27	ATCAGCAGTGACCAGTGTGG	TGGCCACAACTCCTCCAATC	107
IFI44L	ACCCCTAGAAACAGATATAGAACAA	GACGGCTGCATCTTTCAACC	163
IFIT1	GGACCCACAAGAATGTGAAAGC	TCACCATTTGTACACATCTCCACT	85
MMP8	AGCCAGGAGGGGTAGAGTTT	GGCTTATTTATTCTGCTGAACAGT	149
ANXA3	ACCGCGCTTTGGATTAGTGT	CAGCATCCACTGATGGGCTA	123
IL6	CCTTCTCCACAAACATGTAACAAGA	TCACCAGGCAAGTCTCCTCA	142
TNFA	CCTGCTGCACTTTGGAGTGA	GAGGGTTTGCTACAACATGG	143
p21	TCTAGGAGGGAGACACTGGC	TGTCTGACTCCTTGTTCCGC	109
ELOVL2	CCAAATCAGTAGAGTTCCTGGACACAA	TTGTCCACAAGGTATCCAGTTCAAGA	140

Table 2.8.5: List of Primers

2.8.10 Housekeeping Gene Selection

All gene amplifications for human samples during this project were normalised to Ribosomal protein L27 (*RPL27*), which, using NormFinder.xla v0.953 and statistical measures of deviation, was selected as the most stably expressed gene across samples from a panel of potential normalisers: *RPL27*, *18S*, ribosomal protein S13 (*RPS13*), peptidylprolyl isomerase A protein (*PPIA*), TATA-Box binding protein (*TBP*), beta-actin and ornithine decarboxylase antizyme 1 (*OAZ1*). The expression of these genes in 3 samples from a healthy control (HC), disease control (DC), AAV remission and AAV active cohort were analysed for each normaliser. All genes tested showed stable expression across our cohorts indicating that all genes tested would be suitable housekeeping gene candidates (Figure 2.8.2). Although *OAZ1* came out as the best housekeeping candidate gene using Normfinder (Figure 2.8.2 D), this gene showed very high baseline CT values corresponding to very low expression levels and higher deviation than other candidates (Figure 2.8.2 A-B). Standard deviation analysis isolated *RPL27* as the most stable gene across samples (Figure 2.8.2 C), while Normfinder found this to be the second-best housekeeping gene candidate of the seven tested (Figure 2.8.2 D). Considering these results as a whole, *RPL27* was selected as our housekeeping gene moving forward in all qPCR experiments.

Figure 2.8.2:

A.

B.

C.

	18S	ACTB	PPIA	TBP	RPS13	RPL27	OAZ1
std dev [± CP]	0.367134	0.35941	0.450079	0.391872	0.41342	0.342279	0.353246
std dev [± x-fold]	1.289788	1.282901	1.366115	1.312095	1.331839	1.267758	1.277431
coeff. of corr. [r]	0.558	0.661	0.787	0.553	0.726	0.72	0.668

D.

	Gene name	Stability value		Best gene	OAZ1
HC VS DC VS AAV	18S	0.023		Stability value	0.011
	ACTB	0.015			
	PPIA	0.013		Best combination of two genes	RPL27 and OAZ1
	TBP	0.014		Stability value for bestcombination of tv	0.009
	RPS13	0.014			
	RPL27	0.012			
	OAZ1	0.011			

Figure 2.8.2: Housekeeping gene analysis

(A.) The absolute mRNA expression measured in 12 samples for each gene tested. (B.) The absolute mRNA expression of (i.) 18S, (ii.) ACTB, (iii) PPIA, (iv) TBP, (v.) RPS13, (vi) RPL27 and (vii) OAZ1 measured in healthy controls (HC), disease controls (DC), AAV active patients (AAV Active) and AAV remission patients (AAV Remission). (C.) Summary of the deviation measured between samples for each gene using GraphPad Prism statistical analysis. (D.) Summary of Normfinder analysis results for each gene.

2.8.11 qPCR

Primer Preparation:

Each of the stock primers provided by IDT technologies were diluted in 250µl RNA-free water to yield a 100nM stock solution. Working stock solutions of 10nM were prepared by adding 10µl of the forward primer and 10µl of the reverse primer to 80µl of NF-H_2O. 0.4µl of the working stock solution was added to each well of the qPCR plate which contained a total of 10µl, yielding a final concentration of 0.4nM per well.

cDNA Preparation:

1 in 10 dilutions of the previously synthesised cDNA was prepared using NF-H_2O.

Master mix Preparations:

A master mix containing 5µl of SYBR green, 0.4µl of the working primer solution and 2.6µl of NF-H_2O was made for each well used in the qPCR for each gene tested.

All prepared mixtures were briefly vortexed and spun before plating. A 384 well plate was clearly labelled and divided into suitable sections. 2µl of the diluted cDNA was pipetted into the appropriate wells in triplicate, followed by 8µl of the appropriate master mix solution. The plate was centrifuged for 30 seconds and analysed using the QuantStudio 5 qPCR machine.

2.9 Cell Isolation

2.9.1 Neutrophil and PBMC Isolation

Fresh whole blood was transferred into a 50ml falcon tube and an equal volume of filter sterilised 2% dextran was added to this. This mixture was slowly inverted 18-20 times and RBCs allowed to sediment by gravity by standing the falcon tube upright for approximately 30mins. Following this the supernatant from the blood/dextran mixture was removed into a fresh 50ml falcon, being careful to avoid taking any RBCs from the pellet. The supernatant was spun at 200g for 7 mins with no brakes. Once complete, the supernatant was discarded, and the pellet resuspended in 3ml of 55% percoll. This suspension was then slowly layered over 4.5ml of 65% percoll into a 15ml tube using a Pasteur pipette. The tubes were then centrifuged for 30 mins at 1500g with no brakes. Once complete the PBMC layer was (top layer of cells) was removed and placed into a fresh 50ml tube while the remaining supernatant was carefully discarded. The neutrophil and red blood cell layer was subsequently combined by gentle pipetting. PBS was added to both the neutrophil and PBMC suspensions and both samples were centrifuged for 5mins at 400g with the brake on. Supernatants were removed and both pellets were gently resuspended in 10ml of RBC lysis buffer and incubated for 5mins at RT with frequent mixing. Cells were then washed and resuspended in 1-2ml of media (RPMI 0.05% BSA) for counting using Trypan blue.

2.9.2 Cell Counting and Viability

Cell viability was determined via trypan blue exclusion. A 1 in 100 dilution of neutrophil samples were prepared by adding 10μl of the neutrophil cell suspension to 90μl of trypan blue, mixing thoroughly by gently pipetting and then adding 10ul of this suspension to 90μl of trypan blue in a serial dilution. A 1 in 20 dilution of the PBMC samples were prepared by adding 5μl of the PBMC cell suspension to 95μl of trypan blue. At least 10μl of the prepared dilution was then added to a haemocytometer after gentle pipetting up and down. This was viewed under a light microscope and the number of cells present in each of the corner squares of the haemocytometer grid were counted. The total cell count was calculated using the following formula:

Number of cells / ml = (average cell count per haemocytometer grid X 10^4) x (dilution factor)

2.10 Functional Assays

2.10.1 Microscopy

Day 1

Neutrophils were isolated as per the above protocol and resuspended at 1 million cells/ml in RPMI containing 0.5% BSA. 150μl of this cell suspension was added to labelled eppys for each of the desired stimuli (UN, MPO, fMLP, and IgG) and time points (4hr, 3hr, 2hr and 1hr). 2ng/ml of TNFα was added to the eppys designed to have the longest time point (e.g. 4hours) and incubated for 15mins at 37°C. Following 15mins the appropriate stimuli were added to the appropriate eppys (5μg/ml monoclonal anti-MPO, IgG control or fMLP) and left to incubate at 37°C. The TNFα priming step and stimulations were repeated for each time point (3hr, 2hr, 1hr). Meanwhile, using a wax pen, small circles were drawn onto labelled poly-L-lysine glass slides. 30mins before the stimulations are complete, 100μl of each of the stimulated cell suspensions (approx. 1×10^5 cells) were added to their corresponding slides within the drawn circles and the slides were placed over a box with a wet tissue to reduce evaporation. Once all the stimulations were complete the cells were fixed by adding 4% PFA and incubated for 15mins at room temperature. Following this the cells were washed by adding PBS into the corner of the wax circle outline, gently pouring off and repeating for a total of 3 washes. 150μl of 0.5 % Triton X-100 was added to the slides for 1min at room temperature in order to permeabilise cells. The wash step was repeated 3 times. 100μl of blocking buffer (5% goat serum) was subsequently added to the slides and incubated in a humid chamber for 1hr. Anti-histone antibody was diluted in blocking buffer to give a final concentration of 5μg/ml and 100ml was added to each slide. These were incubated at 4°C overnight in the humidity chamber.

Day 2

The slides were washed 3 times with 5min soaks in PBS. The secondary antibody (goat anti-Mouse IgG Alexa Fluor® 568 conjugate) was diluted to 10μg/ml in blocking buffer, 100μl of this was added to each slide and these were incubated for 1hr in the humidity chamber. Following this the slides were washed 3 times with 5min PBS soaks. The DNA was then stained by adding 5μg/ml Hoechst dye to the cells and incubating for 10mins in the dark. The cells were washed twice and then coverslips were mounted using PermaFluor mountant and allowed to dry. The coverslips were sealed using nail varnish

and slides were stored in the cold room until ready to analyse using an Olympus fluorescent microscope.

2.10.2 Cell Preparation for Functional Assays

Neutrophils and PBMCs were isolated as described above. In order to prepare for flow cytometry analysis, the desired cells were resuspended at 2×10^6 cells/ml in media (RPMI 0.5% BSA). 3ml of each cell suspension was added to a separate tube, loaded with 2.5µg/ml DHR123 together with 5µg/ml Cytochalasin B and incubated in the dark for 10 minutes at 37ºC. Following this 98µl of the cell suspension was added to appropriately labelled wells of the 96 well plate (Figure 2.10.1). Wells intended for the 4hr stimulation were subsequently primed by incubation with 2ng/ml TNFα in 2µl aliquots for 15min at 37˚C with gentle mixing at 5 minute intervals. These wells were then left unstimulated or stimulated with either 5µg/ml monoclonal anti-MPO or IgG antibodies, 150µg/ml anti-PR3 monoclonal antibody, 5µg/ml of fMLP for neutrophils or 0.1µg/ml PMA as a positive control for monocyte activation in 100µl aliquots. The 96 well plate was then left to incubate for 2hrs and 45mins at 37°C with intermittent gentle mixing. Following this the priming step and stimulation steps were repeated for the 1hr wells. The plate was then placed back in the incubator to incubate at 37°C for the remaining hour. Once complete, the plate was spun at 100g for 10mins and the supernatants were carefully pipetted from each well into a new, labelled 96 well plate for storage at -20°C. 200µl of 2% FACs buffer was added to the remaining cell pellets and centrifuged for 10mins at 100g. The supernatants were discarded, and the wash step repeated. The cells were then fixed by adding 100µl of 2% PFA and incubating at RT for 10mins. Once complete, 100µl of 2% FACs buffer was added, and the cells centrifuged at 100g for 10mins. Supernatants were discarded and the wash step was repeated. The cells were resuspended in 100µl of 2% FACs buffer and kept at 4°C in the dark overnight before being analysed by flow cytometry.

Figure 2.10.1:
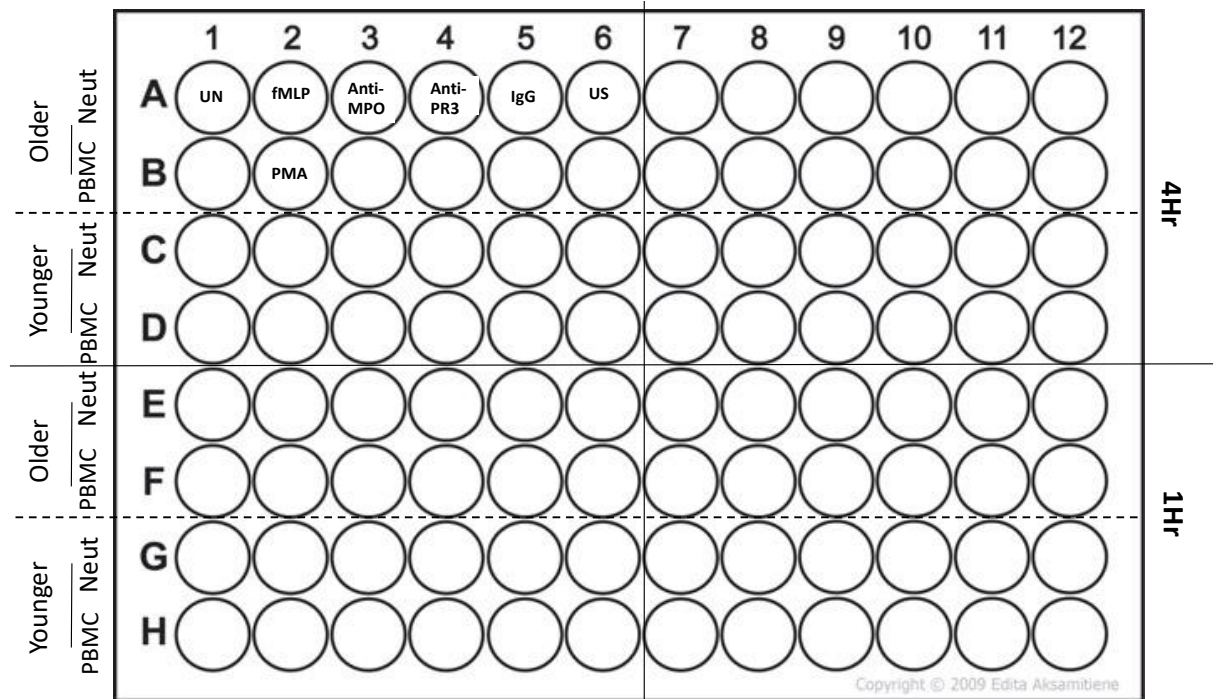
Figure 2.10.1: Example Plate plan for day 1 flow cytometry cell prep.

During the 4 hour incubation period for the flow cytometry plate, further preparation for supernatant and cell lysate collection was undergone. Provided enough cells were obtained, 1ml of PBMCs at $2x10^6$ cells/ml and 1ml of isolated neutrophils at $5x10^6$ cells/ml were added to appropriately labelled wells in a 12 well plate (Figure 2.10.2). All wells were primed using 2ng/ml TNFα incubated for 15min at 37°C with gentle mixing at 5 minute intervals. Wells were then either left unstimulated or stimulated for 4 hours with either 5μg/ml monoclonal anti-MPO or IgG antibodies or 150μg/ml anti-PR3 antibody. 5μg/ml of fMLP, 100ng/ml PMA or 100ng/ml of LPS was used as positive controls. Following the 4 hour incubation, the supernatants of each sample were removed and put in labelled Eppendorf tubes and were centrifuged for 2mins at 12,000g. Meanwhile 600μl of RNA lysis buffer provided within the PureLink RNA extraction kits was added to each well of the 12 well plate. Once centrifugation was complete, the supernatants were carefully transferred into fresh labelled Eppendorf tubes, being sure not to disturb the pellet, before being stored at -20°C. The wells now containing cell lysates were then scrapped using the filtered tips and pipetted into their corresponding cell pellets left from the centrifugation step. These cell lysates were stored at -80°C.

Figure 2.10.2:
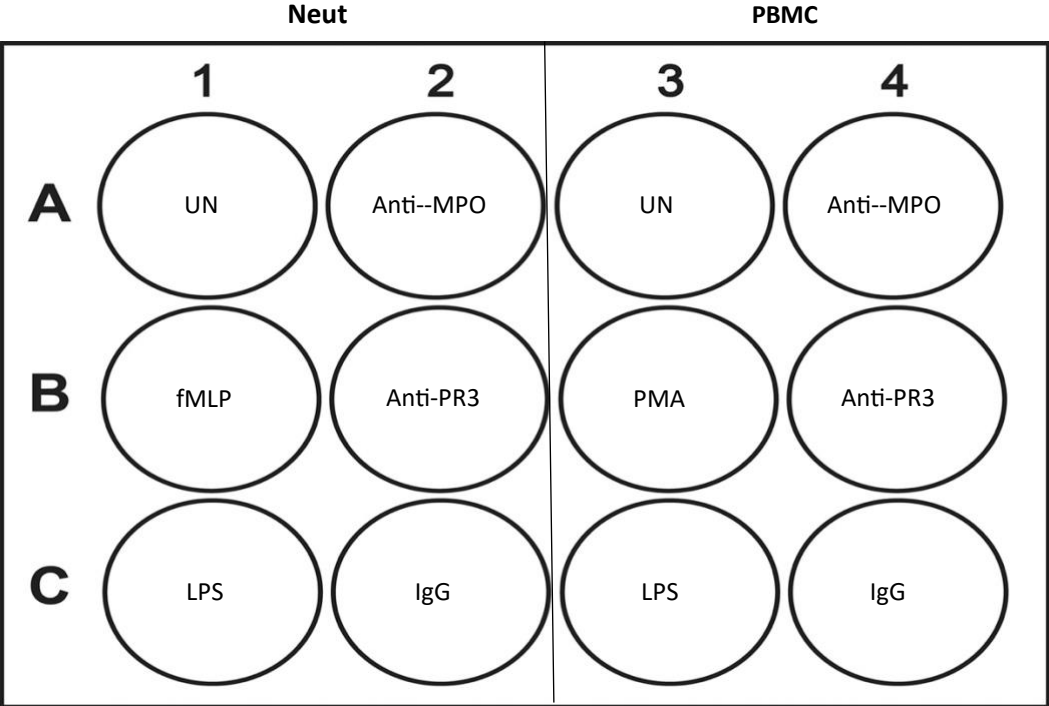
Figure 2.10.2: Example Plate plan for day cell lysate and supernatant cell prep.

2.10.3 Neutrophil and PBMC Flow Cytometry

The DNA dyes, Sytox red and DAPI, were removed from the freezers and allowed to thaw. Meanwhile an antibody mastermix was made following the concentrations described in Table 2.10.1. This antibody mastermix was added to the appropriate wells of the 96 well plate. This was incubated in the dark at RT for 15mins. During this time the nuclear dye mastermix was made using 5nM Sytox red and 0.3nM DAPI diluted in flow buffer. Once the incubation was complete 100µl of flow buffer was added to each well and the plate was then centrifuged for 10mins at 100g. Once complete, supernatants were discarded and 200µl of the nuclear dye mastermix was added to the appropriate wells and the plate was incubated for at least 20 mins in the dark at RT. The samples were then run either on the Luminex cellstream or BD Canto flow cytometers.

Table 2.10.1:

Marker	Clone	Fluorophore	Cellstream Channel	Concentration
CD15	WD63	PerCP-Cy5.5	C6	0.2µg
CD14	61D3	PE-Cy7	D1	0.2µg
CD16	3G8	APC-Cy7	B1	0.2µg
CD45	HI30	PE	D4	0.2µg
DAPI	N/A	Pacific Blue	A2	0.3nM
Sytox Red	N/A	APC	B6	5nM
DHR-123	N/A	FITC	C3	5µg/ml

Table 2.10.1 NETosis and ROS assay flow panel

2.10.4 Whole blood Cell Flow

100µl of whole blood was added to a FACS tube with an equal volume of 2% FACS solution. A mastermix of the desired antibodies (see Table 2.10.2) was added to the blood sample and incubated at RT for 20 minutes. Once complete, 2ml of 1 x BD FACS lyse solution (Stock solution 10x, prepared with ultra-pure H_2O) was added to the tubes, vortexed gently and incubated for 15 minutes in the dark at RT. Following this incubation, 1ml of PBS was added to the samples, vortexed and spun at 400g for 5 minutes. Supernatants were discarded, the pellets were resuspended in 2ml of PBS and spun again at 400g for 5mins. This wash step was repeated twice more or until the supernatant runs

clear. The cell pellets were then resuspended in 300µl of 2% FACs buffer and stored at 4°C in the dark until acquired on the BD Canto flow cytometer.

Table: 2.10.2

Marker	Clone	Fluorophore	Volume	Concentration
CD15	WD63	Per-CPCy5.5	1µl/ test	0.2µg
CD14	61D3	PE-Cy7	1µl/test	0.2µg
CD16	3G8	APC-Cy7	1µl/test	0.2µg
CD45	HI30	Pacific Blue	1µl/test	0.2µg
Anti-MPO	2C7	PE	5µl/test	2.5µg
Anti-PR3	W6M2	FITC	1µl/test	0.25 µg

Table 2.10.2 Whole blood surface expression flow panel

2.10.5 ELISA

ELISAs were carried out following the protocols specific to each kit (BD Biosciences for IL-6, TNFα, MCP-1 and CXCL10; R&D systems for MPO and CCL19). Firstly, the capture antibody was added to each well and left to incubate at 4°C overnight. The plates were washed three times with PBS 0.05% tween before being blocked with assay diluent (10% FCS PBS:BD biosciences, 1%FCS PBS: R&D systems) and left to incubate at room temperature for 1hr. The plates were again washed thrice, and the standards/samples were added to the appropriate wells. These were left to incubate for at least 2 hours at room temperature. Following this the plates were aspirated 5 times and for the BD Biosciences kits i.e., IL-6, TNFα, MCP-1 and CXCL10, 50µl of the working detector (detection antibody and streptavidin HrP) was added and left to incubate for a further hour. For the R&D kits, MPO and CCL19 ELISAs, the detection antibody and streptavidin were added to the plates in two separate steps separated by a 5-wash interval; the first involving the addition of the detection antibody to the wells followed by a 2 hour incubation period and the second involving the addition of the Strep-HrP to each well and a 20min incubation period. Following this the substrate solution was added to each well and the plate left to incubate for up to 45mins. Once complete 25µl of stop solution (1M sulfuric acid) was added and the plate was immediately analysed using a plate reader.

3   Biological age in AAV

3.1 Introduction

Biological ageing refers to a measure of molecular and cellular changes characteristic of physiological deterioration that are associated with chronological ageing [13]. With chronological age being one of the biggest risk factors for some of the world's most prominent disorders, the use of biological ageing in the risk assessment of age-related disease has become a novel and interesting area of research. AAV is a relapsing-remitting autoimmune disease that, unusually for an autoimmune disease, tends to develop later-in-life [133, 147, 190]. Several studies have also reported age-of-onset differences between AAV patients based on ANCA subtype i.e. between anti-MPO and anti-PR3 mediated AAV [192]. Although chronological ageing is widely accepted to be a risk factor for AAV, biological ageing is yet to be explored in the context of this disease.

Several measures of biological age have been described to date, however arguably the most accurate tools to measure this parameter are epigenetic clocks, specifically DNAm-based clocks which measure the methylation of a series of specific CpG sites along the genome and use computational algorithms and modelling to predict ageing [9, 10, 12, 13, 31, 32]. Perhaps the simplest and most cost effective of these clock models is the *ELOVL2* DNAm clock which measures the methylation surrounding a small number of sites within the *ELOVL2* gene promoter region, a gene whose methylation status is highly correlated with both chronological and biological ageing [12, 33, 34]. Importantly however, despite these clocks being considered a superior method of biological age analysis, the effect that environmental factors, such as treatment, have on these measures remains unclear. Very few studies to date have included treatment as a variable in their analysis, however those that have, have recognised the impact that pharmacological intervention can have on DNA methylation and epigenetic age acceleration [40][37]. Sehl *et al.,* for example, reported an increase in epigenetic age acceleration in breast cancer patients post chemotherapy and radiotherapy treatment [40]. In contrast to this, Fahy *et al.* showed that pharmacological intervention can decrease epigenetic ageing in a cohort of healthy male participants [37]. Further investigations into the effect of various treatment types on these clocks are clearly warranted as treatment history is a factor that is often overlooked in studies that use DNAm clocks to analyse biological ageing in a disease setting.

This study therefore aimed to explore biological age in the context of AAV using an *ELOVL2* clock model of epigenetic ageing. We investigated whether AAV patients exhibit DNAm-based age acceleration compared to healthy controls, whether biological ageing differs between anti-MPO and anti-PR3 mediated AAV patients and whether treatment with the anti-inflammatory drugs, cyclophosphamide and rituximab, two commonly used remission-induction therapies for the treatment of AAV, affects DNAm-based epigenetic ageing measures. With the continuous emergence of drugs such as senolytics that target certain age-associated biological processes [90, 96, 97, 221], whether the risks of chronological ageing translate onto a cellular level in AAV is of great interest and biological age modelling of AAV patients could provide further insight into the underlying pathogenesis of this disease.

3.2 Study Design and rational

3.2.1 Hypothesis

Chronological age is a well-recognised risk factor for AAV development however biological ageing is largely understudied in these disorders. We hypothesised that individuals diagnosed with AAV experience accelerated biological ageing, as measured by *ELOVL2* DNAm clock modelling, leaving them at increased risk of morbidity and mortality. Considering the differences in chronological age at diagnosis between anti-MPO and anti-PR3 mediated AAV, we also hypothesised that biological age differs depending on ANCA subtype. Furthermore, we suggest that induction treatment with either cyclophosphamide, a DNA alkylating agent, or rituximab, a monoclonal antibody that results in B cell depletion, may affect DNAm age measures in these patients.

3.2.2 Specific Aims

- To determine whether AAV patients experience DNAm epigenetic age acceleration compared to age-matched healthy controls.
- To determine whether epigenetic ageing differs between ANCA subtypes.
- To investigate the effect that treatment with cyclophosphamide and/or rituximab has on the epigenetic age of these patients.

3.2.3 Sample Selection

Whole blood EDTA samples were previously collected from AAV patients through the RKD biobank following the protocols outlined in section 2.7. DNA samples were isolated and stored from these patients. RKD databases were scanned for DNA samples collected from treatment naïve GPA/MPA participants that had either MPO or PR3 ANCA positivity and all available samples were selected for use in this study. Paired samples that had been collected following a first round of induction treatment with either cyclophosphamide and/or rituximab from the same patients were then identified and selected for use. Finally, age-matched healthy controls were chosen from available biobank samples.

3.2.4 Specific Methods

Validation analysis was carried out using epigenetic methylation array data obtained from collaborators in TILDA and The University of North Carolina, Chapel Hill, USA [134, 222]. *ELOVL2* analysis was undergone using samples obtained from participants recruited through the RKD biobank as outlined in section 2.7. Bisulphite conversion of DNA, PCR amplification and pyrosequencing were undergone as described in sections 2.8.1-2.8.4. qPCR was carried out following our method outlined in section 2.8.11.

3.2.5 Data Analysis and Statistical tests

Raw epigenetic data was processed and analysed using R (version 4.2.1) in collaboration with Matt McElheron. "DNAm Epigenetic Age" was modelled as previously described [12, 33]. In brief, multiple linear regression was used to model *ELOVL2* methylation as a predictor of chronological age in healthy control samples, adjusted for smoking status. This model was then used to generate "DNAm epigenetic age", the predicted age of an individual based on their *ELOVL2* methylation and smoking status;

$$Age_{DNA_m} = f(DNA_m, Smoking) = \hat{\beta}_0 + \hat{\beta}_1(DNA_m) + \hat{\beta}_{Smoking} + \hat{\epsilon}_i$$
$$where \ \epsilon \sim N(0, \hat{\sigma}^2)$$

Two conventional metrics of accelerated DNAm epigenetic age were derived; "Difference" referring to the absolute difference between the predicted age of an individual and their chronological age, and "Residual" referring to the residual of regressing predicted age over chronological age. In both metrics, a positive value refers to advanced accelerated ageing, while a negative implies decelerated ageing. Statistical analyses and visualization of epigenetic data was performed using R (version 4.2.1) and Python (version 3.9.7).

Genetic data was log transformed before analysis and normality was tested using a Shapiro-Wilk test. Spearman correlation analyses were used to determine correlation coefficients and statistical significance for each correlation. The strength of these correlations was defined following published guidelines with Spearman correlation coefficients greater than 0.5 deemed strong, those below 0.3 deemed weak associations while those between 0.3 and 0.5 are acknowledged as moderate associations [223, 224].

Statistical significance between cohorts was analysed using unpaired t tests with the exception of treatment analysis between paired treated and treatment naïve samples in which case paired t tests were utilised.

3.3 Results

3.3.1 Methylation of the *ELOVL2* Promoter Region can be used to Create Accurate DNAm Clocks

DNAm epigenetic clocks are extremely useful tools in the measurement of biological ageing [13]. However, many clocks require extensive sequencing of the genome which can be a very costly venture [225]. Various studies have therefore explored the use of single gene markers in the development of DNAm clocks [12, 33]. *ELOVL2* is a protein coding gene whose methylation has been shown to correlate strongly with chronological age and so, the methylation of several probes surrounding this gene alone has been used in multiple studies to estimate the chronological age of a biological sample [12, 33]. We therefore wanted to explore this approach of DNAm ageing and following statistical protocols outlined by Garagnani *et al.* we investigated the ability of 3 methylation sites along the *ELOVL2* promoter region (positions Chr6:1104466;ID cg21572722, Chr6:11044655;ID cg24724428 and Chr6:11044644;ID cg16867657) to predict biological ageing using previously acquired EPIC chip DNA methylation data from the TILDA dataset [12]. Using this model of DNAm ageing, each methylation probe analysed showed a strong and significant correlation with chronological age. In order to ensure that *ELOVL2* methylation analysis is also an appropriate measure of biological ageing, as opposed to simply chronological ageing, we correlated our DNAm age scores to the GrimAge, PhenoAge and Horvath clock scores previously measured in TILDA [222]. Epigenetic age as measured by markers of *ELOVL2*, GrimAge, PhenoAge and Horvath clock scores correlate strongly and significantly with each other (Figure 3.3.1). Finally, we tested the viability of these models on a small cohort of AAV patients using data obtained by Jones *et al.* in Chapel Hill [134]. Again, a strong and significant association with chronological ageing was found with *ELOVL2* DNAm age according to each probe (Figure 3.3.2) as well as strong and significant associations with the Horvath methylation age and PhenoAge calculated for each sample. Together these results validate the use of *ELOVL2* methylation clocks for biological age assessment.

Figure 3.3.1

(a.)

TILDA Participant Demographics	All	Males	Female
Sex (n)	498	252	246
Age, median (range)	61 (50-87)	61 (50-86)	62 (50-87)
CRP, median (range)	1.8 (1-112)	1.87 (1-112)	1.68 (1-40.35)
Creatinine, median (range)	78 (44-148)	86 (49-148)	69 (44-116)

(b.)
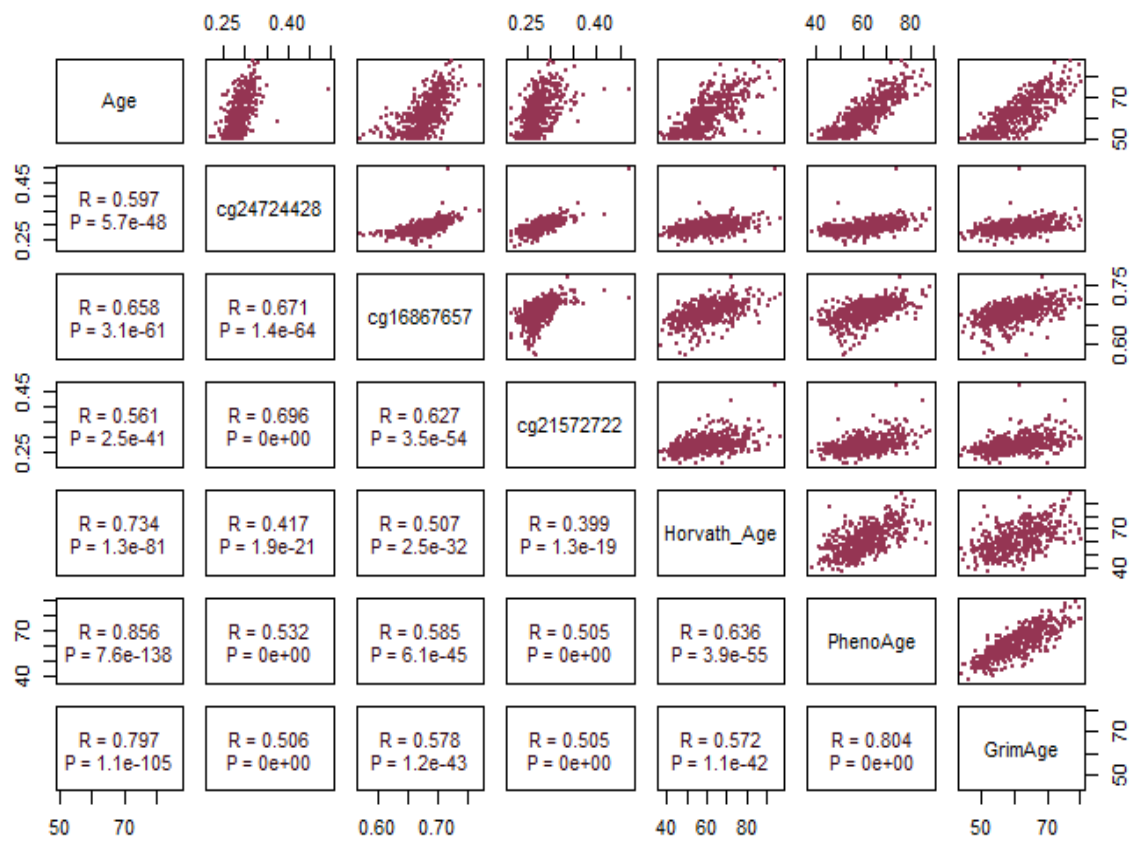
Figure 3.3.1 *ELOVL2* methylation age analysis of the TILDA Cohort.

Both demographic and methylation data previously acquired using the Illumina 850K EPIC methylation chip was obtained on a cohort of 498 older individuals. (a.) Basic demographic information of the TILDA sample cohort (b.) Correlations between epic methylation chip data on 3 specific methylation sites along the *ELOVL2* promoter (cg21572722, cg24724428 and cg16867657) chronological age, Horvath's age, PhenoAge and GrimAge of each individual. Spearman correlation analysis was used to generate correlation coefficient values (R values) and to determine the significance of these relationships (p values).

Figure 3.3.2:

(a.)

Chapel Hill Participant Demographics	HC	AAV Active	AAV Remission
n	4	9	9
Sex, Male: Female (%Male)	1:1 (50)	5:4 (56)	5:4 (56)
Age, median (range)	54.5 (47-57)	53 (24-82)	55 (27-85)
ANCA Specificity, Anti-PR3: Anti-MPO ratio	N/A	6:3	6:3

(b.)
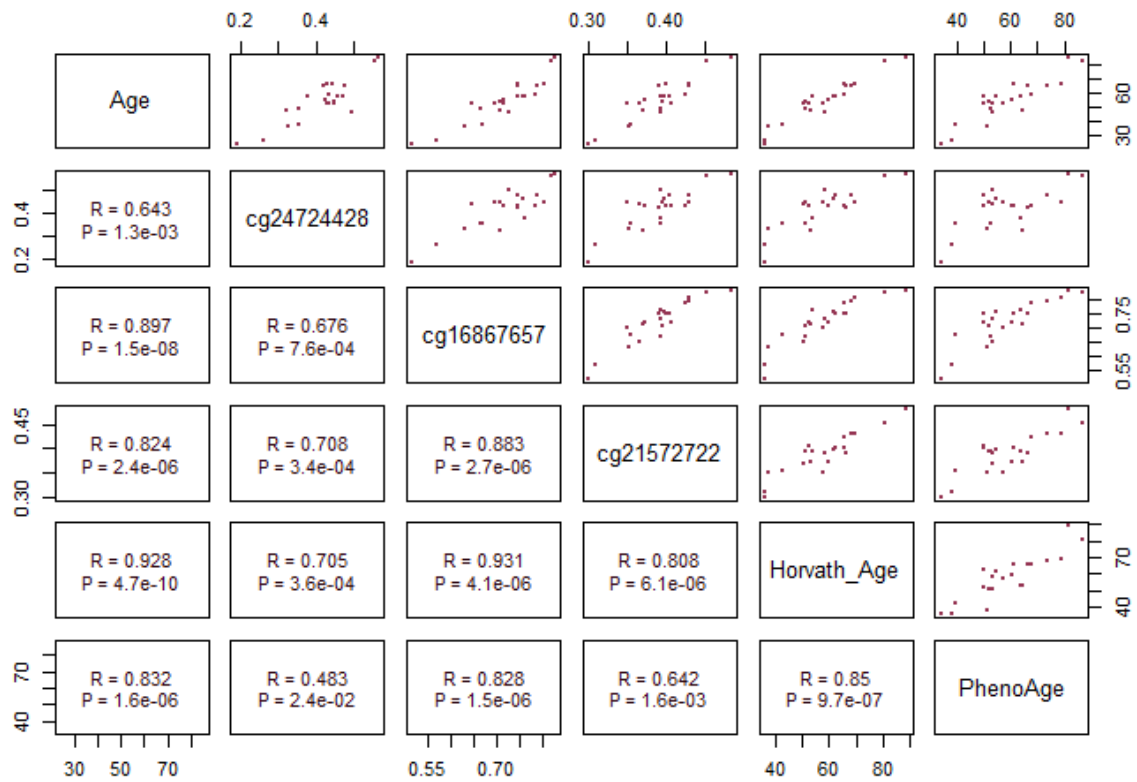
Figure 3.3.2 *ELOVL2* methylation age analysis in the Chapel Hill Cohort.

Both demographic and methylation data previously acquired using the Illumina 450K Infinium BeadChip was obtained on a cohort comprising 22 samples obtained from 13 individuals, 4 of which were healthy controls with the remaining 9 being AAV patients. (a.) Basic demographic information of the Chapel Hill sample cohort (b.) Correlations between epic methylation chip data on 3 specific methylation sites along the *ELOVL2* promoter (cg21572722, cg24724428 and cg16867657) chronological age, Horvath's age and PhenoAge of each individual. Spearman correlation analysis was used to generate correlation coefficient values (R values) and to determine the significance of these relationships (p values).

3.3.2 Participant Demographics

Once our proposed methods were validated, we selected a cohort of healthy controls and AAV samples to investigate. Demographic information on each participant used for this study is shown in the table below (Table 3.3.1). 142 DNA samples from 121 individuals were used in this study consisting of healthy controls (HC; n=24), treatment naïve (Txt N; n=97) and paired treated (Txt; n= 21) AAV patients. Treated samples consist of a sample matched to a treatment naïve sample from the same participant following their first encounter of induction treatment with either cyclophosphamide or rituximab. Doses prescribed to each participant vary.

Table 3.3.1:

Participant Demographics		HC	AAV Txt N		AAV Txt	
			Anti-MPO	Anti-PR3	Anti-MPO	Anti-PR3
n		24	58	39	9	12
Age, median (range)		62.5 (52-83)	72 (40-86)	60 (23-84)	69 (41-82)	59 (48-85)
Sex, Male: Female (%Male)		11:13 (46)	27:31 (47)	24:15 (62)	5:4 (56)	10:2 (83)
Smoking Status, n	Current	3	5	3	2	0
	Previous	16	23	15	5	8
	Never	5	23	11	2	4
	Unknown	0	7	10	0	0
AAV Diagnosis, *n* (%)	GPA	N/A	2 (3)	24 (62)	0 (0)	7 (58)
	MPA	N/A	56 (97)	15 (38)	9 (100)	5 (42)
BVAS, median (range)		N/A	14 (6-29)	17 (2-34)	0 (0)	0 (0)
CRP (mg/dL), median (IQR)		N/A	19 (6-55.5)	62 (24-198.25)	5 (1.5-30.5)	5 (1.75-7.25)
Creatinine (µmol/L), median (IQR)		N/A	286 (189-432)	166 (82-433)	163 (140-189)	126 (96-221)
Immunosuppression treatment, *n* (%)						
	Cyclophosphamide	N/A	N/A	N/A	4	4
	Rituximab	N/A	N/A	N/A	5	5
	Both	N/A	N/A	N/A	0	3

Table 3.3.1 Participants Demographics

Participants have been divided into either healthy control (HC), treatment naïve AAV patients (AAV Txt N) or treated AAV patients (AAV Txt). AAV patients are further subdivided by ANCA status (anti-MPO or anti-PR3). A summary of participant demographics including age, sex, and smoking status is shown as well as clinical characteristics such as AAV diagnosis, Birmingham Vasculitis Activity Score (BVAS), C-reactive protein (CRP) cytokine levels, creatinine and treatment type. IQR; interquartile range, N/A; not applicable.

3.3.3 Individuals with AAV Experience Epigenetic Age Acceleration and This Is Independent of ANCA Subtype

In order to explore biological ageing in AAV we measured the methylation status of 7 CpG sites surrounding the *ELOVL2* promoter region (positions Chr6:11044661, Chr6:11044655, Chr6:11044644, Chr6:11044647, Chr6:11044642, Chr6:11044640 and Chr6:11044634) following methods previously validated by Zbieć-Piekarska [33]. Multiple linear regression modelling using the mean methylation of all 7 CpG sites adjusted for smoking status was used to calculate epigenetic ageing in each sample. Epigenetic age acceleration (EAA) was calculated in each cohort using the residuals for each sample. With this model of DNAm ageing, we showed that Txt N AAV samples exhibit significantly increased DNAm epigenetic age compared to healthy controls (Figure 3.3.3a, i). Ageing residuals were also significantly higher in AAV patients compared to healthy individuals indicating accelerated biological age in these patients (Figure 3.3.3a, ii).

As multiple studies have reported differences in chronological age at diagnosis between anti-MPO and anti-PR3 mediated AAV we also investigated whether ANCA subtype affects DNAm ageing. DNAm age measures and EAA did not differ with ANCA specificity (Figure 3.3.3b).

Figure 3.3.3:

(a.)

(i.)

ELOVL2 Age Prediction

R = 0.66, p = 0.00044
R = 0.46, p = 0.00016

(ii.)

ELOVL2 Age Residual

p = 0.014

HC
AAV Txt N

(b.)

(i.)

ELOVL2 Age Prediction

R = 0.42, p = 0.0067
R = 0.55, p = 0.0098

(ii.)

ELOVL2 Age Residual

p = 0.23

Anti-MPO
Anti-PR3
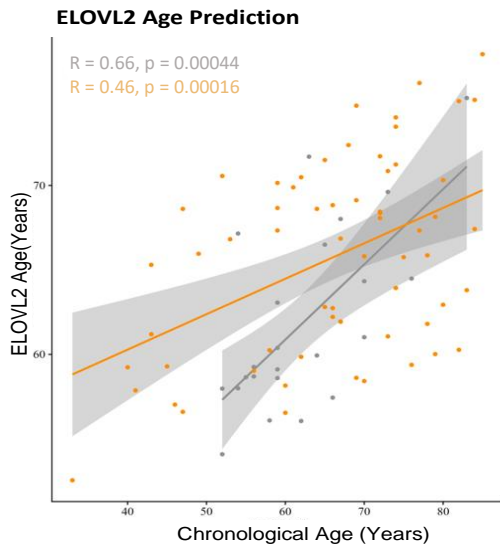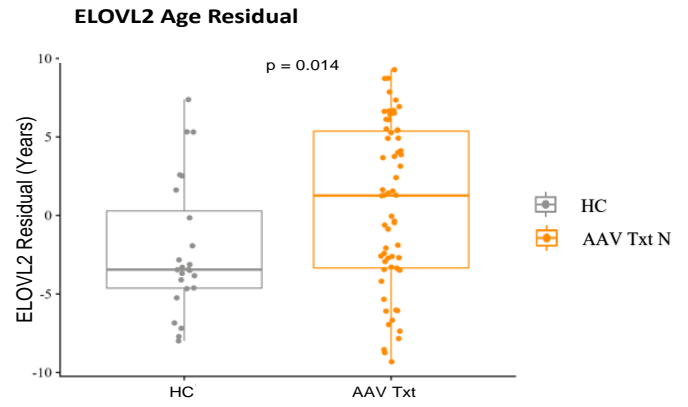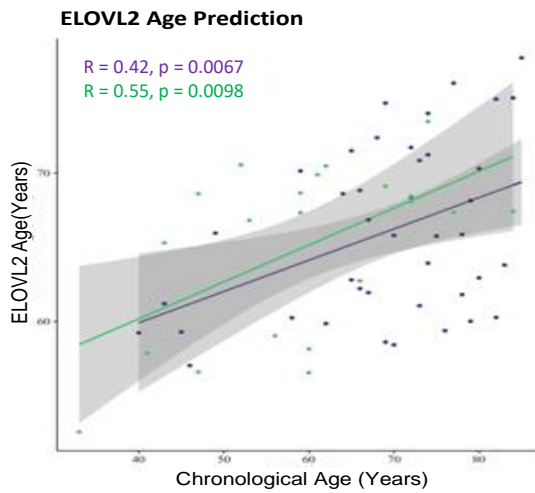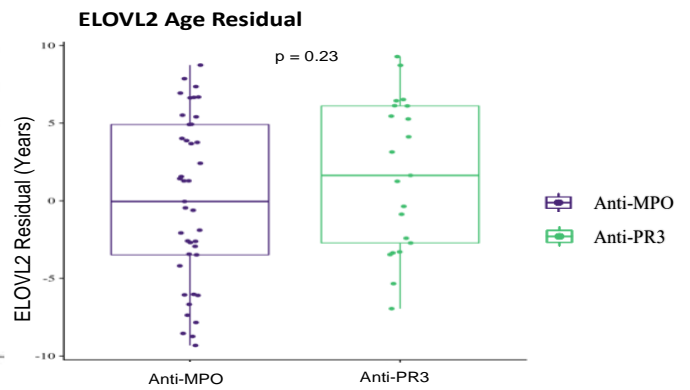
Figure 3.3.3: Analysis of *ELOVL2* DNAm age in Txt N AAV patients and healthy controls
Whole blood samples were obtained from treatment naïve AAV patients (AAV Txt N; n = 97) and age-matched healthy controls (HC; n = 24). DNA was extracted from each sample, bisulphite conversion and PCR amplification of the *ELOVL2* gene performed, followed by pyrosequencing to measure the methylation percentage of 7 CpG sites surrounding the *ELOVL2* promoter region. Simple multi-linear regression of this data was used to create a model for DNAm epigenetic ageing. (a.) (i) The correlation between epigenetic age and chronological age and (ii) the difference in EAA calculated between healthy controls (grey) and AAV Txt N patients (orange) measured using the residual. (b.) AA Txt N samples were further categorised as either anti-MPO AAV patients (Anti-MPO; n = 58) (purple) or anti-PR3 AAV patients (anti-PR3; n = 39) (green) (i) The correlation between epigenetic age and chronological age and (ii) the difference in EAA calculated between anti-MPO AAV patients and anti-PR3 AAV patients measured using the residual. Spearman correlation analysis was used to generate correlation coefficient values (R values) and to determine the statistical significance of these relationships (p values) while unpaired t tests were used to calculate statistical significance between calculated residuals (p value).

3.3.4 Induction Treatment with Cyclophosphamide and/or Rituximab Decreases DNAm Ageing in AAV Patients

The effect that immunosuppressive treatment has on epigenetic clock analysis remains unclear. AAV patients are routinely prescribed cyclophosphamide or rituximab as a remission induction therapy and, given their mechanisms of action, it is possible that these treatments will influence epigenetic ageing [152]. Interestingly, treatment was shown to significantly reduce DNAm epigenetic age in AAV patients, bringing each measure closer to those seen in healthy controls (Figure 3.3.4a). Despite treated patients being chronologically older than treatment naive patients, treatment naïve patient samples showed increased DNAm age and ageing residuals in comparison to their treated counterparts (Figure 3.3.4b). These results hold true for both cyclophosphamide and rituximab treated patients (Figure 3.3.4d). Although all anti-PR3 AAV samples showed a consistent decrease in DNAm epigenetic age and EAA following treatment, not all anti-MPO AAV samples followed this pattern with 3 individuals showing an increase in both DNAm epigenetic age and ageing residuals post-treatment compared to pre-treatment (Figure 3.3.4c).

Figure 3.3.4:
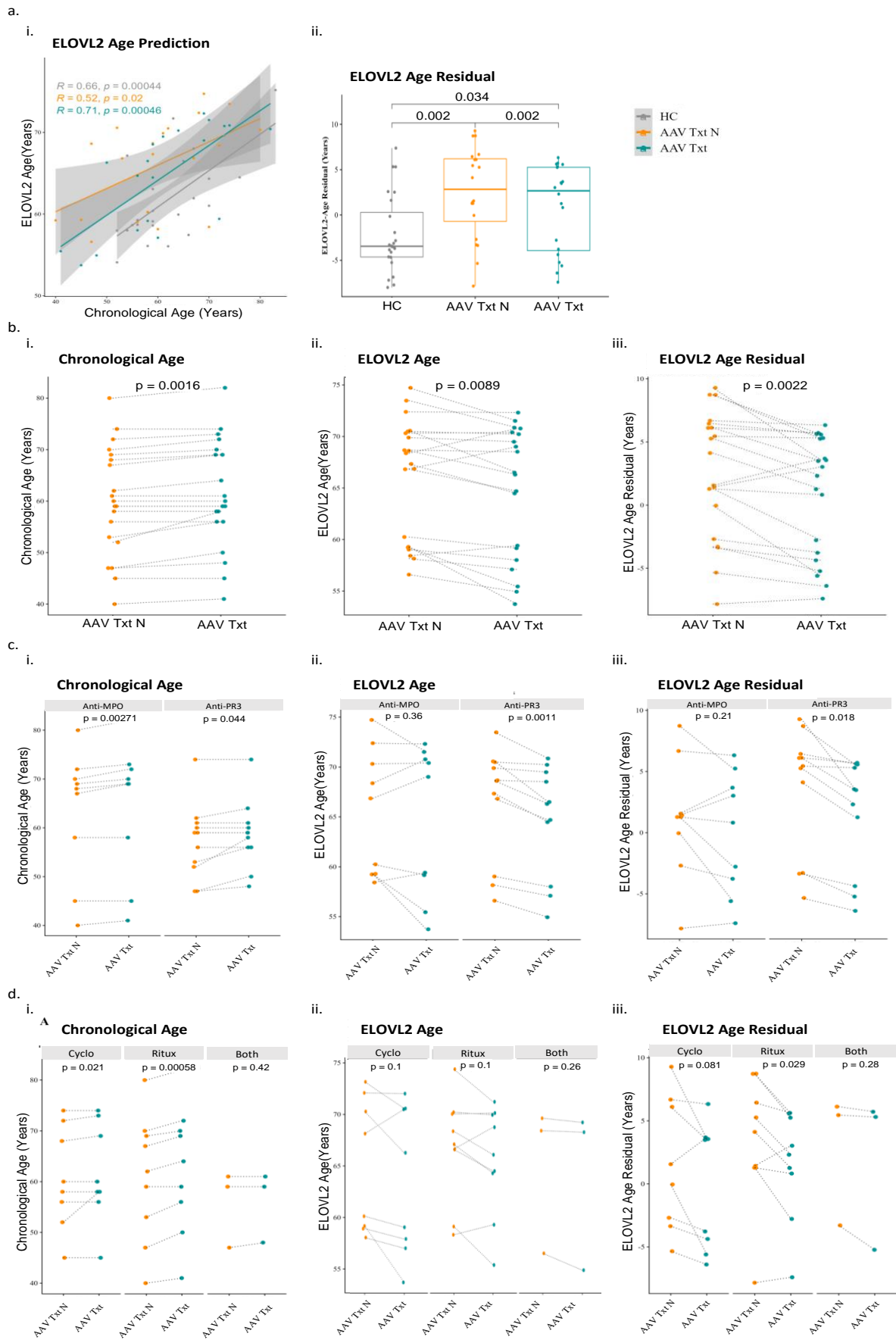
Figure 3.3.4 The effect of treatment on epigenetic age analysis

Whole blood samples were obtained from paired treatment naïve AAV patients (AAV Txt N) and treated AAV patients (AAV Txt) (n = 21) as well as age-matched healthy controls (HC; n = 24). DNA was extracted from each sample, bisulphite conversion and PCR amplification of the *ELOVL2* gene performed, followed by pyrosequencing to measure the methylation percentage on 7 CpG sites surrounding the *ELOVL2* promoter region. Simple multi linear regression of this data was used to create a model for DNAm epigenetic ageing. (a.) (i) The correlation between epigenetic age and chronological age and (ii) the difference in epigenetic age acceleration calculated between healthy controls (grey), AAV Txt N patients (orange) and AAV Txt patients (blue) as measured using the residual. (b.) The difference in (i) chronological age, (ii) epigenetic age and (iii) EAA, measured as a residual, calculated for each AAV patient pre- and post-treatment. (c.) The difference in (i.) chronological age, (ii) epigenetic age and (iii) EAA, measured as a residual, calculated for each AAV patient pre- and post-treatment categorised by ANCA subtype. (d.) The difference in (i.) chronological age, (ii) epigenetic age and (iii) EAA, measured as a residual, calculated for each AAV patient pre- and post-treatment categorised by treatment type. Spearman correlation analysis was used to generate correlation coefficient values (R values) and to determine the statistical significance (p values) of the relationships depicted in (a)(i). All remaining statistical analysis was preformed using either unpaired (healthy control vs AAV) and paired (Txt N vs Txt) student t test.

3.3.5 Epigenetic Age Acceleration Does Not Correlate with Markers of Systemic Inflammation, Disease Activity or Kidney Function

In order to investigate potential explanations for the effect that treatment has on AAV we correlated age residuals with CRP, a cytokine that is often used clinically to measure systemic inflammation (Figure 3.3.5a), the Birmingham Vasculitis Activity Scores (BVAS) for each patient, a score given to AAV patients based on their clinical symptoms at the time of sampling (Figure 3.3.5b) and creatinine a common biomarker of kidney function (Figure3.3.5c). Only weak correlations were noted between ageing residuals and each marker.

Figure 3.3.5:
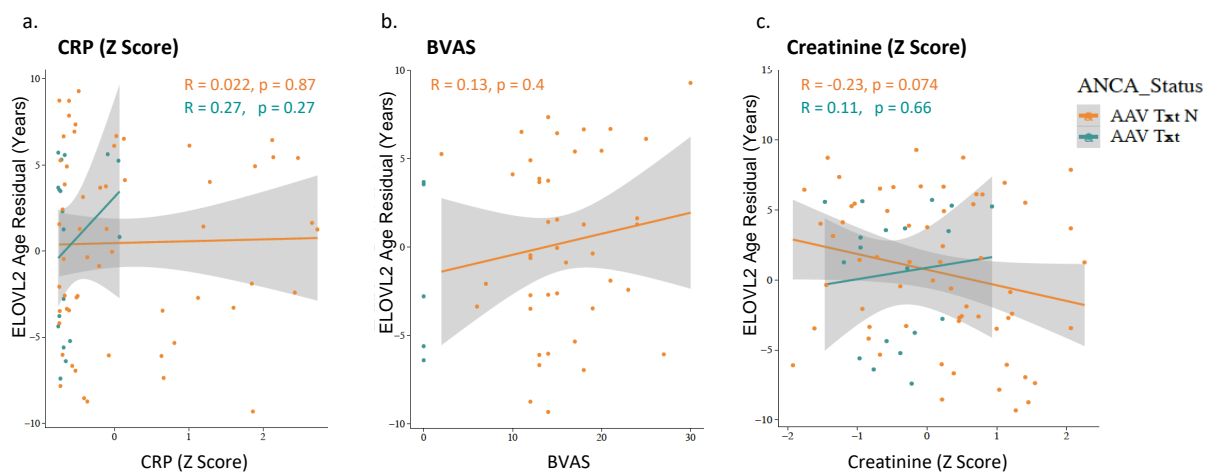
Figure 3.3.5: Correlation of epigenetic age acceleration with clinical measurements of AAV

EAA data, as measured by the residual, calculated for AAV Txt N (n = 97; blue) and AAV Txt (n = 21; orange) samples were correlated with matched (a.) CRP, (b.) BVAS and (c.) Creatinine levels. Spearman correlation analysis was used to generate correlation coefficient values, indicated in the table, and to determine the significance of these relationships. No strong or statistically significant correlations were observed.

3.3.6 Epigenetic Age Acceleration as Measured by *ELOVL2* is Independent of Whole Blood Composition and Sex

Blood cell composition is known to effect epigenetic clock measures. Treatment with both cyclophosphamide and rituximab is known to alter blood cell composition [13, 32]. For this reason, we correlated our results to individual cell counts for each sample. EAA does not correlate with total leukocyte (Figure 3.3.6a), neutrophil (Figure 3.3.6b), lymphocyte (Figure 3.3.6c), monocyte (Figure 3.3.6d), eosinophil (Figure 3.3.6e) or platelet (Figure 3.3.6f) counts.

Males have been reported to experience increased DNAm epigenetic age compared to females correlating to a greater risk of age-related mortality and morbidity [38, 226]. In order to assess any sex specific differences, we segregated male and female data and compared results. Although males did trend towards increasing EAA, as measured using residual values, in each of our cohorts, no significant differences were noted between sexes (Figure 3.3.7).

Figure 3.3.6:
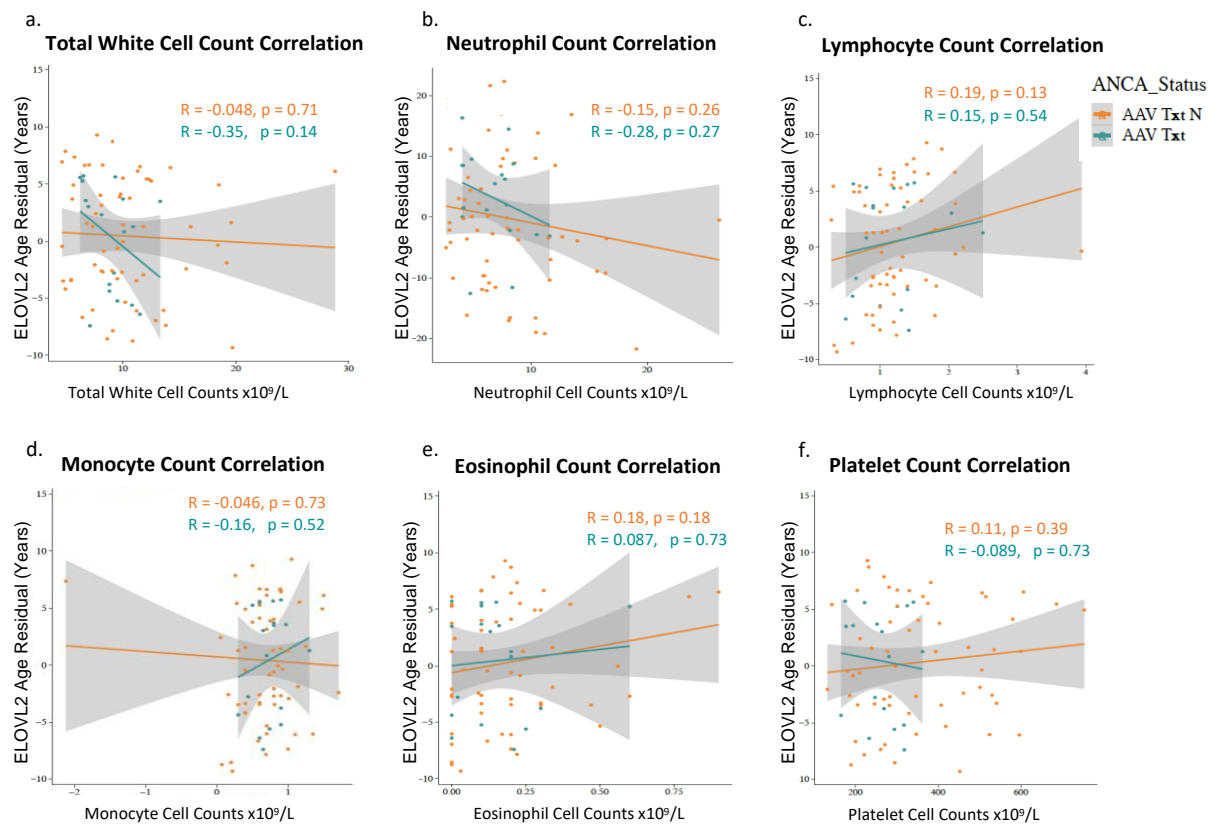
Figure 3.3.6: Correlation of DNAm epigenetic age acceleration with leukocyte cell counts in AAV patients

EAA data, as measured using residual values, calculated for AAV Txt N (n = 97; blue) and AAV Txt (n = 21; orange) samples were correlated with corresponding leukocyte cell counts measured for each participant upon sample collection. Cell count data includes (a.) total white blood cell counts, (b.) neutrophil cell counts, (c.) lymphocyte cell counts, (d.) monocyte cell counts, (f.) eosinophil cell counts and (f.) platelet cell counts. Spearman correlation analysis was used to generate the correlation coefficient values indicated in the table and to determine the significance of these relationships. No significant correlations were noted.

Figure 3.3.7:
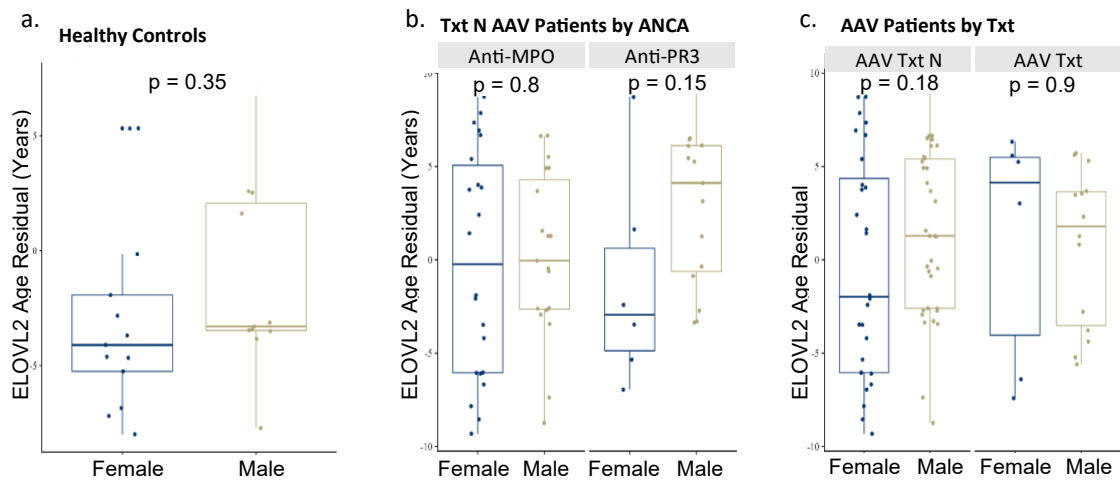
Figure 3.3.7: Sex-specific analysis of DNAm epigenetic age acceleration

EAA data calculated for each sample analysed in this study were analysed on the bases of sex. No differences between males or females were noted when analysing (a.) healthy control samples only, (b.) AAV Txt N samples segregated by ANCA subtype or (c.) AAV samples segregated by treatment status. Statistical analysis was preformed using a student t test.

3.3.7 *ELOVL2* Gene Expression is Significantly Diminished in AAV Patients Compared to Healthy Controls While a Trend Towards Increased *p21* Expression Occurs

In order to explore whether the methylation differences noted between AAV samples and healthy controls translate into transcriptional effects, *ELOVL2* gene expression was measured in a small cohort of individuals from whom we had collected an RNA sample paired to the DNA samples that underwent methylation analysis. AAV samples show significantly decreased *ELOVL2* gene expression compared to healthy controls (Figure 3.3.8a, i). *ELOVL2* gene expression was also shown to negatively correlate with the corresponding mean *ELOVL2* methylation percentages calculated for each sample (Figure 3.3.8a ii).

Decreased *ELOVL2* expression has been reported to result in increased cellular senescence. We therefore measured the expression of *p21*, a genetic marker of cellular senescence, in our cohort. A trend towards increasing *p21* expression in AAV samples was seen compared to HC however this did not reach statistical significance (p=0.13) (Figure 3.3.8b).

Figure 3.3.8:
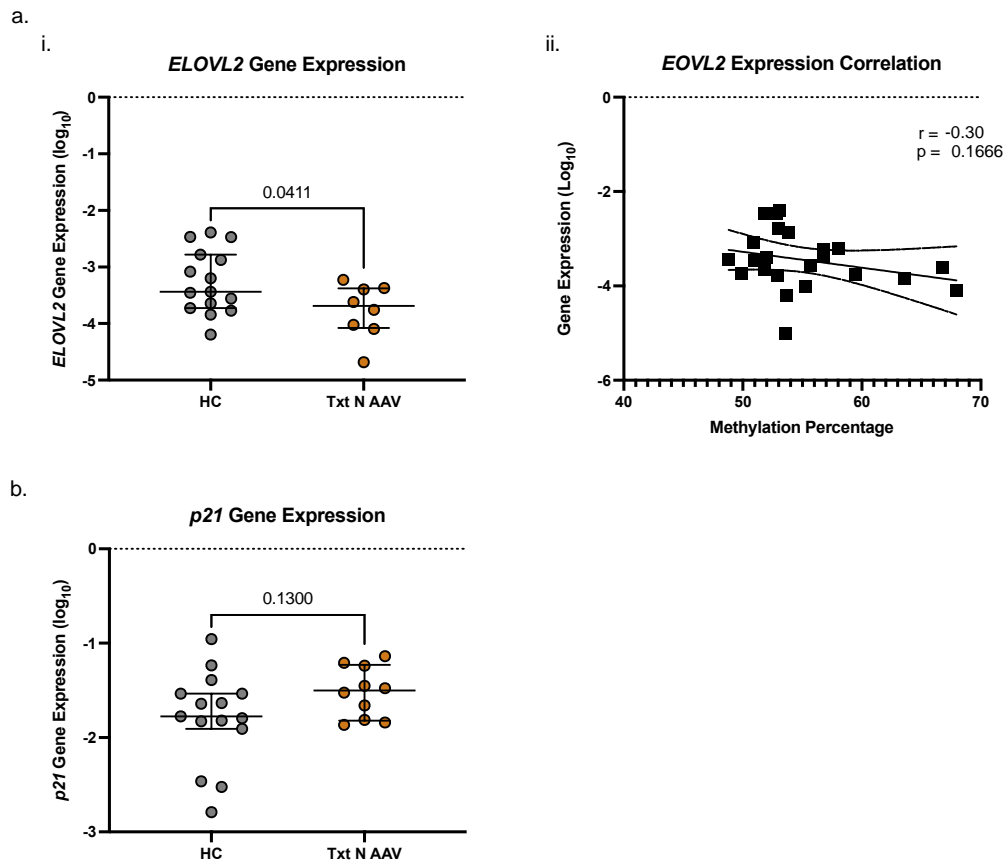
Figure 3.3.8: *ELOVL2* and *p21* Gene Expression in AAV compared to HC.

RNA samples were obtained from healthy controls (HC; n=15) and treatment naïve AAV patients (Txt N AAV; n=10). qPCR was used to quantify gene expression and all data is shown relative to the expression of the endogenous control gene *RPL27* and analysed following the delta CT method. (a.) Relative gene expression of (i) *ELOVL2* and (ii) the correlation of these values with their corresponding *ELOVL2* percent methylation. (b) Relative gene expression of *p21*. Gene expression data are represented as a log transformed value. Unpaired t tests were used to analyse statistical significance between our healthy control and Txt N AAV cohort while Pearson correlations were used to calculate correlation coefficients and statistical significance for the correlation analysis.

3.4 Discussion

ANCA-associated vasculitis is a set of autoimmune diseases that, unusually, occur later-in-life, making chronological age a major risk factor for these disorders. Despite this, biological ageing, a much stronger predictor of age-related morbidity and mortality, has been largely overlooked in AAV. In this study we show for the first time that AAV patients experience accelerated biological ageing as measured by our *ELOVL2* DNAm clock model suggesting a role for age related mechanisms in the development and progression of this disease.

As there is growing evidence and support to further categorise AAV according to ANCA subtype as well as there being multiple reports that indicate a younger chronological age of onset for anti-PR3 AAV compared to anti-MPO AAV, we investigated differences in DNAm epigenetic age between the 2 subtypes. Although no significant differences were noted between our anti-MPO and anti-PR3 AAV samples in terms of DNAm epigenetic age or EAA, differences in EAA in response to treatment were seen between the two groups. We noted that in contrast to anti-PR3 AAV patients, anti-MPO AAV patients do not show a significant decrease in EAA following treatment. Interestingly anti-MPO AAV patients have been reported to have worse outcomes and a lower response to treatment compared to anti-PR3 AAV patients and this may be reflected in our results [184, 186].

It is very important to note however, that this perceived difference regarding the response to treatment between anti-MPO and anti-PR3 AAV patients was driven by the presence of three individuals that, in contrast to every other donor, displayed increased EAA post treatment compared to pre-treatment. More specific analysis regarding ANCA subtype and titres, BVAS, CRP, creatinine, cell counts, sex, treatment type, treatment dose and time from treatment were undergone on these individuals in comparison to all other samples with the only point of commonality noted between these individuals being ANCA subtype; all three individuals were shown to be anti-MPO positive AAV patient donors. There are however many other variables that may have influenced these results including organ and tissue involvement, the presence of comorbidities, vasculitis damage index scores, ethnicity, socio economic status etc. Unfortunately, with such small numbers it may be difficult to draw any conclusions from this data.

We found that treatment with either cyclophosphamide or rituximab abrogates DNAm age acceleration in AAV patient samples. In a report published by Fahy *et al.*, treatment of healthy male adults with recombinant rhGH in combination with DHEA and metformin resulted in decreases in DNAm epigenetic ageing [37]. Fahy *et al.* also noted that markers of systemic inflammation and local morbidity as well as changes in the immune landscape of these individuals occurred post-treatment, indicating a potential link between inflammation and epigenetic ageing [37]. Although similar decreases in DNAm epigenetic age were observed in our AAV cohort following treatment, quite surprisingly, when correlating the EAA of these patients to measures of inflammation, kidney function, disease activity and immune blood cell composition, no strong or significant correlations were noted leaving us uncertain of the mechanisms that drive these treatment effects. The extent to which DNAm epigenetic age is influenced by inflammation is thus unclear, however, we should note that the three individuals who showed increasing EAA following treatment showed only minor changes in CRP compared to other participants indicating a lower systemic effect on inflammatory outcomes compared to other individuals' post-treatment.

In terms of the mechanistic implications of these results and how they may translate biologically we should report on the primary function of *ELOVL2* itself. *ELOVL2* is a gene that codes for a protein involved in very long chain polyunsaturated fatty acid (VLC-PUFA) formation (Figure 3.4.2). A recent paper by Li *et al.* investigated the mechanistic effects of *ELOVL2* depletion in mice and how these drive accelerated ageing [34]. They showed that *ELOVL2* depletion results in an ageing phenotype in mice accompanied by mitochondrial dysfunction, stem cell exhaustion and increased cellular senescence; three hallmarks of biological ageing. Intriguingly, immunomodulation with eicosapentaenoic acid, a PUFA, has been reported to support the treatment of autoimmune small vessel vasculitis [227]. As well as this, our lab group has shown in unpublished work, that monocytes stimulated with ANCA produce significantly increased levels of alpha-linolenic acid and arachidonic acid (Figure 3.4.1), precursor molecules in the PUFA chain. A similar increase in precursor short chain fatty acid build-up was also noted by Li *et al.* in *ELOVL2* knock out mice. In order to investigate this further we measured *ELOVL2* gene expression in a number of AAV samples and healthy controls. We have shown that AAV patients express lower levels of *ELOVL2* compared to healthy controls and that this expression negatively correlates with *ELOVL2* methylation status implicating a potential

transcriptional effect of *ELOVL2* methylation. We also went on to measure a DNA marker of cellular senescence, *p21*, in this cohort and although not statistically significant, a trend towards increased *p21* gene expression was noted in AAV patients compared to healthy controls. We therefore suggest that AAV patients, potentially mediated by the presence of ANCAs, show increased *ELOVL2* methylation and decreased *ELOVL2* gene expression resulting in the inability to complete PUFA formation and a build-up of small-chain fatty acids. This may result in mitochondrial dysfunction, stem cell exhaustion and increased cellular senescence in AAV patients resulting in age-related morbidity.

Figure 3.4.1:
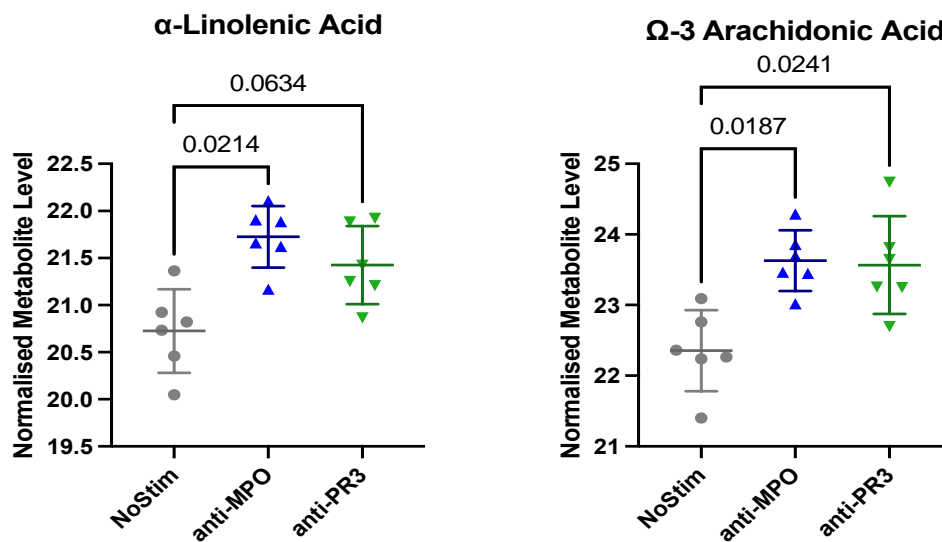
Figure 3.4.1: Metabolic Changes in Isolated Monocytes in Response to ANCA Stimulation CD14+ monocytes were isolated from PBMCs of healthy controls by MACS separation (n=6). Cells were plated and stimulated at 37°C for 4 hours with 5μg/ml monoclonal antibody (mAb) directed against either MPO or PR3. ANCA- monocytes were analysed by Liquid chromatography-mass spectrometry and untargeted metabolomic analysis was completed. Significantly altered features present in all samples of all four treatment groups were annotated based on accurate mass and isotopic distribution, ID scores >70 were analysed by 2-way ANOVA with a Benjamini-Hochberg FDR correction. Log2 and BCA-normalised AUC values for significantly altered metabolites are displayed as individual dot plots. All related data was created and analysed by Dr. Emma Leacy.

There are certain strengths and limitations to note with this work, primarily in relation to sample numbers. Although we have relatively large sample numbers considering the rarity of AAV, when splitting these patients further into anti-MPO and anti-PR3 and

treated versus treatment naïve samples we begin to lose statistical power, and this may diminish the significance of potential differences. Despite sample numbers being relatively low for our treatment group, the fact that these were paired to a treatment naïve sample taken from a single individual across two time points, is a true strength of this analysis. Furthermore, in terms of quantifying DNAm epigenetic age, clocks that require whole methylome analysis may be considered as more accurate predictors of biological age compared to *ELOVL2* clocks, accounting for hundreds of methylation sites as opposed to those surrounding a single gene marker. However, *ELOVL2* has been well validated as an accurate biomarker of both chronological and biological ageing in previous studies and indeed we found a strong correlation between *ELOVL2* methylation clocks, chronological age, GrimAge, PhenoAge and Horvath methylation age using both the TILDA cohort and Chapel Hill Cohort, validating its use in our study [12, 33].

The question remains as to whether these clocks may be good predictors of relapse in AAV this is an avenue that we hope to further explore with future work. Our results also further promote questions regarding the effect of treatment on epigenetic age analysis. Do all drug types effect DNAm epigenetic clock measures? How long will the impact of these medications persist? What is the underlying driver of these differences? What other environmental factors effect epigenetic clock measures? And given these unanswered questions, how reliable are DNAm epigenetic clock models as biological ageing predictors in disease or infectious setting?

3.5 Conclusion

Overall, this work shows for the first time that AAV patients experience accelerated biological ageing as measured by an *ELOVL2* DNAm clock model and that treatment of these patients decreases this effect. These results suggest a role for age-associated processes in the development and progression of AAV and these should be investigated further in order to understand the underlying pathology of this disease.

Figure 3.4.2:
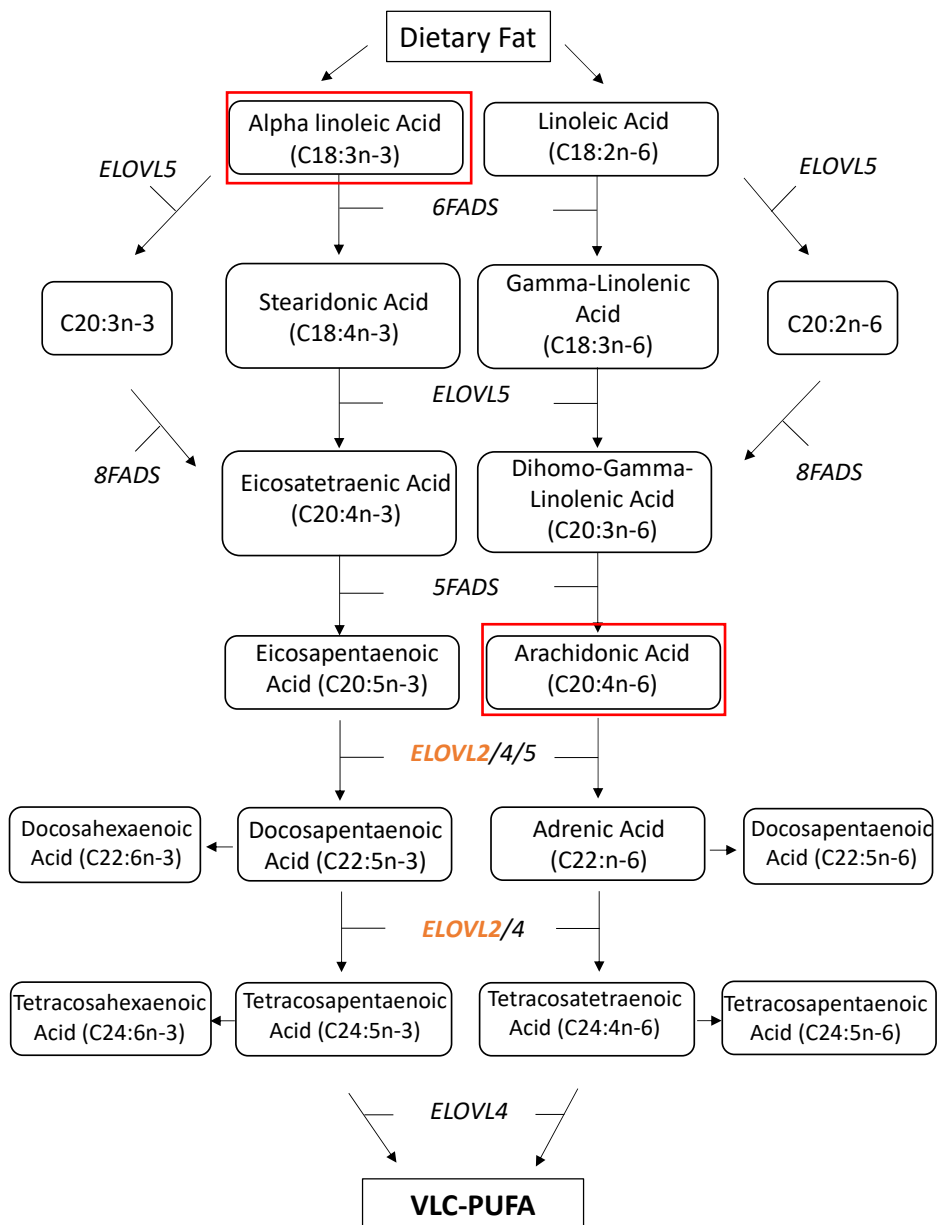
Figure 3.5.1: VLC-PUFA formation pathway

The positioning of ELOVL2 protein (orange) in the VLC-PUFA pathway. Red boxes indicate fatty acids that were shown to be increased in isolated monocytes in response to ANCA stimulation.

4 The Effects of Age on Immune Functions with Respect to AAV

4.1 Introduction

Inflammation, specifically of the small vasculature, is a primary characteristic of ANCA-associated vasculitis and this is often thought to be mediated by the presence of autoantibodies anti-MPO and anti-PR3 [146]. Binding of these ANCAs to their protein targets, present on the surface of immune cells such as monocytes and neutrophils, has been shown to initiate a rapid onset inflammatory response [47, 174, 228][182]. Interestingly and unusually for an autoimmune disorder, AAV predominantly affects older individuals [133, 147, 190]. Despite ageing having a major impact on immune processes, the influence that ageing has with regards to specific AAV immunopathology remains unclear.

Ageing is known to be accompanied by changes to both the innate and adaptive immune systems. While adaptive immune responses generally decline with age in a process known as immunosenescence, innate immune responses are reported to become persistently activated, resulting in a low-grade chronic inflammation, a phenomenon referred to as inflammageing [67, 71, 99]. This phenomenon is characterised by a systemic low-level production and release of pro-inflammatory mediators and can contribute to the development and progression of most age-related diseases [80][78, 79][75][76, 77]. Emerging research is now linking age-related processes such as inflammageing with the development of autoimmune diseases later-in-life [229]. Inflammageing has been suggested to act as a cell priming agent, with monocytes, neutrophils, NK cells and dendritic cells all contributing towards an inflammatory environment characteristic of autoimmune diseases [107, 112, 116-118, 120].

With this in mind, the impact that age-related immune processes have on the pathogenesis of AAV is unclear, particularly regarding response to ANCA stimulation. Pro-inflammatory cytokines, such as IL-6 and TNFα, that are associated with inflammageing, are upregulated in AAV patients, and are thought to contribute to disease activity [230-233]. Age-related severity of AAV has been explored in mouse models of AAV with studies indicating increased systemic inflammatory cytokine production in aged mice compared to younger controls contributing to a more severe prognosis in these mice. [234]. In 2021, Alikhan *et al.* reported enhanced immune responses in older mice

following MPO immunisation compared to younger mice, and this was an ANCA specific observation. Although this study focused on adaptive immune responses, the authors did refer to the likelihood of innate immune changes contributing to their results [83]. Whether these observations translate into human research remains unknown.

With the current surge in ageing and age-modifying studies as well as the availability of drugs, such as senolytics, that target age-related immune processes, further investigation into immune-ageing in AAV, and in particular the responsiveness of immune cells from older donors to ANCAs, could provide important new insights regarding the immunopathology of this disease as well as provide potential therapeutic options for patients.

4.2 Design and rational

4.2.1 Hypothesis

Despite ageing being a significant risk factor for AAV, the impact that ageing has on the immune response to ANCA remains largely unexplored. Immune cells involved in the pathogenesis of AAV such as monocytes and neutrophils can be impacted by age and the effect that this may have in response to ANCA stimulation is unknown. We therefore hypothesise that age related changes to these key immune cells results in aberrant responses to ANCA stimulation, potentially enhancing inflammatory responses and thus leaving older individuals more susceptible to AAV development.

4.2.2 Specific Aims

- To determine whether PBMCs and neutrophils isolated from older individuals show increased inflammatory cytokine production in responses to ANCAs compared to those isolated from younger individuals.
- To examine NETosis and ROS production by neutrophils and PBMCs from younger and older individuals in response to ANCA stimulation.
- To investigate whether ANCA stimulation can induce cellular senescence and whether this differs with age.
- To explore whether surface expression of MPO and PR3 on monocytes and neutrophils changes with age

4.2.3 Sample Selection and Criteria

Healthy younger (<35 years old) and older (>60 years old) participants were recruited, consented and logged following the RKD biobank protocols. Participants were asked to fill out a health status survey prior to sample collection (Appendix 1). All participants were self-proclaimed as healthy. All individuals were free from any form of chronic kidney disease, diabetes, cancer, chronic inflammatory disorders, autoimmune disease, chronic infection, impaired mobility etc. Participants reported to be capable of walking ¼ mile without any issues and were free from infection/vaccination for at least 2 weeks prior to sample collection. Individuals with steroid, immunosuppressant or NSAID treatment were excluded. Blood and urine samples were collected from these individuals

for both immediate use in this project as well as storage in the RKD biobank for downstream studies.

4.2.4   Specific Methods

Neutrophils and PBMCs were isolated and processed following the methods outlined in section 2.9. ELISAs on supernatants were performed following the protocols described in section 2.10.5. qPCRs on cell pellets were performed following protocols in sections 2.8.5, 2.8.7-2.8.11. Microscopy was carried out using the protocols outlined in section 2.10.1. Flow cytometry to measure NETosis and ROS production was performed on both the BD FACS CANTO II and Luminex Cellstream flow cytometers in accordance with the protocols in section 2.10.2-2.10.3. Flow cytometry to look at MPO or PR3 surface expression was performed on whole blood samples using the FACS CANTO II following section 2.10.4.

4.2.5   Data Analysis and Statistical Tests

NETosis was quantified from fluorescent microscopy data using ImageJ Fiji analysis software. Flow cytometry data was analysed using either Kaluza software for BD FACs CANTO II exported FCS files or the Luminex Cellstream analysis software for Luminex Cellstream exported FCS files. All data was subsequently graphed and statistically analysed using GraphPad Prism v9.1.1. Shapiro-Wilk tests were used to determine normality. All data was found to be non-normally distributed. Due to the inclusion of incomplete data sets, paired one-way ANOVA analysis was deemed unfeasible between paired stimulated samples. Therefore, statistical significance between each cohort was determined using either Kruskal-Wallis one-way ANOVA, with Dunn's post hoc multiple comparison tests or Mann-Whitney t tests.

4.3 Results

4.3.1 Cohort Characteristics

A total of 56 participants were recruited for this study comprising of 27 younger individuals (<35 years old) and 29 older individuals (>60 years old). Of those recruited, two participants (one younger and one older) were excluded from the analysis due to a self-reported history of chronic illness. This resulted in a final cohort of 54 individuals, all of whom met our healthy control criteria outlined in section 4.2.3. A female bias was noted in both the younger (65%) and older (64%) cohorts (Table 4.3.1).

Table 4.3.1:
Cohort Summary

		Younger	*Older*
Participants (n)		26	28
Age, median (range), years		24 (19-35)	69 (60-86)
Male, *n* (%)		9 (35)	10 (36)
Smoking status, n (%)	Current	0 (0)	3 (11)
	Never	21 (81)	17 (61)
	Previous	2 (8)	8 (28)
	Unknown	3 (11)	0 (0)

Table 4.3.1: Cohort Summary
All participants have been classified as healthy controls having met our inclusion criteria. Participants have been categorised into two cohorts, younger (<35 years) and older (>60 years), based on age. A summary of the median age, sex and smoking status breakdown is provided on each cohort.

4.3.2 ANCA stimulation significantly increases inflammatory cytokine release, and this response differs by age and ANCA subtype

Inflammageing and age-related morbidity is often associated with elevated levels of inflammatory cytokines such as IL-6 and TNFα. Whether age has an effect on primary immune cells stimulated with ANCAs remains unclear. We thus examined the expression of these two inflammageing-associated cytokines at both a transcriptional and translational level in PBMCs stimulated with ANCAs (anti-MPO and anti-PR3), positive controls (PMA/LPS) and negative controls (UN/IgG) that had been isolated from either healthy younger (<35yrs) or older (>60yrs) donors (Figure 4.3.1. & 4.3.2).

In order to validate our assay and confirm ANCA specific responses, samples stimulated with either positive controls (LPS and PMA) or negative controls (isotype IgG) were analysed with respect to unstimulated samples. As expected, LPS significantly increased *IL6* gene expression (Figure 4.3.1a, i) and protein concentration (Figure 4.3.1a, ii). PMA stimulation increased *TNFA* gene expression (Figure 4.3.1a, iii) and protein concentration (Figure 4.3.1a, iv). No transcriptional or translational changes were seen for either cytokine in response to stimulation with the IgG control (Figure 4.3.1a). No significant differences were noted regarding baseline expression for either cytokine between younger and older participants (Figure 4.3.1b).

Having validated our assay design, we analysed IL-6 and TNFα production in response to ANCA stimulation of isolated PBMCs. Anti-MPO stimulation resulted in no change to *IL6* gene expression (Figure 4.3.2a, i) while resulting in significantly elevated IL-6 protein concentration (Figure 4.3.2a, iv) compared to the isotype control. No significant differences in gene (Figure 4.3.2a, i) or protein concentration (Figure 4.3.2a, iv) were noted in response to anti-PR3 stimulation. *IL6* gene expression from PBMCs stimulated with anti-MPO was significantly increased the older cohort compared to the younger controls (Figure 4.3.2a, ii) and a similar trend was noted for IL-6 protein concentration (Figure 4.3.2a v). No differences in response to anti-PR3 stimulation were noted between our two age cohorts at either a gene (Figure 4.3.2a iii) or protein level (Figure 4.3.2a iii&vi).

Both anti-MPO and anti-PR3 were capable of significantly upregulating TNFα gene (Figure 4.3.2b, i) and protein expression (Figure 4.3.2b iv) relative to the negative control. There were no significant differences in anti-MPO driven *TNFA* gene expression in PBMCs from older versus younger donors, however a trend towards significance was noted, likely driven by several individuals in the older cohort who mounted very high anti-MPO induced *TNFA* expression (p=0.09)(Figure 4.3.2b, ii). This difference is mirrored in TNFα protein concentration with PBMCs isolated from older individuals showing significantly higher TNFα protein production in response to anti-MPO compared to those isolated from younger donors (Figure 4.3.2b, v). No differences in TNFα gene expression or protein concentration were noted with age in response to anti-PR3 stimulation (Figure 4.3.2b, iii&vi).

Figure 4.3.1:

a.

i.

IL6 Gene Expression

ii.

IL-6 Protein Concentration

iii.

TNFA Gene Expression

iv.
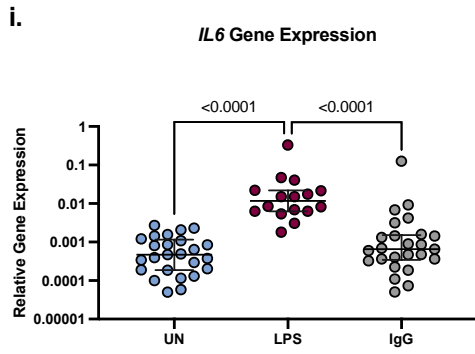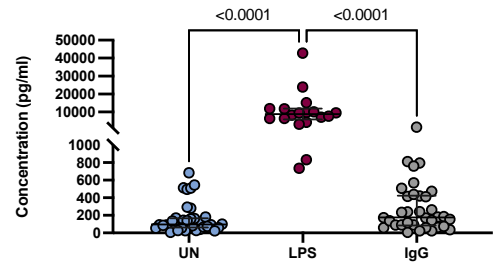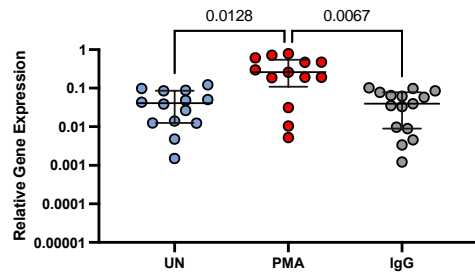
TNFa Protein Concentration
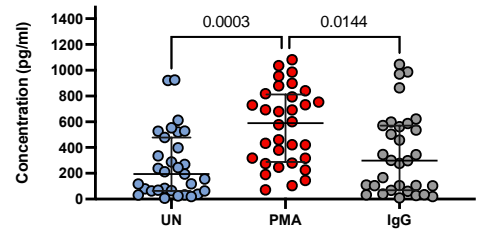
b.

i.

IL6 Gene Expression
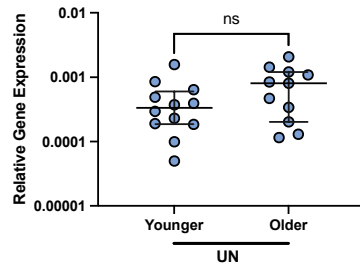
ii.

IL-6 Protein Concentration

iii.

TNFA Gene Expression

iv.
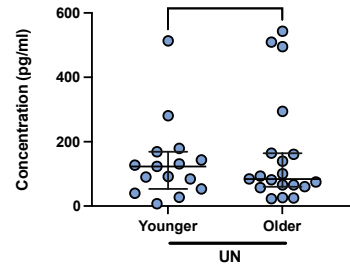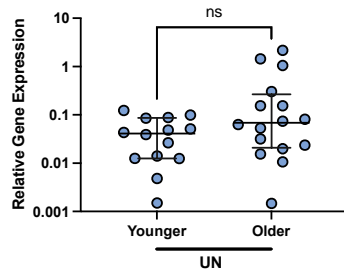
TNFa Protein Concentration
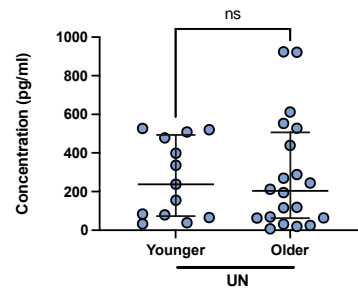
Figure 4.3.1: Assay control and baseline analysis of pro-inflammatory cytokine production
Whole blood samples were collected from healthy younger (n=15) and older (n=20) donors and PBMCs were isolated from each sample. PBMCs were stimulated for 4 hours with either 100ng/ml LPS or PMA, 5μg/ml isotype IgG control or left unstimulated (UN). qPCR was used to quantify gene expression and data was made relative to the expression of the endogenous control gene *RPL27* following the delta delta CT method. Cell supernatants were used to measure protein concentration using ELISA. (a.) Unstimulated (UN; blue) and stimulated (LPS; maroon, PMA; red, IgG; grey) sample analysis. (i.) *IL6* gene expression measurements. (ii) IL-6 protein concentration. (iii) *TNFA* gene expression measurements. (iv) TNFα protein concentration. (b.) Baseline comparisons of younger and older donors. (i.) *IL6* gene expression measurements. (ii) IL-6 protein concentration. (iii) *TNFA* gene expression measurements. (iv) TNFα protein concentration. Each point on the graph represents an individual sample. Whole horizontal lines represent the median and interquartile range (IQR) of each cohort. Statistical analysis was performed using One-Way ANOVA with Dunn's multiple comparison testing or using Mann-Whitney t tests. No significance (ns).

Figure: 4.3.2

a.
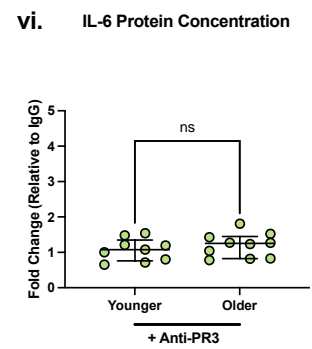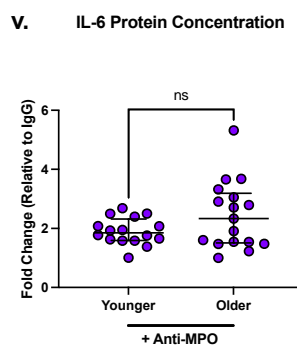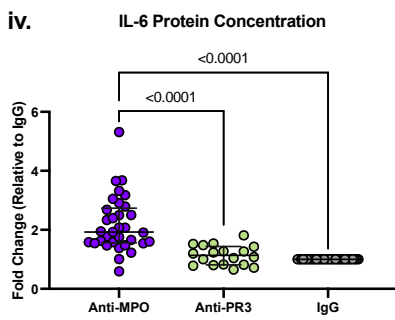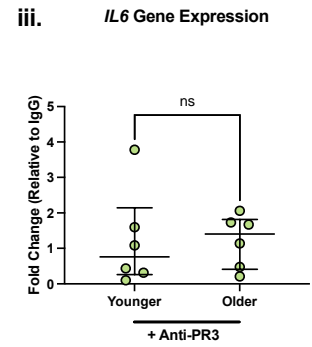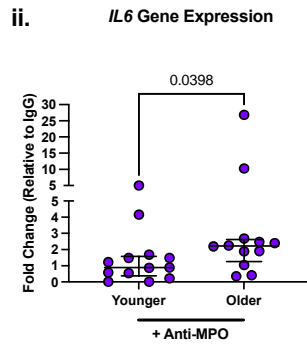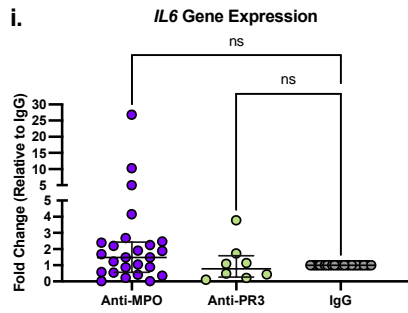
b.
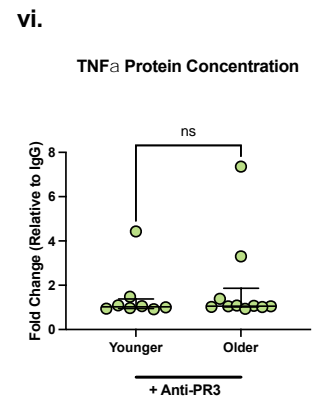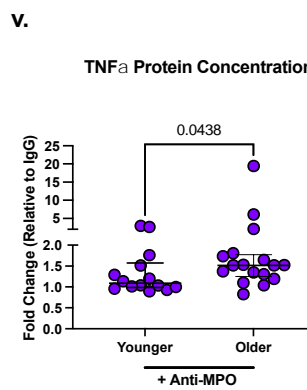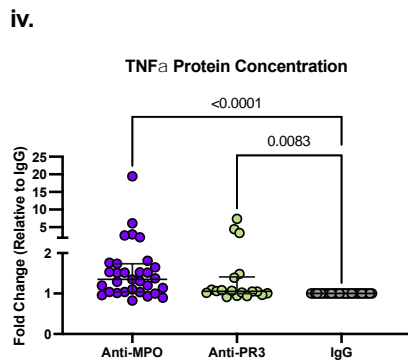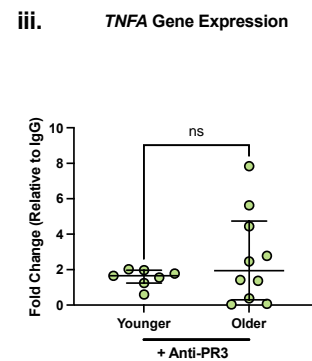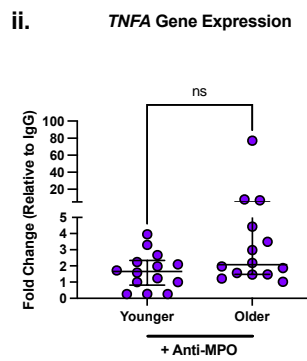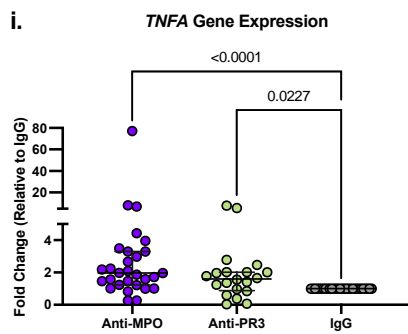
Figure 4.3.2: Pro-inflammatory cytokine production in response to ANCA stimulation with age

Whole blood samples were obtained from healthy younger (n=15) and older (n=20) donors and PBMCs were isolated from each sample. PBMC were stimulated for 4 hours with either 5 μg/ml isotype IgG control, 5μg/ml anti-MPO mAb or 150μg/ml anti-PR3 mAb. qPCR was used to quantify gene expression from RNA extracted from cell lysates and data was made relative to the expression of the endogenous control gene *RPL27* following the delta delta CT method. Cell supernatants were used to measure protein concentration using ELISA. (a.) *IL6* gene expression measurements and protein concentration and (b.) *TNFA* gene expression measurement and protein concentration for samples stimulated with either anti-MPO (purple) or anti-PR3 (green) expressed relative to the IgG control (grey). (i.) Gene expression changes in response to stimulation. (ii.) Gene expression differences in response to anti-MPO stimulation between the younger and older cohorts. (iii.) Gene expression differences in response to anti-PR3 stimulation between the younger and older cohorts. (iv.) Protein concentration changes in response to stimulation. (v.) Protein concentration differences in response to anti-MPO stimulation between the younger and older cohorts. (vi.) Protein concentration differences in response to anti-PR3 stimulation between the younger and older cohorts. Each point on the graph represents an individual sample. Whole horizontal lines represent the median and IQR of each cohort. Statistical analysis was performed using One-Way ANOVA with Dunn's multiple comparison testing or using Mann-Whitney t tests. No significance (ns).

4.3.3 NETosis can be accurately measured using flow cytometry

In order to measure both NETosis and ROS production from isolated neutrophils using a single assay, a modified version of a protocol outlined by Zharkova *et al*. in 2019 that utilises Sytox and DAPI to quantify NETosis was followed. As NETosis is traditionally measured using microscopy, in order to validate our flow cytometry method as an accurate measure of NETosis we isolated and stimulated neutrophils from a small cohort of healthy donors and prepared a subset of these cells for NETosis analysis using fluorescent microscopy, while the remaining sample was simultaneously prepared for flow cytometry analysis. Results were compared and contrasted. NET structures were clearly visualized via the colocalization and expansion of Hoechst dye (blue) and anti-histone antibody (red) following fMLP and anti-MPO stimulation in a time dependent manner using our fluorescent microscopy technique (Figure 4.3.3). For our flow cytometry method, NETs were quantified following the gating strategy outlined previously by Zharkova *et al*. Briefly, total cells were gated on using FSC and SSC gates followed by singlets using either FSC H and FSC A (BD FACs CANTO) or aspect ratio FSC and area FSC (Luminex Cellstream). CD45+ leukocytes were selected and, from this population, CD15+ neutrophils. These cells were then analysed based on DAPI and Sytox red positivity. Double positive cells at this point were deemed to be NETosing neutrophils (Figure 4.3.4). fMLP and anti-MPO stimulation showed a time dependent increase in NETosis rates while the UN and IgG control showed little to no increase for both fluorescent microscopy (Figure 4.3.5a, i) and flow cytometry (Figure 4.3.5a, ii) analysis. Microscopy and flow cytometry NETosis data correlated strongly with one another (Figure 4.3.5b).

Figure 4.3.3:
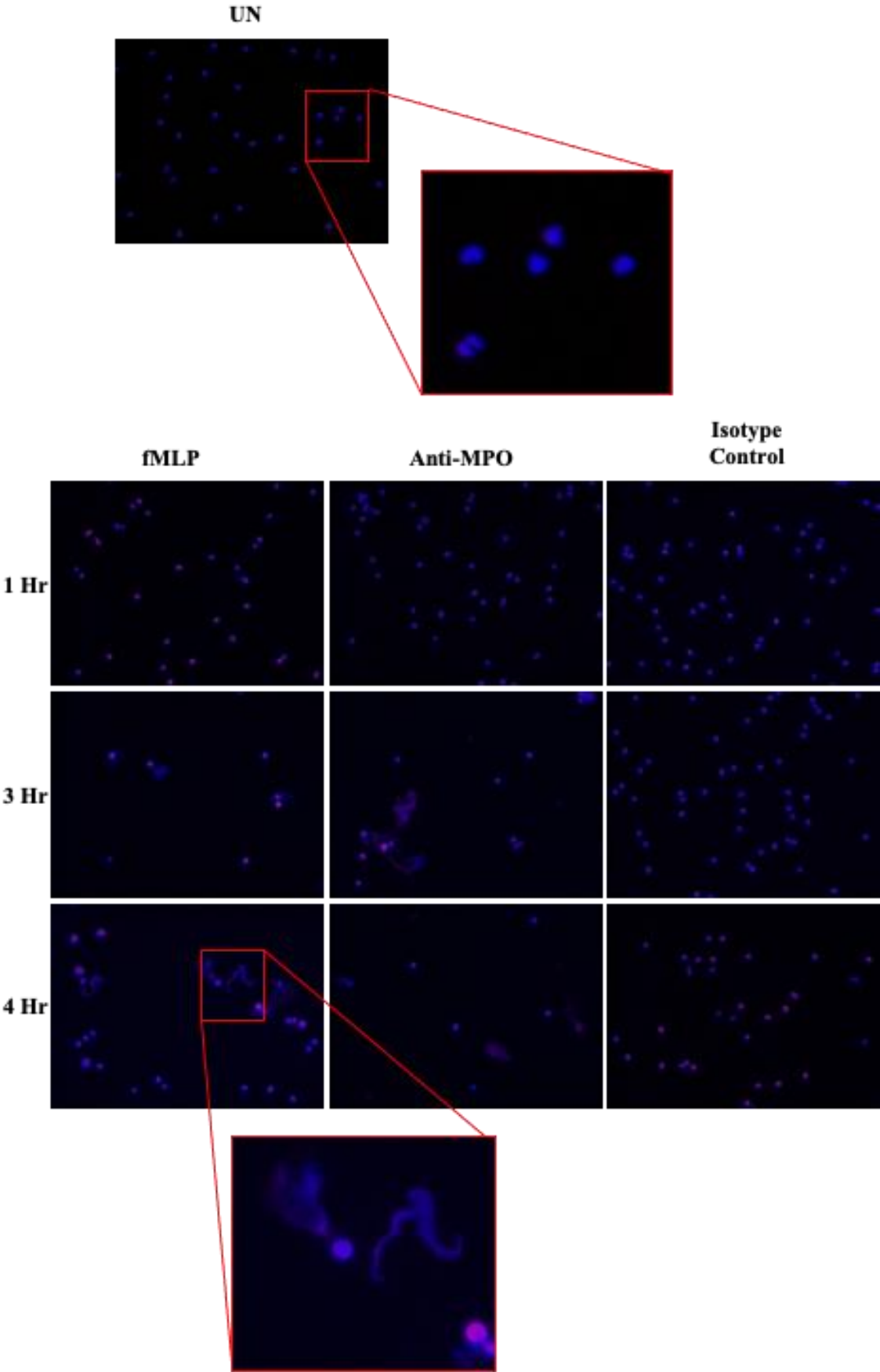
Figure 4.3.3: Microscopy images of neutrophils and NETosis

Whole blood samples were obtained from healthy donors (n=3) and neutrophils were isolated from each sample. Neutrophils and NET structures were visualized using Hoechst dye (blue) and anti-histone antibody (red) following stimulation with 5μg/ml of either fMLP, anti-MPO or isotype control for either 1hr, 3hr or 4hr.

Figure 4.3.4:
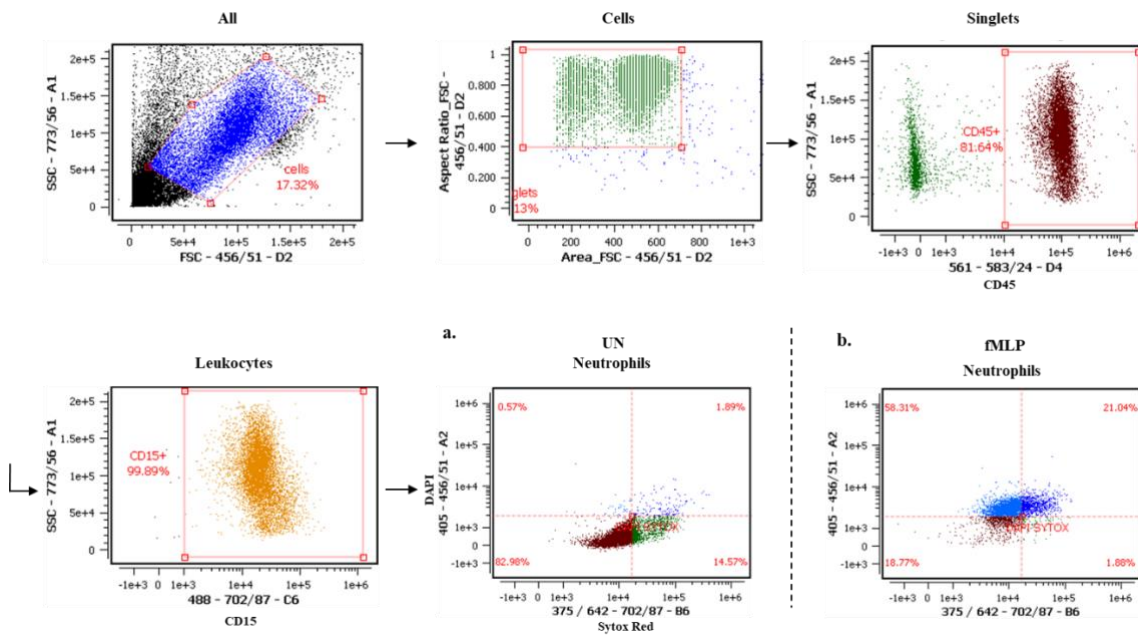
Figure 4.3.4 Flow cytometry gating strategy for NETosis quantification

Total cells were gated on using FSC and SSC gates followed by singlets using aspect ratio FSC and area FSC. Further selection of CD45+ leukocytes and CD15+ neutrophils was performed. Cells were then analysed for DAPI and Sytox red positivity with double positive cells being deemed NETosing neutrophils. (a.) NETosis gating in an unstimulated (UN) sample. (b.) NETosis gating in an fMLP stimulated sample.

Figure 4.3.5:

a.

(i.)

NETosis Rate Measured by Fluorescent Microscopy

(ii.)

NETosis Rate Measured by Flow Cytometry

b.

(i.)

UN

Spearman r = 0.5

(ii.)

IgG

Spearman r = 1

(iii.)

fMLP

Spesrman r = 1

(iv.)

ANTI-MPO

Spearman r = 1
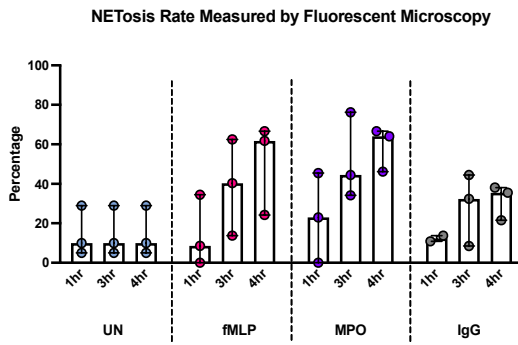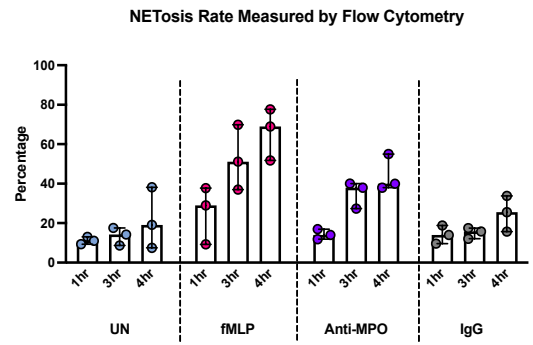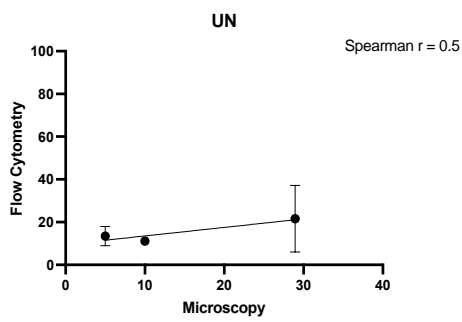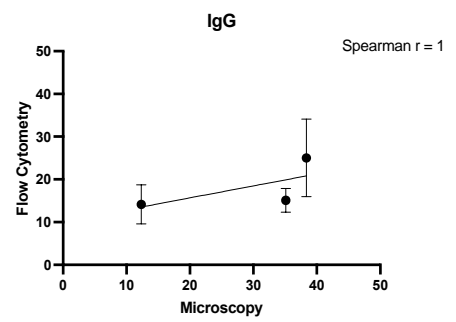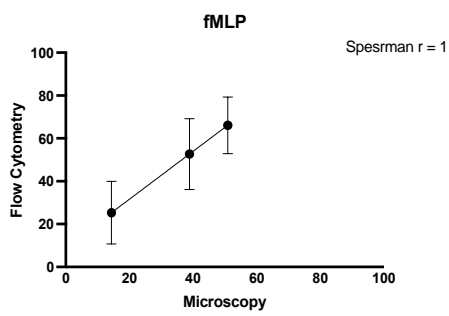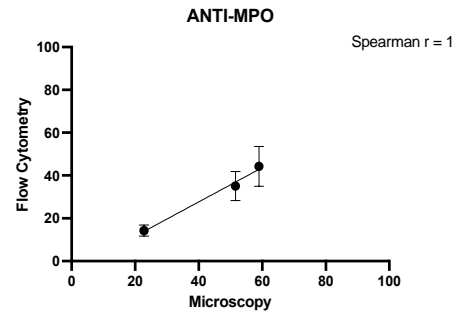
Figure 4.3.5 Comparison of NETosis quantification using microscopy and flow cytometry analysis methods.

Whole blood samples were obtained from healthy controls (n=3) and neutrophils were isolated from each donor. Neutrophils were left unstimulated (blue) or stimulated with 5μg/ml of either fMLP (pink), anti-MPO (purple) or isotype control (grey) for either, 1hr, 3hr or 4hr and NET structures were quantified using both fluorescent microscopy and flow cytometry and results were compared and contrasted between the two methods. (a.)(i) NETosis rate quantified using fluorescent microscopy. (ii.) NETosis rate quantified using flow cytometry. (b.) Correlations between NETosis data generated by flow cytometry and microscopy in (i) unstimulated samples, (ii) IgG stimulated samples, (iii) fMLP stimulated samples and (iv) anti-MPO stimulated samples. Whole horizontal lines represent the median and IQR of each cohort. Spearman analysis was used to calculate correlation coefficients.

4.3.4 No differences in NETosis or degranulation were noted with age in response to ANCA stimulation

NETosis and degranulation are important neutrophil responses that are reportedly dysregulated with age [112, 113]. Interestingly, they are also noted to contribute to the pathogenesis of AAV. Again, the effect that age has on these functions in response to ANCA stimulation is unknown. We therefore aimed to measure these outcomes in neutrophils isolated from either healthy younger (<35yrs) or older (>60yrs) donors stimulated with ANCAs (anti-MPO and anti-PR3), a positive control (fMLP) and negative controls (UN/IgG). NETosis rates were measured using our previously validated flow cytometry method of NETosis analysis while ELISAs to calculate MPO release was used as a surrogate marker of degranulation.

NETosis rates were significantly increased following stimulation with fMLP while no difference from the unstimulated samples were noted following stimulation with an IgG control (Figure 4.3.6a, i). Although not significant, older donors trended towards increased baseline levels of NETosis compared to younger donors (p=0.058) (Figure 4.3.6a, ii). Both anti-MPO and anti-PR3 stimulation were found to significantly increase NETosis rates relative to the isotype control (Figure 4.3.6b, i). No differences in NETosis rates were noted in response to either anti-MPO or anti-PR3 stimulation between the younger and older cohorts (Figure 4.3.6b, ii-iii).

MPO release from isolated neutrophils was measured as a surrogate marker of degranulation. Again, our positive control, fMLP, was shown to significantly increase MPO release from neutrophils while no differences in degranulation were noted between the unstimulated and IgG control measures (Figure 4.3.7a, i). No differences in baseline MPO release were identified with age (Figure 4.3.7a, ii). Specific analysis of ANCA stimulation revealed that anti-PR3 stimulation was capable of significantly upregulating MPO release (Figure 4.3.7b, i). Interestingly, we noted that MPO release was decreased in response to anti-MPO stimulation of isolated neutrophils. No differences in degranulation were noted between younger or older donors in response to anti-MPO or anti-PR3 stimulation (Figure 4.3.7b ii-iii). As this was an unexpected finding, we further analysed the efficacy of the assay in response to anti-MPO stimulation. Supernatants from neutrophils that had previously been stimulated with fMLP and then further spiked with anti-MPO were analysed. These samples showed significant decreases in MPO

concentrations compared to the same sample stimulated with fMLP alone (Figure 4.3.7c) suggesting a technical fault with our assay in response to anti-MPO stimulation and so results from this specific stimulation should be disregarded.

Figure 4.3.6:

Figure 4.3.6: NETosis rates with age in response to ANCA stimulation:

Whole blood samples were collected from healthy younger (n=23) and healthy older (n=24) donors and neutrophils were isolated from each sample. Isolated neutrophils were left unstimulated or stimulated for 4 hours with either 5μg /ml fMLP, 5μg /ml isotype IgG control, 5μg /ml anti-MPO mAb or 150μg /ml anti-PR3 mAb. NETosis was quantified using flow cytometry through the detection of DAPI+Sytox+ cells. (a.) (i.) NETosis rates of assay control samples; UN (blue), fMLP (pink) and IgG (grey). (ii) Baseline comparison of NETosis rates between the younger and older cohorts. (b.) (i.) NETosis rates in response to ANCA stimulation; anti-MPO (purple) and anti-PR3 (green). (ii.) Differences in NETosis between the younger and older cohorts in response to anti-MPO stimulation. (iii.) Differences in NETosis between the younger and older cohorts in response to anti-PR3 stimulation. Data is expressed as either (a.) a percentage relative to the CD15+ Neutrophil gate or (b.-c.) as a fold change relative to the IgG control data. Each point on the graph represents an individual sample. Whole horizontal lines represent the median and IQR of each cohort. Statistical analysis was performed using One-Way ANOVA with Dunn's multiple comparison testing or using Mann-Whitney t tests. No significance (ns).

Figure 4.3.7:

a.

i.

MPO Protein Concentration

ii.

MPO Protein Concentration

b.

i.

MPO Protein Concentration

ii.

MPO Protein Concentration

iii.

MPO Protein Concentration

c.

MPO Protein Concentration

Figure 4.3.7 Degranulation rates with age in response to ANCA stimulation

Whole blood samples were obtained from healthy younger (n=15), and healthy older (n=16) individuals and neutrophils were isolated from each donor. Isolated neutrophils were left unstimulated or stimulated for 4 hours with either 5µg/ml fMLP, 5µg/ml isotype IgG control, 5µg/ml anti-MPO mAb or 150µg/ml anti-PR3 mAb. Degranulation was quantified via MPO release using an ELISA. (a.) (i.) MPO protein concentration of assay control samples; UN (blue), fMLP (pink) and IgG (grey). (ii) Baseline MPO concentration comparison between younger and older cohorts. (b.) (i.) MPO concentration in response to ANCA stimulation; anti-MPO (purple) and anti-PR3 (green). (ii.) Differences in MPO concentration between the younger and older cohorts in response to anti-MPO stimulation. (iii.) Differences in MPO concentration between the younger and older cohorts in response to anti-PR3 stimulation. (c.) MPO concentration measured in fMLP stimulated samples compared to that measured in matched fMLP stimulated, anti-MPO spiked samples. Data is expressed either (a.) as a concentration or (b., c.) as a fold change relative to the IgG control data. Each point on the graph represents an individual sample. Whole horizontal lines represent the median and IQR of each cohort. Statistical analysis was performed using One-Way ANOVA with Dunn's multiple comparison testing or using Mann-Whitney t tests. No significance (ns).

4.3.5 Neutrophils show elevated ROS production in response to ANCA stimulation with age but CD14+ monocytes do not

ROS production is an innate immune response that when dysregulated can result in extensive cellular damage and death. It is a process that is commonly reported to become dysregulated during AAV contributing to the vascular damage noted in these patients. The uncontrolled production of ROS species is also associated with ageing, inflammageing and multiple age-associated diseases. The potential effect that age has on ROS production by immune cells in response to ANCA stimulation is unknown. With this in mind, we measured ROS production in either neutrophils and/or CD14+ monocytes, as gated on by flow cytometry from PBMC samples stimulated with ANCA (anti-MPO and anti-PR3), positive controls (fMLP/PMA) and negative controls (UN/IgG) that had been isolated from either healthy younger (<35 years) or older (>60 years) donors. Figure 4.3.8 outlines the gating strategy used to evaluate ROS production in isolated neutrophils. Figure 4.2.9 outlines the gating strategy used to evaluate ROS production from CD14+ monocytes.

Again, our assay controls showed expected changes in ROS production with fMLP and PMA leading to significantly increased ROS production from isolated neutrophils (Figure 4.3.10a, i) and CD14+ monocytes (Figure 4.3.10c, i) but no differences between the unstimulated and isotype controls were noted. No baseline differences in ROS production were noted from either neutrophil (Figure 4.3.10a, ii) or CD14+ monocytes (Figure 4.3.10c, ii) between the younger and older cohorts.

Both anti-MPO and anti-PR3 significantly increased ROS production from isolated neutrophils relative to the isotype control (Figure 4.3.10b, i). Neutrophils isolated from older individuals displayed increased ROS production compared to those isolated from younger individuals in response to anti-PR3 stimulation (Figure 4.3.10b, iii) but not anti-MPO stimulation (Figure4.3.10b, ii).

ROS production from CD14+ monocytes was significantly increased in response to anti-MPO stimulation only, while no significant increases from baseline were noted with anti-PR3 stimulation of PBMCs (Figure 4.3.10d, i). No significant differences in ROS production were noted between our two age groups in response to ANCA stimulation (Figure 4.3.10d ii-iii).

Notably, anti-MPO was shown to be a superior driver of ROS production in both neutrophils and CD14+ monocytes (Figure 4.3.10), resulting in significantly increased ROS levels in comparison to anti-PR3 stimulations.

Figure 4.3.8:
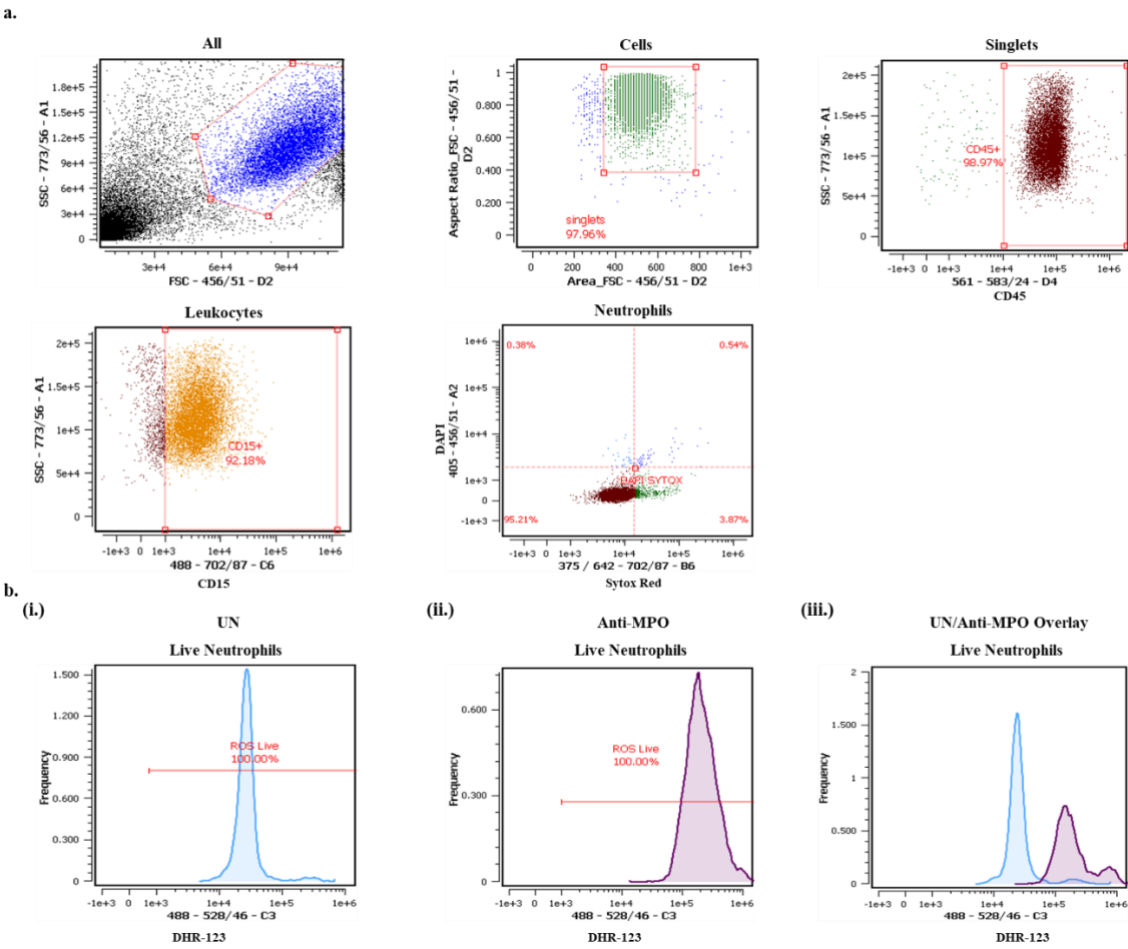
Figure 4.3.8: Flow cytometry gating strategy for quantifying ROS Production in isolated neutrophils

(a.) Total cells were gated on using FSC and SSC gates followed by singlets using aspect ratio FSC and area FSC. Further selection of CD45+ leukocytes and CD15+ neutrophils was performed. DAPI and Sytox red negative live cells were selected, and ROS production quantified as the median fluorescent intensity (MFI) of DHR-123 for these cells. (b.) (i.) ROS production in an UN sample. (ii.) ROS production in a corresponding anti-MPO stimulated sample. (iii) Overlay of ROS production in an UN (blue) and anti-MPO (purple) stimulated sample.
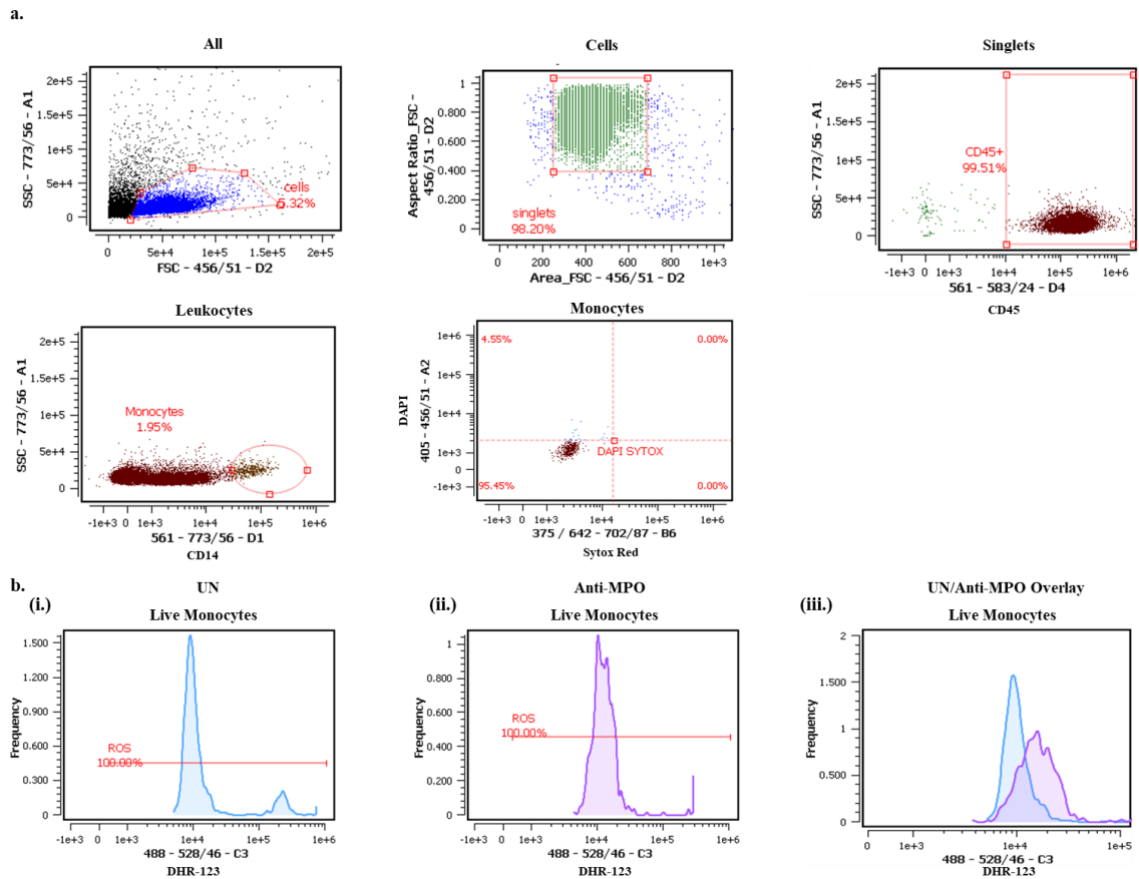
Figure 4.3.9: Flow cytometry gating strategy for quantifying ROS Production in monocytes (a.) Total cells were gated on using FSC and SSC gates followed by singlets using aspect ratio FSC and area FSC. Further selection of CD45+ leukocytes and CD14+ monocytes was performed. DAPI and Sytox red negative live cells were selected, and ROS production quantified as the median fluorescent intensity (MFI) of DHR-123 for these cells. (b.) (i.) ROS production in an UN sample. (ii.) ROS production in a corresponding anti-MPO stimulated sample. (iii) Overlay of ROS production in an UN (blue) and anti-MPO (purple) stimulated sample.

Figure 4.3.10:

CD15+ Neutrophils:

a.
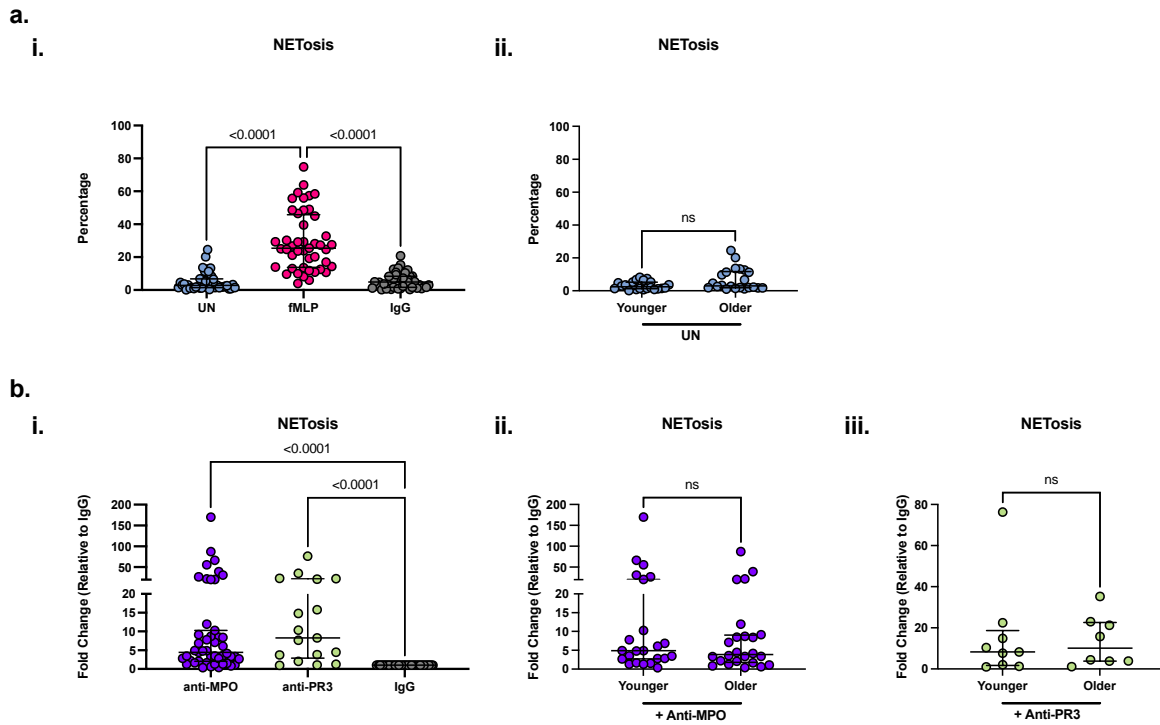

b.

CD14+ Monocytes

c.

d.
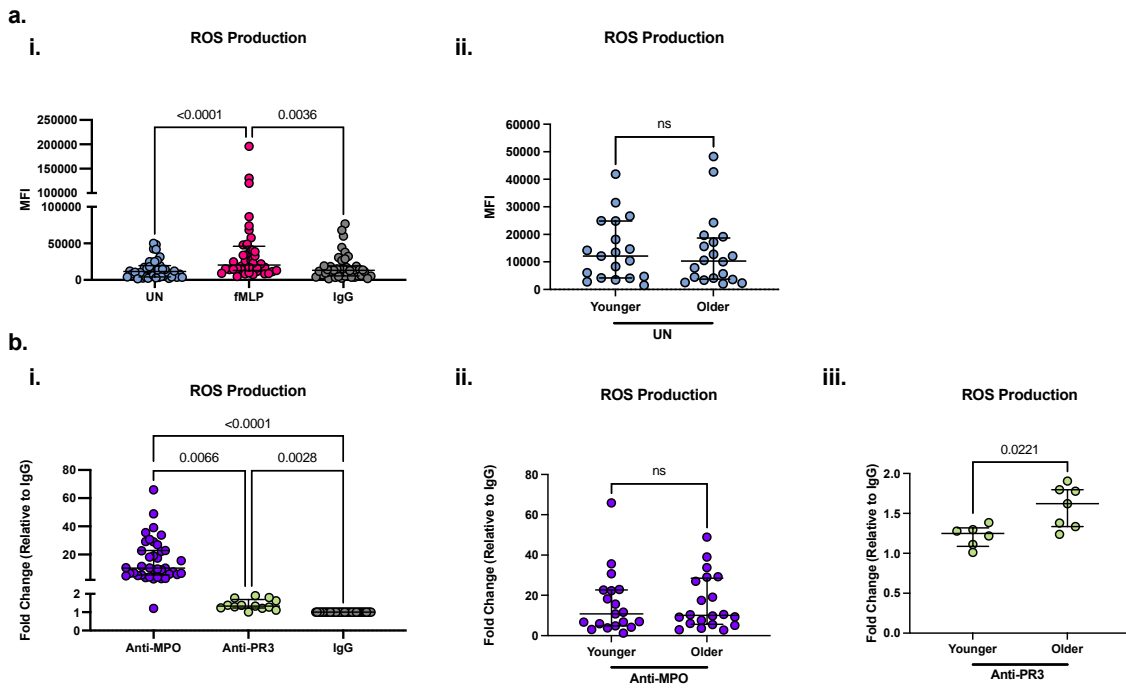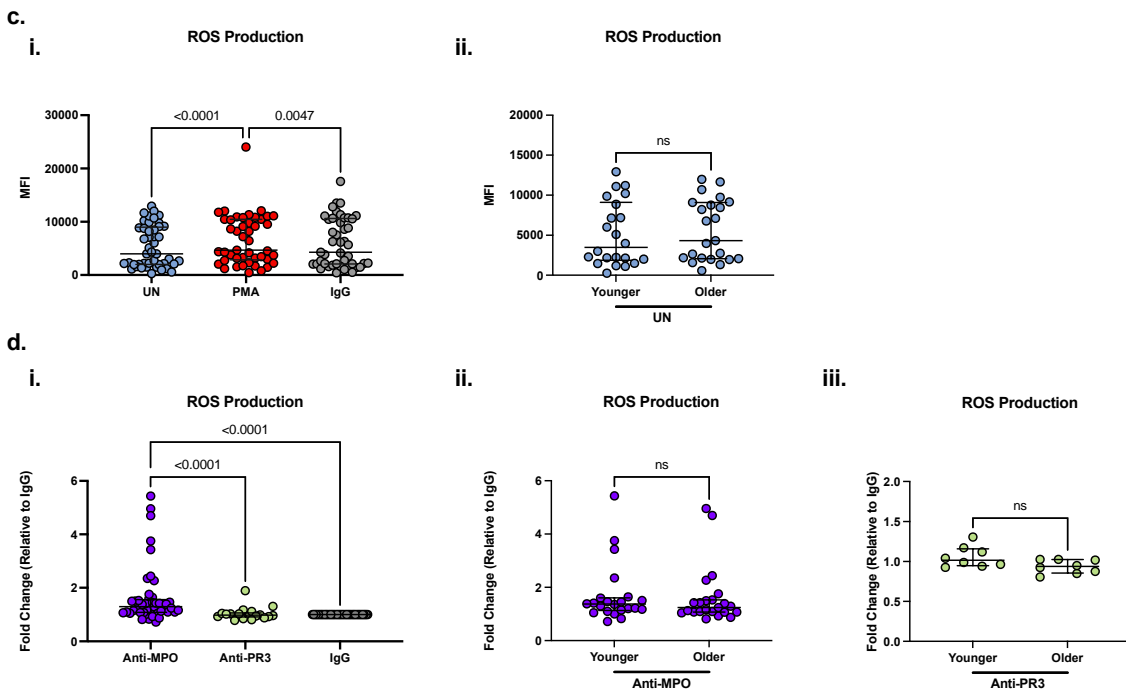
Figure 4.3.10 ROS production with age in response to ANCA stimulation

Whole blood samples were collected from healthy younger (n=22) and healthy older (n=23) individuals and both neutrophils and PBMCs were isolated from each donor. Isolated cells were left unstimulated or stimulated for 1 hour with either 5µg/ml fMLP, 100ng/ml PMA, 5µg/ml isotype IgG control, 5µg/ml anti-MPO mAb or 150µg/ml anti-PR3 mAb. ROS production was quantified via DHR-123 fluorescence using flow cytometry in both (a, b) neutrophils and (c, d) CD14+ monocytes. (a, c) (i.) ROS production from assay control samples; UN (blue), fMLP (pink), PMA (red) and IgG (grey). (ii) Baseline ROS production comparison between the younger and older cohorts. (b, d) (i.) ROS production in response to ANCA stimulation; anti-MPO (purple) and anti-PR3 (green). (ii.) Differences in ROS production between the younger and older cohorts in response to anti-MPO stimulation. (iii.) Differences in ROS between the younger and older cohorts in response to anti-PR3 stimulation. Data is expressed either as median fluorescent intensity (MFI) or as a fold change relative to the IgG control data. Each point on the graph represents an individual sample. Whole horizontal lines represent the median and IQR of each cohort. Statistical analysis was performed using One-Way ANOVA with Dunn's multiple comparison testing or using Mann-Whitney t tests. No significance (ns).
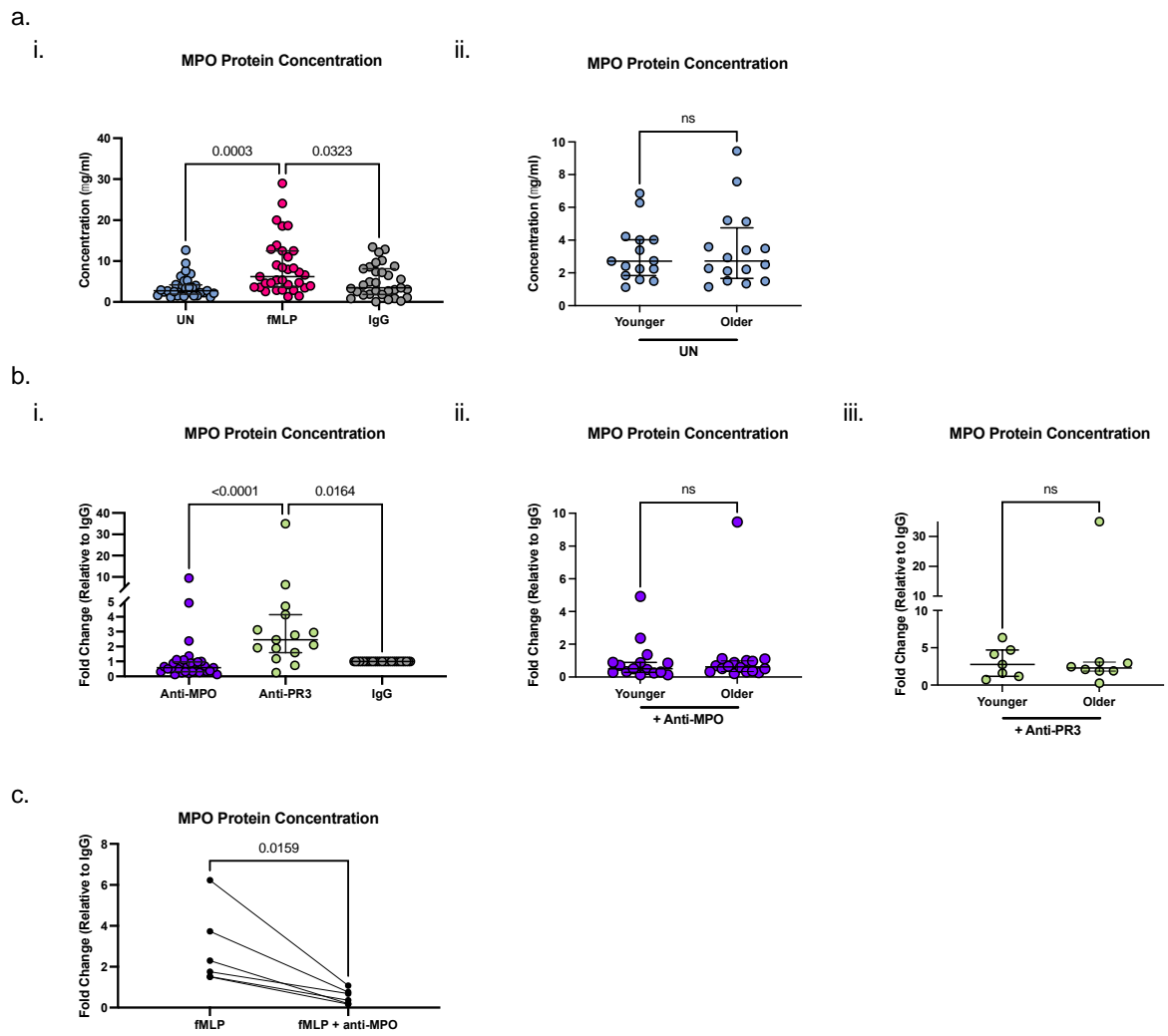
4.3.6 Cellular senescence in response to ANCA stimulation may differ with age

Cellular senescence is an important hallmark of ageing and is known to contribute to the process of inflammageing through the secretion of various inflammatory mediators. Studies are beginning to emerge linking cellular senescence to autoimmunity and AAV [234, 235]. We therefore wanted to investigate whether stimulation with ANCA could drive cellular senescence, as measured by *p21* gene expression, in PBMCs isolated from younger and older donors. There was a trend towards increased *p21* expression in response to PMA stimulation compared to baseline (p=0.06) while no differences were noted between the UN and IgG control samples (Figure 4.3.11a, i). Although not significant, a trend towards increased baseline *p21* expression was seen in older compared to younger donors (p=0.11) (Figure 4.3.11a, ii). *p21* also trended towards increased expression relative to the IgG control in response to anti-MPO stimulation (p=0.08) (Figure 4.3.11b, i). A similar trend was noted when comparing relative *p21* gene expression between our two age groups, with older donors showing increased *p21* gene expression compared to younger donors in response to anti-MPO stimulation (p=0.12) (Figure 4.3.11b, ii).

Figure 4.3.11:
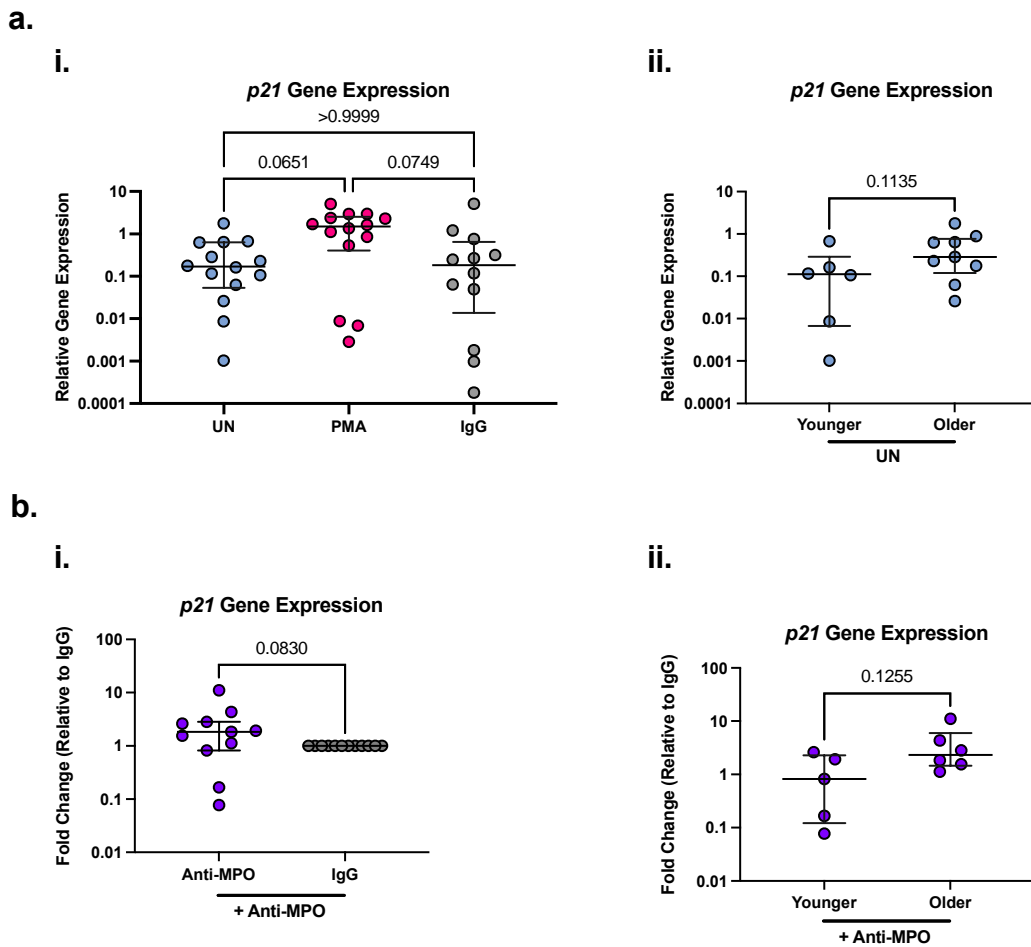
Figure 4.3.11: Cellular Senescence with age in response to ANCA

Whole blood samples were collected from healthy controls from both younger (n=6) and older (n=9) individuals and PBMCs were isolated from each donor. Isolated cells were left unstimulated or stimulated for 4 hours with either, 100ng/ml PMA, 5µg/ml isotype IgG control, 5µg/ml anti-MPO mAb or 150µg/ml anti-PR3 mAb. *p21* gene expression was used as a marker for cellular senescence and quantified using qPCR. All data was made relative to the expression of the endogenous control gene *RPL27* and analysed using the delta delta CT method. (a.) (i.) *p21* gene expression from assay control samples; UN (blue), PMA (red) and IgG (grey). (ii) Comparison of *p21* gene expression in unstimulated sample between the younger and older cohorts. (b) (i.) *p21* gene expression in response to anti-MPO (purple) stimulation made relative to the IgG control (grey). (ii.) Differences in *p21* gene expression between the younger and older cohorts expressed as a fold change relative to the IgG control in response to anti-MPO stimulation. Each point on the graph represents an individual sample. Whole horizontal lines represent the median and IQR of each cohort. Statistical analysis was performed using either One-Way ANOVA with Dunn's multiple comparison testing or using Mann-Whitney t tests.

4.3.7 MPO and PR3 surface expression on neutrophils and monocytes does not differ with age

Cellular activation and a rapid onset inflammatory response is known to follow the binding of ANCAs to their protein targets, MPO and PR3. These proteins are most commonly associated with neutrophils and monocytes, however, are thought to be primarily internal in the cell unless cells have been previously primed, for example with TNFα stimulation which has been shown to bring both MPO and PR3 to the cell surface. We therefore sought to examine whether the baseline surface expression of MPO and PR3 differs with age on neutrophils and monocytes and thus investigate if there is an ageing-associated "priming" effect. No significant differences in either MPO or PR3 expression were noted between younger and older donors for either cell type in this small pilot investigation.

Figure 4.3.12:

a.
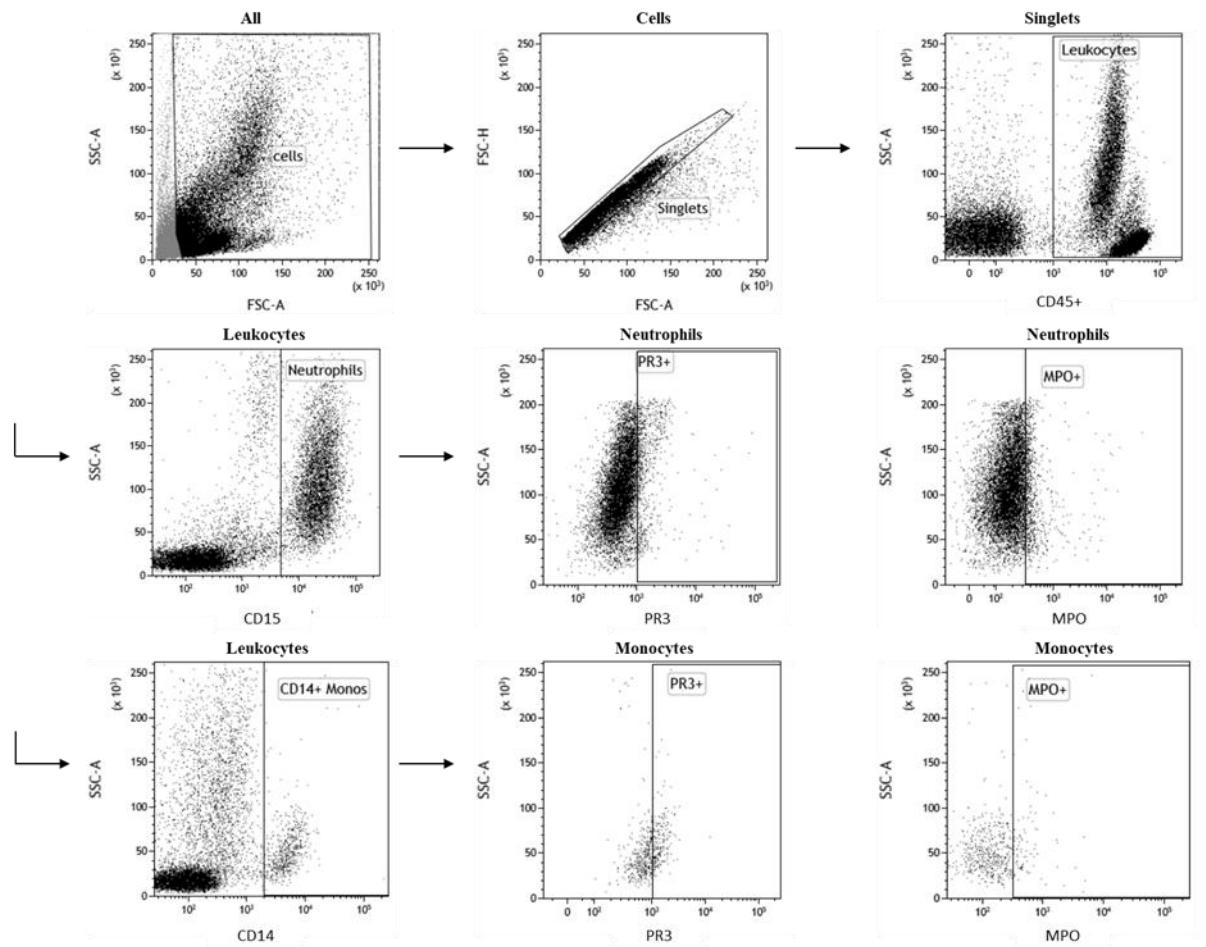
b.

(i.)

Monocyte Surface Expression
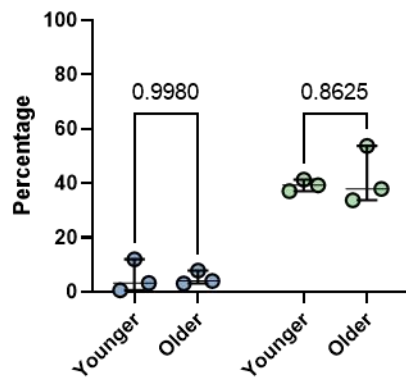
(ii.)

Neutrophil Surface Expression
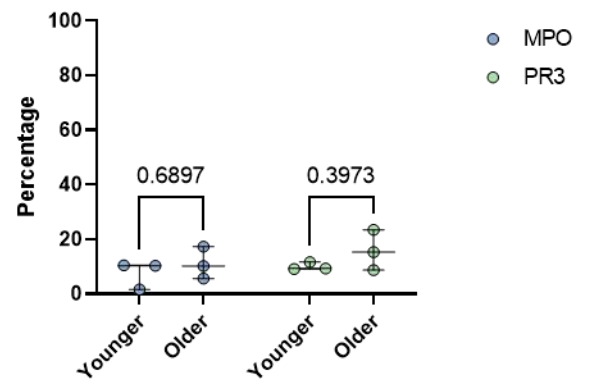
Figure 4.3.12: MPO and PR3 surface expression on innate immune cells with age:
Whole blood samples were collected from healthy younger (n=3) and healthy older (n=3) donors. Surface expression of MPO and PR3 on neutrophils and monocytes was quantified using whole blood flow cytometry. (a.) Gating strategy in whole blood samples to analyse MPO and PR3 surface expression. Total cells were gated on using FSC and SSC gates followed by singlets using FSC height and FSC area and then CD45+ leukocytes. CD14 was used to gate monocytes while CD15 utilised for neutrophil gating. PR3 and MPO surface expression was then quantified on each population using fluorescent antibodies against these proteins. (b.) (i.) MPO (blue) and PR3 (green) surface expression on whole blood gated monocytes from younger and older donors. (ii.) MPO (blue) and PR3 (green) surface expression on whole blood gated neutrophils from younger and older donors. Each point on the graph represents an individual sample. Whole horizontal lines represent the median and IQR of each cohort. Statistical analysis was performed using Mann-Whitney t tests.

4.4 Discussion

Despite ageing being a well-established risk factor for AAV development, the implications that this may have regarding the immunopathology of this disease remains largely unexplored, particularly with regards to human research. Ageing is known to have major impacts on the frequency and function of all immune cell subsets resulting in dysregulated cell signalling and aberrant responses to external stimuli, often leaving older individuals at a higher risk of morbidity and mortality [66, 236]. In this study we have shown that certain aspects of the innate immune system are altered in response to ANCA stimulation with age, likely resulting in increased inflammation (Table 4.4.1).

Table 4.4.1:

		Function	*Anti-MPO*	*Anti-PR3*
PBMC Responses	Inflammatory Cytokines Production	*IL6 Gene expression*	Increased in older cohort	No difference with age
		IL-6 protein concentration	Trend towards Increase in older cohort	No difference with age
		TNFA gene expression	Trend towards Increase in older cohort	No difference with age
		TNFα protein concentration	Increased in older cohort	No difference with age
		Monocyte ROS Production	No difference with age	No difference with age
		p21 Gene Expression	Trend towards increase in older cohort	N/A
Neutrophil Responses		*NETosis*	No difference with age	No difference with age
		Degranulation	No difference with age	No difference with age
		Neutrophil ROS Production	No difference with age	Increased in older cohort

Table 4.4.1: Summary of results

Table summarising the differences in innate immune response between younger and older cohorts found in this study in response to ANCA stimulation.

A failure to adequately control and resolve inflammatory processes can be extremely harmful and is known to result in tissue damage and disease development as is the case in ANCA associated vasculitis [182]. Similar to a multitude of previous studies, our

results indicate that ANCA stimulation is capable of upregulating inflammatory processes such as pro-inflammatory cytokine production, NETosis, degranulation and ROS production and this likely contributes to the inflammation noted in AAV [196, 237-239].

Differences in response to anti-MPO and anti-PR3 stimulations were also consistently noted throughout this study. Pathological differences are often reported between anti-MPO and anti-PR3 mediated AAV patients and many experts are now advocating for separate disease classification criteria based on ANCA subtype [152, 183]. Our results agree with this argument. For example, we have shown that both anti-MPO and anti-PR3 stimulation are capable of upregulating TNFα production while anti-MPO alone drove IL-6 expression in PBMCs isolated from healthy donors. The inability of anti-PR3 to drive IL-6 expression has previously been reported by O'Brien *et al.* who found increased IL-6 production in isolated monocytes in response to anti-MPO stimulation but not anti-PR3 stimulation and this may be indicative of the differential mechanisms of immunopathology noted between the two ANCA types, particularly differences in signal transduction [166]. Despite this, it is important to note that the lack of IL-6 production in response to anti-PR3 stimulation may also be due to assay design. In contrast to our results, Hattar *et al.* reported increased production of IL-6 in response to anti-PR3 stimulation, however, this increase was time dependent. They noted that unlike TNFα, IL-8 and IL-1, IL-6 production by isolated monocytes occurred at a later time point of at least 6 hours, suggesting a differing mechanism of regulation [240].It is therefore plausible that the lack of IL-6 noted in our study in response to anti-PR3 is due to a non-optimal stimulation time point. I would also suggest that differences noted between IL-6 gene expression and protein production in response to anti-MPO stimulation is a result of the stimulation times used.

Interestingly, we have noted that many of the anti-PR3 driven effects observed in this study, with the exception of TNFα production, were directed against isolated neutrophils (NETosis, degranulation and ROS production) and not PBMCs, potentially suggesting a more potent role for neutrophils in anti-PR3 mediated pathogenesis while both PBMCs and neutrophils were responsive to anti-MPO stimulation.

IL-6 and TNFα are inflammatory cytokines that have been implicated in the pathogenesis of a multitude of diseases [66, 77, 78]. Concentrations of both cytokines have been reportedly upregulated in AAV patients compared to healthy controls and are thought to contribute to disease severity in these patients leading to the exploration of IL-6 and TNFα blockade therapies in various AAV animal models [196, 230-232, 237]. This upregulation is, in part, thought to be driven by the presence of ANCAs, anti-MPO and anti-PR3 and results from our study support this hypothesis [166]. Systemic elevations in both of these cytokines are also characteristic of the process of inflammageing, age-related morbidity and mortality, with IL-6 in particular being highly correlated with lifespan [66, 78, 241]. Interestingly, our data reveals differences in both TNFα and IL-6 expression in response to ANCA stimulation with age. PBMCs isolated from older donors showed increased expression and production of these inflammatory cytokines compared to younger donors following stimulation with anti-MPO, suggesting an amplified inflammatory immune response to ANCAs with ageing older donors. Similar observations have also been made in mouse models of AAV. Wang *et al.* investigated pathological differences in anti-MPO autoantibody-mediated glomerulonephritis mice with age, an acute passive transfer model that relies on systemic injection of anti-MPO antibodies into wildtype C57Bl6 mice. Within 7 days, mice develop urinary abnormalities (haematuria, albuminuria and leukocyturia), crescentic glomerulonephritis and vasculitis. Wang *et al.* showed that older mice displayed higher plasma IL-6 and TNFα levels as well as increased renal mRNA expression of inflammatory genes including IL-6 along with higher proportions of circulating neutrophils and monocytes compared to younger mice [234]. Our study is amongst the first to investigate the effect of age on human cells in response to ANCA stimulation. We have shown that while multiple immune processes are not altered in response to ANCAs with age, certain aspects of the immune response are different between older donors compared to younger controls following ANCA stimulation. We therefore, suggest that these dysregulated responses may promote the immunopathology of AAV with age.

Despite seeing differences between younger and older participants in terms of inflammatory cytokine release in response to ANCAs, no differences in NETosis, degranulation or PBMC ROS production were seen between our two cohorts following the same stimulation suggesting that these are not age dependent processes during AAV.

All three of these processes have been shown to play a role in AAV pathogenesis and, importantly, our data does align with numerous previous studies that report the ability of ANCAs to upregulated these immune functions, however we suggest that this may be independent of age [238, 239].

Interestingly, we did see significant increases in neutrophil ROS production in response to anti-PR3, but not anti-MPO, in older participants compared to younger participants. The effect that age has on neutrophil intracellular ROS production is unclear with various reports suggesting increased ROS production with age, others showing decreased ROS in older adults and some noting no difference at all [242-244]. While the few studies to have focused on immune changes with age in AAV have focused on anti-MPO mediated pathology [83, 234], our results suggest that the immunopathology of anti-PR3 mediated AAV is also affected by age.

Cellular senescence is an important hallmark of ageing and has been recently linked to the induction of autoimmunity and is speculated to play a role in AAV [1, 234, 235]. In our study, we have shown that PBMCs isolated from older individuals tend to show increased *p21* expression, a genetic marker of cellular senescence, in response to anti-MPO stimulation compared to those from younger participants. Wang *et al*. also investigated markers of cellular senescence in AAV mouse models with age. Similarly to our results, although they reported no significant differences between younger and aged mice with regards to *p21* gene expression, a trend towards increased expression was seen with age. Interestingly, they also reported significant decreases in *klotho* expression in older mice compared to younger mice. The expression of this gene has previously been noted to reduce premature cellular senescence [234]. Taken together, we would suggest that the role of cellular senescence warrants further investigation in terms of AAV pathogenesis, particularly considering the emergence of senolytics, drugs that specifically target senescent cells.

MPO and PR3 are the primary protein targets of ANCAs and binding of ANCAs to their targets is generally accepted to result in immune cell activation and the promotion of an inflammatory response [182]. However, MPO and PR3 are thought to be largely intracellular proteins that are brought to the surface through a priming event [182, 196]. With this in mind, it is plausible that the process of inflammageing acts to prime immune

cells for subsequent activation by these ANCAs, contributing to some of the differences noted in this study [244]. Despite this, our experiments saw no significant differences in monocyte or neutrophil MPO or PR3 surface expression between younger and older donors suggesting that this did not influence the age-related results noted in our study. However, it is important to note that this was a pilot dataset with a small sample size (n=3 younger, n=3 older) and it is therefore hard to draw conclusions from these experiments.

This study is not without its limitations with sample size being the most obvious of these. Despite having managed to examine multiple aspects of the innate immune response to ANCA, a strength of this work, some of our analysis does suffer from low sample numbers and therefore are subject to type II errors, in particular the cellular senescence and surface expression assays as well as anti-PR3 stimulated sample analysis. Along with this, further isolation of specific immune subsets from PBMCs may have helped to identify leading cell types involved in each response and potentially uncovered further differences among aged cohorts. However, we have explored the immune responses of two prominent cell fractions, neutrophils and PBMCs, and it is worth noting that isolation techniques have been known to alter cellular phenotypes and immune responses and so by analysing PBMC fractions we have minimised these errors [245]. As well as this, further isolation of the PBMC fraction would result in very small cell numbers and this would have limited functional analysis capabilities. MPO release is a common marker of neutrophil degranulation that was utilised in this study; however, we did have technical issues with this assay with respect to anti-MPO stimulation which limited its efficacy in terms of ANCA analysis. We have shown here that anti-MPO stimulation interferes with the kinetics of this assay as stimulation with fMLP followed by the addition of anti-MPO to the supernatant of these samples significantly decreases MPO release measures. This therefore renders our anti-MPO stimulation data for degranulation analysis unreliable. Additional assays including lactoferrin or cathepsin G may resolve this issue in the future. Finally, it is also worth noting that in order to study the effect of age as a single variable without the influence of external factors such as medication, obesity, chronic illness etc., only healthy individuals were recruited for this study. Although this was by design and has best allowed us to approach our specific research question, our older cohort may therefore not be representative of the older population, and this may impact the translation of our results.

In this study we have shown that certain immune responses are altered with age following ANCA stimulation, while others show no age-specific effects. Although we do not always see differences between our two age cohorts in response to ANCA stimulation, we often note a much broader range of responses in our older cohort compared to our younger cohort, with certain individuals showing little to no response to ANCA stimulation and others showing very high responses. Inter-individual variability is a growing area of interest in the field of gerontology and is noted to be a result of sex, genetic and environmental influences [246-248]. The differential responses noted in our study cohorts pose the intriguing question of whether these high responders are at a higher risk of AAV development compared to low responders.

The precise cause of AAV development remains a major knowledge gap in this field of research. Considering the age-related onset and inflammatory nature of AAV, the effect that age has on immune processes in the context of AAV is an important and understudied area of research that could help to bridge this knowledge gap.

4.5   Conclusion

This study was carried out with the overall aim of better understanding the underlying immune processes that are known to drive AAV pathogenesis with age. Our results suggests that immunological differences in response to ANCAs can occur in older compared to younger adults and this may be impacting their risk of AAV development. This study has highlighted the increased ability of immune cells isolated from older participants to undergo inflammatory and age-related processes in response to ANCA stimulation and, with the emergence of "age-reversal" and "anti-ageing" drugs that target these processes, the effect that ageing has on AAV pathology warrants further research.

5 Type I IFN Responses in AAV

5.1 Introduction

Type I IFNs are essential mediators of immune functions and are noted for their anti-viral, anti-proliferative and immuno-regulatory properties [198]. These cytokines regulate a wide range of biological processes and, under normal homeostatic conditions, their activation is tightly regulated [199]. However, the dysregulation of type I IFN signalling can have severe consequences, resulting in chronic inflammation. Research from our lab has shown that these responses become dysregulated with age. We have found that the baseline expression of several type I interferon regulated genes are significantly increased in PBMCs isolated from older adults compared to those from younger controls (unpublished; Figure 5.1.1). Similar results have been noted in both human and mouse studies and this inappropriate interferon response has been suggested to contribute to the process of inflammageing and refractory signalling [209, 210, 249]. This dysregulation can have detrimental effects in older individuals leaving them more susceptible to infection and less responsive to vaccination, as highlighted by the SARS-CoV-2 pandemic [250, 251].

Figure 5.1.1:
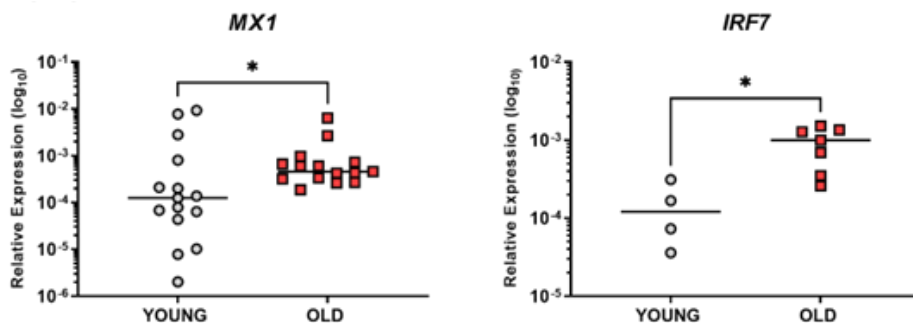
Figure 5.1.1 Baseline type I IFN regulated gene expression in PBMCs isolated from younger and older donors

Whole blood samples were obtained from healthy young and old donors and PBMC were isolated. RNA was extracted from PBMCs, and qPCR was used to quantify gene expression. All data is expressed relative to the endogenous housekeeping gene *18S* using the delta delta Ct method. (A) Relative gene expression of *MX1* measured in PBMCs isolated from young (grey; n=15) and old (red; n=15) donors. (B) Relative gene expression of *IRF7* measured in PBMCs isolated from young (grey; n=4) and old (red; n=7) donors. Statistical significance was tested using Mann-Whitney t testing. (*$p<0.05$)

In recent decades, a role for altered type I interferon responses in the development of autoimmunity has emerged [215, 217]. As mentioned above, dysregulated type I IFN signalling can result in chronic inflammation and this chronic inflammation can contribute to the development of autoinflammatory and autoimmune disease, now specifically classified as type I interferonopathies [213]. First proposed as an independent classification of autoimmune disease in 2011 following the description of a monogenic form of systemic lupus erythematosus, such type I interferonopathies now encompass multiple diseases including Aicardi Goutier syndrome, dermatomyositis and primary Sjogren's syndrome (pSS) among others [207, 215, 217, 218].

Interestingly, along with being an age-associated autoimmune disease, AAV shares both clinical and immunological similarities with known type I interferonopathies such as SLE and past studies have suggested a role for type I IFNs in AAV severity [50, 220]. In 2009, while studying the process of NETosis in AAV, Kessenbrock *et al*. found increased *MxA* expression, a typical interferon regulated gene, in the glomeruli and tubules of active AAV patients. Additionally, they noted increased IFN-α concentrations in the serum of active AAV patients in comparison to AAV remission patients and healthy controls, suggesting a role for these cytokines in AAV activity [50]. In 2017, Ishizu *et al*. examined the gene expression profiles of Japanese MPA patients, noting a decrease in specific IFN regulated gene expression following remission induction treatment, and concluded that these genes are good markers of therapeutic benefit [220].

Despite this, the role of type I IFNs in regards to the initiation or progression of AAV remains unclear and, with specific therapies designed to target various elements of type I IFN responses currently undergoing clinical trials for the treatment of type I interferonopathies, investigations into the role of these cytokines in AAV has become even more pressing [219, 252]. We thus hypothesise that systemic type I IFN responses are dysregulated in AAV. In the present study we measured commonly used markers of type I interferonopathies in AAV patients and compared their expression to disease and healthy controls to determine whether type I IFN responses are dysregulated in AAV.

5.2 Study Design and Rational

5.2.1 Hypothesis

Type I IFNs become dysregulated with age and are known to be characteristic cytokines involved in multiple autoimmune conditions [208-210, 214, 215, 249]. Considering that ageing is a primary risk factor of AAV and the similarities between AAV and other type I interferonopathies, we hypothesise that type I interferons are involved in the immunopathology of AAV.

5.2.2 Specific Aims

- To explore whether type I IFN regulated gene expression is systemically dysregulated in AAV patients.
- To determine whether type I IFN regulated protein expression is systemically dysregulated in AAV patients.
- To investigate whether measures of systemic type I IFNs correlate to clinical measures AAV severity.

5.2.3 Sample Selection

All available whole blood samples that had previously been collected in paxgene tubes through the RKD biobank were selected. RNA was extracted from these and bioanalyzed for RNA quality. A nanodrop spectrophotometer was used for RNA quantification. Samples with RIN values greater than 6.5 and yields higher than 30ng/µl were selected. Remaining samples were carefully phenotyped and any samples with false or uncertain diagnoses were excluded. All available matched serum samples that had been subjected to minimum freeze thaw cycles (1-2) with a minimum aliquot volume of 250µl were then identified and requested for use.

SLE patient samples were obtained from the Leeds Institute of Rheumatic and Musculoskeletal Medicine at the University of Leeds and the NIHR Leeds Biomedical Research Centre. Ethical approval for the use of these samples in such research has been provided by the South Yorkshire research ethics committee. All patients with primary Sjogren's syndrome included in our study met the American-European Consensus classification criteria [253] and were recruited from Royal Victory eye and Ear Hospital, Dublin. The study protocol was conducted in accordance with the Helsinki Declaration

and approved by the institutional review boards of the Royal Victory eye and Ear Hospital. Every participant involved in this study has provided written informed consent.

5.2.4 Specific Methods

RNA was extracted and bioanalysed following the protocols described in sections 2.8.6-2.8.7. qPCR protocols outlined in 2.8.8-2.8.11 were followed. Serum ELISAs were carried out according to the methods described in section 2.10.5.

5.2.5 Data Analysis and Statistical Tests

All statistical analyses were performed using GraphPad Prism v8.4.2 with the exception of the power calculations which were determined using R software. Shapiro-Wilk tests were used to determine normality. All data was found to be non-normally distributed. Therefore, statistical significance between each sample cohort was determined using Kruskal-Wallis one-way ANOVA, with Dunn's post hoc multiple comparison tests, while Spearman's Correlation tests were used to analyse associations between clinical measurements or demographic data and experimental data. The strength of these correlations was defined following published guidelines with Spearman correlation coefficients greater than 0.5 deemed strong, those below 0.3 deemed weak associations while those between 0.3 and 0.5 are acknowledged as moderate associations [223, 224]. We confirmed the power of our analysis using a one-way balanced ANOVA power calculation as a baseline comparison in collaboration with Dr. Arthur White. The mean number of samples per group in our experiments were used as the estimate for the per group sample size, and the conservative assumption that the standardised means of the three disease groups differed from the control group by delta = 0.25, 0.5, and 0.75 in some combination was made.

5.2.6 IFN Score Calculation

An IFN score for each sample was calculated following previously described methods [215, 252]. This was calculated as the median fold change of the seven IRGs for each sample when compared to the median of the healthy control samples. Abnormal IFN scores were defined as those higher than 2 standard deviations from the mean IFN score of healthy control samples i.e., those higher than 4.227 for whole blood gene expression analysis and 7.3 for PBMC gene expression analysis. Samples with an IFN score greater

than this were labelled as IFN positive while any score below this measure were labelled as IFN negative.

5.3 Results

5.3.1 Cohort Characteristics

A total of 217 participants were recruited for this study comprising healthy controls (n=72), disease controls (n=34), AAV active patients (n=48), AAV remission patients (n=35), SLE patients (n=19) and pSS patients (n=9). Four of these participants provided both active and remission matched samples, one DC (anti-GBM) and 3 AAV participants. This resulted in a total of 168 serum samples, 178 whole blood samples and 30 PBMC samples (Table 5.3.1).

Table 5.3.1:

Cohort Summary		*HC*	*DC*	*AAV R*	*AAV A*	*SLE*	*pSS*
N	Participants	72	34	35	48	19	9
	Serum Samples (*n*)	67	31	29	41	0	0
	Whole Blood Samples (*n*)	62	29	27	41	19	0
	PBMC Samples (*n*)	5	4	6	6	0	9
Age, median (range), years		51 (16-83)	60 (16-87)	62 (25-80)	65 (22-84)	44 (28-60)	57 (52-73)
Male, *n* (%)		24 (36)	20 (57)	20 (17)	24 (50)	2 (11)	1 (11)

Table 5.3.1: Cohort Summary

All participants have been categorised as either Healthy controls (HC), Disease controls (DC), AAV patients (Active {A} or Remission{R}), Systemic Lupus Erythematosus (SLE) or primary Sjogren's syndrome (pSS). A summary of the samples obtained as well as the median age and sex breakdown is shown. Age and sex breakdown for the HC cohort is based off of whole blood and serum donors only (n=67) as this data was unavailable for participants involved in PBMC analysis (n=5).

Active AAV disease is clinically defined by a BVAS of ≥ 1. However, in order to exclude cases of persistent mild inflammation from our study our active cohort were selected to have a BVAS ≥ 3. AAV patients in remission were defined by a BVAS of zero. A summary of clinical measurements used to define and study our AAV participants is shown in Table 5.3.2.

Table 5.3.2:

AAV Characteristics			*AAV R*	*AAV A*	
				<u>*Txt*</u>	<u>*Txt Naive*</u>
n	Patients		35	37	11
ANCA status, *n* (%)	Anti-MPO		19 (54)	16 (43)	9 (82)
	Anti-PR3		16 (46)	21 (57)	2 (18)
Diagnosis, *n* (%)	GPA		16 (46)	20 (54)	1 (9)
	MPA		19 (54)	17 (46)	10 (91)
BVAS, median (range)			0	14 (3-32)	14 (12-27)
CRP (mg/dL), median (IQR)			3 (10.8-9.8)	18.5 (5.3-77.8)	46 (39–112)
Creatinine (µmol/L), median (IQR)			119.5 (86.5-166.5)	136.5 (89.5-296.5)	247 (201-416)
eGFR (ml/min), median (IQR)			49.5 (32.3-34.8)	42 (15-73)	17.5 (11–23)
Immunosuppression treatment, *n* (%)					
	Cyclo	0-6 months	5 (13.9)	3 (8.1)	N/A
	Azathioprine	Current	14 (38.9)	4 (10.8)	N/A
	MMF	Current	9 (25)	5 (13.5)	N/A
	Methotrexate	Current	2 (5.6)	0	N/A
	Rituximab	0-6 months	2 (5.6)	2 (5.4)	N/A
	Corticosteroid	Current	24 (66.7)	30 (81.1)	N/A
	Other	Current	7 (19.4)	5 (13.5)	N/A

Table 5.3.2: AAV Characteristics
AAV participants have been divided into AAV R and AAV A cohorts with a further delineation of AAV A into treated (Txt) and treatment naïve (Txt Naïve) participants. A summary of clinical characteristics including ANCA status, diagnosis, BVAS, CRP cytokine levels, creatinine, estimated Glomerular Filtration Rate (eGFR) and treatment history is shown.

To evaluate potential effects of general kidney inflammation and systemic autoimmunity on type I IFN responses, a disease control group comprised of patients diagnosed with a spectrum of kidney diseases and/or autoimmune disorders were included in this study. These included diagnoses of anti-glomerular basement membrane (anti-GBM) disease (n=12), chronic kidney disease (CKD; n=7), classical polyarteritis nodosa (PAN) (n=1), chronic pyelonephritis (n=1), diabetic kidney disease (n=4), IgA vasculitis (n=4), rheumatoid vasculitis (n=1) and rheumatoid arthritis (n=4). Samples collected from known type I interferonopathies (SLE; n=19 and pSS; n=9) were also utilised as positive disease controls in this study. Further information regarding disease activity and treatment of disease controls is shown in Tables 5.3.3 and 5.3.4.

Table 5.3.3:

Diagnosis	Disease Status				TxtN	Treatment received (>6 months)							
	A	*R*	*C*	*NA*		*Cyclo*	*Aza*	*MMF*	*Mtx*	*CS*	*Anti-TNF*	*HCQ*	*O*
Anti-GBM	6	7	-	-	2	2	1	1	-	6	-	-	2
CKD	-	-	7	-	-	-	-	-	-	-	-	-	3
IgA V	2	1	-	1	1	-	-	1	-	2	-	-	-
DKD	-	-	-	4	-	-	-	-	-	-	-	-	1
RV	-	1	-	-	-	-	-	-	1	-	-	-	-
C-PAN	-	1	-	-	-	-	1	-	-	-	-	-	-
CP	-	-	1	-	-	-	-	-	-	-	-	-	1
RA	-	-	4	-	-	-	-	-	-	-	4	-	-
SLE	10	9	-	-	3	-	3	5	2	5	-	11	3
pSS	-	-	9	-		NA	NA	NA	NA	NA	NA	NA	NA

Table 5.3.3: Breakdown of disease control groups, SLE and pSS based on disease status and treatments received.

Disease control diagnoses include anti-glomerular basement membrane (anti-GBM) disease, chronic kidney disease (CKD), classical polyarteritis nodosa (C-PAN), diabetic kidney disease (DKD), IgA Vasculitis (IgA V), rheumatoid vasculitis (RV), chronic pyelonephritis (CP) and rheumatoid arthritis (RA). A; Active, R; Remission, C; chronic, NA; not available, TxN; treatment naïve, Cyclo; cyclophosphamide, Aza; azathioprine, MMF; mycophenolate mofetil, Mtx; methotrexate, CS; corticosteroids, Anti-TNF; anti-tumour necrosis factor; HCQ; hydroxychloroquine, O; other.

Table 5.3.4:

Diagnosis	SLE	pSS
SLEDAI, median (IQR)	4 (2.5-6)	N/A
OSDI, median (IQR)	N/A	41.2 (27.1-50)
ESPRI, median (IQR)	N/A	6.7 (5-7)
NEI VF OP, median (IQR)	N/A	50 (50-50)

Table 5.3.4: A summary of clinical measurement scores used to evaluate SLE or pSS severity. SLEDAI; SLE Disease Activity Index, OSDI; Ocular surface disease index, ESPRI; The EULAR Sjogren's Syndrome Patient Reported Index, NEI VF OP; National Eye Institute Vision Functioning Ocular Pain, IQR; interquartile range.

5.3.2 Whole Blood IRG Expression Is Not Upregulated in AAV

Expression of specific IRGs are elevated in blood from patients with type I interferonopathies and correlate with disease severity in these conditions [208, 215, 254]; therefore, we investigated the expression of a panel of these IRGs (*ISG15, SIGLEC1, STAT1, RSAD2, IFI27, IFI44L* and *IFIT1*) using mRNA extracted from whole blood samples. These genes are upregulated in the presence of type I IFNs and are often adopted as surrogate markers of type I IFN activity which can otherwise be difficult to detect [199, 213, 252, 255, 256]. They are continuously found to be dysregulated in transcriptomic analysis of known type I interferonopathies and are therefore commonly used to investigate the transcriptional activity of type I IFNs in such disease settings (Table 5.3.5) [207, 208, 215, 252]

Table 5.3.5:

	Function	*Type I Interferonopathies*			
		SLE	AG	DM	pSS
ISG15	This gene is reported to have various immune functions. The proteins produced by this gene can act as chemotactic factors for immune cells such as neutrophils during viral infection and have been proposed to function similarly to cytokines with several effects such as NK cell proliferation and DC maturation. As well as this the conjugated forms of these proteins mediate the process of ISGylation. This involves protein conjugation by ISG15, modifying proteins in similar manner to ubiquitination. The exact biological functions of this process remain unknown however ISGylation of viral proteins is known to inhibit viral replication [257, 258].	[208, 252, 259, 260]	[215]		
Siglec1	Codes for a protein present on myeloid cells that acts as an endocytic receptor facilitating clathrin-dependent endocytosis. Allows for the capture of viral components, facilitating the initiation of a specific targeted immune response [261, 262].	[208, 252]	[215]		
RSAD2	Known to inhibit infection/replication of a wide range of viruses including hepatitis C virus (HCV), influenza A virus, human immunodeficiency virus (HIV) etc. Exact mechanism of action remains unclear however studies on influenza A have linked this anti-viral activity to lipid raft disruption, preventing the later stages of viral replication [263-265].	[208, 252]	[215]	[207]	[266]
IFIT1	Codes for proteins that specifically recognise viral RNA sequences, thereby recognising viral invasion and initiating an antiviral response as well as inhibiting viral RNA translation [267, 268].	[208, 252]	[215]	[207]	[266]
IFI27	Thought to have various functions in humans including type I IFN induced apoptosis and viral proteasomal degradation mediated through ubiquitination [269, 270].	[208, 252]	[215]	[207]	[218, 266]
IFI44L	Upregulated in response to various viruses and is reported to inhibit the replication of HCV however mechanisms remain unclear. Also exhibits anti-tumour properties [255, 271].	[208, 252]	[215]	[207]	[266, 272]
STAT1	Codes for a signalling molecule involved in IFN production pathways [198, 273].	[256]		[207]	[218, 266]

MCP-1	An essential chemokine involved in monocyte and macrophage recruitment during inflammation [274].	[217, 275]	[276]	[207, 208]	[277, 278]
CXCL10	Chemokine that mediates immune responses through the recruitment and subsequent activation of numerous immune cells including monocytes, T cells and NK cells [279, 280].	[217, 275]		[207, 208]	[272, 277]
CCL19	A cytokine with various biological functions, most well studied as a chemokine responsible for the migration of T cells and mature dendritic cells during infection and inflammation [281, 282].	[217, 275]		[207, 208]	[277]

Table 5.3.6: Interferon Regulated Gene and Protein Summary. A summary of the functions of each type I interferon regulated gene and protein analysed in this study as well as references indicating their dysregulation in various type I interferonopathies (SLE; Systemic Lupus Erythematosus, AG; Aicardi Goutier Syndrome, DM; Dermatomyositis, pSS; primary Sjogren's Syndrome).

No significant difference in whole blood IRG expression was noted between AAV samples (active or remission), disease controls or healthy control groups, whereas samples collected from a known type I Interferonopathy, SLE, showed notably increased expression across all genes measured with the exception of *STAT1* (Figure 5.3.1a). These results show only weak to moderate correlations with age (Figure 5.3.4a)

In order to ensure that our AAV cohort experience expected transcriptional changes compared to healthy controls, and that our assays were working efficiently, we measured the expression of *MMP8* and *ANXA3*, genes that have been previously shown to be upregulated in AAV patients compared to healthy controls. We observed significantly higher expression of the genes *MMP8* and *AXA3* in our active AAV group compared to HCs ($p < 0.05$)(Figure 5.3.1b.), neither of which are primarily type I IFN regulated [283, 284], indicating that our experimental system can detect such signals. This is consistent with existing literature [285], confirming that our AAV cohort exhibits expected gene expression characteristics, but that systemic IRG expression is not specifically altered in this condition.

We also calculated an IFN score for each sample in our cohort. While SLE samples showed a significantly increased IFN score compared to all other cohorts, no differences in the median IFN score were noted between AAV samples, disease controls and healthy controls (Figure 5.3.1c i). Of the 24 positive IFN score samples detected, 3 (4.8%) were healthy control, 2 (6.7%) disease control, 3 (11.1%) AAV remission patient samples, 3 (7.3%) AAV active patient samples and 13 SLE patient samples (68.4%) (Figure 5.3.1c ii). The percentage of healthy control and interferonopathy groups with a positive IFN score in our study is consistent with those of previous studies [215, 252].

Figure 5.3.1:
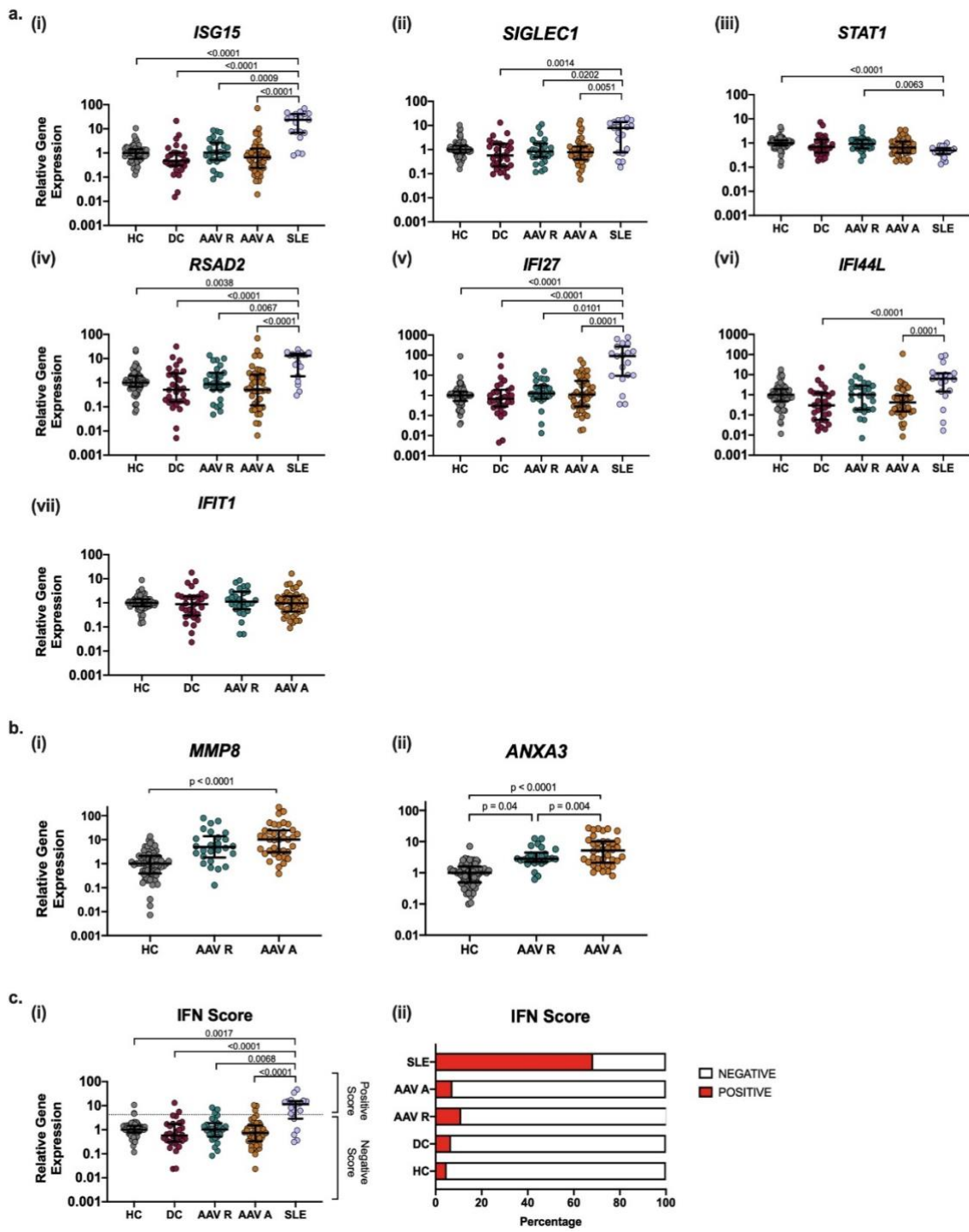
Figure 5.3.1: IRG Expression in AAV Patients and Controls

Whole blood samples were obtained from healthy controls (HC; n=62), disease controls (DC; n=29), AAV remission patients (AAV R; n=27), AAV active patients (AAV A; n=41) and SLE patients (n=19). PBMC samples were obtained from healthy controls (HC; n=5), disease control (DC; n=4), AAV remission (AAV R; n=6), AAV Active (AAV A; n=6) and primary Sjogren's syndrome (pSS; n=9). qPCR was used to quantify gene expression and all data is shown relative to the expression of the endogenous control gene *RPL27* and normalised to the median expression of the healthy control samples ($2^{-\Delta\Delta CT}$). (a.) Gene expression measurements of the IRGs (i) *ISG15*, (ii) *SIGLEC1,* (iii) *STAT1* (iv) *RSAD2* (v) *IFI27,* and (vi) *IFI44L* in whole blood from HC, DC, AAV R, AAV A and SLE groups, (vii) *IFIT1* in HC, DC, AAV R and AAV A groups only. Due to technical issues *IFIT1* expression analysis could not be performed on SLE samples. (b.) Gene expression measurements of (i) *MMP8* and (ii) *ANXA3* in whole blood HC, AAV R and AAV A groups. (c.) (i) IFN scores calculated and plotted for each whole blood sample analysed. (ii) Percentage of positive (red) and negative (white) IFN scores in each cohort studied from whole blood samples. Whole horizontal lines represent the median and IQR of each cohort. Statistical analysis was performed using One-Way ANOVA with Dunn's multiple comparison testing.

5.3.3 IRG Expression is Not Upregulated in Peripheral Blood Mononuclear Cells Isolated from AAV Patients

As peripheral blood mononuclear cells (PBMCs) are the primary producers of type I IFNs and their signalling components within the blood, we examined this IRG signature (*ISG15, SIGLEC1, STAT1 RSAD2, IFI27* and *IFI44L*) within these isolated cell types collected from a smaller cohort of healthy controls, disease controls, AAV and primary Sjogren's syndrome (pSS) patients in order to identify any signals that may have been blunted in the presence of alternative blood fractions. Numerous studies have reported an upregulation of IRGs in the peripheral blood and salivary glands of pSS patients, resulting in its classification as a type I interferonopathy (Table 5.3.5) [218, 286]. We observed upregulation of IRGs in PBMCs collected from pSS patients compared to all other cohorts, yet we again found no significant differences in IRG expression between AAV (active or remission) PBMC samples and both disease and healthy control groups (Figure 5.3.2a). We calculated IFN scores for all samples, which confirmed that pSS samples had significantly increased IFN scores compared to all other cohorts while no significant differences in the median IFN score was noted between AAV samples, disease controls and healthy controls (Figure 5.3.2b). Of the 9 positive IFN score samples detected, 1 was a disease control sample (25%), 1 was an AAV active patient samples (16.7%) and 7 were pSS patient samples (77.8%) (Figure 5.3.2b). Taken in combination with our whole blood analysis, our results confirm that there is no elevation in the IFN transcriptional signature in peripheral blood of AAV patients.

Figure 5.3.2:
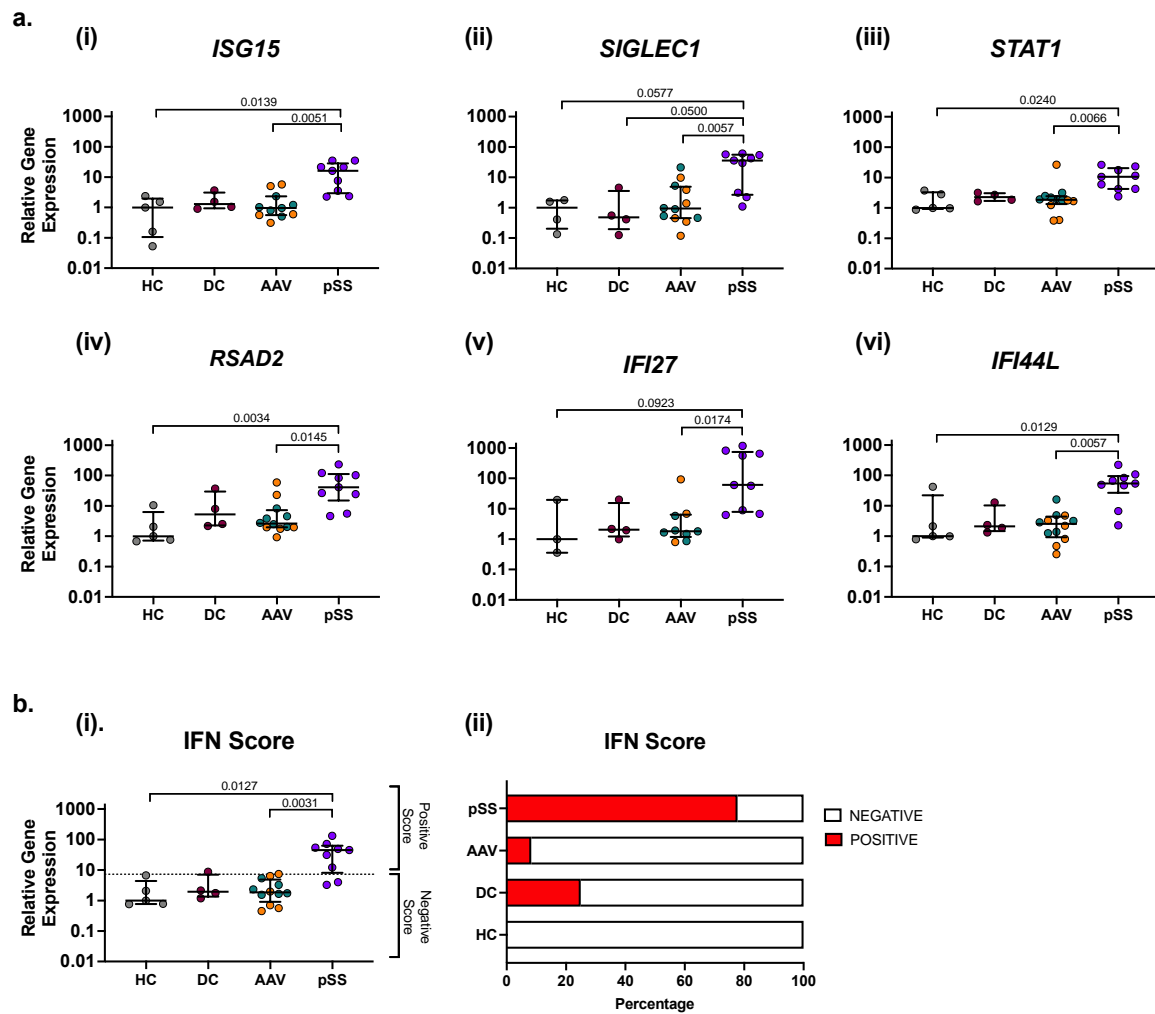
Figure 5.3.2: IRG Expression Measured from the PBMCs of AAV Patients and Controls.
PBMC samples were obtained from healthy controls (HC; n=5), disease controls (DC; n=4), AAV patients (n=12) (AAV R; blue and AAV A; orange) and primary Sjogren's Syndrome patients (pSS; n=9). qPCR was used to quantify gene expression and all data is shown relative to the expression of the endogenous control gene *RPL27* and normalised to the median expression of the healthy control samples ($2^{-\Delta\Delta CT}$). (a.) Gene expression measurements of the IRGs (i) *ISG15*, (ii) *SIGLEC1*, (iii) *STAT1* (iv) *RSAD2* (v) *IFI27*, and (vi) *IFI44L* and in HC, DC, AAV and pSS groups. (b.) (i) IFN scores calculated and plotted for each PBMC sample analysed. (ii.) Percentage of positive (red) and negative (white) IFN scores in each cohort studied from PBMC samples. Whole horizontal lines represent the median and IQR of each cohort. Statistical analysis was performed using One-Way ANOVA with Dunn's multiple comparison testing.

5.3.4 Type I IFN Regulated Protein Expression Does Not Differ Between AAV and Healthy Controls

We next measured the serum concentration of three type I IFN regulated chemokines: MCP-1, CCL19 and CXCL10. Although these chemokines can be regulated by several inflammatory mediators, they have previously been validated as robust biomarkers of type I interferonopathies (Table 5.3.5) [217, 275]. We found no significant differences in the serum concentration of MCP-1, CCL19 or CXCL10 in AAV patients compared to HC and DC (Figure 5.3.3). These results show only a weak to moderate correlation with age (Figure 5.3.4).

Figure 5.3.3:
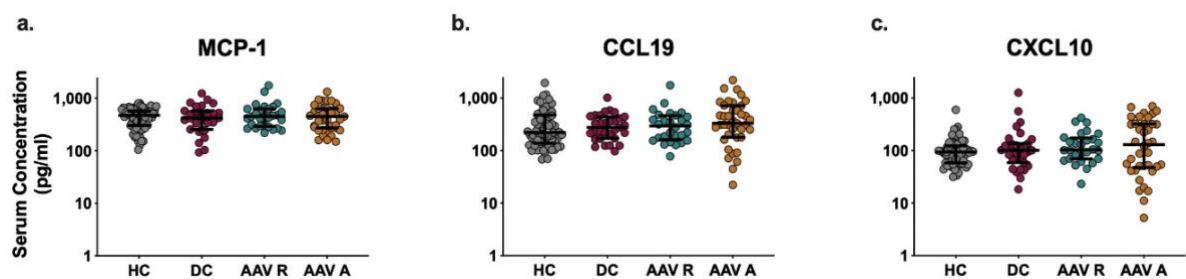
Figure 5.3.3: Serum concentrations of Type I IFN regulated chemokines expression In AAV patients and controls.

Serum samples were obtained from HC (n=67), DC (n=31), AAV R patients (n=29) and AAV A patients (n=41). The concentration of circulating (a.) MCP-1, (b.) CCL19 and (c.) CXCL10 were measured using ELISAs. Whole horizontal lines represent the median and IQR of each cohort. Statistical analysis was performed using One-Way ANOVA with Dunn's multiple comparison testing. No statistical differences were observed.

Figure 5.3.4:

a.

(i)

ISG15

(ii)

SIGLEC1

(iii)

IFIT1

(iv)

RSAD2

(v)

IFI27

(vi)

IFI44L

(vii)

STAT1

b.

(i)

MCP-1

(ii)

CCL19

(iii)

CXCL10
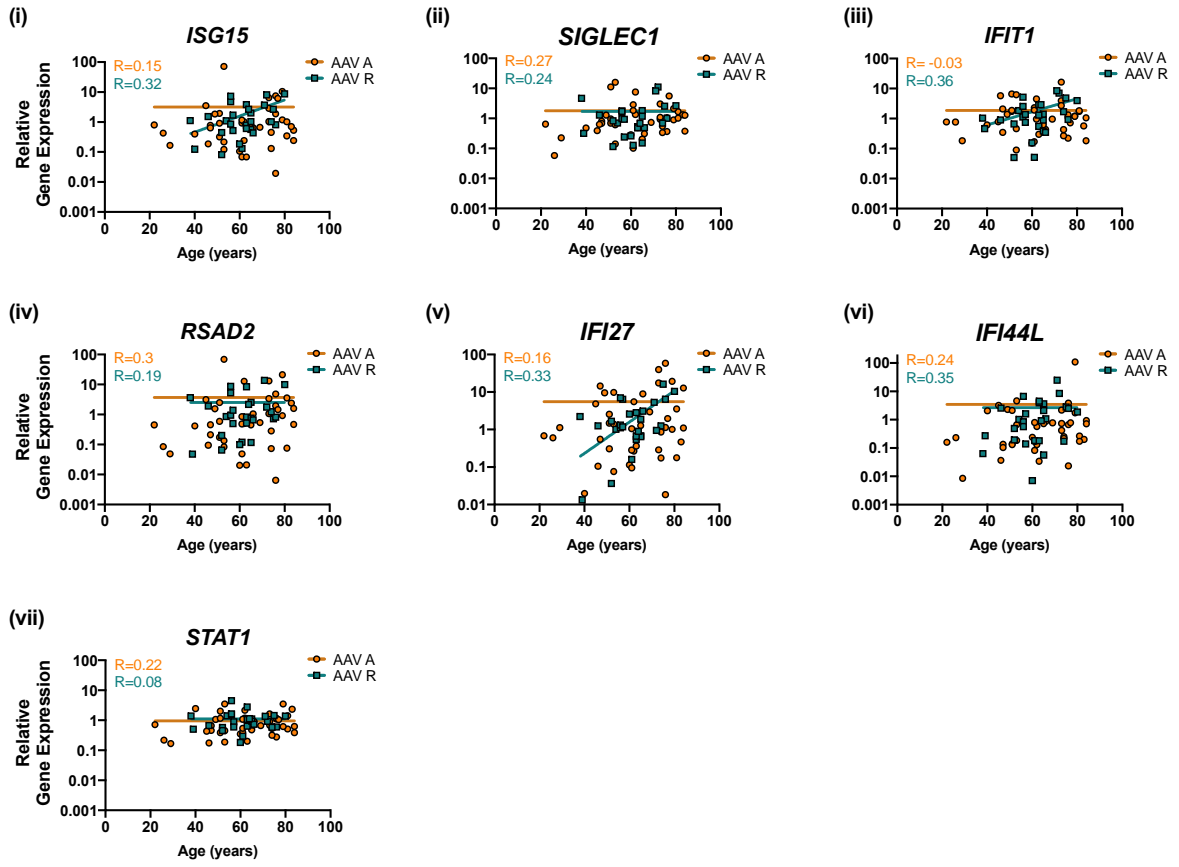
Figure 5.3.4: Correlation of type I IFN responses with age in AAV:

Whole blood samples were obtained from AAV R (n=27) and AAV A patients (n=42). qPCR was used to quantify the expression of seven IRGs. All data was made relative to the expression of the endogenous control gene *RPL27* and normalised to the median expression of the healthy control samples ($2^{-\Delta\Delta CT}$). (a.) The correlation between age and the expression value measured for each of these IRGs (i) *ISG15*, (ii) *IFIT1,* (iii) *SIGLEC1,* (iv) *RSAD2* (v) *IFI27,* (vi) *IFI44L* and (vii) *STAT1* in both AAV A (orange) and AAV R patients (blue). Matching serum samples were collected from AAV R patients (n=29) and AAV A patients (n=42). ELISAs were used to measure the concentration of serum cytokines. (b.) The correlation between age and serum concentrations of circulating (i) MCP-1, (ii) CCL19 and (iii) CXCL10 in both AAV A (orange) and AAV R patients (blue). Trend lines represent either (a.) semi-log non-linear regression lines or (b.) linear regression lines of best fit. Spearman correlations were used to determine correlation coefficients (R) and significance. * = $p < 0.05$.

5.3.5 Type I IFN Responses in AAV Are Independent of Whole Blood Cell Composition and Sex

Changes to whole blood cell composition is common in disease pathology, including in AAV, where patients often exhibit altered leukocyte cell counts [161, 287]. Different cell subsets have different gene expression profiles [288] so varying blood cell composition can affect transcriptional analysis [289, 290]. To assess any potential effects that differential cell counts may have on our analysis, the absolute cell counts available for each participant were correlated with their corresponding IFN scores. Only weak to moderate correlations, none of which were significant, were found between IFN scores and total white blood cell counts, which included cell counts for neutrophils, lymphocytes, eosinophils and platelets (Table 5.3.6).

Type I IFN responses have been reported to show sex-based differences with females often displaying overall higher type I IFN regulated activity [291]. In order to investigate the role of sex our analysis we compared IRG expression levels and IFN protein concentration measures between males and females. No significant differences were noted between the two sexes for each cohort (Figure 5.3.5)

Table 5.3.6:

		IFN Scores		
		DC	**AAV R**	**AAV A**
	WBC	0.14	0.02	-0.23
	Neutrophils	0.24	0.08	-0.14
Cell Counts	*Lymphocytes*	-0.2	-0.18	-0.24
	Eosinophil	-0.04	-0.02	0.08
	Platelets	0.15	-0.09	0.03
	Other	-0.37	0.13	-0.04

Table 5.3.7: Correlation of type I IFN Scores from DC, AAV R and AAV A patients with leukocyte cell counts

Type I IFN score data collected from DC, AAV R and AAV A patients were correlated with corresponding leukocyte cell counts measured for each participant upon sample collection. Leukocyte count data includes total white blood cell counts (WBC), neutrophil cell counts, lymphocyte cell counts, eosinophil cell counts and platelet cell counts. The remaining cells that make-up white blood cell compositions are represented as "other" in the above table. Spearman correlation analysis was used to generate correlation coefficient values, indicated in the table, and to determine the significance of these relationships. No significant correlations were noted.

Figure 5.3.5:

(i) *ISG15*

(ii) *SIGLEC1*

(iii) *IFIT1*

(iv) *RSAD2*

(v) *IFI27*

(vi) *IFI44L*

(vii) *STAT1*

b.

(i) MCP-1

(ii) CCL19

(iii) CXCL10
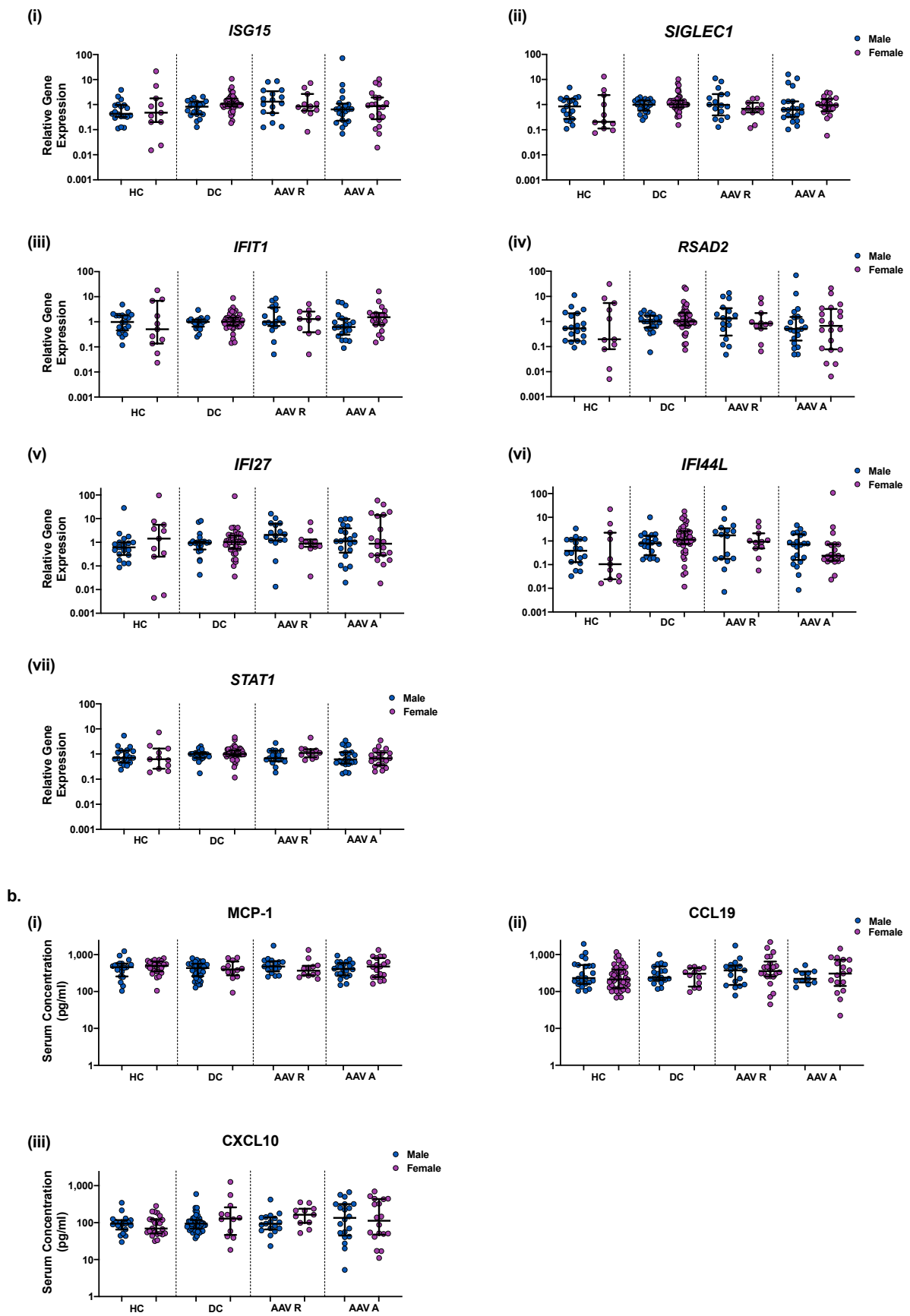
Figure 5.3.5: Sex Analysis of Type I IFN Regulated Gene and Protein Expression:

Whole blood samples were obtained from healthy controls (HC; n=62), disease controls (DC; n=30), AAV remission patients (AAV R; n=27) and AAV active patients (AAV A; n=42). qPCR was used to quantify gene expression and all data was made relative to the expression of the endogenous control gene *RPL27* and normalised to the median expression of the healthy control samples ($2^{-\Delta\Delta CT}$). (a.) Gene expression measurements of seven IRGs (i) *ISG15*, (ii) *IFIT1,* (iii) *SIGLEC1,* (iv) *RSAD2* (v) *IFI27,* (vi) *IFI44L* and (vii) *STAT1* separated and analysed by sex (male; blue, female; pink). Matching serum samples were collected from HC (n=67), DC (n=32), AAV R patients (n=29) and AAV A patients (n=42). (b.) Serum concentrations of circulating (i) MCP-1, (ii) CCL19 and (iii) CXCL10 were measured using ELISAs and separated and analysed by sex (male; blue, female; pink). Whole horizontal lines represent the median and IQR of each cohort and statistical analysis was performed using One-Way ANOVA with Dunn's multiple comparison testing. No significant differences were measured.
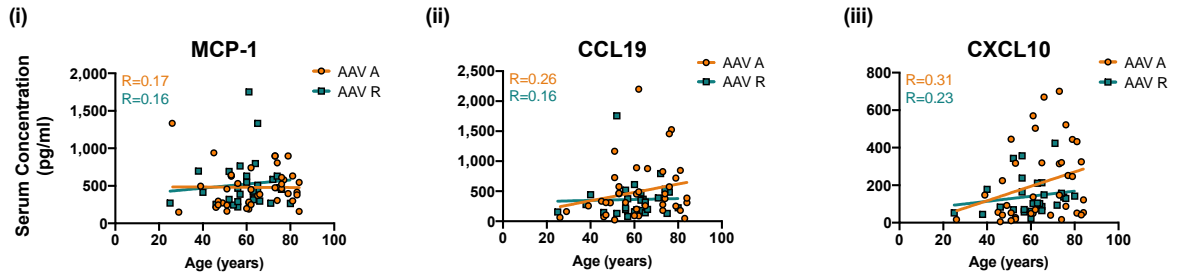
5.3.6 Immunosuppression Treatment Does Not Affect IRG Expression, but AAV Treatment Naïve Patients Have Significantly Increased CXCL10 Serum Concentrations

The immunosuppressive treatments received by AAV patients in this cohort are known to alter the expression of inflammatory mediators. Therefore, we investigated whether treatment naïve patients had elevated expression and the potential effects of these drugs on type I IFN responses in AAV. Immunosuppressive treatment did not affect IRG expression, with treatment naïve (TxN) samples and treated (Tx) samples showing similar levels for all IRGs measured (Figure5.3.6a.).

We also observed no differences in MCP-1 or CCL19 concentrations between treated and treatment naïve samples (Figure 5.3.6b). However, we did observe a significant increase in CXCL10 in treatment naïve samples (Figure 5.3.6b), which was not seen in treatment naïve disease control patients.

Figure 5.3.6:

a.
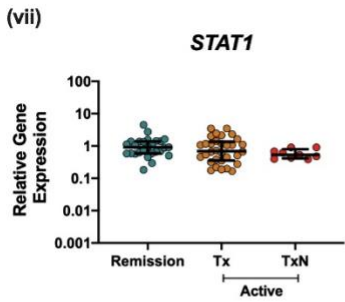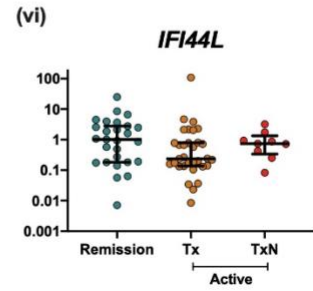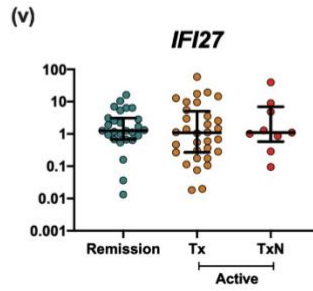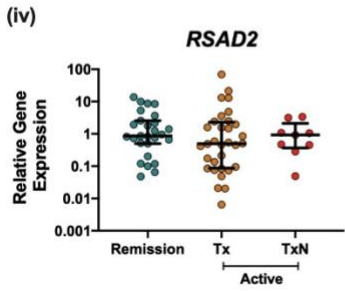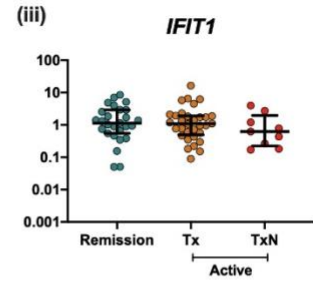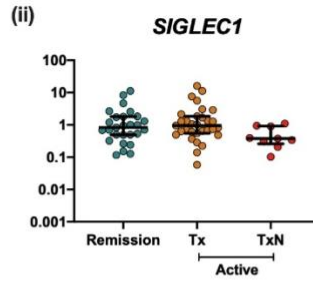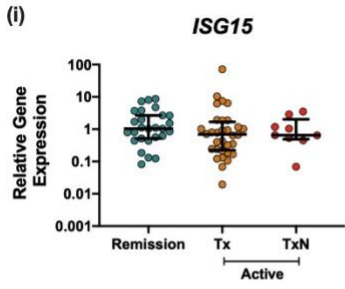
b.
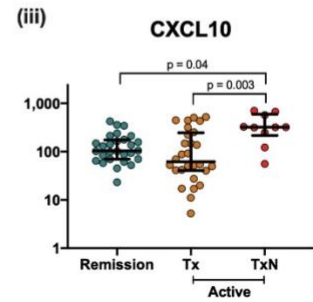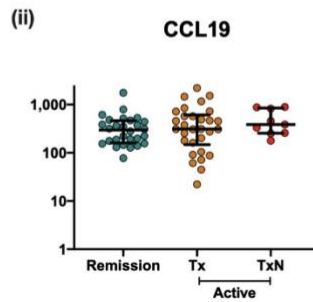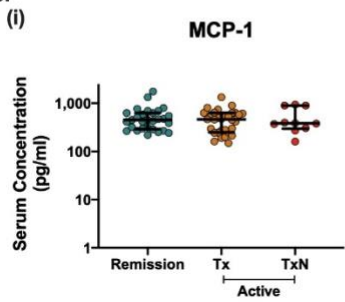
Figure 5.3.6: The effects of immunosuppressive treatment on type I IFN regulated gene expression and protein expression.

Whole blood samples were obtained from treated AAV remission patients (n=27), treated AAV active patients (Tx; n=31) and treatment naïve AAV active patients (TxN; n=10). qPCR was used to quantify the expression of seven IRGs (a.); IRGs (i) *ISG15*, (ii) *IFIT1,* (iii) *SIGLEC1,* (iv) *RSAD2* (v) *IFI27,* (vi) *IFI44L* and (vii) *STAT1*. Gene expression data is shown relative to the expression of the endogenous control gene *RPL27* and normalised to the median expression of the healthy control samples ($2^{-\Delta\Delta CT}$). Matching serum samples were collected from AAV remission (n=29), treated AAV active patients (Tx; n=31) and treatment naïve AAV active patients (TxN; n=10). (b.) Serum concentrations of circulating (i) MCP-1, (ii) CCL19 and (iii) CXCL10 were measured using ELISAs. Whole horizontal lines represent the median and IQR of each cohort and statistical analysis was performed using One-Way ANOVA with Dunn's multiple comparison testing.

5.3.7 Type I IFN Regulation Is Independent of ANCA Subtype

Given the many differences noted between anti-MPO and anti-PR3 mediated AAV we investigated the effect that ANCA subtype may have on our results. When comparing anti-MPO and anti-PR3 AAV samples no significant differences were noted in either IRG expression (Figure 5.3.7a) or IFN regulated protein concentration (Figure 5.3.7b).

Figure 5.3.7:
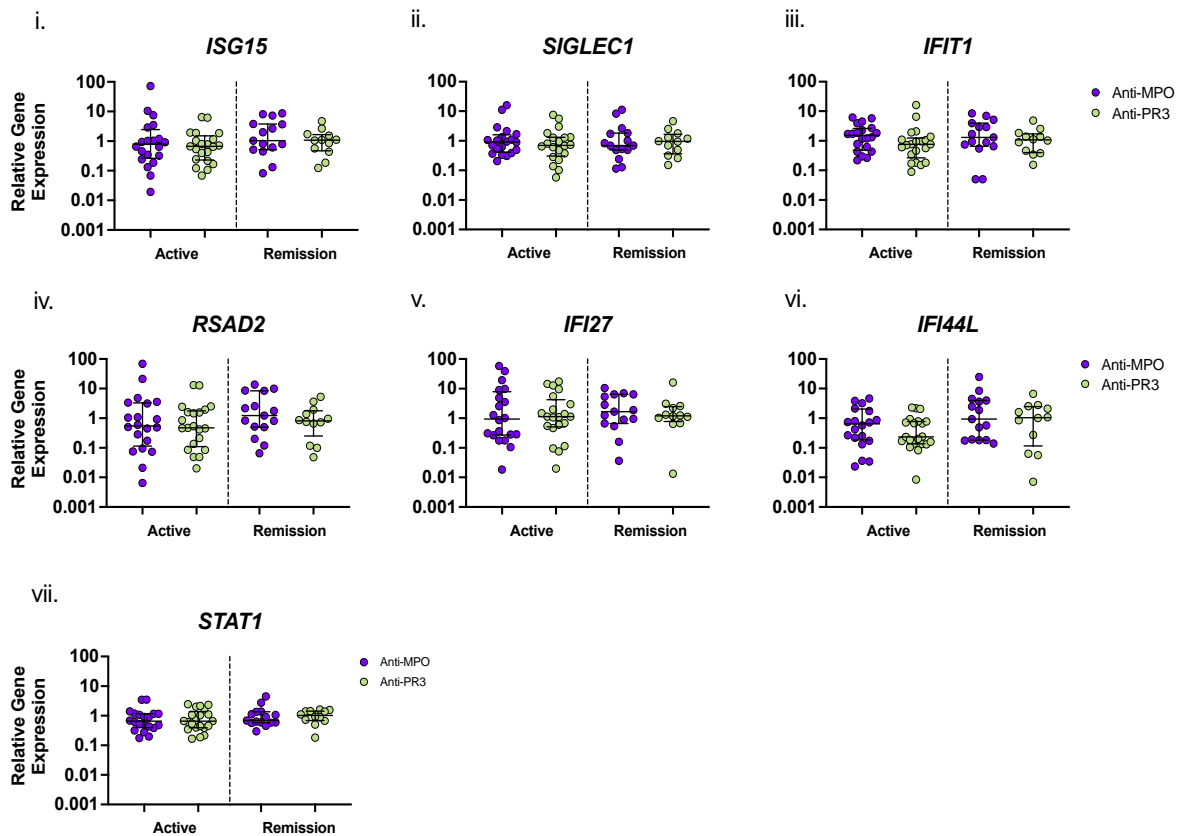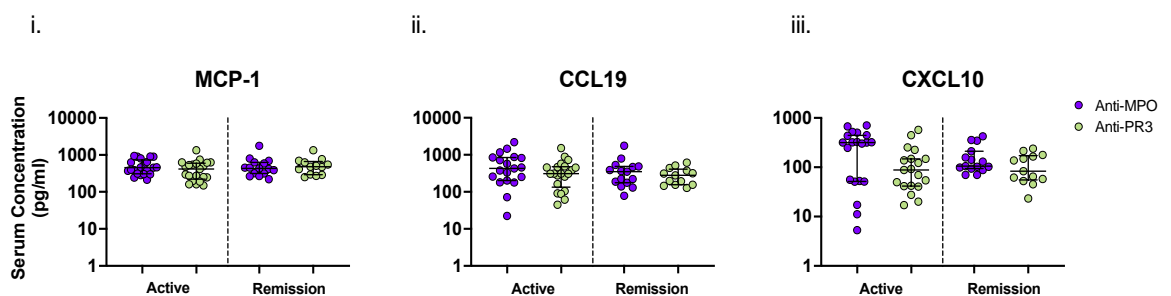
Figure 5.3.7: Type I IFN gene and protein expression by ANCA subtype.

Whole blood and serum samples were obtained from active anti-MPO AAV patients (n=21), active anti-PR3 AAV patients (n=23), remission anti-MPO patients (n=15) and remission anti-PR3 patients (n=13). qPCR was used to quantify the expression of seven IRGs from whole blood. All data was made relative to the expression of the endogenous control gene *RPL27* and normalised to the median expression of the healthy control samples ($2^{-\Delta\Delta CT}$). (a.) The relative gene expression measured for each of these IRGs (i) *ISG15*, (ii) *IFIT1,* (iii) *SIGLEC1,* (iv) *RSAD2* (v) *IFI27,* (vi) *IFI44L* and (vii) *STAT1* in both anti-MPO (lilac) and anti-PR3 patients (green). ELISAs were used to measure the concentration of serum cytokines. (b.) The serum concentrations of circulating (i) MCP-1, (ii) CCL19 and (iii) CXCL10 in both anti-MPO (lilac) and anti-PR3 patients (green). Whole horizontal lines represent the median and IQR of each cohort and statistical analysis was performed using One-Way ANOVA with Dunn's multiple comparison testing.

5.3.8 IRG and Type I IFN Regulated Protein Expression Does Not Correlate with AAV Severity

To explore potential relationships between type I IFN responses and AAV severity, we examined the correlation of type I IFN regulated protein and gene expression with three clinical measurements of AAV severity: BVAS, CRP concentrations and creatinine levels. We found no significant ($p < 0.05$) or strong ($r > 0.5$) correlations between type I IFN regulated gene or protein expression data and any of these clinical measurements (Table 5.3.7).

Table 5.3.7:

		BVAS	*CRP*	*Creatinine*
Gene Expression	*ISG15*	-0.18	0.04	-0.21
	SIGLEC1	-0.05	-0.08	-0.19
	IFIT1	-0.03	-0.06	-0.03
	RSAD2	-0.10	0.07	-0.17
	IFI27	-0.13	0.08	-0.10
	IFI44L	-0.21	-0.12	-0.02
	STAT1	-0.12	0.08	-0.23
Protein Expression	**CXCL10**	0.15	0.19	0.02
	MCP-1	0.05	-0.08	0.18
	CCL19	0.18	0.20	0.13

Table 5.3.8: Correlation of type I IFN responses with clinical measurements of AAV

Whole blood IRG gene expression data, as well as type I IFN regulated protein concentration data, collected from AAV patients (both active and remission) were correlated with matched BVAS, CRP and Creatinine levels. Spearman correlation analysis was used to generate correlation coefficient values, indicated in the table, and to determine the significance of these relationships. No statistically significant correlations were observed.

5.3.9 Data sets in this study are sufficiently powered allowing for accurate statistical analysis

In order to identify the likelihood of a type two error, power calculations using one-way balanced ANOVAs were undergone with data obtained from all gene expression and protein concentration experiments. Our calculated biological power of the analyses ranged from 84% to 87% (Table 5.3.8).

Table 5.3.8:

Variable	*Power*
ISG15	0.846464223
SIGLEC1	0.846464223
IFIT1	0.84896502
RSAD2	0.846464223
IFI27	0.84896502
IFI44L	0.843928587
STAT1	0.84896502
IFN Score	0.851431302
CXCL10	0.856261625
MCP1	0.867756297
CCL19	0.858626319

Table 5.3.9: Power analysis of interferon regulated gene and protein work in whole blood and serum. Power calculated using a one-way balanced ANOVA power calculation for each individual gene and protein analysed. Power calculation was performed by Dr. Arthur White.

5.4 Discussion

Knowing that dysregulated type I IFN signalling contributes to the pathology of various autoimmune diseases, that type I IFN responses become dysregulated with age and that AAV is an autoimmune disease that most commonly occurs later-in-life, we sought to investigate whether systemic type I IFN responses are dysregulated in AAV, indicative of a type I interferonopathy. Both transcriptional and translational mediators of type I IFN responses were measured following previously described methods commonly used in the identification and study of existing type I interferonopathies [208, 275]. Overall, our results indicate no link between systemic type I IFN regulated gene and protein expression and AAV, suggesting that AAV is not a type I interferonopathy and that patients are therefore unlikely to benefit from interferon inhibiting therapies.

Type I IFN activity is known to become dysregulated with age, with older individuals showing altered baseline IFN activity compared to younger controls [209, 210]. Age is therefore an important variable to consider when studying type I IFNs. In this study, we found only weak to moderate correlations between type I IFN activity and age in our AAV cohort. Interestingly these correlations were strongest in remission patients. Although not strong, all correlations were found to be positive, and given that the majority of samples tested were aged between 50 and 70, this is not unexpected, and likely represents a small but consistent increase in type I IFN responses within this age range. Overall results from our study would suggest that AAV patients experience slightly increased type I IFN responses with age however this is similar to those noted in healthy controls and is not exacerbated during AAV pathology.

Diseases such as SLE, Aicardi Goutier syndrome, dermatomyositis and Sjogren's syndrome are examples of autoimmune conditions that have been classified as type I interferonopathies due to alterations in systemic type I IFN responses [207, 215, 217, 218]. Dysregulation of type I IFN responses are implicated as drivers of the meta-inflammation characteristic of these conditions and elevated type I interferon regulated gene and protein expression often act as hallmarks for these type I interferonopathies [208, 215, 216, 275]. As well as showing abnormal IFN regulated expression, IFN activity in type I interferonopathies often directly correlates with clinical severity measurements and

outcomes of these patients. In SLE, for example, IFN responses have been shown to directly correlate with the SLE disease activity index (SLEDAI) [259, 275]. Despite the lack of significant differences in type I IFN regulated gene and protein expression between AAV samples and control samples we explored the idea that type I IFN responses may still have a role in AAV disease severity, postulating that high IFN regulated expression may correlate with the presence of severe acute disease. We found no strong correlations between standard clinical measurements of AAV (including BVAS, creatinine levels and CRP concentrations) and type I IFN regulated expression at either a transcriptional or a translational level. We also did not find any evidence that sex, ANCA status or cellular composition of our samples influenced the IFN scores that we generated in our AAV cohort, however we do note that we did not perform cell type specific analysis, and this is a limitation of our findings. Taken together, our analysis suggests that type I IFNs and associated responses are not key drivers of AAV disease pathogenesis.

These findings do contradict those of Kessler *et al*. who has recently looked at this family of cytokines, predominantly in mouse models of AAV but also in isolated human PBMCs and has reported a type I IFN signature in active anti-MPO AAV [292]. Although many of these differences could be attributed to specificities of the mouse model used, the underlying differences between our results and Kessler's PBMC results remain unresolved. Despite this, I would suggest that these differences are likely a result of cohort variation in both healthy controls and AAV samples. The healthy controls used in Kessler's study were indeed younger than those used here, despite their AAV cohort showing similar age ranges to our AAV cohort. Knowing the importance of ageing on type I IFN responses, we suggest that this has contributed some of the differences in results noted between these two studies. Differences in clinical severity and treatment courses between the AAV cohorts may also add to these conflicting results however this is yet to be confirmed [292].

Treatment for AAV consists of broad immunosuppression and it is possible that immunosuppressive drugs impact on systemic type I IFN responses. We found that treatment naïve AAV patients have significantly higher concentrations of circulating CXCL10 when compared to treated patients suggesting that the immunosuppressive drugs received by these individuals act to suppress CXCL10 production. Interestingly, investigations into the role of type I IFNs in autoimmune Addison's disease (AAD) show

a similar CXCL10 finding between patients and healthy controls [293, 294]. Although AAD has not officially been categorised as a type I interferonopathy, one study has found dysregulation in the negative regulators of type I IFN responses in T cells of patients with AAD following stimulation [293]. This data suggests that, at baseline, type I IFN regulated gene expression is standard in AAD, but T cells isolated from these patients fail to respond appropriately to immune stimulation resulting in alterations to type I IFN regulated responses. This raises the intriguing question of whether basal type I IFN responses also remain intact in AAV but an inability to appropriately respond to immune challenges occurs, or furthermore whether dysregulation of IFN signalling is specific to certain cell types which may become diluted in whole blood analysis. It is important to note, however, that although CXCL10 has been proven to be a useful biomarker of type I interferonopathies in the past [217], it is also known to be upregulated in several other autoimmune disorders, so this upregulation is not necessarily specific to type I interferonopathies [279]. CXCL10 expression can be upregulated by several immune factors in addition to type I IFNs, in particular IFNγ, a type II IFN. IFNγ production is reported to be upregulated in AAV and genes involved in IFNγ signalling pathways have been proposed to have novel roles in AAV pathogenesis suggesting that perhaps the upregulation of CXCL10 seen here in treatment naive AAV active patients is a result of type II IFN activity [295, 296].

Each of the proteins analysed here have been investigated in AAV previously and although our results agree with some of these studies, they contradict the findings of others. For example, similar to our observations, Monach *et al*. showed a significant increase of CXCL10 in AAV serum samples compared to healthy controls, however unlike our study, this find was independent of disease status while also showing no significant effects of treatment [297]. These conflicting results warrant further investigation however may be partially explained through differences in study design. For instance, samples used by Monach *et al*. were received through the RAVE trial, a trial testing the efficacy of rituximab in the treatment of AAV [154, 297]. These patients were therefore undergoing a strict treatment regimen with little to no crossover with other medications. In contrast, participants in our treated cohort were often on various treatment options simultaneously and this has likely affected our results. Variable prednisone treatment before rituximab therapy can affect IFN scores in rheumatoid arthritis patients and so differences in treatment regimens between the studies is clearly an important

variable to note [298]. Although our findings are therefore limited in that they cannot be attributed to the effects of one specific treatment, this is possibly a more realistic overview of treated AAV cohorts with combination therapies being routinely prescribed [299]. Additionally, differences in CXCL10 concentrations observed between the two studies may be a consequence of the differential assay sensitivities noted between our two methods of protein detection, with Monach *et al*. observing discrete but significant differences between their cohorts [297]. Indeed, the median values of circulating CXCL10 were higher in both our remission (103.6pg/ml) and active (130pg/ml) AAV patient samples when compared to that of healthy controls (93.47pg/ml), however this did not reach statistical significance. It is worth noting that the median CXCL10 levels detected in our cohort (AAV, DC and HC) correspond with the serum concentration range of CXCL10 reported in the healthy control cohorts of various studies that use ELISAs as a means of protein detection [300-302]. However, it is clear that the role of CXCL10 in AAV pathogenesis remains to be fully elucidated. Again, our MCP-1 and CCL19 results both agree with [167, 303] and contradict previous studies [304, 305]. However, studies that contradict our findings had sample sizes significantly smaller than those used here [304, 305]. Our large sample size is a strength of this work acting to minimise the likelihood of a type II error in our analysis (Table 5.3.8).

This study is not without limitations, and these are important to note. The focus of this work was to investigate systemic type I IFN responses to determine whether AAV could be classified as a type I interferonopathy, as is standard practice in the study and diagnosis of type I interferonopathies [208, 217]. As such, tissue and organ specific analysis was not investigated so a role for type I IFNs at local sites of inflammation cannot be ruled out. Several autoimmune diseases have site-specific upregulation of type I IFNs responses [306]. Indeed, increased gene expression of *MX1,* an IRG, was observed in the glomeruli of AAV patients with active disease by Kessenbrock *et al*. suggesting a localised change in IFN responses in active AAV patients [50]. However, we have since conducted analysis using the Ingenuity Pathway Analysis (IPA) software system on publicly available RNA-sequencing data sets from the glomeruli of AAV patients in order to better characterise the molecular pathways driving AAV. Type I interferons signalling pathways were not pathways flagged in this analysis when comparing the most differentially expressed genes in AAV patients compared to healthy controls (Appendix 2).

Another limitation is that only four matched active and remission samples were available for this study, three AAV participants and one in the disease control group, thus making robust analysis of matched samples difficult. Although increasing numbers of matched samples would have strengthened investigation of type I IFN responses in AAV disease progression and relapse, the stratification of our AAV cohort into active and remission groups, which even post-stratification had sufficient numbers for well-powered analysis and the availability of matched clinical measurements provides significant insight into relationships between systemic type I IFN responses and disease activity.

The heterogenous nature of our AAV disease control cohort acts as an additional limitation to this study. Samples from a variety of diseases were purposefully chosen to analyse potential contribution of general kidney inflammation and systemic autoimmune disorders to enable the identification of AAV specific upregulation. However, for each group, small numbers, range of disease severities and treatments made singular disease comparison difficult and possibly blunted any signals that may have otherwise been observed in specific disease settings [307].

5.5 Conclusion

Overall, this study was carried out with the aim of better understanding the underlying immune processes behind AAV progression with the potential to provide a more specific target for future treatment of AAV. Despite their role in ageing and inflammageing, our work indicates that systemic type I IFN responses are not key drivers in AAV pathogenesis and so patients are unlikely to benefit from treatments that target these cytokines [219, 252]. We have shown that systemic type I IFN responses are not dysregulated in AAV and that these responses do not correlate with AAV disease severity.

6 Final Discussion

Ageing is a complex concept that is often associated with an increased risk of disease development. With a rapidly expanding ageing population, the underlying cellular processes that drive this risk association with age, a concept known as biological ageing, has become a major focus of current gerontological research [1, 7, 8]. Unusually for an autoimmune disease, AAV commonly develops later-in-life, with incidence rates for AAV peaking in the sixth-seventh decades [133, 147, 190]. Despite this association with chronological age, the biological mechanisms driving this risk remain unknown. There is currently no cure for AAV patients, and although the available therapeutic options have greatly improved patient outcomes, they can have severe adverse effects with treatment complications being the leading cause of death in AAV patients within the first year of diagnosis [154, 194, 195]. The need for more specific treatment options is clear and therefore there is a need to better understand the biological processes driving AAV. Thus, further investigation into age-related processes could help to reveal important pathways involved in AAV development and progression.

Chapter 3 of this project aimed to estimate and explore biological age in AAV patients. We have shown for the first time that AAV patients experience accelerated biological ageing compared to healthy controls, measured using an *ELOVL2* epigenetic clock model. Intriguingly, the increase in epigenetic age was shown to be diminished following induction treatment with either cyclophosphamide or rituximab, highlighting that treatment directly affects this particular measure of accelerated biological ageing. Furthermore, we found that the changes in *ELOVL2* methylation detected in AAV patients and controls may result in transcriptional differences between cohorts, with increased DNA methylation correlating to decreased *ELOVL2* gene expression. Taken together, these results suggest that the risk associated with chronological age in AAV translates onto a biological scale.

AAV is characterised by severe inflammation of the small blood vessels. Having demonstrated an association between biological age and AAV, we continued on to explore the effects that age-related immune system changes have on AAV pathogenesis [150, 182]. Changes to both the innate and adaptive immune system are known to occur with age with dysregulated inflammation recently being recognised as a key hallmark of biological ageing [1, 8, 66, 236]. We thus investigated the effect that age has on various innate immune functions in response to ANCA stimulation. We found that various inflammatory

processes such as cytokine secretion, ROS production and cellular senescence induction were increased in response to ANCA stimulation of immune cells. This response was higher in healthy older individuals compared to younger controls, although this was often cell and ANCA specific. These results are similar to those previously outlined in mouse models [234]. The results described in chapter 4 indicate that age-related changes to immune cells may make them more responsive to ANCAs and thus, may be contributing towards the characteristic immunopathology of AAV.

Finally, considering the impact of ageing on innate immunity in response to ANCA stimulation, we went on to perform an in-depth investigation into an important arm of the innate immune response, type I IFN signalling, in AAV patients. We have previously shown that type I IFN regulated immunity is altered with age (unpublished; Figure 5.1.1) and considering various reports that have noted a potential role for these cytokines in AAV [50, 220], as well as their well-established role in the immunopathology of several other prominent inflammatory autoimmune diseases, we sought to conclusively examine the role of type I IFN responses in AAV pathogenesis. Here we quantified the expression of type I IFN regulated genes and proteins and investigated their relationship with disease severity. We showed that type I IFN regulated expression is not dysregulated in AAV compared to healthy or disease controls. As well as this, measures of type I IFN responses did not correlate with measures of disease severity in AAV patients. We therefore suggest that type I IFN signalling is not systemically dysregulated in AAV and that AAV should not be considered as a type I interferonopathy.

It is important to discuss that accelerated ageing is a phenomenon found to occur in several other age-related disease settings, and so, it is not specific to AAV [38, 39, 226, 308, 309]. The effect that treatment had on DNAm-based ageing measures found in this study may also translate into other disease states and is a factor that needs further consideration and exploration. Several studies have reported DNAm-based age differences post pharmacological intervention calling into question the reliability of these clocks during infectious or disease conditions [37, 40, 308]. The variability of these clocks under such conditions may therefore support their use as biomarkers for certain age-related pathologies and indeed multiple studies to date have explored and confirmed this concept [38, 40, 309, 310]. Given our results, this may be a beneficial avenue of research to explore in AAV.

Considering the key role of inflammation in biological ageing and age-related disease including AAV, we did expect that our DNAm-based age measures would likely be influenced by dysregulated inflammatory responses. However, the lack of any strong correlations between DNAm-based age measures, markers of systemic inflammation such as CRP and immune cell frequencies would indicate otherwise, leaving us unclear as to the specific mechanisms driving DNAm-based ageing in AAV patients. It is likely that this phenomenon is a product of an accumulation of environmental and genetic factors over time and cannot be attributed to one such process. The answer to this specific question remains beyond the scope of this project.

The specific roles of ANCAs in AAV are still somewhat debated [173, 183]. We, like various other studies, have reported that ANCAs are capable of driving pro-inflammatory processes such as cytokine secretion, ROS production, NETosis and degranulation supporting the model that ANCAs exacerbate the immunopathology seen in AAV [196, 234, 238, 239]. Unlike most other studies however, we have shown that aspects of this pro-inflammatory response are heightened in older individuals in certain contexts. We suggest that this is linked to inflammageing in older donors, elevating their response to certain stimuli possibly through the priming of unstimulated cells [83, 234]. Importantly, we noted differences in immune responses between our anti-MPO and anti-PR3 stimulated cells indicating a potentially divergent mechanism of action between the two autoantibodies. This would support the recent motion of further categorising AAV patients based on ANCA subtype [150, 183]. Throughout this work, when investigating AAV patient samples we further categorised and analysed cohorts based on ANCA subtype. We have shown that both anti-MPO and anti-PR3 mediated AAV patients experience significant DNAm age acceleration compared to healthy controls. Although we saw no significant differences in DNAm age between anti-MPO and anti-PR3 patients we did note potential differences regarding response to induction treatment. Despite this, no difference between these two patient cohorts were noted when analysing type I IFN signalling. Overall, our results suggest that anti-MPO and anti-PR3 mediated AAV result in very similar clinical pathologies that overlap in many respects but may result from divergent immune related pathways.

In terms of the immunopathology of AAV, our work indicates a role for cellular senescence in this disease. The accumulation of senescent cells accompanied by SASP secretion has been implicated to contribute to multiple age-related pathologies including Alzheimer's disease, cardiovascular disease and cancer [221, 311, 312]. Emerging evidence has linked cellular senescence to the development of several autoimmune diseases including systemic sclerosis, SLE and RA, where SASP factors provide a pro-inflammatory environment that contributes towards tissue damage and fibrosis while simultaneously promoting the activation of autoreactive B and T cells and subsequent production of autoantibodies [313-316]. The accumulation of cellular senescence with age may therefore promote the development of autoimmunity later-in-life, an idea that has only recently begun to be explored [132, 234]. Indeed, cellular senescence is a relatively novel area of research with respect to AAV with most work to date focusing on senescent T cells. Elevations in circulating senescent T cells, that show diminished expression of the costimulatory molecule CD28, has been reported in AAV patients compared to controls. These cells are thought to be a source of pro-inflammatory mediator production contributing to chronic inflammation as well as autoreactivity in AAV [235, 317]. Our work suggests that cellular senescence may be systemically increased in AAV patients compared to healthy controls. PBMCs isolated from older individuals and stimulated with anti-MPO also show increased *p21* expression, a marker of cellular senescence, compared to those isolated from younger donors. We therefore suggest that the presence of ANCAs may promote cellular senescence with age in AAV patients and, considering the work outlined by Li. *et al*. who showed that a loss of *ELOVL2* gene expression resulted in mitochondrial dysfunction, cellular stress and a resultant increase in cellular senescence, we propose that this could potentially be mediated by *ELOVL2* expression. Given the emergence of senolytic drugs that target senescent cell accumulation, in-depth knowledge regarding the role of cellular senescence in AAV could provide more specific and targeted treatment options to patients and we would therefore advocate for further research into the role of cellular senescence in AAV.

In summary, we have shown that AAV patients experience accelerated DNAm age as well as highlighting the differential impact that ageing has on ANCA-driven immune responses. We have also conclusively demonstrated that type I IFNs are not systemically dysregulated in AAV and so AAV should not be classified as a type I interferonopathy. Overall, our results point to the importance of ageing and, more specifically, biological

ageing in the pathogenesis of AAV and suggest that the mechanisms associated with age be further studied in AAV patients.

6.1 Future work

The work outlined in this thesis has helped to highlight the importance of biological age and age-related immune processes in the pathogenesis of AAV. The establishment of *ELOVL2* methylation as a marker for epigenetic ageing in AAV has led to some interesting future avenues of research. Firstly, we would hope to continue our investigation into the mechanistic effects that increasing *ELOVL2* methylation has on these patients. Although we have already established that methylation changes translate into transcriptional effects, we would further like to explore ELOVL2 protein expression as well as the potential effects that this has on mitochondrial function and stem cell exhaustion as was highlighted in mouse models. We are curious about the role of ANCAs in this process and plan to further investigate whether ANCA stimulation of isolated cells can mimic the results seen in AAV patient samples. Furthermore, the viability of this gene as a biomarker for disease activity and relapse in AAV is an area of great interest that we hope to delve into with future work.

The effect that treatment had on DNAm-based age measurements is a very interesting and important find from this project and has raised many questions regarding the efficacy of epigenetic modelling in a disease context. Future work should further explore these results in different disease settings as well as potentially dive into the mechanistic drivers of this in more detail.

Although we explored many aspects of the innate immune response during this project, as discussed in Chapter 4 some of this work was underpowered in terms of participant numbers, and so future work would have to be carried out in order to confirm these findings. As well as this, one important pathway that we were unable to explore was the complement system. The complement system refers to a series of pathways that play a crucial role in pathogen defence and immunomodulation. It can be further categorised into 3 specific pathways: classical, lectin and alternative [318, 319]. Interestingly, recent studies have demonstrated that age significantly alters complement levels and functionality in a healthy population [318]. Dysregulated activation of the alternative pathway has also been shown necessary in the development of ANCA associated vasculitis. Avacopan, a complement component inhibitor, has recently been shown to promote sustained remission in AAV patients and this has since gained approval for

clinical use [195]. The links between ageing, complement activation and AAV is therefore a very interesting prospect for future research.

Finally, this thesis has focused primarily on innate immune cell function with age. Both innate and adaptive immune responses are altered with age and indeed both innate and adaptive immunity are implicated in the pathogenesis of AAV. Previous work undergone on mouse models of AAV have suggested an increased sensitivity to MPO immunisation with age, a response largely driven by the B and T cells. How changes to the adaptive immune response effect AAV development in humans should be explored further in the future.

6.2   Final Remarks

The effect that biological ageing has on AAV development is an extremely understudied area of research. With chronological ageing being arguably the most important risk factor in relation to initial AAV development, the biological implications that this has in terms of AAV pathogenesis are important to uncover. Through this research I aimed to investigate the relationship between ageing and AAV activity with a specific focus on biological ageing and innate immune cell functions. The key finding from this work are as followed.

- Biological ageing is accelerated in AAV patients compared to healthy controls as measured using an *ELOVL2* epigenetic clock model.

- Induction treatment with either cyclophosphamide or rituximab effects DNAm-based epigenetic age analysis, decreasing EAA in AAV patients.

- Changes in *ELOVL2* methylation correlate with transcriptional changes in *ELOVL2* gene expression.

- Certain innate immune functions differ with age in response to ANCA stimulation with cells isolated from older donors often showing heightened pro-inflammatory induction.

- Type I regulated IFN responses are not dysregulated with age and therefore AAV should not be considered a type I interferonopathy.

Overall, our work has demonstrated that biological ageing and age-related processes are involved in AAV pathogenesis and further investigation into this will help in our understanding of the AAV pathology and potentially lead to more specific treatment options for these patients (Figure 6.2.1).

Figure 6.2.1:
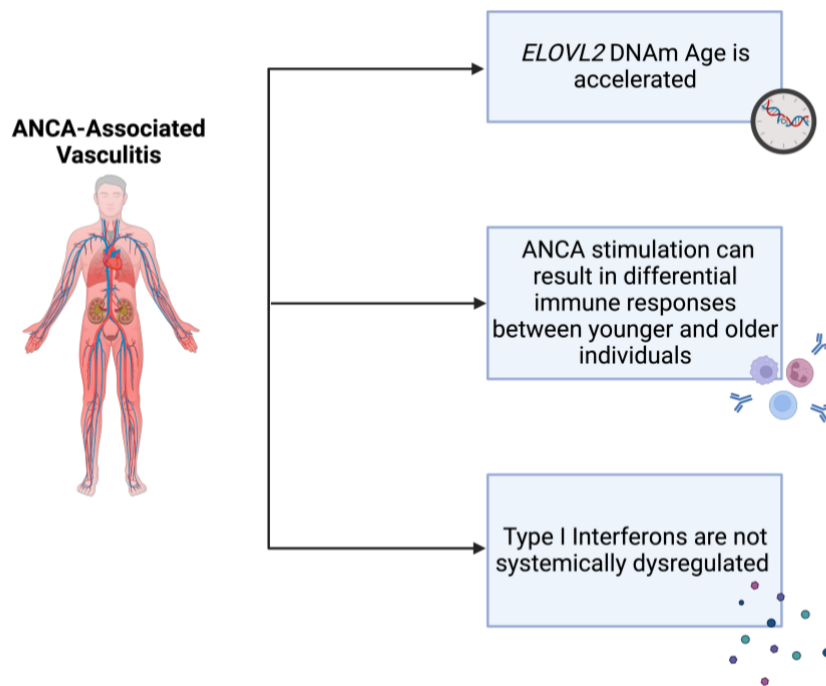
Figure 6.2.1 Summary of Main Results

7 References

1.   López-Otín, C., et al., *The hallmarks of aging.* Cell, 2013. **153**(6): p. 1194-217.
2.   Scott, K.R. and A.M. Barrett, *Dementia syndromes: evaluation and treatment.* Expert Rev Neurother, 2007. **7**(4): p. 407-22.
3.   Kalogeropoulos, A.P., et al., *Echocardiography, natriuretic peptides, and risk for incident heart failure in older adults: the Cardiovascular Health Study.* JACC Cardiovasc Imaging, 2012. **5**(2): p. 131-40.
4.   North, B.J. and D.A. Sinclair, *The intersection between aging and cardiovascular disease.* Circ Res, 2012. **110**(8): p. 1097-108.
5.   Zinger, A., W.C. Cho, and A. Ben-Yehuda, *Cancer and Aging - the Inflammatory Connection.* Aging Dis, 2017. **8**(5): p. 611-627.
6.   Bektas, A., et al., *Aging, inflammation and the environment.* Exp Gerontol, 2018. **105**: p. 10-18.
7.   Partridge, L., J. Deelen, and P.E. Slagboom, *Facing up to the global challenges of ageing.* Nature, 2018. **561**(7721): p. 45-56.
8.   López-Otín, C., et al., *Hallmarks of aging: An expanding universe.* Cell, 2023. **186**(2): p. 243-278.
9.   Levine, M.E., et al., *An epigenetic biomarker of aging for lifespan and healthspan.* Aging (Albany NY), 2018. **10**(4): p. 573-591.
10.   Lu, A.T., et al., *DNA methylation GrimAge strongly predicts lifespan and healthspan.* Aging (Albany NY), 2019. **11**(2): p. 303-327.
11.   Belsky, D.W., et al., *Quantification of the pace of biological aging in humans through a blood test, the DunedinPoAm DNA methylation algorithm.* Elife, 2020. **9**.
12.   Garagnani, P., et al., *Methylation of ELOVL2 gene as a new epigenetic marker of age.* Aging Cell, 2012. **11**(6): p. 1132-4.
13.   Horvath, S. and K. Raj, *DNA methylation-based biomarkers and the epigenetic clock theory of ageing.* Nat Rev Genet, 2018. **19**(6): p. 371-384.
14.   *Image created using Biorender.com*. Available from: https://www.biorender.com.
15.   Watson, J.D. and F.H. Crick, *Molecular structure of nucleic acids. A structure for deoxyribose nucleic acid. 1953.* Rev Invest Clin, 2003. **55**(2): p. 108-9.
16.   Alberts Bruce, J.A., Lewis Julian, Raff Martin, Roberts Keith, Walter Peter, *Molecular Biology of the Cell*. Fifth ed. 2008: Garland Science.
17.   Allis, C.D. and T. Jenuwein, *The molecular hallmarks of epigenetic control.* Nat Rev Genet, 2016. **17**(8): p. 487-500.
18.   Booth, L.N. and A. Brunet, *The Aging Epigenome.* Mol Cell, 2016. **62**(5): p. 728-44.
19.   Zhang, X., et al., *Genome-wide analysis of epigenetic dynamics across human developmental stages and tissues.* BMC Genomics, 2019. **20**(Suppl 2): p. 221.
20.   Tiffon, C., *The Impact of Nutrition and Environmental Epigenetics on Human Health and Disease.* Int J Mol Sci, 2018. **19**(11).
21.   Buro-Auriemma, L.J., et al., *Cigarette smoking induces small airway epithelial epigenetic changes with corresponding modulation of gene expression.* Hum Mol Genet, 2013. **22**(23): p. 4726-38.
22.   Pandey, S.C., et al., *Brain chromatin remodeling: a novel mechanism of alcoholism.* J Neurosci, 2008. **28**(14): p. 3729-37.

23.   Tobi, E.W., et al., *DNA methylation signatures link prenatal famine exposure to growth and metabolism.* Nat Commun, 2014. **5**: p. 5592.
24.   Dayeh, T., et al., *DNA methylation of loci within ABCG1 and PHOSPHO1 in blood DNA is associated with future type 2 diabetes risk.* Epigenetics, 2016. **11**(7): p. 482-8.
25.   Xu, K., et al., *Epigenome-wide association analysis revealed that SOCS3 methylation influences the effect of cumulative stress on obesity.* Biol Psychol, 2018. **131**: p. 63-71.
26.   Surace, A.E.A. and C.M. Hedrich, *The Role of Epigenetics in Autoimmune/Inflammatory Disease.* Front Immunol, 2019. **10**: p. 1525.
27.   De Carvalho, D.D., et al., *DNA methylation screening identifies driver epigenetic events of cancer cell survival.* Cancer Cell, 2012. **21**(5): p. 655-67.
28.   Jones, P.A., et al., *Epigenetic therapy in immune-oncology.* Nat Rev Cancer, 2019. **19**(3): p. 151-161.
29.   Moore, L.D., T. Le, and G. Fan, *DNA methylation and its basic function.* Neuropsychopharmacology, 2013. **38**(1): p. 23-38.
30.   Bird, A.P., *CpG-rich islands and the function of DNA methylation.* Nature, 1986. **321**(6067): p. 209-13.
31.   Horvath, S., *DNA methylation age of human tissues and cell types.* Genome Biol, 2013. **14**(10): p. R115.
32.   Hannum, G., et al., *Genome-wide methylation profiles reveal quantitative views of human aging rates.* Mol Cell, 2013. **49**(2): p. 359-367.
33.   Zbieć-Piekarska, R., et al., *Examination of DNA methylation status of the ELOVL2 marker may be useful for human age prediction in forensic science.* Forensic Sci Int Genet, 2015. **14**: p. 161-7.
34.   Li, X., et al., *Lipid metabolism dysfunction induced by age-dependent DNA methylation accelerates aging.* Signal Transduct Target Ther, 2022. **7**(1): p. 162.
35.   Wang, Y., et al., *Epigenetic influences on aging: a longitudinal genome-wide methylation study in old Swedish twins.* Epigenetics, 2018. **13**(9): p. 975-987.
36.   Sturm, G., et al., *Human aging DNA methylation signatures are conserved but accelerated in cultured fibroblasts.* Epigenetics, 2019. **14**(10): p. 961-976.
37.   Fahy, G.M., et al., *Reversal of epigenetic aging and immunosenescent trends in humans.* Aging Cell, 2019. **18**(6): p. e13028.
38.   Theodoropoulou, E., et al., *Different epigenetic clocks reflect distinct pathophysiological features of multiple sclerosis.* Epigenomics, 2019. **11**(12): p. 1429-1439.
39.   Fransquet, P.D., et al., *The epigenetic clock as a predictor of disease and mortality risk: a systematic review and meta-analysis.* Clin Epigenetics, 2019. **11**(1): p. 62.
40.   Sehl, M.E., et al., *The acute effects of adjuvant radiation and chemotherapy on peripheral blood epigenetic age in early stage breast cancer patients.* NPJ Breast Cancer, 2020. **6**: p. 23.
41.   Chaplin, D.D., *Overview of the immune response.* J Allergy Clin Immunol, 2010. **125**(2 Suppl 2): p. S3-23.
42.   Alberts B, J.A., Lewis J, et al., *Molecular Biology of the Cell*. 4th edition ed. Innate Immunity. 2002, New York: Garland Science.
43.   Alberts B, J.A., Lewis J, et al., *Molecular Biology of the Cell*. 4th Edition ed. Chapter 24, The Adaptive Immune System. 2002, New York: Garland Science.

44. Systems, B.-R.D. *A Guide to Human Immune Cell Characterization by Flow Cytometry*. Cell Markers Guide for Human Immune Cell Characterization by Flow Cytometry; Available from: https://resources.rndsystems.com/images/site/br_imm-cell-character-fc_rsdfy20-8243-w-mp.pdf.

45. Marshall, J.S., et al., *An introduction to immunology and immunopathology.* Allergy Asthma Clin Immunol, 2018. **14**(Suppl 2): p. 49.

46. Pillay, J., et al., *In vivo labeling with 2H2O reveals a human neutrophil lifespan of 5.4 days.* Blood, 2010. **116**(4): p. 625-7.

47. Ui Mhaonaigh, A., et al., *Low Density Granulocytes in ANCA Vasculitis Are Heterogenous and Hypo-Responsive to Anti-Myeloperoxidase Antibodies.* Front Immunol, 2019. **10**: p. 2603.

48. Lehman, H.K. and B.H. Segal, *The role of neutrophils in host defense and disease.* J Allergy Clin Immunol, 2020. **145**(6): p. 1535-1544.

49. Fuchs, T.A., et al., *Novel cell death program leads to neutrophil extracellular traps.* J Cell Biol, 2007. **176**(2): p. 231-41.

50. Kessenbrock, K., et al., *Netting neutrophils in autoimmune small-vessel vasculitis.* Nat Med, 2009. **15**(6): p. 623-5.

51. Guilliams, M., A. Mildner, and S. Yona, *Developmental and Functional Heterogeneity of Monocytes.* Immunity, 2018. **49**(4): p. 595-613.

52. Boyette, L.B., et al., *Phenotype, function, and differentiation potential of human monocyte subsets.* PLoS One, 2017. **12**(4): p. e0176460.

53. Weller, P.F. and L.A. Spencer, *Functions of tissue-resident eosinophils.* Nat Rev Immunol, 2017. **17**(12): p. 746-760.

54. Dorosz, A., et al., *Eosinophils and Neutrophils-Molecular Differences Revealed by Spontaneous Raman, CARS and Fluorescence Microscopy.* Cells, 2020. **9**(9).

55. LeBien, T.W. and T.F. Tedder, *B lymphocytes: how they develop and function.* Blood, 2008. **112**(5): p. 1570-80.

56. McHeyzer-Williams, L.J. and M.G. McHeyzer-Williams, *Antigen-specific memory B cell development.* Annu Rev Immunol, 2005. **23**: p. 487-513.

57. Medzhitov, R., *Inflammation 2010: new adventures of an old flame.* Cell, 2010. **140**(6): p. 771-6.

58. Amoureux, M.C., et al., *Peptidoglycan and bacterial DNA induce inflammation and coagulation markers in synergy.* Mediators Inflamm, 2005. **2005**(2): p. 118-20.

59. Yang, K.H., et al., *The main functions and structural modifications of tripeptide N-formyl-methionyl-leucyl-phenylalanine (fMLP) as a chemotactic factor.* Pharmazie, 2008. **63**(11): p. 779-83.

60. Takeuchi, O. and S. Akira, *Pattern recognition receptors and inflammation.* Cell, 2010. **140**(6): p. 805-20.

61. Kusiak, A. and G. Brady, *Bifurcation of signalling in human innate immune pathways to NF-kB and IRF family activation.* Biochem Pharmacol, 2022. **205**: p. 115246.

62. Gong, T., et al., *DAMP-sensing receptors in sterile inflammation and inflammatory diseases.* Nat Rev Immunol, 2020. **20**(2): p. 95-112.

63. Liu, T., et al., *NF-κB signaling in inflammation.* Signal Transduct Target Ther, 2017. **2**.

64. Platanias, L.C., *Mechanisms of type-I- and type-II-interferon-mediated signalling.* Nat Rev Immunol, 2005. **5**(5): p. 375-86.

65. Schneider, W.M., M.D. Chevillotte, and C.M. Rice, *Interferon-stimulated genes: a complex web of host defenses.* Annu Rev Immunol, 2014. **32**: p. 513-45.

66. Franceschi, C. and J. Campisi, *Chronic inflammation (inflammaging) and its potential contribution to age-associated diseases.* J Gerontol A Biol Sci Med Sci, 2014. **69 Suppl 1**: p. S4-9.

67. Ferrucci, L. and E. Fabbri, *Inflammageing: chronic inflammation in ageing, cardiovascular disease, and frailty.* Nat Rev Cardiol, 2018. **15**(9): p. 505-522.

68. Collino, S., et al., *Metabolic signatures of extreme longevity in northern Italian centenarians reveal a complex remodeling of lipids, amino acids, and gut microbiota metabolism.* PLoS One, 2013. **8**(3): p. e56564.

69. Biagi, E., et al., *Through ageing, and beyond: gut microbiota and inflammatory status in seniors and centenarians.* PLoS One, 2010. **5**(5): p. e10667.

70. Kennedy, B.K., et al., *Geroscience: linking aging to chronic disease.* Cell, 2014. **159**(4): p. 709-13.

71. De Martinis, M., et al., *Inflamm-ageing and lifelong antigenic load as major determinants of ageing rate and longevity.* FEBS Lett, 2005. **579**(10): p. 2035-9.

72. Franceschi, C., et al., *Inflammaging and 'Garb-aging'.* Trends Endocrinol Metab, 2017. **28**(3): p. 199-212.

73. Zitvogel, L., O. Kepp, and G. Kroemer, *Decoding cell death signals in inflammation and immunity.* Cell, 2010. **140**(6): p. 798-804.

74. Jylhä, M., et al., *Interleukin-1 receptor antagonist, interleukin-6, and C-reactive protein as predictors of mortality in nonagenarians: the vitality 90+ study.* J Gerontol A Biol Sci Med Sci, 2007. **62**(9): p. 1016-21.

75. Walker, K.A., et al., *Midlife Systemic Inflammation Is Associated With Frailty in Later Life: The ARIC Study.* J Gerontol A Biol Sci Med Sci, 2019. **74**(3): p. 343-349.

76. Cushman, M., et al., *C-reactive protein and the 10-year incidence of coronary heart disease in older men and women: the cardiovascular health study.* Circulation, 2005. **112**(1): p. 25-31.

77. Cesari, M., et al., *Inflammatory markers and onset of cardiovascular events: results from the Health ABC study.* Circulation, 2003. **108**(19): p. 2317-22.

78. Tegeler, C., et al., *The inflammatory markers CRP, IL-6, and IL-10 are associated with cognitive function--data from the Berlin Aging Study II.* Neurobiol Aging, 2016. **38**: p. 112-117.

79. Schram, M.T., et al., *Systemic markers of inflammation and cognitive decline in old age.* J Am Geriatr Soc, 2007. **55**(5): p. 708-16.

80. Leonardi, G.C., et al., *Ageing: from inflammation to cancer.* Immun Ageing, 2018. **15**: p. 1.

81. Aryan, Z., et al., *Baseline High-Sensitivity C-Reactive Protein Predicts Macrovascular and Microvascular Complications of Type 2 Diabetes: A Population-Based Study.* Ann Nutr Metab, 2018. **72**(4): p. 287-295.

82. Prattichizzo, F., et al., *Inflammageing and metaflammation: The yin and yang of type 2 diabetes.* Ageing Res Rev, 2018. **41**: p. 1-17.

83. Alikhan, M.A., et al., *Ageing enhances cellular immunity to myeloperoxidase and experimental anti-myeloperoxidase glomerulonephritis.* Rheumatology (Oxford), 2022. **61**(5): p. 2132-2143.

84. Adamson, A., et al., *Signal transduction controls heterogeneous NF-κB dynamics and target gene expression through cytokine-specific refractory states.* Nat Commun, 2016. **7**: p. 12057.

85. Shen-Orr, S.S., et al., *Defective Signaling in the JAK-STAT Pathway Tracks with Chronic Inflammation and Cardiovascular Risk in Aging Humans.* Cell Syst, 2016. **3**(4): p. 374-384.e4.

86. Di Micco, R., et al., *Cellular senescence in ageing: from mechanisms to therapeutic opportunities.* Nat Rev Mol Cell Biol, 2021. **22**(2): p. 75-95.

87. Li, Y., et al., *Embryonic senescent cells re-enter cell cycle and contribute to tissues after birth.* Cell Res, 2018. **28**(7): p. 775-778.

88. Demaria, M., et al., *An essential role for senescent cells in optimal wound healing through secretion of PDGF-AA.* Dev Cell, 2014. **31**(6): p. 722-33.

89. Born, E., et al., *Eliminating Senescent Cells Can Promote Pulmonary Hypertension Development and Progression.* Circulation, 2023. **147**(8): p. 650-666.

90. Xu, M., et al., *Senolytics improve physical function and increase lifespan in old age.* Nat Med, 2018. **24**(8): p. 1246-1256.

91. Ahmed, A.A., et al., *Loss of DNA polymerase β induces cellular senescence.* Environ Mol Mutagen, 2018. **59**(7): p. 603-612.

92. Bidault, G., et al., *Progerin Expression Induces Inflammation, Oxidative Stress and Senescence in Human Coronary Endothelial Cells.* Cells, 2020. **9**(5).

93. Sherr, C.J., *Ink4-Arf locus in cancer and aging.* Wiley Interdiscip Rev Dev Biol, 2012. **1**(5): p. 731-41.

94. Zhang, Y., et al., *A cis-element within the ARF locus mediates repression of p16 INK4A expression via long-range chromatin interactions.* Proc Natl Acad Sci U S A, 2019.

95. Xu, M., et al., *JAK inhibition alleviates the cellular senescence-associated secretory phenotype and frailty in old age.* Proc Natl Acad Sci U S A, 2015. **112**(46): p. E6301-10.

96. Zhu, Y., et al., *Identification of a novel senolytic agent, navitoclax, targeting the Bcl-2 family of anti-apoptotic factors.* Aging Cell, 2016. **15**(3): p. 428-35.

97. Hickson, L.J., et al., *Senolytics decrease senescent cells in humans: Preliminary report from a clinical trial of Dasatinib plus Quercetin in individuals with diabetic kidney disease.* EBioMedicine, 2019. **47**: p. 446-456.

98. Wang, R., et al., *Rapamycin inhibits the secretory phenotype of senescent cells by a Nrf2-independent mechanism.* Aging Cell, 2017. **16**(3): p. 564-574.

99. Aiello, A., et al., *Immunosenescence and Its Hallmarks: How to Oppose Aging Strategically? A Review of Potential Options for Therapeutic Intervention.* Front Immunol, 2019. **10**: p. 2247.

100. Wertheimer, A.M., et al., *Aging and cytomegalovirus infection differentially and jointly affect distinct circulating T cell subsets in humans.* J Immunol, 2014. **192**(5): p. 2143-55.

101. Palmer, S., et al., *Thymic involution and rising disease incidence with age.* Proc Natl Acad Sci U S A, 2018. **115**(8): p. 1883-1888.

102. Srinivasan, J., et al., *Age-Related Changes in Thymic Central Tolerance.* Front Immunol, 2021. **12**: p. 676236.

103. Gibson, K.L., et al., *B-cell diversity decreases in old age and is correlated with poor health status.* Aging Cell, 2009. **8**(1): p. 18-25.

104. Frasca, D., et al., *Aging down-regulates the transcription factor E2A, activation-induced cytidine deaminase, and Ig class switch in human B cells.* J Immunol, 2008. **180**(8): p. 5283-90.

105. Shi, Y., et al., *Regulation of aged humoral immune defense against pneumococcal bacteria by IgM memory B cell.* J Immunol, 2005. **175**(5): p. 3262-7.

106. Fecteau, J.F., G. Côté, and S. Néron, *A new memory CD27-IgG+ B cell population in peripheral blood expressing VH genes with low frequency of somatic mutation.* J Immunol, 2006. **177**(6): p. 3728-36.

107. Pinke, K.H., et al., *Proinflammatory profile of in vitro monocytes in the ageing is affected by lymphocytes presence.* Immun Ageing, 2013. **10**(1): p. 22.

108. Becker, L., et al., *Age-dependent shift in macrophage polarisation causes inflammation-mediated degeneration of enteric nervous system.* Gut, 2018. **67**(5): p. 827-836.

109. Cui, C.Y., et al., *Skewed macrophage polarization in aging skeletal muscle.* Aging Cell, 2019. **18**(6): p. e13032.

110. Linehan, E. and D.C. Fitzgerald, *Ageing and the immune system: focus on macrophages.* Eur J Microbiol Immunol (Bp), 2015. **5**(1): p. 14-24.

111. Stranks, A.J., et al., *Autophagy Controls Acquisition of Aging Features in Macrophages.* J Innate Immun, 2015. **7**(4): p. 375-91.

112. Martinod, K., et al., *Peptidylarginine deiminase 4 promotes age-related organ fibrosis.* J Exp Med, 2017. **214**(2): p. 439-458.

113. Perskin, M.H. and B.N. Cronstein, *Age-related changes in neutrophil structure and function.* Mech Ageing Dev, 1992. **64**(3): p. 303-13.

114. Uciechowski P., R.L., *Neutrophil Granulocyte Functions in the Elderly.*, in *Handbook on Immunosenescence*, D. Springer, Editor. 2009.

115. Mathur, S.K., et al., *Age-related changes in eosinophil function in human subjects.* Chest, 2008. **133**(2): p. 412-9.

116. Agrawal, A., et al., *Altered innate immune functioning of dendritic cells in elderly humans: a role of phosphoinositide 3-kinase-signaling pathway.* J Immunol, 2007. **178**(11): p. 6912-22.

117. Solana, R., et al., *Innate immunosenescence: effect of aging on cells and receptors of the innate immune system in humans.* Semin Immunol, 2012. **24**(5): p. 331-41.

118. Gounder, S.S., et al., *Effect of Aging on NK Cell Population and Their Proliferation at Ex Vivo Culture Condition.* Anal Cell Pathol (Amst), 2018. **2018**: p. 7871814.

119. Chidrawar, S.M., et al., *Ageing is associated with a decline in peripheral blood CD56bright NK cells.* Immun Ageing, 2006. **3**: p. 10.

120. Le Garff-Tavernier, M., et al., *Human NK cells display major phenotypic and functional changes over the life span.* Aging Cell, 2010. **9**(4): p. 527-35.

121. Almeida-Oliveira, A., et al., *Age-related changes in natural killer cell receptors from childhood through old age.* Hum Immunol, 2011. **72**(4): p. 319-29.

122. Frasca, D. and B.B. Blomberg, *Aging induces B cell defects and decreased antibody responses to influenza infection and vaccination.* Immun Ageing, 2020. **17**(1): p. 37.

123. Frasca, D., et al., *The generation of memory B cells is maintained, but the antibody response is not, in the elderly after repeated influenza immunizations.* Vaccine, 2016. **34**(25): p. 2834-40.

124. Britanova, O.V., et al., *Age-related decrease in TCR repertoire diversity measured with deep and normalized sequence profiling.* J Immunol, 2014. **192**(6): p. 2689-98.

125. Yager, E.J., et al., *Age-associated decline in T cell repertoire diversity leads to holes in the repertoire and impaired immunity to influenza virus.* J Exp Med, 2008. **205**(3): p. 711-23.

126. Weng, N.P., A.N. Akbar, and J. Goronzy, *CD28(-) T cells: their role in the age-associated decline of immune function.* Trends Immunol, 2009. **30**(7): p. 306-12.

127. Hobbs, M.V., et al., *Cell proliferation and cytokine production by CD4+ cells from old mice.* J Cell Biochem, 1991. **46**(4): p. 312-20.

128. John Hopkins Hospital, D.o.P.G. *Definitions of Autoimmunity and Autoimmune Disease*. Definitions of Autoimmunity and Autoimmune Disease; Available from: https://pathology.jhu.edu/autoimmune/definitions.

129. Salinas, G.F., et al., *The role of B lymphocytes in the progression from autoimmunity to autoimmune disease.* Clin Immunol, 2013. **146**(1): p. 34-45.

130. Hayter, S.M. and M.C. Cook, *Updated assessment of the prevalence, spectrum and case definition of autoimmune disease.* Autoimmun Rev, 2012. **11**(10): p. 754-65.

131. John Hopkins Hospital, D.o.P., *Prevalence of Autoimmune Diseases*.

132. Watad, A., et al., *Autoimmunity in the Elderly: Insights from Basic Science and Clinics - A Mini-Review.* Gerontology, 2017. **63**(6): p. 515-523.

133. Berti, A., et al., *The Epidemiology of Antineutrophil Cytoplasmic Autoantibody-Associated Vasculitis in Olmsted County, Minnesota: A Twenty-Year US Population-Based Study.* Arthritis Rheumatol, 2017. **69**(12): p. 2338-2350.

134. Jones, B.E., et al., *Gene-Specific DNA Methylation Changes Predict Remission in Patients with ANCA-Associated Vasculitis.* J Am Soc Nephrol, 2017. **28**(4): p. 1175-1187.

135. Lyons, P.A., et al., *Genetically distinct subsets within ANCA-associated vasculitis.* N Engl J Med, 2012. **367**(3): p. 214-23.

136. Chalan, P., et al., *Rheumatoid Arthritis, Immunosenescence and the Hallmarks of Aging.* Curr Aging Sci, 2015. **8**(2): p. 131-46.

137. Catalina, M.D., et al., *Gene expression analysis delineates the potential roles of multiple interferons in systemic lupus erythematosus.* Commun Biol, 2019. **2**: p. 140.

138. Rullo, O.J. and B.P. Tsao, *Recent insights into the genetic basis of systemic lupus erythematosus.* Ann Rheum Dis, 2013. **72 Suppl 2**: p. ii56-61.

139. Papendorf, J.J., E. Krüger, and F. Ebstein, *Proteostasis Perturbations and Their Roles in Causing Sterile Inflammation and Autoinflammatory Diseases.* Cells, 2022. **11**(9).

140. Agrawal, A., et al., *Dendritic cells and aging: consequences for autoimmunity.* Expert Rev Clin Immunol, 2012. **8**(1): p. 73-80.

141. Attanasio, R., et al., *Age-related autoantibody production in a nonhuman primate model.* Clin Exp Immunol, 2001. **123**(3): p. 361-5.

142. Shome, M., et al., *Serum autoantibodyome reveals that healthy individuals share common autoantibodies.* Cell Rep, 2022. **39**(9): p. 110873.

143. Weksler, M.E., *Changes in the B-cell repertoire with age.* Vaccine, 2000. **18**(16): p. 1624-8.

144.   Clemens, M.J., W.J. van Venrooij, and L.B. van de Putte, *Apoptosis and autoimmunity.* Cell Death Differ, 2000. **7**(1): p. 131-3.

145.   Utz, P.J., T.J. Gensler, and P. Anderson, *Death, autoantigen modifications, and tolerance.* Arthritis Res, 2000. **2**(2): p. 101-14.

146.   Khan, I. and R.A. Watts, *Classification of ANCA-associated vasculitis.* Curr Rheumatol Rep, 2013. **15**(12): p. 383.

147.   Pearce, F.A., et al., *Incidence of ANCA-associated vasculitis in a UK mixed ethnicity population.* Rheumatology (Oxford), 2016. **55**(9): p. 1656-63.

148.   Watts, R.A., et al., *Global epidemiology of vasculitis.* Nat Rev Rheumatol, 2022. **18**(1): p. 22-34.

149.   Romeu, M., et al., *Survival of patients with ANCA-associated vasculitis on chronic dialysis: data from the French REIN registry from 2002 to 2011.* QJM, 2014. **107**(7): p. 545-55.

150.   Watts, R.A. and J. Robson, *Introduction, epidemiology and classification of vasculitis.* Best Pract Res Clin Rheumatol, 2018. **32**(1): p. 3-20.

151.   Trivioli, G., et al., *Genetics of ANCA-associated vasculitis: role in pathogenesis, classification and management.* Nat Rev Rheumatol, 2022. **18**(10): p. 559-574.

152.   Furuta, S. and D. Jayne, *Emerging therapies in antineutrophil cytoplasm antibody-associated vasculitis.* Curr Opin Rheumatol, 2014. **26**(1): p. 1-6.

153.   Ahlmann, M. and G. Hempel, *The effect of cyclophosphamide on the immune system: implications for clinical cancer therapy.* Cancer Chemother Pharmacol, 2016. **78**(4): p. 661-71.

154.   Stone, J.H., et al., *Rituximab versus cyclophosphamide for ANCA-associated vasculitis.* N Engl J Med, 2010. **363**(3): p. 221-32.

155.   Jones, R.B., et al., *A multicenter survey of rituximab therapy for refractory antineutrophil cytoplasmic antibody-associated vasculitis.* Arthritis Rheum, 2009. **60**(7): p. 2156-68.

156.   Scott, J., et al., *ANCA-associated vasculitis in Ireland: a multi-centre national cohort study.* HRB Open Res, 2022. **5**: p. 80.

157.   Schreiber, A., et al., *C5a receptor mediates neutrophil activation and ANCA-induced glomerulonephritis.* J Am Soc Nephrol, 2009. **20**(2): p. 289-98.

158.   Brouwer, E., et al., *Neutrophil activation in vitro and in vivo in Wegener's granulomatosis.* Kidney Int, 1994. **45**(4): p. 1120-31.

159.   Ohlsson, S., et al., *Neutrophils from ANCA-associated vasculitis patients show an increased capacity to activate the complement system via the alternative pathway after ANCA stimulation.* PLoS One, 2019. **14**(6): p. e0218272.

160.   Ge, S., et al., *Neutrophils in ANCA-associated vasculitis: Mechanisms and implications for management.* Front Pharmacol, 2022. **13**: p. 957660.

161.   Ahn, S.S., et al., *Neutrophil to lymphocyte ratio at diagnosis can estimate vasculitis activity and poor prognosis in patients with ANCA-associated vasculitis: a retrospective study.* BMC Nephrol, 2018. **19**(1): p. 187.

162.   Hakroush, S., et al., *Comparative Histological Subtyping of Immune Cell Infiltrates in MPO-ANCA and PR3-ANCA Glomerulonephritis.* Front Immunol, 2021. **12**: p. 737708.

163.   Ciavatta, D.J., et al., *Epigenetic basis for aberrant upregulation of autoantigen genes in humans with ANCA vasculitis.* J Clin Invest, 2010. **120**(9): p. 3209-19.

164. Rousselle, A., R. Kettritz, and A. Schreiber, *Monocytes Promote Crescent Formation in Anti-Myeloperoxidase Antibody-Induced Glomerulonephritis.* Am J Pathol, 2017. **187**(9): p. 1908-1915.

165. Vegting, Y., et al., *Monocytes and macrophages in ANCA-associated vasculitis.* Autoimmun Rev, 2021. **20**(10): p. 102911.

166. Eóin C. O'Brien , W.H.A., Abraham Rutgers , Minke G. Huitema , Vincent P. O'Reilly , Alice M. Coughlan , Mark Harrington , Peter Heeringa , Mark A. Little   and Fionnuala B. Hickey, *Intermediate monocytes in ANCA vasculitis: increased surface expression of ANCA autoantigens and IL-1β secretion in response to anti-MPO antibodies.* Scientific reports, 2015.

167. Tam, F.W., et al., *Urinary monocyte chemoattractant protein-1 (MCP-1) is a marker of active renal vasculitis.* Nephrol Dial Transplant, 2004. **19**(11): p. 2761-8.

168. Zhao, L., et al., *M2 macrophage infiltrates in the early stages of ANCA-associated pauci-immune necrotizing GN.* Clin J Am Soc Nephrol, 2015. **10**(1): p. 54-62.

169. Furuta, S., T. Iwamoto, and H. Nakajima, *Update on eosinophilic granulomatosis with polyangiitis.* Allergol Int, 2019. **68**(4): p. 430-436.

170. Wechsler, M.E., et al., *Mepolizumab or Placebo for Eosinophilic Granulomatosis with Polyangiitis.* N Engl J Med, 2017. **376**(20): p. 1921-1932.

171. Martinez Valenzuela, L., et al., *T-lymphocyte in ANCA-associated vasculitis: what do we know? A pathophysiological and therapeutic approach.* Clin Kidney J, 2019. **12**(4): p. 503-511.

172. von Borstel, A., et al., *Cellular immune regulation in the pathogenesis of ANCA-associated vasculitides.* Autoimmun Rev, 2018. **17**(4): p. 413-421.

173. Watts, R.A., et al., *Classification, epidemiology and clinical subgrouping of antineutrophil cytoplasmic antibody (ANCA)-associated vasculitis.* Nephrol Dial Transplant, 2015. **30 Suppl 1**: p. i14-22.

174. Robbins, S.L. and R.S. Cotran, *Robbins and Cotran Pathologic Basis of Disease*. 7th ed, ed. V. Kumar, K. Abul, and N. Fausto. 2005, The Curtis Center, 170 S Independent Mall W 300E, Philadelphia, Pennsylvania 19106: Elsevier Saunders. 9.

175. Thompson, G.E., et al., *Clinical Utility of Serial Measurements of Antineutrophil Cytoplasmic Antibodies Targeting Proteinase 3 in ANCA-Associated Vasculitis.* Front Immunol, 2020. **11**: p. 2053.

176. Fijolek, J., et al., *Antineutrophil cytoplasmic antibodies and their relationship with disease activity and presence of staphylococcal superantigens in nasal swabs in patients having granulomatosis with polyangiitis: results of a study involving 115 patients from a single center.* Clin Rheumatol, 2019. **38**(11): p. 3297-3305.

177. Shochet, L., S. Holdsworth, and A.R. Kitching, *Animal Models of ANCA Associated Vasculitis.* Front Immunol, 2020. **11**: p. 525.

178. Finkielman, J.D., et al., *Antiproteinase 3 antineutrophil cytoplasmic antibodies and disease activity in Wegener granulomatosis.* Ann Intern Med, 2007. **147**(9): p. 611-9.

179. Fijołek, J. and E. Wiatr, *Antineutrophil cytoplasmic antibodies (ANCA) - their role in pathogenesis, diagnosis, and treatment monitoring of ANCA-associated vasculitis.* Cent Eur J Immunol, 2020. **45**(2): p. 218-227.

180. Brunetta, E., et al., *Serum ANCA and Overall Mortality: A 10-Year Retrospective Cohort Study on 1,024 Italian Subjects.* Front Immunol, 2021. **12**: p. 714174.

181. Deshpande, P., et al., *Low level autoantibodies can be frequently detected in the general Australian population.* Pathology, 2016. **48**(5): p. 483-90.

182. McKinney, E.F., et al., *The immunopathology of ANCA-associated vasculitis.* Semin Immunopathol, 2014. **36**(4): p. 461-78.

183. Berti, A. and U. Specks, *Remission maintenance in ANCA-associated vasculitis: does one size fit all?* Expert Rev Clin Immunol, 2019. **15**(12): p. 1273-1286.

184. Wu, T., et al., *Differences between myeloperoxidase-antineutrophil cytoplasmic autoantibody (ANCA) and proteinase 3-ANCA associated vasculitis: A retrospective study from a single center in China.* Exp Ther Med, 2021. **21**(6): p. 561.

185. Bantis, K., et al., *Different Types of ANCA Determine Different Clinical Phenotypes and Outcome in ANCA-Associated Vasculitis (AAV).* Front Med (Lausanne), 2021. **8**: p. 783757.

186. Hilhorst, M., et al., *Proteinase 3-ANCA Vasculitis versus Myeloperoxidase-ANCA Vasculitis.* J Am Soc Nephrol, 2015. **26**(10): p. 2314-27.

187. Arnhold, J., *The Dual Role of Myeloperoxidase in Immune Response.* Int J Mol Sci, 2020. **21**(21).

188. Hess, C., S. Sadallah, and J.A. Schifferli, *Induction of neutrophil responsiveness to myeloperoxidase antibodies by their exposure to supernatant of degranulated autologous neutrophils.* Blood, 2000. **96**(8): p. 2822-7.

189. van Rossum, A.P., et al., *Constitutive membrane expression of proteinase 3 (PR3) and neutrophil activation by anti-PR3 antibodies.* J Leukoc Biol, 2004. **76**(6): p. 1162-70.

190. Watts, R.A., et al., *Epidemiology of systemic vasculitis: a ten-year study in the United Kingdom.* Arthritis Rheum, 2000. **43**(2): p. 414-9.

191. Krafcik, S.S., et al., *Wegener's granulomatosis in the elderly.* Chest, 1996. **109**(2): p. 430-7.

192. Wójcik, K., et al., *Association of antineutrophil cytoplasmic antibody (ANCA) specificity with demographic and clinical characteristics of patients with ANCA-associated vasculitides.* Pol Arch Intern Med, 2022. **132**(3).

193. Berglin, E., et al., *Anti-neutrophil cytoplasmic antibodies predate symptom onset of ANCA-associated vasculitis. A case-control study.* J Autoimmun, 2021. **117**: p. 102579.

194. Berden, A., et al., *Diagnosis and management of ANCA associated vasculitis.* BMJ, 2012. **344**: p. e26.

195. Jayne, D.R.W., et al., *Avacopan for the Treatment of ANCA-Associated Vasculitis.* N Engl J Med, 2021. **384**(7): p. 599-609.

196. O'Brien, E.C., et al., *Intermediate monocytes in ANCA vasculitis: increased surface expression of ANCA autoantigens and IL-1β secretion in response to anti-MPO antibodies.* Sci Rep, 2015. **5**: p. 11888.

197. Walter, M.R., *The Role of Structure in the Biology of Interferon Signaling.* Front Immunol, 2020. **11**: p. 606489.

198. Lee, A.J. and A.A. Ashkar, *The Dual Nature of Type I and Type II Interferons.* Front Immunol, 2018. **9**: p. 2061.

199. Porritt, R.A. and P.J. Hertzog, *Dynamic control of type I IFN signalling by an integrated network of negative regulators.* Trends Immunol, 2015. **36**(3): p. 150-60.

200. Soucy-Faulkner, A., et al., *Requirement of NOX2 and reactive oxygen species for efficient RIG-I-mediated antiviral response through regulation of MAVS expression.* PLoS Pathog, 2010. **6**(6): p. e1000930.

201. Fuertes, M.B., et al., *Type I interferon response and innate immune sensing of cancer.* Trends Immunol, 2013. **34**(2): p. 67-73.

202. Gessani, S., et al., *Type I interferons as regulators of human antigen presenting cell functions.* Toxins (Basel), 2014. **6**(6): p. 1696-723.

203. Paquette, R.L., et al., *Interferon-alpha and granulocyte-macrophage colony-stimulating factor differentiate peripheral blood monocytes into potent antigen-presenting cells.* J Leukoc Biol, 1998. **64**(3): p. 358-67.

204. Ogasawara, K., et al., *Requirement of the IFN-alpha/beta-induced CXCR3 chemokine signalling for CD8+ T cell activation.* Genes Cells, 2002. **7**(3): p. 309-20.

205. Le Bon, A., et al., *Type i interferons potently enhance humoral immunity and can promote isotype switching by stimulating dendritic cells in vivo.* Immunity, 2001. **14**(4): p. 461-70.

206. Litinskiy, M.B., et al., *DCs induce CD40-independent immunoglobulin class switching through BLyS and APRIL.* Nat Immunol, 2002. **3**(9): p. 822-9.

207. Baechler, E.C., et al., *An interferon signature in the peripheral blood of dermatomyositis patients is associated with disease activity.* Mol Med, 2007. **13**(1-2): p. 59-68.

208. Rice, G.I., et al., *Assessment of Type I Interferon Signaling in Pediatric Inflammatory Disease.* J Clin Immunol, 2017. **37**(2): p. 123-132.

209. Li, G., et al., *Age-Associated Failure To Adjust Type I IFN Receptor Signaling Thresholds after T Cell Activation.* J Immunol, 2015. **195**(3): p. 865-74.

210. Rasa, S.M.M., et al., *Inflammaging is driven by upregulation of innate immune receptors and systemic interferon signaling and is ameliorated by dietary restriction.* Cell Rep, 2022. **39**(13): p. 111017.

211. Gresser, I., et al., *Lethality of interferon preparations for newborn mice.* Nature, 1975. **258**(5530): p. 76-8.

212. Lebon, P., et al., *Intrathecal synthesis of interferon-alpha in infants with progressive familial encephalopathy.* J Neurol Sci, 1988. **84**(2-3): p. 201-8.

213. Crow, Y.J., *Type I interferonopathies: a novel set of inborn errors of immunity.* Ann N Y Acad Sci, 2011. **1238**: p. 91-8.

214. Crow, Y.J. and D.B. Stetson, *The type I interferonopathies: 10 years on.* Nat Rev Immunol, 2022. **22**(8): p. 471-483.

215. Rice, G.I., et al., *Assessment of interferon-related biomarkers in Aicardi-Goutières syndrome associated with mutations in TREX1, RNASEH2A, RNASEH2B, RNASEH2C, SAMHD1, and ADAR: a case-control study.* Lancet Neurol, 2013. **12**(12): p. 1159-69.

216. Ganguly, D., *Do Type I Interferons Link Systemic Autoimmunities and Metabolic Syndrome in a Pathogenetic Continuum?* Trends Immunol, 2018. **39**(1): p. 28-43.

217.   Connelly, K.L., et al., *Longitudinal association of type 1 interferon-induced chemokines with disease activity in systemic lupus erythematosus.* Sci Rep, 2018. **8**(1): p. 3268.

218.   Kimoto, O., et al., *Activation of the interferon pathway in peripheral blood of patients with Sjogren's syndrome.* J Rheumatol, 2011. **38**(2): p. 310-6.

219.   Morand, E.F., et al., *Trial of Anifrolumab in Active Systemic Lupus Erythematosus.* N Engl J Med, 2020. **382**(3): p. 211-221.

220.   Ishizu, A., et al., *Prediction of response to remission induction therapy by gene expression profiling of peripheral blood in Japanese patients with microscopic polyangiitis.* Arthritis Res Ther, 2017. **19**(1): p. 117.

221.   Owens, W.A., et al., *Senescence and senolytics in cardiovascular disease: Promise and potential pitfalls.* Mech Ageing Dev, 2021. **198**: p. 111540.

222.   McCrory, C., et al., *Epigenetic clocks and allostatic load reveal potential sex-specific drivers of biological ageing.* J Gerontol A Biol Sci Med Sci, 2019.

223.   Mukaka, M.M., *Statistics corner: A guide to appropriate use of correlation coefficient in medical research.* Malawi Med J, 2012. **24**(3): p. 69-71.

224.   Akoglu, H., *User's guide to correlation coefficients.* Turk J Emerg Med, 2018. **18**(3): p. 91-93.

225.   Mehrmohamadi, M., et al., *A Comparative Overview of Epigenomic Profiling Methods.* Front Cell Dev Biol, 2021. **9**: p. 714687.

226.   Horvath, S., et al., *An epigenetic clock analysis of race/ethnicity, sex, and coronary heart disease.* Genome Biol, 2016. **17**(1): p. 171.

227.   Hirahashi, J., et al., *Immunomodulation with eicosapentaenoic acid supports the treatment of autoimmune small-vessel vasculitis.* Sci Rep, 2014. **4**: p. 6406.

228.   Hunder, G.G., et al., *The American College of Rheumatology 1990 criteria for the classification of vasculitis. Introduction.* Arthritis Rheum, 1990. **33**(8): p. 1065-7.

229.   Perdaens, O. and V. van Pesch, *Molecular Mechanisms of Immunosenescene and Inflammaging: Relevance to the Immunopathogenesis and Treatment of Multiple Sclerosis.* Front Neurol, 2021. **12**: p. 811518.

230.   Deguchi, Y., N. Shibata, and S. Kishimoto, *Enhanced expression of the tumour necrosis factor/cachectin gene in peripheral blood mononuclear cells from patients with systemic vasculitis.* Clin Exp Immunol, 1990. **81**(2): p. 311-4.

231.   Berti, A., et al., *Interleukin-6 in ANCA-associated vasculitis: Rationale for successful treatment with tocilizumab.* Semin Arthritis Rheum, 2015. **45**(1): p. 48-54.

232.   Berti, A., et al., *The association of serum interleukin-6 levels with clinical outcomes in antineutrophil cytoplasmic antibody-associated vasculitis.* J Autoimmun, 2019. **105**: p. 102302.

233.   McAdoo, S.P. and C.D. Pusey, *Is there a role for TNFα blockade in ANCA-associated vasculitis and glomerulonephritis?* Nephrol Dial Transplant, 2017. **32**(suppl_1): p. i80-i88.

234.   Wang, Q., et al., *Age-determined severity of anti-myeloperoxidase autoantibody-mediated glomerulonephritis in mice.* Nephrol Dial Transplant, 2017. **32**(2): p. 254-264.

235.   Żabińska, M., et al., *Immune Cells Profiling in ANCA-Associated Vasculitis Patients-Relation to Disease Activity.* Cells, 2021. **10**(7).

236.   Mogilenko, D.A., I. Shchukina, and M.N. Artyomov, *Immune ageing at single-cell resolution.* Nat Rev Immunol, 2022. **22**(8): p. 484-498.

237.   Noronha, I.L., et al., *In situ production of TNF-alpha, IL-1 beta and IL-2R in ANCA-positive glomerulonephritis.* Kidney Int, 1993. **43**(3): p. 682-92.

238.   Schreiber, A., et al., *Necroptosis controls NET generation and mediates complement activation, endothelial damage, and autoimmune vasculitis.* Proc Natl Acad Sci U S A, 2017. **114**(45): p. E9618-E9625.

239.   Falk, R.J., et al., *Anti-neutrophil cytoplasmic autoantibodies induce neutrophils to degranulate and produce oxygen radicals in vitro.* Proc Natl Acad Sci U S A, 1990. **87**(11): p. 4115-9.

240.   Hattar, K., et al., *Wegener's granulomatosis: antiproteinase 3 antibodies induce monocyte cytokine and prostanoid release-role of autocrine cell activation.* J Leukoc Biol, 2002. **71**(6): p. 996-1004.

241.   Albani, D., et al., *Interleukin-6 plasma level increases with age in an Italian elderly population ("The Treviso Longeva"-Trelong-study) with a sex-specific contribution of rs1800795 polymorphism.* Age (Dordr), 2009. **31**(2): p. 155-62.

242.   Sauce, D., et al., *Reduced Oxidative Burst by Primed Neutrophils in the Elderly Individuals Is Associated With Increased Levels of the CD16bright/CD62Ldim Immunosuppressive Subset.* J Gerontol A Biol Sci Med Sci, 2017. **72**(2): p. 163-172.

243.   Kovalenko, E.I., et al., *ROS production, intracellular HSP70 levels and their relationship in human neutrophils: effects of age.* Oncotarget, 2014. **5**(23): p. 11800-12.

244.   Ogawa, K., et al., *The association of elevated reactive oxygen species levels from neutrophils with low-grade inflammation in the elderly.* Immun Ageing, 2008. **5**: p. 13.

245.   Nguyen, M.T., et al., *Quiescence of Human Monocytes after Affinity Purification: A Novel Method Apt for Monocyte Stimulation Assays.* Biomolecules, 2022. **12**(3).

246.   Martinez-Jimenez, C.P., et al., *Aging increases cell-to-cell transcriptional variability upon immune stimulation.* Science, 2017. **355**(6332): p. 1433-1436.

247.   Howlett, S.E., Rutenberg, A.D. & Rockwood, K., *The degree of frailty as a translational measure of health in aging*. 2021: *Nat Aging*. p. 651–665.

248.   Piasecka, B., et al., *Distinctive roles of age, sex, and genetics in shaping transcriptional variation of human immune responses to microbial challenges.* Proc Natl Acad Sci U S A, 2018. **115**(3): p. E488-E497.

249.   D'Souza, S.S., et al., *Type I Interferon signaling controls the accumulation and transcriptomes of monocytes in the aged lung.* Aging Cell, 2021. **20**(10): p. e13470.

250.   Lopez, L., et al., *Dysregulated Interferon Response Underlying Severe COVID-19.* Viruses, 2020. **12**(12).

251.   Beer, J., et al., *Impaired immune response drives age-dependent severity of COVID-19.* J Exp Med, 2022. **219**(12).

252.   Yao, Y., et al., *Development of Potential Pharmacodynamic and Diagnostic Markers for Anti-IFN-α Monoclonal Antibody Trials in Systemic Lupus Erythematosus.* Hum Genomics Proteomics, 2009. **2009**.

253. Vitali, C., et al., *Classification criteria for Sjögren's syndrome: a revised version of the European criteria proposed by the American-European Consensus Group.* Ann Rheum Dis, 2002. **61**(6): p. 554-8.

254. Dominguez-Gutierrez, P.R., et al., *Reduced levels of CCL2 and CXCL10 in systemic lupus erythematosus patients under treatment with prednisone, mycophenolate mofetil, or hydroxychloroquine, except in a high STAT1 subset.* Arthritis Res Ther, 2014. **16**(1): p. R23.

255. Schoggins, J.W., et al., *A diverse range of gene products are effectors of the type I interferon antiviral response.* Nature, 2011. **472**(7344): p. 481-5.

256. Li, Q.Z., et al., *Interferon signature gene expression is correlated with autoantibody profiles in patients with incomplete lupus syndromes.* Clin Exp Immunol, 2010. **159**(3): p. 281-91.

257. Perng, Y.C. and D.J. Lenschow, *ISG15 in antiviral immunity and beyond.* Nat Rev Microbiol, 2018. **16**(7): p. 423-439.

258. Zhang, D. and D.E. Zhang, *Interferon-stimulated gene 15 and the protein ISGylation system.* J Interferon Cytokine Res, 2011. **31**(1): p. 119-30.

259. Feng, X., et al., *Association of increased interferon-inducible gene expression with disease activity and lupus nephritis in patients with systemic lupus erythematosus.* Arthritis Rheum, 2006. **54**(9): p. 2951-62.

260. Ding, Y., et al., *Identification of a gene-expression predictor for diagnosis and personalized stratification of lupus patients.* PLoS One, 2018. **13**(7): p. e0198325.

261. Akiyama, H., et al., *Interferon-Inducible CD169/Siglec1 Attenuates Anti-HIV-1 Effects of Alpha Interferon.* J Virol, 2017. **91**(21).

262. Gaudet, P., et al., *Phylogenetic-based propagation of functional annotations within the Gene Ontology consortium.* Brief Bioinform, 2011. **12**(5): p. 449-62.

263. Fitzgerald, K.A., *The interferon inducible gene: Viperin.* J Interferon Cytokine Res, 2011. **31**(1): p. 131-5.

264. Wang, X., E.R. Hinson, and P. Cresswell, *The interferon-inducible protein viperin inhibits influenza virus release by perturbing lipid rafts.* Cell Host Microbe, 2007. **2**(2): p. 96-105.

265. Nasr, N., et al., *HIV-1 infection of human macrophages directly induces viperin which inhibits viral production.* Blood, 2012. **120**(4): p. 778-88.

266. Emamian, E.S., et al., *Peripheral blood gene expression profiling in Sjögren's syndrome.* Genes Immun, 2009. **10**(4): p. 285-96.

267. Kumar, P., et al., *Inhibition of translation by IFIT family members is determined by their ability to interact selectively with the 5'-terminal regions of cap0-, cap1- and 5'ppp- mRNAs.* Nucleic Acids Res, 2014. **42**(5): p. 3228-45.

268. Fensterl, V. and G.C. Sen, *Interferon-induced Ifit proteins: their role in viral pathogenesis.* J Virol, 2015. **89**(5): p. 2462-8.

269. Mihalich, A., et al., *Interferon-inducible genes, TNF-related apoptosis-inducing ligand (TRAIL) and interferon inducible protein 27 (IFI27) are negatively regulated in leiomyomas: implications for a role of the interferon pathway in leiomyoma development.* Gynecol Endocrinol, 2012. **28**(3): p. 216-9.

270. Rosebeck, S. and D.W. Leaman, *Mitochondrial localization and pro-apoptotic effects of the interferon-inducible protein ISG12a.* Apoptosis, 2008. **13**(4): p. 562-72.

271. Huang, W.C., et al., *IFI44L is a novel tumor suppressor in human hepatocellular carcinoma affecting cancer stemness, metastasis, and drug resistance via regulating met/Src signaling pathway.* BMC Cancer, 2018. **18**(1): p. 609.

272. Björk A, R.A.E., Imgenberg-Kreuz J, et al., *Protein and DNA methylation-based scores as surrogate markers for interferon system activation in patients with primary Sjögren's syndrome.* RMD Open, 2020.

273. Cheon, H. and G.R. Stark, *Unphosphorylated STAT1 prolongs the expression of interferon-induced immune regulatory genes.* Proc Natl Acad Sci U S A, 2009. **106**(23): p. 9373-8.

274. Deshmane, S.L., et al., *Monocyte chemoattractant protein-1 (MCP-1): an overview.* J Interferon Cytokine Res, 2009. **29**(6): p. 313-26.

275. Bauer, J.W., et al., *Interferon-regulated chemokines as biomarkers of systemic lupus erythematosus disease activity: a validation study.* Arthritis Rheum, 2009. **60**(10): p. 3098-107.

276. Cuadrado, E., et al., *Phenotypic variation in Aicardi-Goutières syndrome explained by cell-specific IFN-stimulated gene response and cytokine release.* J Immunol, 2015. **194**(8): p. 3623-33.

277. Blokland, S.L.M., et al., *Emerging roles for chemokines and cytokines as orchestrators of immunopathology in Sjögren's syndrome.* Rheumatology (Oxford), 2019.

278. Balarini, G.M., et al., *Serum calprotectin is a biomarker of carotid atherosclerosis in patients with primary Sjögren's syndrome.* Clin Exp Rheumatol, 2016. **34**(6): p. 1006-1012.

279. Antonelli, A., et al., *Chemokine (C-X-C motif) ligand (CXCL)10 in autoimmune diseases.* Autoimmun Rev, 2014. **13**(3): p. 272-80.

280. Vazirinejad, R., et al., *The biological functions, structure and sources of CXCL10 and its outstanding part in the pathophysiology of multiple sclerosis.* Neuroimmunomodulation, 2014. **21**(6): p. 322-30.

281. Yan, Y., et al., *CCL19 and CCR7 Expression, Signaling Pathways, and Adjuvant Functions in Viral Infection and Prevention.* Front Cell Dev Biol, 2019. **7**: p. 212.

282. Pietilä, T.E., et al., *Multiple NF-kappaB and IFN regulatory factor family transcription factors regulate CCL19 gene expression in human monocyte-derived dendritic cells.* J Immunol, 2007. **178**(1): p. 253-61.

283. Yan, C. and D.D. Boyd, *Regulation of matrix metalloproteinase gene expression.* J Cell Physiol, 2007. **211**(1): p. 19-26.

284. Perron, B., et al., *Can enzymatic activity, or otherwise, be inferred from structural studies of annexin III?* J Biol Chem, 1997. **272**(17): p. 11321-6.

285. McKinney, E.F., et al., *T-cell exhaustion, co-stimulation and clinical outcome in autoimmunity and infection.* Nature, 2015. **523**(7562): p. 612-6.

286. Yao, Y., et al., *Type I interferons in Sjögren's syndrome.* Autoimmun Rev, 2013. **12**(5): p. 558-66.

287. Goupil, R., et al., *Lymphopenia and treatment-related infectious complications in ANCA-associated vasculitis.* Clin J Am Soc Nephrol, 2013. **8**(3): p. 416-23.

288. H, J.J.a.J., *Methods to analyze cell type-specific gene expression profiles from heterogeneous cell populations.* Animal Cells and Systems, 2016.

289. Diao, B., et al., *Reduction and Functional Exhaustion of T Cells in Patients With Coronavirus Disease 2019 (COVID-19).* Front Immunol, 2020. **11**: p. 827.

290. Kolling, U.K., et al., *Leucocyte response and anti-inflammatory cytokines in community acquired pneumonia.* Thorax, 2001. **56**(2): p. 121-5.

291. Webb, K., et al., *Sex and Pubertal Differences in the Type 1 Interferon Pathway Associate With Both X Chromosome Number and Serum Sex Hormone Concentration.* Front Immunol, 2018. **9**: p. 3167.

292. Kessler, N., et al., *Monocyte-derived macrophages aggravate pulmonary vasculitis via cGAS/STING/IFN-mediated nucleic acid sensing.* J Exp Med, 2022. **219**(10).

293. Edvardsen, K., et al., *Peripheral Blood Cells from Patients with Autoimmune Addison's Disease Poorly Respond to Interferons In Vitro, Despite Elevated Serum Levels of Interferon-Inducible Chemokines.* J Interferon Cytokine Res, 2015. **35**(10): p. 759-70.

294. Bratland, E., A. Hellesen, and E.S. Husebye, *Induction of CXCL10 chemokine in adrenocortical cells by stimulation through toll-like receptor 3.* Mol Cell Endocrinol, 2013. **365**(1): p. 75-83.

295. Lúdvíksson, B.R., et al., *Active Wegener's granulomatosis is associated with HLA-DR+ CD4+ T cells exhibiting an unbalanced Th1-type T cell cytokine pattern: reversal with IL-10.* J Immunol, 1998. **160**(7): p. 3602-9.

296. Lee, K.S., et al., *Genetic Variants in Antineutrophil Cytoplasmic Antibody-Associated Vasculitis: A Bayesian Approach and Systematic Review.* J Clin Med, 2019. **8**(2).

297. Monach, P.A., et al., *Serum proteins reflecting inflammation, injury and repair as biomarkers of disease activity in ANCA-associated vasculitis.* Ann Rheum Dis, 2013. **72**(8): p. 1342-50.

298. de Jong, T.D., et al., *Effect of prednisone on type I interferon signature in rheumatoid arthritis: consequences for response prediction to rituximab.* Arthritis Res Ther, 2015. **17**: p. 78.

299. Wallace, Z.S. and E.M. Miloslavsky, *Management of ANCA associated vasculitis.* BMJ, 2020. **368**: p. m421.

300. El-Gohary, A., et al., *Serum and Urinary Interferon-Gamma-Inducible Protein 10 in Lupus Nephritis.* J Clin Lab Anal, 2016. **30**(6): p. 1135-1138.

301. Han, J.H., et al., *Association of CXCL10 and CXCL13 levels with disease activity and cutaneous manifestation in active adult-onset Still's disease.* Arthritis Res Ther, 2015. **17**: p. 260.

302. Gotsch, F., et al., *CXCL10/IP-10: a missing link between inflammation and anti-angiogenesis in preeclampsia?* J Matern Fetal Neonatal Med, 2007. **20**(11): p. 777-92.

303. Ohlsson, S., J. Wieslander, and M. Segelmark, *Circulating cytokine profile in anti-neutrophilic cytoplasmatic autoantibody-associated vasculitis: prediction of outcome?* Mediators Inflamm, 2004. **13**(4): p. 275-83.

304. Land, J., et al., *Regulatory and effector B cell cytokine production in patients with relapsing granulomatosis with polyangiitis.* Arthritis Res Ther, 2016. **18**: p. 84.

305. Torheim, E.A., et al., *Increased expression of chemokines in patients with Wegener's granulomatosis - modulating effects of methylprednisolone in vitro.* Clin Exp Immunol, 2005. **140**(2): p. 376-83.

306. Yao, Y., et al., *Type I interferon: potential therapeutic target for psoriasis?* PLoS One, 2008. **3**(7): p. e2737.

307. Romanova, Y., et al., *Proteomic Analysis of Human Serum from Patients with Chronic Kidney Disease.* Biomolecules, 2020. **10**(2).

308. Okazaki, S., et al., *Decelerated epigenetic aging associated with mood stabilizers in the blood of patients with bipolar disorder.* Transl Psychiatry, 2020. **10**(1): p. 129.

309. Segura, À., et al., *Epigenetic clocks in relapse after a first episode of schizophrenia.* Schizophrenia (Heidelb), 2022. **8**(1): p. 61.

310. Joyce, B.T., et al., *Epigenetic Age Acceleration Reflects Long-Term Cardiovascular Health.* Circ Res, 2021. **129**(8): p. 770-781.

311. Bhat, R., et al., *Astrocyte senescence as a component of Alzheimer's disease.* PLoS One, 2012. **7**(9): p. e45069.

312. Krtolica, A., et al., *Senescent fibroblasts promote epithelial cell growth and tumorigenesis: a link between cancer and aging.* Proc Natl Acad Sci U S A, 2001. **98**(21): p. 12072-7.

313. Del Rey, M.J., et al., *Senescent synovial fibroblasts accumulate prematurely in rheumatoid arthritis tissues and display an enhanced inflammatory phenotype.* Immun Ageing, 2019. **16**: p. 29.

314. Martyanov, V., M.L. Whitfield, and J. Varga, *Senescence Signature in Skin Biopsies From Systemic Sclerosis Patients Treated With Senolytic Therapy: Potential Predictor of Clinical Response?* Arthritis Rheumatol, 2019. **71**(10): p. 1766-1767.

315. Gu, Z., et al., *p53/p21 Pathway involved in mediating cellular senescence of bone marrow-derived mesenchymal stem cells from systemic lupus erythematosus patients.* Clin Dev Immunol, 2013. **2013**: p. 134243.

316. Gao, L., et al., *Cell Senescence in Lupus.* Curr Rheumatol Rep, 2019. **21**(2): p. 1.

317. Vogt, S., et al., *Shortening of telomeres: Evidence for replicative senescence of T cells derived from patients with Wegener's granulomatosis.* Kidney Int, 2003. **63**(6): p. 2144-51.

318. Gaya da Costa, M., et al., *Age and Sex-Associated Changes of Complement Activity and Complement Levels in a Healthy Caucasian Population.* Front Immunol, 2018. **9**: p. 2664.

319. Zheng, R., et al., *The Complement System, Aging, and Aging-Related Diseases.* Int J Mol Sci, 2022. **23**(15).

320. Grayson, P.C., et al., *Metabolic pathways and immunometabolism in rare kidney diseases.* Ann Rheum Dis, 2018. **77**(8): p. 1226-1233.

Appendix 1: Health Status Survey for Healthy Control Recruitment

Section 1: Declaration of Health:
Please initial the box if you agree with this statement

Initial

I am, to the best of my knowledge, a healthy individual with no underlying chronic medical conditions	

Section 2: Demographic and Clinical Information
Please answer the following questions

What is your date of birth? (dd/mm/yyyy)
What is your sex? (male/female)
Which of the following best describes your smoking status? Circle the appropriate answer. Current smoker Previous smoker Never smoker
What is your current weight (kg)?
What is your current height (cm)?
What is your ethnicity?

White Irish	Bangladeshi
White British	Chinese
White and Black Caribbean	Any other Asian Background
White and Black African	Caribbean
White and Asian	African
Any other White Background	Any other Black Background
Indian	Any other Mixed Background
Pakistani	Any other ethnic group

Section 3: Medical History:

Please answer yes (Y) or no (N) unless otherwise specified   **Y/N**

Do you have a medical history of any of the following? • heart disease • cancer • chronic kidney disease • diabetes • chronic infection • autoimmunity (e.g., arthritis, multiple sclerosis, systemic lupus erythematosus, inflammatory bowel disease, etc.)	
Do you attend any outpatient clinics?	
Are you capable of comfortably walking ¼ mile (1/2 kilometre)?	
Have you been exposed to any recent infections (within 2 weeks)?	
Have you received any recent vaccinations (within 2 weeks)?	
Have you received a COVID19 vaccination to date?	
If yes, please specify the vaccine type (i.e., AstraZeneca, Pfizer, Johnson & Johnson, Moderna etc.) and date of vaccine(s).	
Vaccine type:	
Date of dose 1 (dd/mm/yyyy)	
Date of dose 2 (if applicable) (dd/mm/yyyy):	
Date of 3rd dose (if applicable) (dd/mm/yyyy)	
Date of 4th dose (if applicable) (dd/mm/yyyy)	
Date of Covid 19 infection (if applicable) (dd/mm/yyyy)	
Are you currently on any forms of medication?	
If yes, please specify the medication(s) type, dose and frequency of intake:	

Appendix 2: Ingenuity Pathway Analysis of AAV Samples

IPA from publicly available RNAseq datasets (GSE108109)[320] on human AAV glomeruli samples compared to healthy controls. Orange represents signalling pathways that were downregulated in AAV samples compared to HC while blue represents pathways that were found to be upregulated in AAV. IPA was performed by Dr. Conor Finlay.